University of Alberta

Analysis of mitochondrial outer membrane import complex components in *Neurospora crassa.*

by

Sebastian William Keith Lackey

A thesis submitted to the Faculty of Graduate Studies and Research

in partial fulfillment of the requirements for the degree of

Doctor of Philosophy

in

Molecular Biology and Genetics

Department of Biological Sciences

Spring 2014

Edmonton, Alberta

Abstract

The TOB (Topogenesis of Outer membrane β-barrel proteins) complex is composed of the core proteins Tob55 (Sam50), Tob37 (Sam37) and Tob38 (Sam35). The complex facilitates the insertion of all β-barrel and some α-helically anchored integral proteins into the mitochondrial outer membrane (MOM). Little is understood about the architecture of the TOB complex and the protein-protein interactions required for complex stability and function. We have shown that the three TOB_{core} proteins are essential in *Neurospora crassa* making *in vivo* analysis of simple TOB knockout strains impossible. However, I have shown that severe depletion of Tob37 or Tob38 protein in heterokaryotic cultures leads to disruption of β-barrel protein import as well as the import of at least one α-helically anchored MOM protein, Tom22. In addition, I identified a key topological feature located near the C-terminus of Tob37. This region contains novel dual α-helices, one of which acts as the transmembrane domain (TMD) anchor for Tob37 that stabilizes the association of the protein with the complex. I have also shown that Tob38 is severely reduced in the absence of Tob37 and that Tob38 likely interacts with Tob37.

In a second project I examined the topology of *N. crassa* Tom40, the essential core β-barrel protein of the TOM (Translocase of the Outer Membrane) complex. Tom40 forms the pore through which the vast majority of mitochondrial proteins must pass through to enter the organelle. I used substituted cysteine accessibility mapping (SCAM) to define the topology and identify the structural β-strand arrangement of specific amino acid residues in a region of Tom40. These data, together with previous data from our laboratory allowed the development of a partial model based on empirical molecular evidence that we compared to various *in silico* developed models. The analysis favors the recently proposed model of a β-barrel protein containing 19 β-strands that was developed

in other laboratories using the structure of the related protein VDAC (or porin) as a model.

TABLE OF CONTENTS

1. Introduction

List of Figures

List of Tables

List of Abbreviations

3D	three dimensional
A	adenine
Å	Angstroms
AAC	ATP/ADP carrier
ADP	adenosine diphosphate
ATOM	archaic translocase of the outer mitochondrial membrane
ATP	adenosine triphosphate
Ben	benomyl
BLAST	basic local alignment search tool
BNGE	blue native gel electrophoresis
bp	base pair
BSA	bovine serum albumin
C	cytosine
°C	degrees Celsius
cDNA	complementary DNA
CL	cardiolipin
Cys	cysteine
Δ	deletion
Da	Dalton
DMSO	dimethylsulfoxide
EM	electron microscopy
ERMES	endoplasmic reticulum-mitochondria encounter structure
ETC	electron transport chain
$F_1\beta$	β subunit of the F_1 ATP synthase
Fe-S	iron sulfur
fpa	fluorophenylalanine
G	guanine
g	gravity
gDNA	genomic DNA
GIP	general import pore
GTP	guanine triphosphate
His	histidine
hr	hour
Hsp	heat shock protein
hyg	hygromycin
IMS	intermembrane space
IP	immunoprecipitate
kbp	kilobasepair
kDa	kiloDalton

L	litre
µg	microgram
µL	microliter
µm	micrometer
M	molar
MAPL	mitochondrial-anchored protein
Mas	mitochondrial assembly protein
mdm	mitochondrial distribution and morphology
MDV	mitochondria-derived vesicle
mg	milligrams
MIM	mitochondrial inner membrane
mL	milliliter
mM	millimolar
mmm	maintaining mitochondrial morphology
min	minute
Mia	mitochondria IMS assembly
MOM	mitochondrial outer membrane
MOPS	4-morpholinepropanesulfonic acid
mRNA	messenger RNA
mtDNA	mitochondrial DNA
NADH	nicotinamide adenine dinucleotide reduced form
Ni-NTA	nickel-nitrilotriacetic acid
OMV	outer membrane vesicles
OXA	oxidase assembly
OXPHOS	oxidative phosphorylation
PAGE	polyacrylamide gel electrophoresis
PAM	presequence translocase associated protein import motor
PCR	polymerase chain reaction
PK	proteinase K
PMSF	phenylmethylsulfonyl fluoride
PVDF	polyvinylidenefluoride
RIP	repeat induced point mutations
RNA	ribonucleic acid
rRNA	ribosomal RNA
rpm	revolutions per minute
SAM	sorting and assembly machinery
SDS	sodium dodecyl sulfate
T	thymine
TCA	trichloroacetic acid
TMD	transmembrane domain

TOB	topogenesis of outer membrane β-barrels
TOM	translocase of the outer mitochondrial membrane
TPR	tetratricopeptide repeat
Tris	tris (hydroxymethyl) aminomethane
UTR	untranslated region

Chapter 1. Introduction

1.1 Mitochondrial structure and function

Mitochondria are double membrane bound eukaryotic organelles with four identifiable subcompartments: the mitochondrial outer membrane (MOM), the intermembrane space (IMS), the mitochondrial inner membrane (MIM) and the matrix (Nicastro *et al.*, 2000). The MIM can be further differentiated into two distinct regions: the inner boundary membrane (IBM) and the cristae membrane (CM) separated by narrow tubular cristae junctions (Vogel *et al.*, 2006). The cristae are specialized invaginations of the MIM created to maximize surface area for the housing of a concentrated population of electron transport chain (ETC) complexes to optimize oxidative phosphorylation (OXPHOS). The IBM acts primarily to maintain the electrical potential between the matrix and IMS while maintaining close proximity with the MOM to allow efficient bidirectional transport of proteins and solutes between the cell and all mitochondrial compartments (Reichert and Neupert, 2002).

Besides their role in energy production mitochondria carry out several additional important functions including: Fe-S cluster metabolism (Lill, 2009), calcium regulation (Drago *et al.*, 2011), β-oxidation of fatty acids (Bartlett and Eaton, 2004), lipid trafficking and signaling (Osman *et al.*, 2011; Toulmay and Prinz, 2011), steroid synthesis (Midzak *et al.*, 2011) and apoptotic regulation (Wang and Youle, 2009). Adenosine triphosphate (ATP) synthesis in mitochondria is the result of oxidation of electron carriers and the reduction of molecular oxygen (Saraste, 1999). The ETC is composed of four large membrane bound redox complexes (Complexes I, II, III and IV) as well as the small electron carriers ubiquinone and cytochrome *c*. (Lenaz and Genova, 2009). Electrons from glycolysis, β-oxidation and the Krebs cycle are carried by $NADH + H^+$ and $FADH_2$ to Complex I (NADH dehydrogenase) and Complex II (Succinate dehydrogenase),

respectively. These electrons are then passed via ubiquinone (coenzyme Q), Complex III (cytochrome *c* reductase), cytochrome c and Complex IV (cytochrome *c* oxidase) to finally reduce oxygen. As electrons pass through Complexes I, III and IV protons are pumped from the matrix to the IMS creating a proton gradient that is harnessed by Complex V (ATP synthase) to phosphorylate ADP.

Mitochondria possess their own remnant genome left over from their endosymbiotic origins (Gray *et al.*, 1999). Mitochondrial genomes vary in size ranging from 6 Kb in *Plasmodium falciparum* (Feagin, 2000) to 11.3Mb in the angiosperm *Silene conica* (Sloan *et al.*, 2012). The mitochondrial genome of *N. crassa* is a circular 64.8 Kb molecule and contains 26 ORFs, 2 rRNAs and 27 tRNAs (Borkovich *et al.*, 2004). The capacity of mitochondrial genomes ranges between 3 (*Plasmodium falciparum*) and 100 (*Andalucia godoyi*) protein coding genes (Lang *et al.*, 1997; Feagin, 2000; Burger *et al.*, 2013). Thus, the vast majority of the approximately 1000 mitochondrial proteins is coded in the nuclear genome, translated on cytoplasmic ribosomes and localized to the mitochondria for import and assembly (Neupert and Herrmann, 2007; Kutik *et al.*, 2009; Schmidt *et al.*, 2010) . Therefore, proper communication between the mitochondria and the nucleus is essential for the maintenance of all mitochondrial processes. Continued mitochondrial function is ensured by constant maintenance regulated by retrograde communication from the organelle to the nucleus (Collins *et al.*, 2012; Jazwinski, 2013).

Mitochondria are constantly under threat by the damaging effects of oxidative stress from Reactive Oxygen Species (ROS) produced as a result of imperfect ETC function. The primary ROS created is superoxide ($O_2^{\cdot-}$) but it is quickly converted by superoxide dismutase into the more benign hydrogen peroxide (H_2O_2). Hydrogen peroxide is believed to be the key ROS signaling molecule from the mitochondria to the

nucleus regulating protein expression and/or the induction of mitophagy or apoptotic pathways (Jazwinski, 2013).

Mitochondria Derived Vesicles (MDVs) have been shown to exist in some mammalian tissue culture cell lines. These small structures act as selective cargo rafts transporting mitochondrial wastes to lysosomes and peroxisomes for degradation or further metabolic processing (Neuspiel *et al.*, 2008; Andrade-Navarro *et al.*, 2009; Soubannier *et al.*, 2012). MDVs, characterized by the presence of the MOM protein Tom20, transport proteins damaged via oxidative stresses to lysosomes where they are catabolized. MDVs destined for the functionally related peroxisome aid regulation of mitochondrial morphology and fission through the sequestration of their characteristic MAPL (mitochondrial-anchored protein ligase) protein (Neuspiel *et al.*, 2008; Braschi *et al.*, 2009). Thus far, discovery of MDVs has been restricted to animals. Some Gram-negative bacteria utilize similar outer-membrane vesicles (OMVs) for a variety of extracellular functions (Kulp and Kuehn, 2010). Considering the endosymbiotic origins of mitochondria, it would be intriguing to determine if MDV capabilities have been conserved from an endosymbiont, or are a novel convergent function.

Mitochondria are also known to be physically coupled with specific patches of the endoplasmic reticulum (ER) called the mitochondrial associated membranes (MAM). This proximate interaction allows for the transfer of lipids and calcium required for homeostasis (Hayashi *et al.*, 2009; Grimm, 2012; Michel and Kornmann, 2012).

1.2 Mitochondria, Ageing and Disease

Mitochondrial dysfunction has long been associated with the etiology of many diseases and the process of ageing (Koopman *et al.*, 2012; Nunnari and Suomalainen, 2012; Breuer *et al.*, 2013). Amyotrophic Lateral Sclerosis (ALS), Alzheimers, Charcot-

Marie-Tooth Disease, Huntingtons, Hereditary Spastic Paraparesis (HSP), Optic Atrophy, Parkinsons and Spinocerebellar Ataxia are a sampling of the many neuro-degenerative pathologies with known specific mitochondrial dysfunctions associated with their onset (Filosto *et al.*, 2011; Schon and Przedborski, 2011; Nunnari and Suomalainen, 2012; Ylikallio and Suomalainen, 2012). However, whether mitochondrial dysfunction is the cause or merely a consequence of neurodegeneration is still being debated in many cases. Certain cell lineages in the brain affected by various mutant or damaged proteins suggests that the high energetic and metabolic demands of neurons causes an increased susceptibility to mitochondrial phenotypes that leave other tissues unharmed. Children and young adults can still fall victim to various genetic myopathies and encephalopathies that unquestionably can be attributed to bioenergetic OXPHOS defects, or a general lack of mitochondrial "housekeeping" (Ylikallio and Suomalainen, 2012).

The process of ageing is a phenomenon that is conserved among nearly all organisms. While we do not yet completely understand the mechanisms of senescence it is believed that it is a multifactorial process that involves the progressive deterioration of various cellular components. Two prominent ageing theories: the "free-radical" and "mitochondrial" models, speculate that ageing is related to the progressive decline in mitochondrial function due to accumulation of oxidative damage (Harman, 1956, 1972; Miquel *et al.*, 1980; Bratic and Trifunovic, 2010; Cui *et al.*, 2012). Continuing ROS related mitochondrial dysfunction is thought to result in even greater ROS production via a sustained progressive cycle of mitochondrial impairment. In mammals it is known that increasing age correlates with more mitochondrial DNA (mtDNA) mutations and ETC dysfunction (Piko *et al.*, 1988; Del Bo *et al.*, 2002; Theves *et al.*, 2006). The obvious connection between mitochondrial energy balance and ageing indicates that mitochondria play an integral role in senescence. On the other hand, mitochondria have further been

implicated in pathways related to increased longevity (Bratic and Trifunovic, 2010; Cui *et al.*, 2012).

1.3 Mitochondrial Evolution

Symbiogenesis, the concept that large complex cells evolved from a symbiotic relationship between simpler cells was first postulated by Konstantin Mereschkowski in his Russian works: Translated *[The nature and origins of chromatophores in the plant kingdom]* (1905) and *[The theory of two plasms as the basis of symbiogenesis, a new study on the origins of organisms]* (1910). Other works by numerous individuals in the late 19th century and subsequent publications in the first half of the 20th century suggested plastids as symbiotic entities in plant cells (Hackstein *et al.*, 2006). This early insight was shunned by the scientific community until Lynn Sagan née Margulis revived endosymbiotic theory when she published *On the origin of mitosing cells* in 1967 (Sagan, 1967).

It is now unequivocally accepted that mitochondria are monophyletic, deriving from a single endosymbiosis involving an ancient α-proteobacterial ancestor (Yang *et al.*, 1985; Gray *et al.*, 1999; Gray *et al.*, 2004; Cavalier-Smith, 2006). Molecular evidence was first presented with comparisons of the 16S rRNA subunits of wheat mitochondria, *E. coli* and the archaebactreium *H. volcanii* providing compelling support for a eubactrial origin of mitochondria (Spencer *et al.*, 1984). Reconstruction of mitochondrial phylogeny within the α-proteobacteria using modern bioinformatic approaches has shown that the Rickettsiales are the closest extant order to mitochondria (Fitzpatrick *et al.*, 2006). However this makes no suggestion that mitochondria evolved from a Rickettsia species as proto-mitochondria are estimated to have arisen ~ 1.5 Gya (billion) years prior to the origin of the Rickettsiales (Davidov and Jurkevitch, 2009). Since the endosymbiosis,

mitochondria have undergone a massive genome reduction resulting in the outright loss of, or transfer of, many genes to the host nuclear genome. This is highlighted by comparison of the gene content of the largest known mitochondrial genome with 100 genes (Burger *et al.*, 2013), while present day α-proteobacterial genomes code between 834 (*Rickettsia prowazekii*) – 6700 + (*Mesorhizhobuim loti)* potential protein coding genes (Feagin, 2000; Kaneko *et al.*, 2000; Andersson *et al.*, 2003; Khachane *et al.*, 2007).

Mitochondrial genomes only code for a small fraction of the mitochondrial proteome. The majority of mitochondrial proteins is coded in the nucleus. Surprisingly very few mitochondrial proteins (~10%) can be traced unequivocally to an α-proteobacterial origin, over half of the mitochondrial proteome shows no homology to any bacterial orthologs (Karlberg *et al.*, 2000; Kurland and Andersson, 2000). Therefore, in addition to reducing their original genome, modern mitochondria have utilized many nuclear genes for novel functions. Proteins of α-proteobacterial origin have also been discovered in peroxisomes, the ER and other non-endosymbiotic organelles (Esser *et al.*, 2004; Gabaldon *et al.*, 2006). This suggests that the nucleus has acquired, recycled and targeted α-proteobacterial genes for non-mitochondrial purposes.

While the ancestry of mitochondria is relatively clear, the nature of the host that acquired the proto-mitochondrion is far less obvious and a topic of considerable debate (Embley and Martin, 2006; Martin, 2011; Vesteg and Krajcovic, 2011). Eukaryotes possess chimeric, polyphyletic genomes derived from an archaeal ancestor but also contain eubacterial genes that arose by lateral gene transfers (Ribeiro and Golding, 1998; Rivera and Lake, 2004). Explanations of the origin of eukaryotes propose that the three domains; archaea, bacteria and eukarya, are monophyletic with eukaryota and archaea sharing a common ancestor (Woese *et al.*, 1990), or that eukaryota are descendant from

an anastomosic branch (eocytes) of paraphyletic archaea (Lake *et al.*, 1984). Mounting evidence supports the latter scenario (Cox *et al.*, 2008; Foster *et al.*, 2009).

All eukaryotes possess mitochondria or one of the the mitochondria derived organelles; mitosomes or hydrogenosomes. Mitosomes do not produce ATP, but still possess a double membrane and the machinery for Fe-S cluster synthesis (Tovar *et al.*, 1999; Hackstein *et al.*, 2006). Nearly all hydrogenosomes lack a genome but maintain a double membrane, Fe-S cluster synthesis and ATP/H_2 production via anaerobic pathways (Muller, 1993; Andersson and Kurland, 1999; Embley *et al.*, 2003; Sutak *et al.*, 2004; Lill and Muhlenhoff, 2005; Hackstein *et al.*, 2006). Notably, the ciliate *N. ovalis* possesses a hydrogenosomal genome clearly derived from a *bona fide* mitochondrion, providing an intermediate evolutionary link between the organelles (Boxma *et al.*, 2005). Mitochondria, mitosomes and hydrogenosomes have some related proteins and similar import pathway machineries. Various studies have shown shared characteristics and compatibility between the protein import systems of the three organelles (Dyall *et al.*, 2000; Plumper *et al.*, 2000; Embley *et al.*, 2003; van der Giezen *et al.*, 2003; Dacks *et al.*, 2006; Rada *et al.*, 2011)

There have been several hypotheses proposed for eukaryogenesis (Martin *et al.*, 2001; Embley and Martin, 2006) , but all can be allocated to fall within four broader models:

[1] Fusion. Suggests an initial fusion between an archaeal and bacterial cell to create a hybrid proto-eukaryote with an additional subsequent endosymbiosis of the mitochondrial ancestor.

[2] Dual endosymbiosis. A host of unknown origin engulfs both an archaeal and bacterial cell to become the nucleus and mitochondria respectively (Lake and Rivera, 1994; Horiike *et al.*, 2001).

Both models [1] and [2] make a case for an amalgamation involving three separate organisms. However the notion that the nucleus is an endosymbiont as proposed in model 2 has been strongly rejected (Poole and Penny, 2001) and genetic evidence for three-way input is lacking (Martin *et al.*, 2001; Esser *et al.*, 2004)

[3] Phagotrophic. The phagotrophic hypothesis suggests that the host organism was some intermediate mitochondria lacking, proto-eukaryote (archaezoon) with a developed endomembrane system and phagocytic abilities. The host is thus assumed to have phagocytosed a free living α-proteobacteria. The model then assumes this prey to have avoided digestion and somehow escaped endomembrane envelopment and continued to survive in a mutualistic manner within the hosts cytoplasm (Sagan, 1967; Margulis, 1993). Support for the phagotrophy model was bolstered by the apparent discovery of amitochondriate eukaryotes purportedly harking back to a lineage of pre-mitochondrial proto-eukaryotes. Eventually support of this theory waned when it was shown that these unicellular anaerobes originally thought to lack mitochondria, actually contained mitosomes or hydrogenosomes. Both of these are mitochondrial derived organelles that evolved independently in a convergent manner in several diverse lineages (Lindmark and Muller, 1973; Tovar *et al.*, 1999; Embley *et al.*, 2003; van der Giezen, 2009). These recent observations weakened the concept of a pre-existing proto-eukaryote, and spawned several syntrophic hypotheses (Zillig *et al.*, 1989; Martin and Muller, 1998; Moreira and Lopez-Garcia, 1998; Lopez-Garcia and Moreira, 1999).

[4] Syntrophy. The hydrogen hypothesis (Martin and Muller, 1998) has garnered the strongest following among the syntrophic theories. The theory proposes that a methanogenic archaeal host entered into a proximate mutual interaction with a hydrogen producing α-proteobacteria. The host required H_2 and CO_2 which were ambient waste products of the heterotrophic α-proteobacteria. Any inhibitory effects of waste accumulation surrounding the bacterium were conveniently alleviated with the uptake of excess H_2 by the archaea. Eventually the relationship became obligate and the system was optimized via evolutionary steps leading to the complete surrounding and eventual engulfment of the symbiont. It has also been suggested that this step eventually led to the evolution of other characteristic features of eukaryotes, namely; the nucleus, introns, and the endomembrane system (Poole and Penny, 2001; Martin and Koonin, 2006; Poole, 2006; Poole and Penny, 2007b; Davidov and Jurkevitch, 2009).

Occam's razor or the principle of "maximization of parsimony" and the rebuttal against the phagotrophic/archaezoa theory [3] would suggest the syntrophy model as the most feasible theory for mitochondrial endosymbiosis and eukaryogenesis, yet there is no consensus among academics and the debate is certain to continue (Cavalier-Smith, 2006; Martin and Koonin, 2006; Poole, 2006; de Duve, 2007; Poole and Penny, 2007a; Poole and Penny, 2007b; Cavalier-Smith, 2009; O'Malley, 2010; Forterre, 2011; Martin, 2011).

1.4 Mitochondrial Morphology and Dynamics

Modern mitochondria undergo fusion and fission events in a strictly orchestrated fashion resulting in dynamic, branched tubular networks that maneuver along cytoskeletal structures and interact with other organelles (Okamoto and Shaw, 2005; Hoppins *et al.*, 2007a; Michel and Kornmann, 2012). Disruption of mitochondrial

morphology and distribution has been observed in many fungal mutants (Burgess *et al.*, 1994; Sogo and Yaffe, 1994; Berger *et al.*, 1997; Hermann *et al.*, 1997; Dimmer *et al.*, 2002; Boldogh *et al.*, 2003; Youngman *et al.*, 2004; Altmann and Westermann, 2005). The proteins identified are involved in a variety of different processes including: mitochondrial transport (Fzo1, Dnm1 and Mdm33) (Hoppins *et al.*, 2007a), phospholipid synthesis and trafficking (Mdm10, Mdm12, Mdm31, Mdm32, Mdm35, Mmm1, Mmm2, Ups1 and Ups2) (Dimmer *et al.*, 2002; Dimmer *et al.*, 2005; Kornmann *et al.*, 2009; Osman *et al.*, 2009; Tamura *et al.*, 2009; Kuroda *et al.*, 2011), cytoskeletal tethering and mitochondrial genome maintenance (Mdm10, Mdm12, Mmm1 and Mmm2) (Boldogh *et al.*, 2003), mitochondrial inheritance (Gem1) (Frederick *et al.*, 2004), ER and cell membrane associations (Num1, Mdm10, Mdm12, Mdm36, Mmm1 and Mmm2) (Kornmann *et al.*, 2009; Hammermeister *et al.*, 2010) and mitochondrial protein import and assembly (Tom7, Tom70, Tom71, Tob37, Tob55, Mdm10, Mdm12, Mmm1 and Mmm2) (Grad *et al.*, 1999; Meisinger *et al.*, 2004; Meisinger *et al.*, 2007; Kondo-Okamoto *et al.*, 2008; Wideman *et al.*, 2010; Wideman *et al.*, 2013). Clearly some of these proteins have multiple roles, exemplifying the interconnected nature of diverse mitochondrial processes. Four of the above mentioned proteins; Mdm10, Mdm12, Mmm1 and Mmm2 have been shown to form the ERMES (Endoplasmic Reticulum Mitochondria Encounter Structure) complex (Kornmann *et al.*, 2009). ERMES acts primarily as a tether between the ER and MOM and its importance is highlighted by the pleiotropic effects seen in mutants of the individual components.

Mitochondrial shape and movement are strictly controlled as changes in spatial arrangements influence the activity of the organelle (McBride *et al.*, 2006; Hoppins *et al.*, 2007a; McBride and Scorrano, 2013). Mitochondria cannot be synthesized *de novo* in the cell, thus all mitochondria are inherently products of constant fusion and fission. These

processes require complex management of both mitochondrial membranes to maintain compartmental composition and integrity of the organelle. Dynamin related protein (DRP) GTPases act as the key components of division and fusion. In *S. cerevisiae,* fusion requires the membrane potential across the inner membrane and the DRP GTPases Fzo1 (mammalian Mfn1/2) of the MOM, and Mgm1 (mammalian Opa1) in the MIM. The MOM localized Ugo1is also required to form a double membrane spanning complex that acts as a trans-organelle tether prior to the GTP dependent fusion of the respective membranes (Hoppins *et al.*, 2007a; Hoppins and Nunnari, 2009). Fission is controlled by another DRP GTPase, Dnm1 (mammalian Drp1). An intricate Dnm1 ring-like complex is recruited to the MOM at ER-contact sites by Fis1 and Mdv1, where GTP-dependent constriction of the ring cleaves the mitochondrial tubule (Lackner and Nunnari, 2009; Friedman *et al.*, 2011). Disruption of the fusion pathway causes mitochondrial hyper-fragmentation, whereas hyper-fusion is created by a fission disruption and leads to enlarged mitochondria. Abolition of both systems leaves the mitochondria with relatively normal appearances (Sesaki and Jensen, 1999; Hoppins *et al.*, 2007a).

In *S. cerevisiae* mitochondria use attachment to actin filaments via the Mdm complex (Mdm10, Mdm12, and Mmm1) to control their movement, morphology and inheritance (Boldogh *et al.*, 2003). *N. crassa, Schizosaccharomyces pombe* and mammalian mitochondria have similar associations with microtubules instead of actin (Heggeness *et al.*, 1978; Yaffe *et al.*, 1996; Fuchs *et al.*, 2002). Mechanistic conservation of function has been shown in a study where *N. crassa* Mmm1 rescued mitochondrial morphology and inheritance in *Δmmm1* yeast strains (Kondo-Okamoto *et al.*, 2003)

1.5 Mitochondrial quality control

Fission and fusion collectively play a role in the maintenance of mitochondrial function and components of these processes have further been implicated in mitophagy. Mammalian studies have shown one mechanism of mitophagy to be regulated by the Parkinsons disease associated proteins PINK1 and Parkin (Jin and Youle, 2012). Mitochondrial dysfunction, marked by depolarization of MIM membrane potential, leads to the accumulation of PINK1 in the MOM rather than its usual degradation, resulting in recruitment of the ubiquitin E3 ligase Parkin to the mitochondria (Lazarou *et al.*, 2012). Parkin then proceeds to ubiquitinylate cytosol exposed components of the fission/fusion machinery (Fis1, Mfn1 and Mfn2) and the TOM complex (Tom20, Tom40 and Tom70) resulting in either total mitophagy, or the rupture and proteosomal degradation of the MOM (Yoshii *et al.*, 2011; Jin and Youle, 2012).

Fungi lack PINK1/Parkin homologues but in *S. cerevisiae* Mdm30 has been shown to ubiquitinylate Fzo1 (mammalian Mfn1/Mfn2) and Mmm2 while *N. crassa* Mus10 (ubiquitin E3 ligase) has been shown to be involved in regulation of mitochondrial maintenance (Escobar-Henriques *et al.*, 2006; Ota *et al.*, 2008; Kato *et al.*, 2010). Additionally, Tom70 and Mdm12 were also identified as ubiquitinylated proteins in yeast (Starita *et al.*, 2012) highlighting the possible conservation of MOM protein ubiquitynlation and degradation/mitophagy between mammals and fungi.

1.6 Mitochondrial Protein Import and Assembly

There are roughly 1000 proteins estimated in the mitochondrial proteome of *N. crassa* (Borkovich *et al.*, 2004; Keeping *et al.*, 2011). With 26 potential protein coding ORFs in the mtDNA, the remainder is encoded in the nuclear genome, translated into precursors by cytosolic ribosomes, targeted to mitochondria and imported and assembled into the correct mitochondrial compartment. Import and assembly are facilitated by the

activity of several protein complexes in the MOM, IMS and MIM (Figure 1.1) (Schmidt *et al.*, 2010; Dukanovic and Rapaport, 2011; Endo *et al.*, 2011; Gebert *et al.*, 2011). The MOM contains two major protein import complexes. The TOM (Translocase of the Outer Membrane) complex functions as the general import pore that initially recognizes most precursors prior to passage through the OM (Dekker *et al.*, 1998; Kunkele *et al.*, 1998; Ahting *et al.*, 1999). The TOB (Topogenesis of Outer membrane β-barrels) complex, also known as the SAM (Sorting and Assembly Machinery) complex, functions to insert several proteins into the MOM including all β-barrels (Kozjak *et al.*, 2003; Paschen *et al.*, 2003; Wiedemann *et al.*, 2003). MIM1/2 is an OM complex that aids the insertion of single and multispan α-helical trans-membrane domain (TMD) proteins directly into the MOM (Becker *et al.*, 2008a; Popov-Celeketic *et al.*, 2008; Becker *et al.*, 2011a; Papic *et al.*, 2011).

The IMS contains the chaperone-like small TIM (Translocase of the Inner Membrane) complexes, Tim8/13 and Tim9/10 that act to transport inbound hydrophobic precursors from the TOM complex to either the TOB or TIM22 complexes (Koehler *et al.*, 1998a; Bauer *et al.*, 2000; Paschen *et al.*, 2000; Hoppins and Nargang, 2004). There is also the mitochondrial disulphide Mia/Erv relay system responsible for importing IMS proteins lacking presequences (Herrmann and Riemer, 2012).

The MIM has three major import complexes; TIM22, TIM23 and OXA. The TIM22 complex assembles multispan carrier proteins into the MIM, while TIM23 translocates precursors with N-terminal presequence targeting signals to the matrix or the MIM. The OXA (Oxidase Assembly) complex integrates ETC components and other multispan proteins from the matrix into the MIM, making it the only “inside-out” protein pathway.

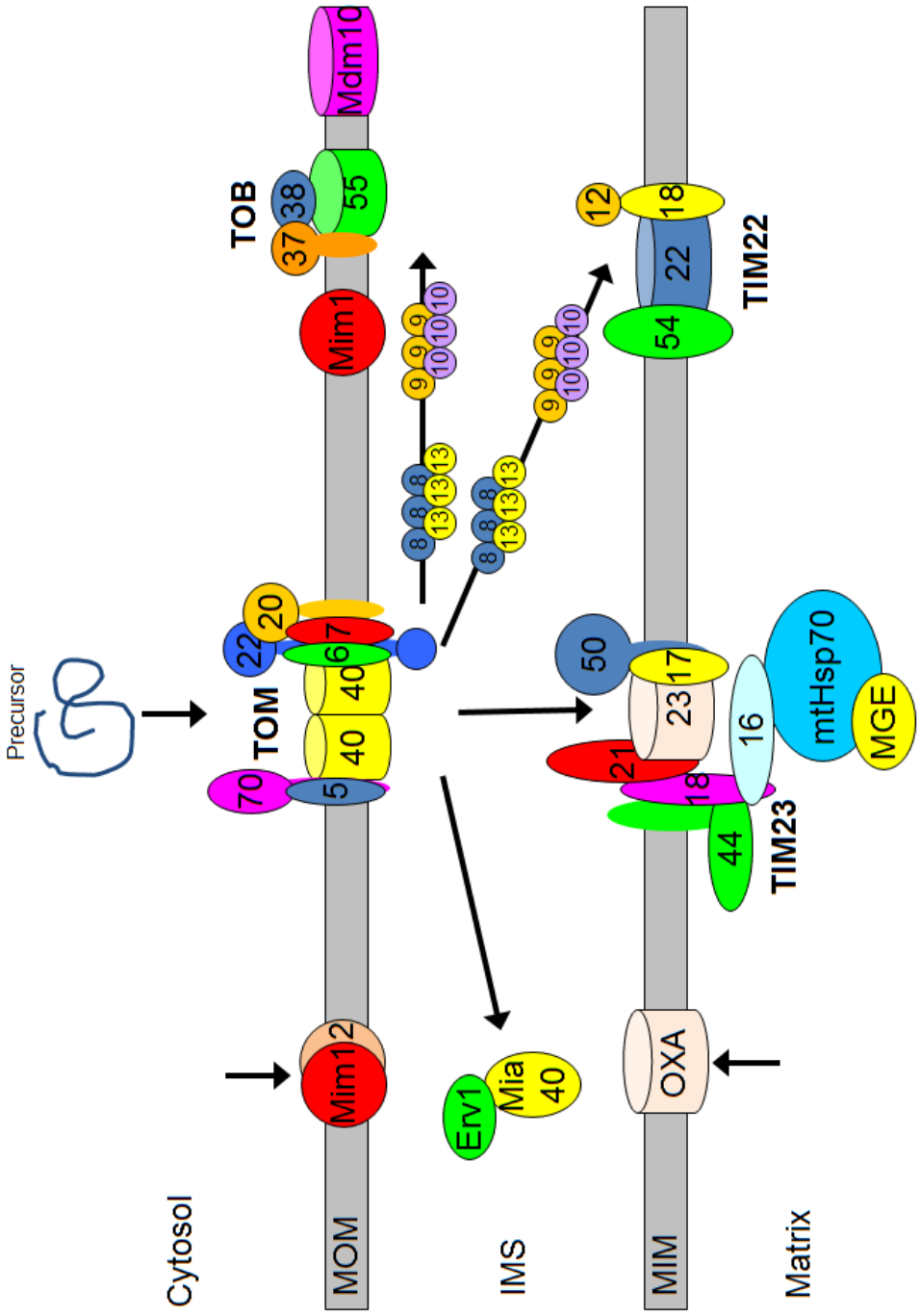

Figure 1.1 General overview of mitochondrial protein import complexes. This schematic shows the complexes and their components. In most cases protein stoichiometry or complex architecture are unknown.

Further details of these complexes will be addressed in their following specific sections.

1.6.1 Targeting signals

Precursor proteins are localized to their final mitochondrial destinations by subcompartment specific amino acid targeting sequences (Davis *et al.*, 1998; Nargang *et al.*, 1998; Brix *et al.*, 1999; Egan *et al.*, 1999; Pfanner, 2000; Wattenberg and Lithgow, 2001; Pfanner and Chacinska, 2002; Rapaport, 2003; Rehling *et al.*, 2003; Waizenegger *et al.*, 2003; Chacinska *et al.*, 2009). Matrix destined proteins have a cleavable amphipathic α-helical presequence peptide. After passing through the MIM, the Matrix Processing Peptidase (MPP) removes this signal sequence allowing the proteins to mature into their native tertiary structures (Mossmann *et al.*, 2012). The targeting signals for other compartments differ in that they are not cleavable sequences but instead are specific combinations/alignments of integral residues of the mature proteins. MIM proteins possess α-helical TMDs that contain the internal signal sequence responsible for their insertion into the membrane. IMS proteins are recognized by a specific Mitochondrial Intermembrane Space Signal (MISS) consisting of conserved cysteine and hydrophobic residues (Chacinska *et al.*, 2009).

There are two classes of MOM proteins with unique targeting signals. β-barrels are cylindrical proteins consisting of a wrapped sheet of anti-parallel β-strands. The exterior face of the barrel is hydrophobic while the lumen is hydrophilic. β-barrels have a defined C-terminal β-signal required for their recognition and incorporation into the MOM. How β-barrels are recognized initially by the TOM complex remains unknown. MOM proteins with either N- or C-terminal α-helical TMDs are localized by signals

within these TMD regions. In some instances positive residues flanking the TMDs are required.

1.6.2 The TOM complex

Nearly all nuclear encoded mitochondrial proteins must pass through the MOM via the pore forming TOM complex. The complex consists of Tom40; the receptors Tom20, Tom22 and Tom70; and the accessory small Toms, Tom5, Tom6 and Tom7 (Becker *et al.*, 2008b; Chacinska *et al.*, 2009; Dukanovic and Rapaport, 2011).

1.6.2.1 Tom40

Tom40 was shown in *S. cerevisiae* and *N. crassa* to be the essential, central pore forming β-barrel of the complex (Vestweber *et al.*, 1989; Kiebler *et al.*, 1990; Hill *et al.*, 1998; Ahting *et al.*, 2001; Taylor *et al.*, 2003). The topology of the protein has yet to be accurately defined. Computer predictions and circular dichroism spectroscopy on *S. cerevisiae* and *N. crassa* Tom40 have estimated the β-sheet content to be between 30-46% of the protein (Hill *et al.*, 1998; Ahting *et al.*, 2001; Becker *et al.*, 2005). Comparative studies have shown a relationship between Tom40 and another MOM β-barrel protein, porin or VDAC (Zeth, 2010; Gessmann *et al.*, 2011). The crystal structure of porin has been determined and the protein was found to contain 19 β-strands (Bayrhuber *et al.*, 2008; Ujwal *et al.*, 2008; Hiller *et al.*, 2010). A similar structure has been suggested for Tom40 based on alignments with porin and preliminary biochemical evidence (Qiu *et al.*, 2013). However, it should be noted that there is some debate about the porin crystal structure. Discrepancies between biochemical data and the crystal structure models suggest the porin crystal structures may not represent the native conformation (Colombini, 2009)(see Chapter 3).

1.6.2.2 TOM complex receptor proteins

Studies in *S. cerevisiae* have shown that up to 65% of nuclear encoded mitochondrial proteins have mRNAs that localize to the organelle with the protein being imported in a co-translational manner (Fujiki and Verner, 1993; Ahmed *et al.*, 2006; Saint-Georges *et al.*, 2008; Garcia *et al.*, 2010; Weis *et al.*, 2013). The remaining precursors are transported to the mitochondria in a protected, loosely folded (or unfolded) state by cytosolic chaperones such as Hsp70 and MSF (Mitochondrial import Stimulating Factor) (Komiya *et al.*, 1997; Beddoe and Lithgow, 2002). Precursors are then recognized by one or more of the three TOM receptors, which possess large cytosolic domains to accommodate the interactions (Hines *et al.*, 1990; Harkness *et al.*, 1994b; Mayer *et al.*, 1995a; Endo and Kohda, 2002).

Tom70 has an N-terminal TMD anchor and a large C-terminal cytosolic domain with seven TPR (Tetratrico Peptide Repeat) motifs that also function as a dimerization domain (Hase *et al.*, 1984; Hines *et al.*, 1990; Millar and Shore, 1993). Tom70 specifically recognizes and binds MIM proteins with internal targeting signals and multiple TMDs such as the carrier proteins (e.g. ADP/ATP carrier, AAC) precursors. (Komiya *et al.*, 1997; van Wilpe *et al.*, 1999). These precursors are highly hydrophobic and require chaperones to escort them during their transfer to the TOM receptors. Tom70 has been shown to interact with the chaperone Hsp70, MSF (mitochondrial import-stimulating factor), and the cargo AAC precursor. MSF is released via ATP hydrolysis and the precursor is then transferred to the Tom20-Tom22 receptor (see below) where it is guided to the Tom40 pore for translocation. Mutants lacking Tom70 in *N. crassa* and *S. cerevisiae* are still capable of importing AAC albeit at a slower rate via Tom20-Tom22 (Steger *et al.*, 1990; Hachiya *et al.*, 1995; Komiya *et al.*, 1997). Additionally, these mutants exhibit morphological defects, however a growth defect is only seen in *N. crassa* (Schlossmann *et al.*, 1996; Grad *et al.*, 1999).

Tom20 contains an N-terminal α-helical TMD anchor, the C-terminal domain is exposed to the cytosol and contains a TPR motif required for precursor interactions (Harkness *et al.*, 1994b; Blatch and Lassle, 1999). Tom22 also acts as a receptor but differs structurally from the other two receptors by having a centralized TMD resulting in both cytosolic and IMS precursor binding domains (Lithgow *et al.*, 1994; Nargang *et al.*, 1995; van Wilpe *et al.*, 1999). Research on the substrate specificity of Tom20 and Tom22 has revealed complex interactions between the two receptors themselves, and incoming presequences (Sollner *et al.*, 1989; Kiebler *et al.*, 1993; Moczko *et al.*, 1993; Harkness *et al.*, 1994b; Moczko *et al.*, 1994; Haucke *et al.*, 1995; Mayer *et al.*, 1995a; Terada *et al.*, 1997; Yano *et al.*, 2000).

Precursor proteins containing amphipathic, positively charged presequence signals are recognized and bound by a dual Tom20-Tom22 receptor (Saitoh *et al.*, 2007; Yamano *et al.*, 2008b; Komuro *et al.*, 2013) the cytosolic domain of which forms the so-called “cis”-binding site (Dietmeier *et al.*, 1997; Rapaport *et al.*, 1997)(see section 1.6.2.5). Structural studies have shown that the cytosolic domain of Tom20 forms multiple α-helices resulting in a grooved superstructure capable of binding a variety of amphipathic presequences via hydrophobic interactions. A motif preceding the binding site has been identified as the WHxBHH (W=hydrophilic, H=Hydrophobic, B=Basic) motif structure. Tom22 contributes an acidic receptor domain that can bind basic residues contained within the signal presequence helix (Abe *et al.*, 2000; Muto *et al.*, 2001; Endo and Kohda, 2002; Obita *et al.*, 2003; Yamano *et al.*, 2008b; Komuro *et al.*, 2013).

Tom20 and Tom22 are both essential in *N. crassa* (Harkness *et al.*, 1994a; Nargang *et al.*, 1995), while in *S. cerevisiae* mutants lacking either are viable but have severely impaired growth characteristics (Ramage *et al.*, 1993; Moczko *et al.*, 1994; van Wilpe *et al.*, 1999). All three receptors are required for efficient precursor recognition.

However, while Tom70 appears to act to increase the efficiency of importing specific classes of protein, either Tom20 or Tom22 (or both in *N.crassa*) must be present for transfer of all precursors to the TOM pore in addition to roles in precursor recognition. All three receptors and Tom40 have further been shown to fulfill a chaperone-like role in maintaining unfolded precursors as they transition through the pore (Esaki *et al.*, 2003; Yamamoto *et al.*, 2009; Yamamoto *et al.*, 2011).

S. cerevisiae has an additional MOM receptor Tom71 which has lower expression than other TOM components but shares 53% identity and the seven TPR motifs with its homologue Tom70 (Bomer *et al.*, 1996; Schlossmann *et al.*, 1996). Tom70/71 has also been shown to play a role in the recruitment of soluble mitochondrial morphology proteins to the cytosolic face of the MOM indicating a broader role for what was thought to be exclusively a precursor receptor (Kondo-Okamoto *et al.*, 2008). In *N. crassa* Tom70 is believed to fulfill the roles that the orthologues Tom70/Tom71 perform in yeast (Schlossmann and Neupert, 1995; Grad *et al.*, 1999)

Mitochondrial protein import can be stimulated or inhibited via the regulatory phosphorylation of the import receptors Tom20, Tom22 and Tom70 (and Mim1) by the cytosolic kinases CK2 and PKA (Schmidt *et al.*, 2011). CK2 promotes TOM complex biogenesis via phosphorylation of Tom22 and Mim1 whereas phosphorylation of Tom70 by PKA inhibits its receptor activity and thus impairs the import of MIM carriers.

1.6.2.3 The small Toms

The small Toms; Tom5, Tom6 and Tom7, are anchored to the MOM by α-helical TMDs and are involved in TOM complex assembly, stability, and formation of precursor interaction sites (Dekker *et al.*, 1998; Ahting *et al.*, 1999; Model *et al.*, 2001; Sherman *et al.*, 2005). *S. cerevisiae* mutants lacking Tom5 had reduced growth rates and were

deficient for import of all tested precursors suggesting a major role in protein import for this protein (Dietmeier *et al.*, 1997). Interestingly, the negatively charged N-terminal cytosolic domain appears not to have an essential role in precursor binding as the TMD containing C-terminal constructs integrate into the complex and rescue the *Δtom5* phenotype (Horie *et al.*, 2003). This implies that the Tom5 TMD acts as the functional structural domain for complex stability and that the cytosolic domain plays no integral role in TOM activity. Despite the apparent importance of Tom5 in *S. cerevisiae*, *N. crassa* shows no import or growth defects in the absence of Tom5. Surprisingly, *N. crassa* Tom5 can alleviate the temperature-sensitive growth phenotype observed in yeast *Δtom5* suggesting correct TOM receptor function is reliant upon Tom5 presence in yeast and not *N. crassa* (Schmitt *et al*., 2005).

Mutants lacking Tom6 in *S. cerevisiae* show import deficiencies for matrix and MIM destined precursors, while in *N. crassa* the only import phenotype was a slight reduction in $F_1\beta$ import (Alconada *et al.*, 1995; Sherman *et al.*, 2005). Tom6 from *S. cerevisiae* and *N. crassa* respectively can only correctly assemble in the organism of their origin, suggesting a divergence in the Tom6 import/assembly mechanisms (Dembowski *et al.*, 2001).

Tom7 deficient mutants in *N. crassa* were defective in importing the MOM β-barrel porin and the matrix targeted $F_1\beta$. Import of the MIM targeted AAC protein was unaffected (Sherman *et al.*, 2005). A similar porin import phenotype was seen in *S. cerevisiae* lacking Tom7 (Meisinger *et al.*, 2006). Both organisms show an increase in Tom40 import in the absence of Tom7 (Honlinger *et al.*, 1996; Sherman *et al.*, 2005; Meisinger *et al.*, 2006). Interestingly, *Δtom7 S. cerevisiae* mutants were found to have an enlarged mitochondrial morphology (Meisinger *et al.*, 2006). Deletion of Tom5 or Tom6 did not affect mitochondrial morphology.

In *S. cerevisiae, Δtom5* is synthetically lethal when combined with lack of Tom6, Tom7, Tom20, Tom70 or Tob37 (Honlinger *et al.*, 1996; Dietmeier *et al.*, 1997). In *N. crassa* the *tom5/tom6* double knockout (KO) showed no growth defects but had a reduction in $F_1\beta$ import that was slightly worse than the Tom6 single mutant. The *tom5/tom7* double KO also showed no growth defects and had import phenotypes similar to the single Tom7 KO mutants where porin and $F_1\beta$ import were reduced. The *tom6/tom7* double KO had severe growth reduction that prevented adequate culturing for further import analysis. Attempts to construct a triple KO in *N. crassa* failed suggesting synthetic lethality (Sherman *et al.*, 2005). Knockdown of any of the small Toms in human tissue culture showed no effect on precursor import. However, depletion of any two-fold combination of the proteins resulted in TOM complex instability and matrix destined protein import defects (Kato and Mihara, 2008).

1.6.2.4 Structure of the TOM complex

All the components of the TOM complex are conserved among opisthokonts (fungi and animals) suggesting their common unikont ancestor also possessed a complete TOM complex (Likic *et al.*, 2005; Chan *et al.*, 2006). Despite what is known about the components and the function of the complex, the stoichiometry and organization of the complex is less well understood. Early experiments revealed very loose associations between the receptors Tom20 and Tom70 and the remainder of the complex. For example, Tom70 was barely detected in coimmunoprecipitation experiments using TOM component antibodies whereas Tom20 failed to remain in the complex under the standard conditions used for blue-native gel electrophoresis (BNGE) (Dekker *et al.*, 1998). However, the association appeared to be dependent on the concentration of detergent used to solubilize the mitochondrial membrane since Tom20 was retained in the complex in BNGE experiments using 0.1% digitonin instead of 1% (Meisinger *et al.*, 2001).

Tom40, Tom22 and the small Toms form a stable complex of ~400kDa under normal BNGE conditions (Kiebler *et al.*, 1993; Alconada *et al.*, 1995; Nakai and Endo, 1995; Dekker *et al.*, 1996; Honlinger *et al.*, 1996; Dietmeier *et al.*, 1997; Kunkele *et al.*, 1998). Tom40 and Tom22 form the very stable functional core unit (Meisinger *et al.*, 2001). A novel site-specific photo cross-linking experiment showed that the TMD of a single Tom22 interacts with two Tom40 β-barrels (Shiota *et al.*, 2011). This agrees with a TOM model based on cryo-electron microscopy (EM) data that showed nitriloacetic acid-gold labeled Tom22 located between adjacent Tom40 pores in the complex (Model *et al.*, 2008).

The β-barrel structure of Tom40 forms the hydrophilic pore through which precursors pass (Vestweber *et al.*, 1989; Hill *et al.*, 1998; Kunkele *et al.*, 1998; Ahting *et al.*, 2001; Taylor *et al.*, 2003). A variety of methods has shown the diameter of the pore is ~20-22 Å (Vestweber and Schatz, 1989; Hill *et al.*, 1998; Kunkele *et al.*, 1998; Ahting *et al.*, 1999; Model *et al.*, 2002). In *N. crassa* and *S. cerevisiae* the TOM complex has been shown as a triple-pore structure (i.e. three Tom40 β-barrels) using EM and cryo-EM of tagged and purified complex reconstituted into liposomes or applied to carbon-coated copper EM grids (Kunkele *et al.*, 1998; Model *et al.*, 2002; Model *et al.*, 2008). However, when purified from *S. cerevisiae* mitochondria lacking Tom20 and Tom70 a 400 kDa twin-pore TOM complex was observed (Meisinger *et al.*, 2001; Model *et al.*, 2002; Model *et al.*, 2008). The current model (Model *et al.*, 2008) suggests that the observed triple-pore complex represents the native wildtype TOM structure. Loss of Tom20 results in the complex shedding a Tom40 molecule and assuming an apparently basal twin-pore configuration (Model *et al.*, 2008).

The small Toms have long been implicated in TOM assembly and stability though differences in phenotypic effects in knockouts in different organisms suggests

some divergence of function. Lack of the individual small Toms in *N. crassa* results in minor destabilization of the complex (Schmitt *et al.*, 2005; Sherman *et al.*, 2005). In human tissue culture depletion of Tom7 but not of Tom5 or Tom6 resulted in severe TOM instability as did depletion of any dual combination of the three (Kato and Mihara, 2008). In yeast, significant TOM instability is observed in strains lacking Tom5 and more so Tom6 (Alconada *et al.*, 1995; Model *et al.*, 2001; Schmitt *et al.*, 2005). Yeast Tom7 deletion actually stabilizes the interactions between Tom40, Tom20 and Tom22 suggesting an opposite role to Tom6 (Honlinger *et al.*, 1996; Yamano *et al.*, 2010b). Loss of both Tom6 and Tom7 in yeast results in a TOM complex that is marginally more stable than in the Tom6 single knockout (Dekker *et al.*, 1998). In *N. crassa* loss of Tom6 and Tom7 together results in major TOM destabilization and reduced Tom5, Tom20 and Tom22 levels. In *S. cerevisiae*, absence of Tom22 results in the three small Toms forming a stable ~100kDa complex with Tom40 (Dekker *et al.*, 1998). Structurally, *N. crassa* Tom6 and Tom7 physically interact with Tom40 while in yeast this has only been shown for Tom6 which is required for Tom22 incorporation into a stable complex (Dekker *et al.*, 1998; Rapaport *et al.*, 1998; Dembowski *et al.*, 2001). Tom7 has further been shown to associate with Mdm10 of the ERMES/TOB complexes acting as a regulatory subunit of β-barrel import by sequestering Mdm10 and thus controlling the distribution equilibrium between; Mdm10-TOB↔Mdm10-Tom7↔Mdm10-ERMES (Meisinger *et al.*, 2004; Wideman *et al.*, 2010; Yamano *et al.*, 2010b)(discussed in section 1.6.3).

1.6.2.5 The TOM complex: Precursor recognition and translocation

Some mitochondria-destined precursors are escorted by cytosolic HSP chaperones that dock with the TPR domain of Tom70 where the precursor is offloaded forming a Tom70-precursor multimer (see section 1.6.2.2)(Young *et al.*, 2003; Fan *et al.*,

2006; Becker *et al.*, 2009). The precursor is then delivered to the TOM cis-receptor site located on the cytosolic face of the complex. The cytosolic domains of Tom20, Tom22 and perhaps Tom5 and Tom40 contribute to the architecture of this site (Dietmeier *et al.*, 1997; Rapaport *et al.*, 1997). The precursor will pass from the cis-site, through the pore and associate with the trans-site on the IMS face of the complex (Mayer *et al.*, 1995b). The IMS domains of Tom22, Tom7 and Tom40 all contribute to the formation of the trans-site (Honlinger *et al.*, 1996; Rapaport *et al.*, 1997; Stan *et al.*, 2000; Esaki *et al.*, 2003; Gabriel *et al.*, 2003).

The acid chain hypothesis suggests that the translocation of the presequence containing precursors through the TOM involves the sequential binding of the basic/amphiphillic presequence to acidic receptor sites of increasing affinity forming an acidic track through the pore (Bolliger *et al.*, 1995; Moczko *et al.*, 1997; Komiya *et al.*, 1998). However the requirement for these acidic residues has been called into question and some reports have shown them to not be essential for precursor import (Nakai *et al.*, 1995; Court *et al.*, 1996; Nargang *et al.*, 1998). Despite the conflicting results regarding the acid chain hypothesis the overlying concept of a sequential unidirectional outside-in migration from Tom20→Tom22→Tom22(IMS)→Tim23 through the pore is well supported (Komiya *et al.*, 1998).

1.6.3 The TOB complex

The 140 kDa TOB_{core} complex consists of three proteins: the β-barrel protein Tob55, the integral MOM protein Tob37; and the peripherally associated MOM protein Tob38 (Kozjak *et al.*, 2003; Paschen *et al.*, 2003; Wiedemann *et al.*, 2003; Ishikawa *et al.*, 2004; Meisinger *et al.*, 2004; Waizenegger *et al.*, 2004; Habib *et al.*, 2005; Lackey *et al.*, 2011; Klein *et al.*, 2012). An alternate nomenclature for the complex and its

components is used in *S. cerevisiae.* The TOB complex was named the SAM (Sorting and Assembly Machinery) and the components include Sam50 (Tob55), Sam37 (Tob37) and Sam35 (Tob38). In mammalian species a homologous complex is present but Tob37 and Tob38 only show weak similarity to their respective mammalian counterparts, Metaxin1 and Metaxin2. Mammalian Sam50 on the other hand shares greater conservation with fungal Sam50/Tob55 (Humphries *et al.*, 2005; Kozjak-Pavlovic *et al.*, 2007). Metaxin1 was the first mammalian component identified in mice and was found between the thrombospondin3 and glucocerebrosidase genes, and drew its name "metaxin" from the greek translation of "in between"(Bornstein *et al.*, 1995). Evidence from import analysis suggests that Mammalian Sam50 and the metaxins function similarly to fungal TOB/SAM complexes (Armstrong *et al.*, 1997; Armstrong *et al.*, 1999; Kozjak-Pavlovic *et al.*, 2007; Xie *et al.*, 2007).

The TOB_{core} complex can also associate with the MOM β-barrel Mdm10 to form the TOB_{holo} complex (Meisinger *et al.*, 2004; Wideman *et al.*, 2010; Lackey *et al.*, 2011; Klein *et al.*, 2012). An association of the TOB_{core} complex with Mim1 has also been reported (Becker *et al.*, 2008a). The stoichiometry of the TOB complex in *N. crassa* is 1:1:1 (Tob55: Tob38: Tob37, for the core complex) and 1:1:1:1 (Tob55: Tob38: Tob37: Mdm10) for the complex containing Mdm10 (Klein *et al.*, 2012). The TOB complex functions to insert/assemble all MOM β-barrels precursors and some integral MOM proteins with C-terminal α-helical TMDs such as Tom5, Tom6 and Tom22 (Stojanovski *et al.*, 2007; Becker *et al.*, 2010; Thornton *et al.*, 2010; Becker *et al.*, 2011b). The modular TOB_{core} and TOB_{holo} complexes are thought to play specific roles in regulating assembly of precursors in the maturing TOM complex (discussed further in the following sections)(Stojanovski *et al.*, 2007; Thornton *et al.*, 2010; Becker *et al.*, 2011b).

1.6.3.1 Tob55

Three groups independently identified Tob55 via three different methods: a proteomic screen of *N. crassa* MOM proteins (Paschen *et al.*, 2003); *S. cerevisiae* SAM complex purification using protein A tagged Sam37 (Kozjak *et al.*, 2003); and a bioinformatics approach identifying bacterial OMP85 homologues in eukaryotes (Gentle *et al.*, 2004). Tob55 is essential in *N. crassa* and *S. cerevisiae* and homologues have been found in all studied mitochondria and Gram-negative bacteria (Kozjak *et al.*, 2003; Paschen *et al.*, 2003; Gentle *et al.*, 2004; Voulhoux and Tommassen, 2004; Hoppins *et al.*, 2007b). The functional homologue in bacteria is the 16-stranded OMP85 family member, BamA, responsible for β-barrel assembly in the bacterial OM (Gentle *et al.*, 2004; Wu *et al.*, 2005; Hewitt *et al.*, 2011).

Since Tob55 is itself a β-barrel, it is responsible for assembling precursors of itself as well as other β-precursors after they have passed through the TOM complex into the IMS. Tob55 possesses an N-terminal protrusion into the IMS that contains a POTRA (polypeptide transport associated) domain. The POTRA domain was initially thought to recognize β-barrel precursors as had been shown in *in vitro* studies (Habib *et al.*, 2007). However, subsequent work has shown the POTRA domain to be required for efficient release of newly assembled precursors from the TOB complex, but not necessary for β-signal recognition or insertion into the MOM (Kutik *et al.*, 2008; Stroud *et al.*, 2011).

In vitro assays using *S. cerevisiae* mitochondria show reduced import and assembly of Tob55 in mutants lacking Tob37 or depleted of Tob38 or Tob55 (Habib *et al.*, 2005). In *N. crassa* depletion of any TOB component reduces steady state Tob55 levels reducing import and assembly of all tested β-precursors suggesting that Tob55 requires a functional TOB complex for assembly (Lackey *et al.*, 2011)(Chapter 2). Additionally, the requirement of the TOM complex for the initial steps of importing β-barrels through the MOM was shown in *in vitro* import studies using Tom40 mutants and

saturating levels of the recombinant precursor pSu9-DHFR (Paschen *et al.*, 2003; Habib *et al.*, 2005).

N. crassa has three alternatively spliced Tob55 isoforms: short, intermediate and long. No defects in growth, import or protein levels could be detected in strains designed to express only the short or intermediate forms. However, strains expressing only the long Tob55 isoform showed growth and β-barrel assembly defects under the stressed conditions of growth at 37˚C and high NaCl concentrations (Hoppins *et al.*, 2007b). The reason for the evolution of these isoforms and possible differences in function between them remains a mystery. Interestingly an additional OMP85 homologue, Sam51, is found in *C. albicans* and most clades of yeast. It too is involved in TOB function. However phylogenetic analysis shows monophyly of Sam51, thus it represents a separate subgroup of OMP85 proteins from Tob55 (Hewitt *et al.*, 2012).

1.6.3.2 Tob37

Tob37 was first identified in *S. cerevisiae* as a temperature sensitive mutant for growth on glycerol and was thought to be part of a hetero-oligomeric receptor complex with Tom70 that bound incoming MSF-associated precursors (Gratzer *et al.*, 1995; Hachiya *et al.*, 1995; Schlossmann and Neupert, 1995). Subsequent work demonstrated that Tob37 does not complex with Tom70 and that Tob37 is a component of the TOB complex (Ryan *et al.*, 1999; Wiedemann *et al.*, 2003; Habib *et al.*, 2005). In yeast Tob37 is thought to be a peripheral OM protein associated with the cytosolic face of the complex (Ryan *et al.*, 1999), whereas evidence suggests mammalian Metaxin1 has a C-terminal TMD anchor (Armstrong *et al.*, 1997). Tob37 is not essential in yeast, however knockouts grew poorly (on glucose) or not at all (on glycerol) at restrictive temperatures (37˚C) (Gratzer *et al.*, 1995; Wiedemann *et al.*, 2003). Notably, yeast Tob37 is itself

imported independently of the TOM complex, and only requires Tob38 and Tob55 to be present (Habib *et al.*, 2005). Tob55 mutants lacking the N-terminal IMS exposed region showed reduced Tob37 levels, possibly as a result of reduced complex stability (Habib *et al.*, 2007). Recently Tob37 has been implicated in retention of mtDNA and the mitochondrial dependent maintenance of cell wall integrity in *C. albicans* suggesting novel roles of the TOB complex in fungi (Qu *et al.*, 2012).

1.6.3.3 Tob38

Tob38 was found in complexes purified with tagged Tob37 and Tob55 and had been identified in MOM proteomic studies. Tob38 is essential in *S. cerevisiae* and *N. crassa* and in both species appears to be a cytosolic peripheral MOM associated protein (Ishikawa *et al.*, 2004; Meisinger *et al.*, 2004; Waizenegger *et al.*, 2004; Schmitt *et al.*, 2006; Lackey *et al.*, 2011). Yeast mutants lacking Tob37 or depleted for Tob55 showed respectively, slight or severe reductions in Tob38 levels. Tob38 depleted yeast showed reduced β-barrel protein levels while all other classes of mitochondrial protein were unaffected (Ishikawa *et al.*, 2004; Waizenegger *et al.*, 2004). Pulldown experiments have shown a stronger affinity between Tob38 and Tob55 than with Tob37, and Tob38 and Tob55 can associate in the absence of Tob37 (Waizenegger *et al.*, 2004; Habib *et al.*, 2005).

1.6.3.4 β-barrel import and assembly

Incoming β-barrel precursors maintain a partially folded conformation that is recognized by the TOM complex receptors Tom20 and Tom22 (Rapaport and Neupert, 1999; Yamano *et al.*, 2008b). This suggests that the receptors recognize a 3-dimensional signal arrangement rather than a linear sequence of residues contained in the precursor. β-barrel import and assembly further requires the TOB complex to be present in the MOM

suggesting it may play a supplemental role in β-precursor recognition (Walther *et al.*, 2009a). Following translocation through the TOM pore, the β-precursor associates with the small Tim complexes of the IMS which escort the substrate to the IMS face of the TOB complex in the MOM (Hoppins and Nargang, 2004; Wiedemann *et al.*, 2004). Contained within the most C-terminal β-strand of β-precursors is the β-signal; xPxGxxHxH (P – Polar residue, H – hydrophobic residue) which is universally conserved across eukaryotes (Imai *et al.*, 2008; Kutik *et al.*, 2008). The sequence is required for β-barrel insertion into the MOM and is recognized by the Tob38 protein (Kutik *et al.*, 2008). The peripherally associated Tob38 is assumed to embed itself in the proteinaceous environment of the Tob55 pore exposing its as yet, unresolved β-signal recognition domain, to the IMS (Kutik *et al.*, 2008).

In vitro import assays have shown that mitochondria lacking Tob37 have reduced levels of β-barrel assembly intermediates and final complexes (Wiedemann *et al.*, 2003; Meisinger *et al.*, 2006; Lackey *et al.*, 2011). It has been proposed that the function of Tob37 is to assist in the release of substrates from the TOB complex with the aid of Mdm10 and/or Mim1 in specific circumstances (Chan and Lithgow, 2008; Dukanovic *et al.*, 2009; Becker *et al.*, 2010; Yamano *et al.*, 2010a). The role of the accessory TOB component Mdm10 is unclear. Lack of Mdm10 decreases Tom40 and porin assembly in *N. crassa* whereas in *S. cerevisiae* Tom40 is also reduced but porin import increases over controls (Meisinger *et al.*, 2004; Wideman *et al.*, 2010; Yamano *et al.*, 2010a, b). Different models suggest that Mdm10 either specifically facilitates the release of Tom40 from the TOB complex (Meisinger *et al.*, 2004) or it plays a role in the import of all MOM β-barrels (Wideman *et al.*, 2010; Yamano *et al.*, 2010a). Other reports have suggested that the β-barrel import phenotypes are a secondary result of reduced Mdm10

dependent Tom22 assembly into the TOM complex (Thornton *et al.*, 2010; Becker *et al.*, 2011b).

Normal MOM β-barrel assembly has also been shown to be dependent upon the presence of two other ERMES components Mmm1 and Mdm12 (Meisinger *et al.*, 2007; Wideman *et al.*, 2010). Unlike Mdm10, these components belong exclusively to the ERMES complex. In *Δmmm*1 and *Δmdm12* mitochondria, assembly of Tom40 precursor to a protease protected state and the accumulation of Intermediate I (see section 1.6.3.5 below) with efficiencies similar to wildtype suggests that ERMES may play an explicit role post-TOB in β-barrel complex assembly (Meisinger *et al.*, 2007). On the other hand, the β-barrel import phenotypes could be secondary to other ERMES phenotypes. Though initially overlooked, the concept that lipids may be selectively assembled into proteinaceous complexes adds a new dimension to MOM biogenesis studies. For example, it has been shown that cardiolipin mutants exhibit altered TOM and TOB complex characteristics in addition to selective impairment of MOM protein assembly (Gebert *et al.*, 2009).

It is not yet understood how the precursor, once associated with the TOB complex, is subsequently assembled into its tertiary barrel structure by the TOB complex or how it is laterally released into the lipid phase. There is much debate concerning the three main model propositions:

[1] The precursor is translocated and assembled within a pore formed by a single Tob55 molecule that opens to release the protein into the MOM (Paschen *et al.*, 2003). This model is often dismissed as it is thermodynamically very unfavorable for the requisite disruption of the many hydrogen bonds between adjacent β-strands (Johnson and Jensen, 2004; Ryan, 2004). However, studies on prokaryotic OM β-barrel insertion have

suggested that some β-barrel precursors can fold in the periplasm prior to insertion (Tamm *et al.*, 2001; Tamm *et al.*, 2004) and a recent structural study on BamA homologues has suggested lateral opening of the β-barrel as a feasible means of substrate release into the lipid environment (Noinaj *et al.*, 2013).

[2] The precursor is assembled within a pore created between numerous Tob55 molecules forming an oligomeric complex (Tommassen, 2007; Dimmer and Rapaport, 2012). However, stoichiometric data indicate that only a sole Tob55 molecule exists in the core TOB complex (Klein *et al.*, 2012).

[3] The TOB complex or Tob55 serve as an internal scaffold which the inserting barrel precursor assembles around (Ryan, 2004; Dimmer and Rapaport, 2012).

Regardless of which, if any, of the above models is proven correct it is assumed that the process is driven by the thermodynamically favorable integration of hydrophobic residues into the lipid environment (Paschen *et al.*, 2003; Johnson and Jensen, 2004; Ryan, 2004; Tommassen, 2007; Dimmer and Rapaport, 2012).

1.6.3.5 Tom40 specific import pathway

The import pathway of Tom40 is the most extensively studied of the MOM β-barrels. A procedure using import of *in vitro* radiolabelled precursors into isolated mitochondria followed by BNGE has led to the definition of intermediate assembly complexes as shown in Figure 1.2 and described below. The Tom40 precursor protein passes transiently through the TOM complex and is escorted by the small Tims to the TOB complex. These initial associations cannot be visualized on blue-native gels (Model *et al.*, 2001; Taylor *et al.*, 2003; Wiedemann *et al.*, 2004). An assembly intermediate (Intermediate I, ~200-250 kDa) that represents the association of a Tom40 precursor with

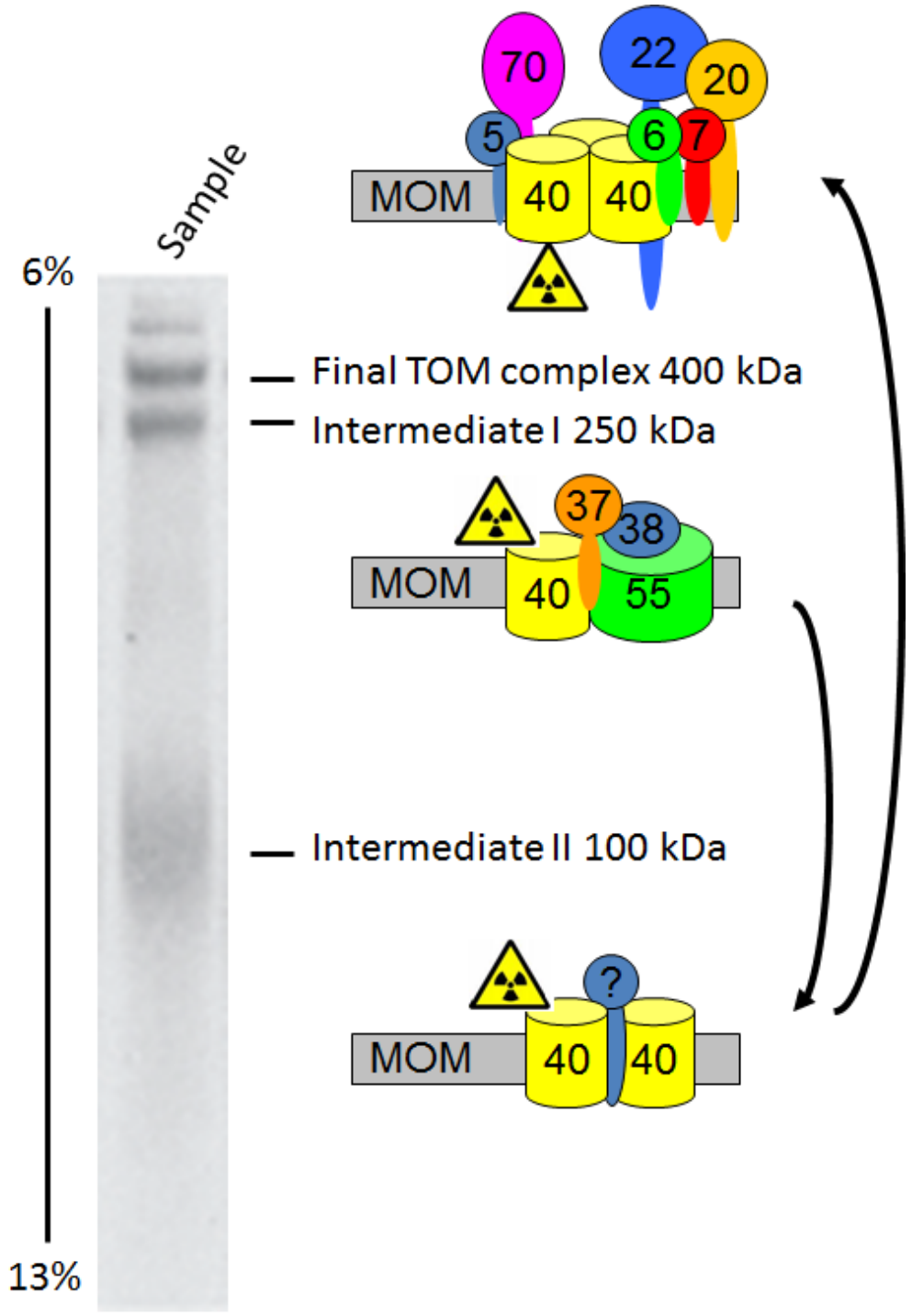

Figure 1.2 Sample autoradiograph showing Tom40 assembly intermediates. The 3 defined Tom40 assembly intermediates (with schematic representations) are shown on a standard 6-13% gradient blue-native acrylamide gel.

the TOB complex is observed in *N. crassa* and *S. cerevisiae* (Paschen *et al.*, 2003; Taylor *et al.*, 2003; Wiedemann *et al.*, 2003; Milenkovic *et al.*, 2004; Pfanner *et al.*, 2004; Waizenegger *et al.*, 2004; Hoppins *et al.*, 2007b; Qiu *et al.*, 2013). In contrast, studies of human Tom40 assembly in isolated human mitochondria have shown no detectable Tom40-TOB intermediate I. However, a novel Tom40-TOM intermediate is observed (Humphries *et al.*, 2005). Following the requisite folding and assembly of the Tom40 protein it is released laterally into the lipid bilayer where it associates with a preexisting membrane inserted Tom40 molecule and a small Tom to form Intermediate II (~100 kDa) (Model *et al.*, 2001; Wiedemann *et al.*, 2003; Humphries *et al.*, 2005; Paschen *et al.*, 2005). Higher resolution blue-native gel electrophoresis, supershift assays and pulldown experiments have identified a previously unresolved Tom40/Tom5/6-TOB intermediate Ib located between conventional intermediates I and II (Becker *et al.*, 2010; Thornton *et al.*, 2010). In *S. cerevisiae* the association of a small fraction of Tom5 molecules to the TOB complex is required for the correct folding/assembly of the Tom40 β-barrel structure at the TOB complex (Qiu *et al.*, 2013). Furthermore, it has been suggested that Tom22 of the TOM complex may also associate with the TOB complex and aid the assembly of the β-barrel proteins (Qiu *et al.*, 2013). Intermediate II then accrues the remaining complex components to form the final ~400 kDa TOM complex (Dekker *et al.*, 1998; Model *et al.*, 2001; Taylor *et al.*, 2003).

1.6.3.6 TOB complex and α-helical proteins

In addition to its role in β-barrel biogenesis the TOB complex has been shown to play an essential role in the insertion of MOM proteins with single-span C-terminal α-helical TMDs (Stojanovski *et al.*, 2007; Becker *et al.*, 2008a). It has been suggested that the TOB complex assumes two distinct modular forms with specific roles in α-helical protein insertion. TOB-Tom5/Tom40 in association with Mim1 facilitates the integration

of the small Toms whereas TOB-Mdm10 specifically inserts Tom22 into the membrane (Thornton *et al.*, 2010). Tob37 but not Tob38 or Tob55 is essential for the membrane integration of the small Toms. Depletion of any TOB component results in decreased import efficiency and steady state levels of Tom22. MOM multipass TMD and N-terminal anchored proteins show no requirement of the TOB complex for import (Stojanovski *et al.*, 2007).

1.6.3.7 A TOM-TOB supercomplex

Studies have shown that the translocation of β-barrel precursors through the TOM complex to a protease-protected environment inside the MOM was impaired in various TOB mutants (Paschen *et al.*, 2003; Wiedemann *et al.*, 2003; Ishikawa *et al.*, 2004; Habib *et al.*, 2007). This suggested that the TOB complex may have role in precursor recognition and may be directly or indirectly associated with the TOM complex. However, until recently the TOM and TOB were defined as independent complexes (Neupert and Herrmann, 2007; Endo and Yamano, 2010; Schmidt *et al.*, 2010; Dukanovic and Rapaport, 2011; Hewitt *et al.*, 2011; Klein *et al.*, 2012; Shiota *et al.*, 2012). Recent studies using a combination of stable isotope labeling with amino acids in cell culture (SILAC) and mass spectrometry demonstrated that Tom40, Tom22 and Tom20 copurified with the TOB complex. Furthermore pulldown experiments using tagged Tob55 and Tom22 revealed that each protein was able to pulldown components of both TOM and TOB complexes suggesting a fraction of TOM and TOB complexes associate in a supercomplex (Qiu *et al.*, 2013). Optimization of the protein:detergent ratios reducing the dissociation of highly labile complexes allowed the first identification of the putative TOM-TOB_{core} supercomplex (~650 kDa, 1 TOM (~400 kDa:1 TOB (~250 kDa)) via BNGE. Notably, mutants lacking Tom22 or Tob37 are unable to form this supercomplex, and loss of the small TIM chaperone complexes of the

IMS inhibits formation of the supercomplex (Qiu *et al.*, 2013). It was also shown via cross-linking and affinity purification experiments that the N-terminal cytosolic domain of Tom22 associates directly with Tob55 facilitating some aspect of the folding of β-barrel precursors associated with the TOB complex. The Tom22-Tob55 association is at least in part responsible for the formation of the TOM-TOB supercomplex (Qiu *et al.*, 2013).

1.6.4 The MIM complex

Mim1 and Mim2 constitute the recently identified fungal MIM (mitochondrial import) complex (Dimmer *et al.*, 2012). Mim1 has long been known for its involvement in integration and assembly of TOM complex components into the MOM. Mim1 has a single span centralized TMD with a conserved GxxxG motif for helix-helix homo-oligomerization, which is essential for complex function (Popov-Celeketic *et al.*, 2008). Mim1 was originally identified to be involved in Tom40 assembly (Ishikawa *et al.*, 2004; Waizenegger *et al.*, 2005). Subsequently, it has been shown to play a role with Mim2 in OM insertion of TOM components containing both N- (Tom20 and Tom70) and C-terminal (small Toms) TMDs in addition to MOM proteins with multispan TMDs (Ugo1, Fzo1, Fis1 and Scm4) (Becker *et al.*, 2008a; Hulett *et al.*, 2008; Popov-Celeketic *et al.*, 2008; Becker *et al.*, 2011a; Papic *et al.*, 2011; Dimmer *et al.*, 2012). *S. cerevisiae* Mim1 requires Mim2 for correct assembly. *Δmim1*, *Δmim2* and *Δmim1/Δmim2* mutants all show retarded growth phenotypes on both fermentable and non-fermentable media however *Δmim2* and the double mutant were significantly worse than *Δmim1* (Becker *et al.*, 2011a; Dimmer *et al.*, 2012). MIM complex disruptions lead to TOM complex instability and import defects likely caused as a downstream effect of small Tom deficiencies (Ishikawa *et al.*, 2004; Waizenegger *et al.*, 2005; Becker *et al.*, 2010; Dimmer *et al.*, 2012). In *N. crassa* Mim1 is essential (Nargang Lab, unpublished

observations), probably due to greater reliance upon Tom20 than *S. cerevisiae*. Although not yet tested, it is expected that Mim2 will also be essential. Fungal MOM proteins with multispan TMDs require Tom70 and the MIM complex for their correct assembly (Becker *et al.*, 2011a; Papic *et al.*, 2011; Dimmer *et al.*, 2012). Equivalent human multispan TMD proteins require only Tom70 in a novel MOM insertion pathway (Otera *et al.*, 2007) perhaps representing a streamlined evolutionary adaptation not requiring the MIM complex.

1.6.5 Unassisted MOM insertion

Certain *S. cerevisiae* proteins with single span TMDs at either terminus can integrate into the MOM without the apparent assistance of any proteinaceous complexes (eg OM45, Mcr1 and Fis1) (Kemper *et al.*, 2008; Meineke *et al.*, 2008; Merklinger *et al.*, 2012). Details of this phenomenon are unclear, however the unique lipid composition of the MOM is believed to be a contributing factor. The *S. cerevisiae* MOM has nearly no ergosterol and a relatively high lipid:protein ratio (Zinser *et al.*, 1991; Schneiter *et al.*, 1999; Kemper *et al.*, 2008). Studies using synthetic lipid bilayers have shown the TMD of one such protein, OM45, to display a higher affinity for MOM-like membranes over other forms (Merklinger *et al.*, 2012). *N. crassa* has homologues of some of these proteins, yet also has a distinctly different MOM composition with ten times the amount of ergosterol compared with the *S. cerevisiae* MOM (Hallermayer and Neupert, 1974; Bay and Court, 2009). Therefore the “unique” lipid composition required may be less stringent than suggested, though it is also possible that changes in lipid compositions have co-evolved with recognition sites on these proteins. It also remains possible that *in vivo* other undefined components may facilitate this process.

1.6.6 The small Tims

The small Tims: Tim8, Tim9, Tim10 and Tim13 function as chaperones to ferry hydrophobic precursors through the IMS from the TOM complex to their next destination in either the TOB or TIM22 dependent pathways. All four have evolved from one ancestral IMS protein and thus share sequence similarities and conserved function while also having subtle differences that have created diverse substrate specificities (Webb *et al.*, 2006; Gentle *et al.*, 2007; Beverly *et al.*, 2008; Alcock *et al.*, 2012). In many lineages a fifth small Tim exists derived from independent gene duplication events. Tim12, found in *S. cerevisiae* (Tim10 related) and animals (Tim9 related) is essential in its role with the TIM22 complex (Koehler *et al.*, 1998a; Sirrenberg *et al.*, 1998). The other small TIM proteins form heterohexameric complexes containing Tim8/Tim13 or Tim9/10 with three of each respective component (Koehler *et al.*, 1998b; Koehler *et al.*, 1999; Hoppins and Nargang, 2004; Webb *et al.*, 2006). Tim9 and Tim10 are essential while Tim8 or Tim13 knockouts show no growth phenotypes (Hoppins and Nargang, 2004; Chacinska *et al.*, 2009). Tim8 and Tim13 function exclusively complexed with each other whereas small fractions of both Tim9 and Tim10 associate with the TIM22 complex (Petrakis *et al.*, 2009). There is as yet no distinction between the chaperoning functions of the TIM8/13 and TIM9/10 complexes as they both escort incoming MIM carrier precursors to the TIM22 complex or β-barrel precursors to the TOB complex (Koehler *et al.*, 1998b; Sirrenberg *et al.*, 1998; Hoppins and Nargang, 2004; Wiedemann *et al.*, 2004; Chacinska *et al.*, 2009; Petrakis *et al.*, 2009).

Despite causing no discernible phenotypes in fungi, mutations in the human Tim8 homologue DDP1 can cause the neurodegenerative Mohr-Tranebjaerg syndrome (Roesch *et al.*, 2002).

1.6.7 The IMS disulphide redox system

Many proteins of the intermembrane space (IMS) lack presequences and are localized to the IMS via the IMS disulphide redox system. This is an oxidation-driven reaction that is reliant upon the activity of the mitochondrial disulfide relay proteins Mia40 and Erv1. Both components of the Mia40/Erv1 IMS import pathway are essential (Chacinska *et al.*, 2004; Bihlmaier *et al.*, 2007; Herrmann and Kohl, 2007; Terziyska *et al.*, 2007; Stojanovski *et al.*, 2008; Endo *et al.*, 2010; Herrmann and Riemer, 2012). Mia40 (Mitochondrial IMS import and Assembly) has a highly conserved domain in which there are six invariant cysteine residues present in a redox-active CPC and twin CX_9C motifs. These motifs contribute to form a substrate binding groove. IMS substrates that are dependent upon this system, notably the small Tims, must pass through the TOM pore in a reduced state. These precursors contain twin internal CX_3C motifs that are recognized by the oxidized form of the oxidoreductase Mia40 with which they form intermolecular disulphide bonds. Mia40 arranges the precursor to form intramolecular disulphide bonds and subsequently releases the oxidized protein into the IMS. Mia40 is then re-oxidized by Erv1 (Essential for Respiratory growth and Viability) allowing the system to cycle repeatedly. Erv1 is re-oxidized by donating electrons to cytochrome c in the ETC providing a small contribution to maintaining membrane potential and ATP synthesis (Herrmann and Riemer, 2012). Alternatively, Erv1 can also reduce molecular oxygen directly to produce hydrogen peroxide (Dabir *et al.*, 2007). Although unrelated with respect to its components, the IMS disulphide redox relay is functionally similar to the Dsb (disulphide bond) system present in the bacterial periplasm (Kadokura *et al.*, 2004).

1.6.8 TIM22 and TIM23/PAM

The TIM22 complex is responsible for the assembly of multispan α-helical MIM carrier proteins (eg, AAC). The complex consists of the central twin pore forming Tim22

and the accessory proteins Tim54 and Tim18 (Chacinska *et al.*, 2009). Tim54 is an integral MIM protein with a large exposed IMS domain that may bind the incoming precursors with the Tim9/Tim10 (and Tim12 in *S. cerevisiae*) complex (Kerscher *et al.*, 1997; Wagner *et al.*, 2008). Tim18 is also membrane embedded. Its function is yet to be determined although recent evidence suggests it has a role in TIM22 complex assembly (Wagner *et al.*, 2008). The carrier precursors are inserted into the pore in a membrane-potential dependent manner and laterally released into the MIM via an unknown mechanism (Rehling *et al.*, 2003).

The TIM23 complex translocates matrix targeted proteins across the MIM. It also can insert specific presequence containing TMD anchored proteins into the MIM via a stop-transfer mechanism (Mokranjac and Neupert, 2010; van der Laan *et al.*, 2010). Some of these TIM23 dependent TMD proteins are further cleaved by IMS or MIM proteases releasing the mature product into the IMS. The pore of Tim23 itself is voltage-gated. Presence of a membrane potential induces a disruption to the structure of an α-helix within the lumen that "opens" the pore due to the conformational shift (Malhotra *et al.*, 2013). Presequence precursors are first driven into the TIM23 pore with the electrophoretic assistance of the membrane-potential acting on the positively charged presequence. Force required for the remaining polypeptide translocation is harnessed via ATP hydrolysis by the matrix localized PAM (presequence translocase-associated motor). The PAM is one of the most intricate Hsp70 systems known (Chacinska *et al.*, 2009). PAM consists of the central mtHsp70 molecular chaperone and five accessory components (Mge1, Tim44, Pam16, Pam 17 and Pam18). The accessory PAM proteins orchestrate the ATP dependent activity of mtHsp70 and the association of the PAM with TIM23 and incoming precursors. There are two proposed mechanisms for PAM induced vectorial motion of precursors: the "Trapping/Brownian ratchet" model or the

"Pulling/Power stroke" model (Neupert and Brunner, 2002). In the trapping model mtHsp70 binds the precursor as it emerges from TIM23 into the matrix and acts as a ratchet to prevent any back-sliding. Brownian kinetics will then ensure that more polypeptide will eventually pass into the matrix where it is bound by additional mtHsp70s favouring the inward import of the precursor (Okamoto *et al.*, 2002; Liu *et al.*, 2003; Yamano *et al.*, 2008a). The pulling model suggests that after mtHsp70 binds the precursor, an ATP dependent conformational shift of the PAM actively forces the bound precursor into the matrix. It is proposed numerous such "pulls" would be required (Chauwin *et al.*, 1998). Interestingly neither mechanism appears to be able to exclusively explain PAM function. Functional studies indicate that the PAM may operate using a combination of both models (Krayl *et al.*, 2007). Following import the N-terminal presequence is cleaved in the matrix by MPP (Matrix Processing Peptidase) (Chacinska *et al.*, 2009; Mokranjac and Neupert, 2010; van der Laan *et al.*, 2010; Mossmann *et al.*, 2012).

The TOM and TIM23 complexes have been shown to tether together *in vivo* via interactions between the IMS domains of Tom22 and Tim50 (Shiota *et al.*, 2011). This supercomplex forms mitochondrial contact sites holding the two membranes in close proximity to assist precursors transitioning between the pores (Schulke *et al.*, 1997; Schulke *et al.*, 1999; Chacinska *et al.*, 2009; Mokranjac and Neupert, 2010; van der Laan *et al.*, 2010).

1.6.9 The OXA complex

The OXA (oxidase assembly) system constitutes the only "inside-out" import pathway known to date. It functions to insert precursors into the MIM from the matrix. The OXA complex assembles several integral membrane proteins encoded by the

mtDNA and translated on mitochondrial ribosomes (He and Fox, 1997; Hell *et al.*, 2001). In addition, some presequence-containing nuclear encoded proteins such as F_0F_1-ATPase subunit 9, Oxa1 and Cox18 that have already passed through the TIM23 complex are routed back into the MIM via the OXA translocase (Rojo *et al.*, 1995; Herrmann *et al.*, 1997; Funes *et al.*, 2004). Certain proteins utilize a co-operative system in which the precursor is released laterally into the MIM via the TIM23 stop-transfer mechanism while the N-terminal matrix portion is subsequently integrated into the MIM via the OXA system (Bohnert *et al.*, 2010). The OXA complex consists of the core component Oxa1 and five accessory proteins (Mba1, Mdm38, Cox18, Pnt1 and Mss2)(Chacinska *et al.*, 2009). Notably, Oxa1 is homologous to the bacterial inner membrane export protein YidC (Bonnefoy *et al.*, 1994; Preuss *et al.*, 2005).

1.6.10 The MINOS complex and Protein Import

Recently, three independent groups identified a MIM associated structural protein complex called MINOS (Mitochondrial Inner membrane Organizing System) (von der Malsburg *et al.*, 2011), MICOS (Mitochondrial Contact Site) (Harner *et al.*, 2011) or MitOS (Mitochondrial Organizing Structure) (Hoppins *et al.*, 2011). The complex is composed of Fcj1(formation of cristae junctions, aka Mitofilin), Mio10 (mitochondrial inner membrane organization), Mio27, Aim5 (altered inheritance of mitochondria), Aim13 and Aim37. Bioinformatics show Fcj1 and Mio10 are highly conserved in eukaryotes, Aim5 appears to be specific to fungi while the other components display some conservation or contain conserved features in other eukaryotes (Harner *et al.*, 2011; Hoppins *et al.*, 2011). Fcj1 was originally found to be involved in the formation of cristae junctions at the sites where distinct cristae meet the inner boundary membranes of the MIM (John *et al.*, 2005; Rabl *et al.*, 2009). MINOS has since been proposed to be involved in regulation of cristae junction structure and interactions

between the MOM and MIM at mitochondrial contact sites (Harner *et al.*, 2011; Korner *et al.*, 2012). MINOS associates with the MOM proteins; Ugo1, porin, Tob55 and Tom40 (Xie *et al.*, 2007; Darshi *et al.*, 2011; Harner *et al.*, 2011; Hoppins *et al.*, 2011; von der Malsburg *et al.*, 2011; Alkhaja *et al.*, 2012; Korner *et al.*, 2012; Ott *et al.*, 2012; Zerbes *et al.*, 2012). Interaction of MINOS with both TOM (Tom40) and TOB (Tob55) components potentially links MINOS to protein import. Evidence in support of this concept shows that MINOS mutants have import defects for Mia/Erv dependent IMS proteins (von der Malsburg *et al.*, 2011). Also minor effects on β-barrel import have been observed in strains overexpressing Fcj1, but considering TOB defects affect cristae and cristae junctions it may be that TOB and MINOS have similar mild secondary phenotypes due to morphological disruptions at contact sites (Korner *et al.*, 2012).

A recent hypothesis has proposed that the MINOS, ERMES, TOM and TOB complexes associate to form an intricate triple-membrane-spanning, dual-organellar structure called ERMIONE (ER-Mitochondria Organizing Network) that controls membrane architecture and biogenesis (van der Laan *et al.*, 2012). The presence of such a structure could explain the diverse array of phenotypes seen in mutant strains lacking ERMIONE proteins. Removal of one component affects the entire network resulting in the downstream pleiotropy often observed.

1.7 Evolution of mitochondrial protein import

As the α-proteobacterial endosymbiont evolved into the mitochondria, many genes were transferred to the host nuclear genome. These displaced genes needed to be transcribed and translated, and the proteins targeted to, and imported into the evolving organelle using adaptation to pre-existing systems. Core elements of these novel pathways must have evolved from extant proteins while subsequent accessory

components may have been added by re-allocation of host or symbiont genes. Interestingly, some unicellular eukaryotic parasites possess a highly reduced mitochondrial-related organelle called the mitosome (see section 1.3). These organelles, despite massive simplification, retain "skeletal" import pathways which may represent those present in the first eukaryotes (Heinz and Lithgow, 2013).

Prior to gene loss from the symbiont genome, pathways for substrate (proteins/metabolites) import/export must have existed to enable transfer of materials between the cytoplasm, periplamic space, outer membrane and outside environment. It is reasonable to assume that a pore protein in the OM of the early endosymbiont must have evolved into the core component of an early Tom40 translocase. Membrane embedded β-barrels exist exclusively in the outer membranes of Gram-negative bacteria, mitochondria and chloroplasts and one of the original endosymbiont β-barrels could have fulfilled the required role of an early polypeptide translocation pore. It has been shown that renatured Tom40 alone, reconstituted into liposomes, forms pores capable of translocating presequence peptides (Becker *et al.*, 2005). Therefore the ancestral Tom40 β-barrel alone could have acted as a primitive TOM complex. As mentioned in section 1.6.2.1 Tom40 appears to share a common evolutionary ancestor and structure with the metabolite channel porin (VDAC) (Zeth, 2010; Gessmann *et al.*, 2011; Bay *et al.*, 2012). Despite the presence of numerous and diverse OM β-barrels in prokaryotes including OmpF and LamB porins (passive transporters) and FhaC and PulD type II transporters (active translocation), no known bacterial OM β-barrel fits the profile as the common ancestor of eukaryotic porin and Tom40 (Gabriel *et al.*, 2001; Dolezal *et al.*, 2006; Walther *et al.*, 2009b; Zeth and Thein, 2010; Liu *et al.*, 2011).

The recent discovery of the MOM β-barrel ATOM (Archaic TOM) protein family in trypanosomes has altered the debate on Tom40/TOM evolution. ATOM is

required for mitochondrial protein import in trypanosomes which purportedly lack an obvious Tom40-like protein. ATOM was originally thought to be orthologous to the bacterial outer membrane YtfM (TamA) export protein, which is a member of the OMP85 superfamily (Pusnik *et al.*, 2011; Selkrig *et al.*, 2012). However, conflicting data derived from differing *in silico* and electrophysiological methodologies have suggested ATOM may be a highly divergent "classical" Tom40 homologue and not be related to YtfM (Harsman *et al.*, 2012; Zarsky *et al.*, 2012). As a β-barrel ATOM is dependent upon another OMP85 superfamily member, trTob55 (trypanosome Tob55), for import and assembly (Pusnik *et al.*, 2011). Despite sharing equivalent functions, a consensus on the ancestry of ATOM is yet to be reached (Pusnik *et al.*, 2012; Zarsky *et al.*, 2012). OMP85 proteins have 16 β-strands whereas Tom40 is modeled to have 19 based on the crystal structure of the homologous porin protein. However, as stated earlier (section 1.6.2.1), it has been suggested that the porin structure may represent a non-native conformation as it conflicts with much of the accumulated porin biochemical data (Colombini, 2009). Thus the debate on Tom40 origin and structure is not yet settled (Hiller *et al.*, 2010).

All other components of the TOM complex lack homologues in bacteria, suggesting they are novel host contributions. An ancestral TOM complex consisting of Tom40, Tom7, Tom22 and Tom70 is predicted to have existed in the last common eukaryotic ancestor (LCEA). These components are sufficiently prevalent across the extremely divergent supergroups to be considered ubiquitous among eukaryotes - excluding rare cases of subsequent gene losses (Macasev *et al.*, 2004; Lithgow and Schneider, 2010; Tsaousis *et al.*, 2011). All TOM components have been conserved between mammals and fungi (Kato and Mihara, 2008).

Tob55 is homologous to bacterial BamA, another OMP85 family member that acts as the β-barrel insertase of the bacterial OM (Gentle *et al.*, 2004; Wu *et al.*, 2005; Hewitt *et al.*, 2011; Liu *et al.*, 2011; Jiang *et al.*, 2012; Webb *et al.*, 2012). Membrane insertion of β-barrels is a highly conserved process evidenced by the fact that bacterial and chloroplast β-precursors can be correctly assembled into the MOM (Walther *et al.*, 2009a; Kozjak-Pavlovic *et al.*, 2011; Ulrich *et al.*, 2012) and, reciprocally, mitochondrial β-barrels can insert into Gram-negative OMs (Walther *et al.*, 2010). Despite the conservation, differences in the mechanism of β-insertion exist (Walther *et al.*, 2009b). BamA/OMP85 has 5 POTRA domains exposed in the periplasmic space, one of which is essential for β-barrel insertion into the bacterial OM (Bos *et al.*, 2007). Tob55 has only one POTRA domain in the IMS, yet unlike bacterial OMP85 the POTRA domain is not essential for β-barrel insertion into the MOM (Kutik *et al.*, 2008) despite being shown to bind β-precursors *in vitro* (Habib et al., 2007) and be required for subsequent release of the assembled β-barrel (Stroud *et al.*, 2011). Tob37 and Tob38 are not considered homologous to the BAM accessory components BamB, C (F in α-proteobacteria), D and E. Of these 4 lipoproteins only BamD is essential (Malinverni *et al.*, 2006; Walther *et al.*, 2009b). It has been proposed that the ancestral BAM was a two-subunit complex (BamA-BamD) (Anwari *et al.*, 2012). Interestingly Tob37 and Tob38, which are required for efficient mitochondrial β-barrel import, are superfluous for the integration of bacterial β-barrels into the MOM (Jiang *et al.*, 2011). Phylogenetic analysis in *Xenopus* on the Tob37 and Tob38 homologues, Metaxin1 and Metaxin2 respectively, has revealed a common ancestry despite considerable sequence divergence (Adolph, 2005). Nonetheless, there has been a high degree of conservation of functions and topologies of Tob37 and Tob38 homologues across opisthokonts (Kozjak-Pavlovic *et al.*, 2007).

Components of the Mia/Erv system and small TIMs also have no homologues in bacteria. However the analogous proteins DsbC and Skp/SurA respectively are present in the bacterial periplasm suggesting that convergent evolution is responsible for the mitochondrial equivalents (Walther *et al.*, 2009b; Hewitt *et al.*, 2011).

The Tim22 and Tim23 proteins are the pore forming components of the TIM22 and TIM23 complexes, respectively. The two proteins are homologous and likely arose as a result of a gene duplication of a common ancestral protein. It has been suggested that Tim22 and Tim23 are homologous to the bacterial LivH family of amino-acid permeases (Rassow *et al.*, 1999) but there is much ambiguity in the data presented thus far and a challenging hypothesis has emerged suggesting that the progenitor of these proteins was first established in the host (Gross and Bhattacharya, 2011). Tim44 and Pam18 of the TIM23 complex are homologous to α-proteobacterial TimA and TimB, respectively, yet the latter function distinctly from LivH in separate complexes. It has been proposed that simple point mutations in both TimA and TimB would allow for the assembly of a primitive yet functional molecular machine (LivH, TimA, TimB, Hsp70) analogous to the PAM (Clements *et al.*, 2009; Liu *et al.*, 2011).

In bacteria an OXA complex homologue YidC functions in concert with SecY to assemble proteins into the cytoplasmic membrane (Hewitt *et al.*, 2011). Notably, the Jakobid protist *Reclinomonas americana* of the eukaryotic supergroup Excavata has retained the SecY gene in its mtDNA despite also having TIM components (Tong *et al.*, 2011).

The evidence provided above suggests that modern mitochondrial import machines are hybrid complexes resulting from the cumulative utilization of both novel host contributions and extant symbiont proteins. Whether evolution of mitochondrial

import machineries was initially driven by the host ("Outside" view), the symbiont ("Inside" view) or both, remains to be clarified (Gross and Bhattacharya, 2009; Alcock *et al.*, 2010; Hewitt *et al.*, 2011).

1.8 Focus of this study: Structural and functional analysis of TOB complex components and other MOM proteins

My first objective was to determine the effects of Tob37 and Tob38 knockdown on β-barrel import and steady-state protein composition in *N. crassa.* The data showed that maximum viable depletion of Tob37 and Tob38 significantly reduced β-barrel assembly. The topology of Tob37 was investigated, focusing on two predicted hydrophobic C-terminal α-helical domains. It was shown that the most N-terminal domain represented a *bona fide* TMD anchor giving *N. crassa* Tob37 an analogous topology to mammalian Metaxin1 that is not conserved in *S. cerevisiae.* It was shown that neither the TMD or C-terminal region were required for mitochondrial or TOB localization of Tob37 but affected complex integrity. Examination of the import properties of mutants lacking these domains indicated their involvement in assembly and release of different β-barrels. Analysis of knockdowns and mutants suggested intra-TOB complex protein associations. Analysis of additional TOB mutants highlighted some intriguing phenotypes which will also be presented in this thesis along with supplementary experiments that have contributed to the published works of collaborators and the Nargang lab.

The second project in this thesis describes experiments aimed to biochemically define the structure and topology of a controversial region of Tom40. This was undertaken to shed light on the validity of structural predictions based on comparisons with porin and its crystal structure. Determination of the arrangement of the residues in

an amphipathic β-strand and its flanking loops was achieved using the SCAM (scanning cysteine accessibility mapping) method. These results were integrated with similar results from other regions of the protein collected by past members of the Nargang lab. The contribution of these results to the growing body of *in silico* and empirical data will hopefully allow a consensus Tom40 topology to be established so evolutionary and functional studies can proceed with more confidence.

1.9 References

Abe, Y., Shodai, T., Muto, T., Mihara, K., Torii, H., Nishikawa, S., Endo, T., and Kohda, D. (2000). Structural basis of presequence recognition by the mitochondrial protein import receptor Tom20. Cell *100*, 551-560.

Adolph, K.W. (2005). Characterization of the cDNA and amino acid sequences of *Xenopus* Metaxin 3, and relationship to *Xenopus* Metaxins 1 and 2. DNA Seq *16*, 252-259.

Ahmed, A.U., Beech, P.L., Lay, S.T., Gilson, P.R., and Fisher, P.R. (2006). Import-associated translational inhibition: novel in vivo evidence for cotranslational protein import into *Dictyostelium discoideum* mitochondria. Eukaryot Cell *5*, 1314-1327.

Ahting, U., Thieffry, M., Engelhardt, H., Hegerl, R., Neupert, W., and Nussberger, S. (2001). Tom40, the pore-forming component of the protein-conducting TOM channel in the outer membrane of mitochondria. J Cell Biol *153*, 1151-1160.

Ahting, U., Thun, C., Hegerl, R., Typke, D., Nargang, F.E., Neupert, W., and Nussberger, S. (1999). The TOM core complex: the general protein import pore of the outer membrane of mitochondria. J Cell Biol *147*, 959-968.

Alcock, F., Clements, A., Webb, C., and Lithgow, T. (2010). Evolution. Tinkering inside the organelle. Science *327*, 649-650.

Alcock, F., Webb, C.T., Dolezal, P., Hewitt, V., Shingu-Vasquez, M., Likic, V.A., Traven, A., and Lithgow, T. (2012). A small Tim homohexamer in the relict mitochondrion of *Cryptosporidium*. Mol Biol Evol *29*, 113-122.

Alconada, A., Kubrich, M., Moczko, M., Honlinger, A., and Pfanner, N. (1995). The mitochondrial receptor complex: the small subunit Mom8b/Isp6 supports association of receptors with the general insertion pore and transfer of preproteins. Mol Cell Biol *15*, 6196-6205.

Alkhaja, A.K., Jans, D.C., Nikolov, M., Vukotic, M., Lytovchenko, O., Ludewig, F., Schliebs, W., Riedel, D., Urlaub, H., Jakobs, S., and Deckers, M. (2012). MINOS1 is a conserved component of mitofilin complexes and required for mitochondrial function and cristae organization. Mol Biol Cell *23*, 247-257.

Altmann, K., and Westermann, B. (2005). Role of essential genes in mitochondrial morphogenesis in *Saccharomyces cerevisiae*. Mol Biol Cell *16*, 5410-5417.

Andersson, S.G., Karlberg, O., Canback, B., and Kurland, C.G. (2003). On the origin of mitochondria: a genomics perspective. Philos Trans R Soc Lond B Biol Sci *358*, 165-177; discussion 177-169.

Andersson, S.G., and Kurland, C.G. (1999). Origins of mitochondria and hydrogenosomes. Curr Opin Microbiol *2*, 535-541.

Andrade-Navarro, M.A., Sanchez-Pulido, L., and McBride, H.M. (2009). Mitochondrial vesicles: an ancient process providing new links to peroxisomes. Curr Opin Cell Biol *21*, 560-567.

Anwari, K., Webb, C.T., Poggio, S., Perry, A.J., Belousoff, M., Celik, N., Ramm, G., Lovering, A., Sockett, R.E., Smit, J., Jacobs-Wagner, C., and Lithgow, T. (2012). The evolution of new lipoprotein subunits of the bacterial outer membrane BAM complex. Mol Microbiol *84*, 832-844.

Armstrong, L.C., Komiya, T., Bergman, B.E., Mihara, K., and Bornstein, P. (1997). Metaxin is a component of a preprotein import complex in the outer membrane of the mammalian mitochondrion. J Biol Chem *272*, 6510-6518.

Armstrong, L.C., Saenz, A.J., and Bornstein, P. (1999). Metaxin 1 interacts with metaxin 2, a novel related protein associated with the mammalian mitochondrial outer membrane. J Cell Biochem *74*, 11-22.

Bartlett, K., and Eaton, S. (2004). Mitochondrial beta-oxidation. Eur J Biochem *271*, 462-469.

Bauer, M.F., Hofmann, S., Neupert, W., and Brunner, M. (2000). Protein translocation into mitochondria: the role of TIM complexes. Trends Cell Biol *10*, 25-31.

Bay, D.C., and Court, D.A. (2009). Effects of ergosterol on the structure and activity of *Neurospora* mitochondrial porin in liposomes. Canadian journal of microbiology *55*, 1275-1283.

Bay, D.C., Hafez, M., Young, M.J., and Court, D.A. (2012). Phylogenetic and coevolutionary analysis of the beta-barrel protein family comprised of mitochondrial porin (VDAC) and Tom40. Biochim Biophys Acta *1818*, 1502-1519.

Bayrhuber, M., Meins, T., Habeck, M., Becker, S., Giller, K., Villinger, S., Vonrhein, C., Griesinger, C., Zweckstetter, M., and Zeth, K. (2008). Structure of the human voltage-dependent anion channel. Proc Natl Acad Sci U S A *105*, 15370-15375.

Becker, D., Krayl, M., Strub, A., Li, Y., Mayer, M.P., and Voos, W. (2009). Impaired interdomain communication in mitochondrial Hsp70 results in the loss of inward-directed translocation force. J Biol Chem *284*, 2934-2946.

Becker, L., Bannwarth, M., Meisinger, C., Hill, K., Model, K., Krimmer, T., Casadio, R., Truscott, K.N., Schulz, G.E., Pfanner, N., and Wagner, R. (2005). Preprotein translocase of the outer mitochondrial membrane: reconstituted Tom40 forms a characteristic TOM pore. J Mol Biol *353*, 1011-1020.

Becker, T., Guiard, B., Thornton, N., Zufall, N., Stroud, D.A., Wiedemann, N., and Pfanner, N. (2010). Assembly of the mitochondrial protein import channel: role of Tom5 in two-stage interaction of Tom40 with the SAM complex. Mol Biol Cell *21*, 3106-3113.

Becker, T., Pfannschmidt, S., Guiard, B., Stojanovski, D., Milenkovic, D., Kutik, S., Pfanner, N., Meisinger, C., and Wiedemann, N. (2008a). Biogenesis of the mitochondrial

TOM complex: Mim1 promotes insertion and assembly of signal-anchored receptors. J Biol Chem *283*, 120-127.

Becker, T., Vogtle, F.N., Stojanovski, D., and Meisinger, C. (2008b). Sorting and assembly of mitochondrial outer membrane proteins. Biochim Biophys Acta *1777*, 557-563.

Becker, T., Wenz, L.S., Kruger, V., Lehmann, W., Muller, J.M., Goroncy, L., Zufall, N., Lithgow, T., Guiard, B., Chacinska, A., Wagner, R., Meisinger, C., and Pfanner, N. (2011a). The mitochondrial import protein Mim1 promotes biogenesis of multispanning outer membrane proteins. J Cell Biol *194*, 387-395.

Becker, T., Wenz, L.S., Thornton, N., Stroud, D., Meisinger, C., Wiedemann, N., and Pfanner, N. (2011b). Biogenesis of mitochondria: dual role of Tom7 in modulating assembly of the preprotein translocase of the outer membrane. J Mol Biol *405*, 113-124.

Beddoe, T., and Lithgow, T. (2002). Delivery of nascent polypeptides to the mitochondrial surface. Biochim Biophys Acta *1592*, 35-39.

Berger, K.H., Sogo, L.F., and Yaffe, M.P. (1997). Mdm12p, a component required for mitochondrial inheritance that is conserved between budding and fission yeast. J Cell Biol *136*, 545-553.

Beverly, K.N., Sawaya, M.R., Schmid, E., and Koehler, C.M. (2008). The Tim8-Tim13 complex has multiple substrate binding sites and binds cooperatively to Tim23. J Mol Biol *382*, 1144-1156.

Bihlmaier, K., Mesecke, N., Terziyska, N., Bien, M., Hell, K., and Herrmann, J.M. (2007). The disulfide relay system of mitochondria is connected to the respiratory chain. J Cell Biol *179*, 389-395.

Blatch, G.L., and Lassle, M. (1999). The tetratricopeptide repeat: a structural motif mediating protein-protein interactions. Bioessays *21*, 932-939.

Bohnert, M., Rehling, P., Guiard, B., Herrmann, J.M., Pfanner, N., and van der Laan, M. (2010). Cooperation of stop-transfer and conservative sorting mechanisms in mitochondrial protein transport. Curr Biol *20*, 1227-1232.

Boldogh, I.R., Nowakowski, D.W., Yang, H.C., Chung, H., Karmon, S., Royes, P., and Pon, L.A. (2003). A protein complex containing Mdm10p, Mdm12p, and Mmm1p links mitochondrial membranes and DNA to the cytoskeleton-based segregation machinery. Mol Biol Cell *14*, 4618-4627.

Bolliger, L., Junne, T., Schatz, G., and Lithgow, T. (1995). Acidic receptor domains on both sides of the outer membrane mediate translocation of precursor proteins into yeast mitochondria. EMBO J *14*, 6318-6326.

Bomer, U., Pfanner, N., and Dietmeier, K. (1996). Identification of a third yeast mitochondrial Tom protein with tetratrico peptide repeats. FEBS Lett *382*, 153-158.

Bonnefoy, N., Chalvet, F., Hamel, P., Slonimski, P.P., and Dujardin, G. (1994). OXA1, a *Saccharomyces cerevisiae* nuclear gene whose sequence is conserved from prokaryotes to eukaryotes controls cytochrome oxidase biogenesis. J Mol Biol *239*, 201-212.

Borkovich, K.A., Alex, L.A., Yarden, O., Freitag, M., Turner, G.E., Read, N.D., Seiler, S., Bell-Pedersen, D., Paietta, J., Plesofsky, N., Plamann, M., Goodrich-Tanrikulu, M., Schulte, U., Mannhaupt, G., Nargang, F.E., Radford, A., Selitrennikoff, C., Galagan, J.E., Dunlap, J.C., Loros, J.J., Catcheside, D., Inoue, H., Aramayo, R., Polymenis, M., Selker, E.U., Sachs, M.S., Marzluf, G.A., Paulsen, I., Davis, R., Ebbole, D.J., Zelter, A., Kalkman, E.R., O'Rourke, R., Bowring, F., Yeadon, J., Ishii, C., Suzuki, K., Sakai, W., and Pratt, R. (2004). Lessons from the genome sequence of Neurospora crassa: tracing the path from genomic blueprint to multicellular organism. Microbiol Mol Biol Rev *68*, 1-108.

Bornstein, P., McKinney, C.E., LaMarca, M.E., Winfield, S., Shingu, T., Devarayalu, S., Vos, H.L., and Ginns, E.I. (1995). Metaxin, a gene contiguous to both thrombospondin 3 and glucocerebrosidase, is required for embryonic development in the mouse: implications for Gaucher disease. Proc Natl Acad Sci U S A *92*, 4547-4551.

Bos, M.P., Robert, V., and Tommassen, J. (2007). Functioning of outer membrane protein assembly factor Omp85 requires a single POTRA domain. EMBO Rep *8*, 1149-1154.

Boxma, B., de Graaf, R.M., van der Staay, G.W., van Alen, T.A., Ricard, G., Gabaldon, T., van Hoek, A.H., Moon-van der Staay, S.Y., Koopman, W.J., van Hellemond, J.J., Tielens, A.G., Friedrich, T., Veenhuis, M., Huynen, M.A., and Hackstein, J.H. (2005). An anaerobic mitochondrion that produces hydrogen. Nature *434*, 74-79.

Braschi, E., Zunino, R., and McBride, H.M. (2009). MAPL is a new mitochondrial SUMO E3 ligase that regulates mitochondrial fission. EMBO Rep *10*, 748-754.

Bratic, I., and Trifunovic, A. (2010). Mitochondrial energy metabolism and ageing. Biochim Biophys Acta *1797*, 961-967.

Breuer, M.E., Koopman, W.J., Koene, S., Nooteboom, M., Rodenburg, R.J., Willems, P.H., and Smeitink, J.A. (2013). The role of mitochondrial OXPHOS dysfunction in the development of neurologic diseases. Neurobiol Dis *51*, 27-34.

Brix, J., Rudiger, S., Bukau, B., Schneider-Mergener, J., and Pfanner, N. (1999). Distribution of binding sequences for the mitochondrial import receptors Tom20, Tom22, and Tom70 in a presequence-carrying preprotein and a non-cleavable preprotein. J Biol Chem *274*, 16522-16530.

Burger, G., Gray, M.W., Forget, L., and Lang, B.F. (2013). Strikingly Bacteria-Like and Gene-Rich Mitochondrial Genomes throughout Jakobid Protists. Genome biology and evolution *5*, 418-438.

Burgess, S.M., Delannoy, M., and Jensen, R.E. (1994). MMM1 encodes a mitochondrial outer membrane protein essential for establishing and maintaining the structure of yeast mitochondria. J Cell Biol *126*, 1375-1391.

Cavalier-Smith, T. (2006). Origin of mitochondria by intracellular enslavement of a photosynthetic purple bacterium. Proc Biol Sci *273*, 1943-1952.

Cavalier-Smith, T. (2009). Predation and eukaryote cell origins: a coevolutionary perspective. Int J Biochem Cell Biol *41*, 307-322.

Chacinska, A., Koehler, C.M., Milenkovic, D., Lithgow, T., and Pfanner, N. (2009). Importing mitochondrial proteins: machineries and mechanisms. Cell *138*, 628-644.

Chacinska, A., Pfannschmidt, S., Wiedemann, N., Kozjak, V., Sanjuan Szklarz, L.K., Schulze-Specking, A., Truscott, K.N., Guiard, B., Meisinger, C., and Pfanner, N. (2004). Essential role of Mia40 in import and assembly of mitochondrial intermembrane space proteins. EMBO J *23*, 3735-3746.

Chan, N.C., Likic, V.A., Waller, R.F., Mulhern, T.D., and Lithgow, T. (2006). The C-terminal TPR domain of Tom70 defines a family of mitochondrial protein import receptors found only in animals and fungi. J Mol Biol *358*, 1010-1022.

Chan, N.C., and Lithgow, T. (2008). The peripheral membrane subunits of the SAM complex function codependently in mitochondrial outer membrane biogenesis. Mol Biol Cell *19*, 126-136.

Chauwin, J.F., Oster, G., and Glick, B.S. (1998). Strong precursor-pore interactions constrain models for mitochondrial protein import. Biophys J *74*, 1732-1743.

Clements, A., Bursac, D., Gatsos, X., Perry, A.J., Civciristov, S., Celik, N., Likic, V.A., Poggio, S., Jacobs-Wagner, C., Strugnell, R.A., and Lithgow, T. (2009). The reducible complexity of a mitochondrial molecular machine. Proc Natl Acad Sci U S A *106*, 15791-15795.

Collins, Y., Chouchani, E.T., James, A.M., Menger, K.E., Cocheme, H.M., and Murphy, M.P. (2012). Mitochondrial redox signalling at a glance. J Cell Sci *125*, 801-806.

Colombini, M. (2009). The published 3D structure of the VDAC channel: native or not? Trends Biochem Sci *34*, 382-389.

Court, D.A., Nargang, F.E., Steiner, H., Hodges, R.S., Neupert, W., and Lill, R. (1996). Role of the intermembrane-space domain of the preprotein receptor Tom22 in protein import into mitochondria. Mol Cell Biol *16*, 4035-4042.

Cox, C.J., Foster, P.G., Hirt, R.P., Harris, S.R., and Embley, T.M. (2008). The archaebacterial origin of eukaryotes. Proc Natl Acad Sci U S A *105*, 20356-20361.

Cui, H., Kong, Y., and Zhang, H. (2012). Oxidative stress, mitochondrial dysfunction, and aging. Journal of signal transduction *2012*, 646354.

Dabir, D.V., Leverich, E.P., Kim, S.K., Tsai, F.D., Hirasawa, M., Knaff, D.B., and Koehler, C.M. (2007). A role for cytochrome c and cytochrome c peroxidase in electron shuttling from Erv1. EMBO J *26*, 4801-4811.

Dacks, J.B., Dyal, P.L., Embley, T.M., and van der Giezen, M. (2006). Hydrogenosomal succinyl-CoA synthetase from the rumen-dwelling fungus *Neocallimastix patriciarum*; an energy-producing enzyme of mitochondrial origin. Gene *373*, 75-82.

Darshi, M., Mendiola, V.L., Mackey, M.R., Murphy, A.N., Koller, A., Perkins, G.A., Ellisman, M.H., and Taylor, S.S. (2011). ChChd3, an inner mitochondrial membrane protein, is essential for maintaining crista integrity and mitochondrial function. J Biol Chem *286*, 2918-2932.

Davidov, Y., and Jurkevitch, E. (2009). Predation between prokaryotes and the origin of eukaryotes. Bioessays *31*, 748-757.

Davis, A.J., Ryan, K.R., and Jensen, R.E. (1998). Tim23p contains separate and distinct signals for targeting to mitochondria and insertion into the inner membrane. Mol Biol Cell *9*, 2577-2593.

de Duve, C. (2007). The origin of eukaryotes: a reappraisal. Nat Rev Genet *8*, 395-403.

Dekker, P.J., Muller, H., Rassow, J., and Pfanner, N. (1996). Characterization of the preprotein translocase of the outer mitochondrial membrane by blue native electrophoresis. Biol Chem *377*, 535-538.

Dekker, P.J., Ryan, M.T., Brix, J., Muller, H., Honlinger, A., and Pfanner, N. (1998). Preprotein translocase of the outer mitochondrial membrane: molecular dissection and assembly of the general import pore complex. Mol Cell Biol *18*, 6515-6524.

Del Bo, R., Bordoni, A., Martinelli Boneschi, F., Crimi, M., Sciacco, M., Bresolin, N., Scarlato, G., and Comi, G.P. (2002). Evidence and age-related distribution of mtDNA D-loop point mutations in skeletal muscle from healthy subjects and mitochondrial patients. J Neurol Sci *202*, 85-91.

Dembowski, M., Kunkele, K.P., Nargang, F.E., Neupert, W., and Rapaport, D. (2001). Assembly of Tom6 and Tom7 into the TOM core complex of *Neurospora crassa*. J Biol Chem *276*, 17679-17685.

Dietmeier, K., Honlinger, A., Bomer, U., Dekker, P.J., Eckerskorn, C., Lottspeich, F., Kubrich, M., and Pfanner, N. (1997). Tom5 functionally links mitochondrial preprotein receptors to the general import pore. Nature *388*, 195-200.

Dimmer, K.S., Fritz, S., Fuchs, F., Messerschmitt, M., Weinbach, N., Neupert, W., and Westermann, B. (2002). Genetic basis of mitochondrial function and morphology in *Saccharomyces cerevisiae*. Mol Biol Cell *13*, 847-853.

Dimmer, K.S., Jakobs, S., Vogel, F., Altmann, K., and Westermann, B. (2005). Mdm31 and Mdm32 are inner membrane proteins required for maintenance of mitochondrial shape and stability of mitochondrial DNA nucleoids in yeast. J Cell Biol *168*, 103-115.

Dimmer, K.S., Papic, D., Schumann, B., Sperl, D., Krumpe, K., Walther, D.M., and Rapaport, D. (2012). A crucial role for Mim2 in the biogenesis of mitochondrial outer membrane proteins. J Cell Sci *125*, 3464-3473.

Dimmer, K.S., and Rapaport, D. (2012). Unresolved mysteries in the biogenesis of mitochondrial membrane proteins. Biochim Biophys Acta *1818*, 1085-1090.

Dolezal, P., Likic, V., Tachezy, J., and Lithgow, T. (2006). Evolution of the molecular machines for protein import into mitochondria. Science *313*, 314-318.

Drago, I., Pizzo, P., and Pozzan, T. (2011). After half a century mitochondrial calcium in- and efflux machineries reveal themselves. EMBO J *30*, 4119-4125.

Dukanovic, J., Dimmer, K.S., Bonnefoy, N., Krumpe, K., and Rapaport, D. (2009). Genetic and functional interactions between the mitochondrial outer membrane proteins Tom6 and Sam37. Mol Cell Biol *29*, 5975-5988.

Dukanovic, J., and Rapaport, D. (2011). Multiple pathways in the integration of proteins into the mitochondrial outer membrane. Biochim Biophys Acta *1808*, 971-980.

Dyall, S.D., Koehler, C.M., Delgadillo-Correa, M.G., Bradley, P.J., Plumper, E., Leuenberger, D., Turck, C.W., and Johnson, P.J. (2000). Presence of a member of the mitochondrial carrier family in hydrogenosomes: conservation of membrane-targeting pathways between hydrogenosomes and mitochondria. Mol Cell Biol *20*, 2488-2497.

Egan, B., Beilharz, T., George, R., Isenmann, S., Gratzer, S., Wattenberg, B., and Lithgow, T. (1999). Targeting of tail-anchored proteins to yeast mitochondria in vivo. FEBS Lett *451*, 243-248.

Embley, T.M., and Martin, W. (2006). Eukaryotic evolution, changes and challenges. Nature *440*, 623-630.

Embley, T.M., van der Giezen, M., Horner, D.S., Dyal, P.L., and Foster, P. (2003). Mitochondria and hydrogenosomes are two forms of the same fundamental organelle. Philos Trans R Soc Lond B Biol Sci *358*, 191-201; discussion 201-192.

Endo, T., and Kohda, D. (2002). Functions of outer membrane receptors in mitochondrial protein import. Biochim Biophys Acta *1592*, 3-14.

Endo, T., and Yamano, K. (2010). Transport of proteins across or into the mitochondrial outer membrane. Biochim Biophys Acta *1803*, 706-714.

Endo, T., Yamano, K., and Kawano, S. (2010). Structural basis for the disulfide relay system in the mitochondrial intermembrane space. Antioxid Redox Signal *13*, 1359-1373.

Endo, T., Yamano, K., and Kawano, S. (2011). Structural insight into the mitochondrial protein import system. Biochim Biophys Acta *1808*, 955-970.

Esaki, M., Kanamori, T., Nishikawa, S., Shin, I., Schultz, P.G., and Endo, T. (2003). Tom40 protein import channel binds to non-native proteins and prevents their aggregation. Nat Struct Biol *10*, 988-994.

Escobar-Henriques, M., Westermann, B., and Langer, T. (2006). Regulation of mitochondrial fusion by the F-box protein Mdm30 involves proteasome-independent turnover of Fzo1. J Cell Biol *173*, 645-650.

Esser, C., Ahmadinejad, N., Wiegand, C., Rotte, C., Sebastiani, F., Gelius-Dietrich, G., Henze, K., Kretschmann, E., Richly, E., Leister, D., Bryant, D., Steel, M.A., Lockhart, P.J., Penny, D., and Martin, W. (2004). A genome phylogeny for mitochondria among alpha-proteobacteria and a predominantly eubacterial ancestry of yeast nuclear genes. Mol Biol Evol *21*, 1643-1660.

Fan, A.C., Bhangoo, M.K., and Young, J.C. (2006). Hsp90 functions in the targeting and outer membrane translocation steps of Tom70-mediated mitochondrial import. J Biol Chem *281*, 33313-33324.

Feagin, J.E. (2000). Mitochondrial genome diversity in parasites. Int J Parasitol *30*, 371-390.

Filosto, M., Scarpelli, M., Cotelli, M.S., Vielmi, V., Todeschini, A., Gregorelli, V., Tonin, P., Tomelleri, G., and Padovani, A. (2011). The role of mitochondria in neurodegenerative diseases. J Neurol *258*, 1763-1774.

Fitzpatrick, D.A., Creevey, C.J., and McInerney, J.O. (2006). Genome phylogenies indicate a meaningful alpha-proteobacterial phylogeny and support a grouping of the mitochondria with the *Rickettsiales*. Mol Biol Evol *23*, 74-85.

Forterre, P. (2011). A new fusion hypothesis for the origin of Eukarya: better than previous ones, but probably also wrong. Res Microbiol *162*, 77-91.

Foster, P.G., Cox, C.J., and Embley, T.M. (2009). The primary divisions of life: a phylogenomic approach employing composition-heterogeneous methods. Philos Trans R Soc Lond B Biol Sci *364*, 2197-2207.

Frederick, R.L., McCaffery, J.M., Cunningham, K.W., Okamoto, K., and Shaw, J.M. (2004). Yeast Miro GTPase, Gem1p, regulates mitochondrial morphology via a novel pathway. J Cell Biol *167*, 87-98.

Friedman, J.R., Lackner, L.L., West, M., DiBenedetto, J.R., Nunnari, J., and Voeltz, G.K. (2011). ER tubules mark sites of mitochondrial division. Science *334*, 358-362.

Fuchs, F., Prokisch, H., Neupert, W., and Westermann, B. (2002). Interaction of mitochondria with microtubules in the filamentous fungus *Neurospora crassa*. J Cell Sci *115*, 1931-1937.

Fujiki, M., and Verner, K. (1993). Coupling of cytosolic protein synthesis and mitochondrial protein import in yeast. Evidence for cotranslational import in vivo. J Biol Chem *268*, 1914-1920.

Funes, S., Nargang, F.E., Neupert, W., and Herrmann, J.M. (2004). The Oxa2 protein of Neurospora crassa plays a critical role in the biogenesis of cytochrome oxidase and defines a ubiquitous subbranch of the Oxa1/YidC/Alb3 protein family. Mol Biol Cell *15*, 1853-1861.

Gabaldon, T., Snel, B., van Zimmeren, F., Hemrika, W., Tabak, H., and Huynen, M.A. (2006). Origin and evolution of the peroxisomal proteome. Biology direct *1*, 8.

Gabriel, K., Buchanan, S.K., and Lithgow, T. (2001). The alpha and the beta: protein translocation across mitochondrial and plastid outer membranes. Trends Biochem Sci *26*, 36-40.

Gabriel, K., Egan, B., and Lithgow, T. (2003). Tom40, the import channel of the mitochondrial outer membrane, plays an active role in sorting imported proteins. EMBO J *22*, 2380-2386.

Garcia, M., Delaveau, T., Goussard, S., and Jacq, C. (2010). Mitochondrial presequence and open reading frame mediate asymmetric localization of messenger RNA. EMBO Rep *11*, 285-291.

Gebert, N., Joshi, A.S., Kutik, S., Becker, T., McKenzie, M., Guan, X.L., Mooga, V.P., Stroud, D.A., Kulkarni, G., Wenk, M.R., Rehling, P., Meisinger, C., Ryan, M.T., Wiedemann, N., Greenberg, M.L., and Pfanner, N. (2009). Mitochondrial cardiolipin involved in outer-membrane protein biogenesis: implications for Barth syndrome. Curr Biol *19*, 2133-2139.

Gebert, N., Ryan, M.T., Pfanner, N., Wiedemann, N., and Stojanovski, D. (2011). Mitochondrial protein import machineries and lipids: a functional connection. Biochim Biophys Acta *1808*, 1002-1011.

Gentle, I., Gabriel, K., Beech, P., Waller, R., and Lithgow, T. (2004). The Omp85 family of proteins is essential for outer membrane biogenesis in mitochondria and bacteria. J Cell Biol *164*, 19-24.

Gentle, I.E., Perry, A.J., Alcock, F.H., Likic, V.A., Dolezal, P., Ng, E.T., Purcell, A.W., McConnville, M., Naderer, T., Chanez, A.L., Charriere, F., Aschinger, C., Schneider, A., Tokatlidis, K., and Lithgow, T. (2007). Conserved motifs reveal details of ancestry and structure in the small TIM chaperones of the mitochondrial intermembrane space. Mol Biol Evol *24*, 1149-1160.

Gessmann, D., Flinner, N., Pfannstiel, J., Schlosinger, A., Schleiff, E., Nussberger, S., and Mirus, O. (2011). Structural elements of the mitochondrial preprotein-conducting channel Tom40 dissolved by bioinformatics and mass spectrometry. Biochim Biophys Acta *1807*, 1647-1657.

Grad, L.I., Descheneau, A.T., Neupert, W., Lill, R., and Nargang, F.E. (1999). Inactivation of the Neurospora crassa mitochondrial outer membrane protein TOM70 by repeat-induced point mutation (RIP) causes defects in mitochondrial protein import and morphology. Curr Genet *36*, 137-146.

Gratzer, S., Lithgow, T., Bauer, R.E., Lamping, E., Paltauf, F., Kohlwein, S.D., Haucke, V., Junne, T., Schatz, G., and Horst, M. (1995). Mas37p, a novel receptor subunit for protein import into mitochondria. J Cell Biol *129*, 25-34.

Gray, M.W., Burger, G., and Lang, B.F. (1999). Mitochondrial evolution. Science *283*, 1476-1481.

Gray, M.W., Lang, B.F., and Burger, G. (2004). Mitochondria of protists. Annu Rev Genet *38*, 477-524.

Grimm, S. (2012). The ER-mitochondria interface: the social network of cell death. Biochim Biophys Acta *1823*, 327-334.

Gross, J., and Bhattacharya, D. (2009). Mitochondrial and plastid evolution in eukaryotes: an outsiders' perspective. Nat Rev Genet *10*, 495-505.

Gross, J., and Bhattacharya, D. (2011). Endosymbiont or host: who drove mitochondrial and plastid evolution? Biology direct *6*, 12.

Habib, S.J., Waizenegger, T., Lech, M., Neupert, W., and Rapaport, D. (2005). Assembly of the TOB complex of mitochondria. J Biol Chem *280*, 6434-6440.

Habib, S.J., Waizenegger, T., Niewienda, A., Paschen, S.A., Neupert, W., and Rapaport, D. (2007). The N-terminal domain of Tob55 has a receptor-like function in the biogenesis of mitochondrial beta-barrel proteins. J Cell Biol *176*, 77-88.

Hachiya, N., Mihara, K., Suda, K., Horst, M., Schatz, G., and Lithgow, T. (1995). Reconstitution of the initial steps of mitochondrial protein import. Nature *376*, 705-709.

Hackstein, J.H., Tjaden, J., and Huynen, M. (2006). Mitochondria, hydrogenosomes and mitosomes: products of evolutionary tinkering! Curr Genet *50*, 225-245.

Hallermayer, G., and Neupert, W. (1974). Lipid composition of mitochondrial outer and inner membranes of *Neurospora crassa*. Hoppe-Seyler's Zeitschrift fur physiologische Chemie *355*, 279-288.

Hammermeister, M., Schodel, K., and Westermann, B. (2010). Mdm36 is a mitochondrial fission-promoting protein in *Saccharomyces cerevisiae*. Mol Biol Cell *21*, 2443-2452.

Harkness, T.A., Metzenberg, R.L., Schneider, H., Lill, R., Neupert, W., and Nargang, F.E. (1994a). Inactivation of the *Neurospora crassa* gene encoding the mitochondrial protein import receptor MOM19 by the technique of "sheltered RIP". Genetics *136*, 107-118.

Harkness, T.A., Nargang, F.E., van der Klei, I., Neupert, W., and Lill, R. (1994b). A crucial role of the mitochondrial protein import receptor MOM19 for the biogenesis of mitochondria. J Cell Biol *124*, 637-648.

Harman, D. (1956). Aging: a theory based on free radical and radiation chemistry. Journal of gerontology *11*, 298-300.

Harman, D. (1972). The biologic clock: the mitochondria? J Am Geriatr Soc *20*, 145-147.

Harner, M., Korner, C., Walther, D., Mokranjac, D., Kaesmacher, J., Welsch, U., Griffith, J., Mann, M., Reggiori, F., and Neupert, W. (2011). The mitochondrial contact site complex, a determinant of mitochondrial architecture. EMBO J *30*, 4356-4370.

Harsman, A., Niemann, M., Pusnik, M., Schmidt, O., Burmann, B.M., Hiller, S., Meisinger, C., Schneider, A., and Wagner, R. (2012). Bacterial origin of a mitochondrial outer membrane protein translocase: new perspectives from comparative single channel electrophysiology. J Biol Chem *287*, 31437-31445.

Hase, T., Muller, U., Riezman, H., and Schatz, G. (1984). A 70-kd protein of the yeast mitochondrial outer membrane is targeted and anchored via its extreme amino terminus. EMBO J *3*, 3157-3164.

Haucke, V., Lithgow, T., Rospert, S., Hahne, K., and Schatz, G. (1995). The yeast mitochondrial protein import receptor Mas20p binds precursor proteins through electrostatic interaction with the positively charged presequence. J Biol Chem *270*, 5565-5570.

Hayashi, T., Rizzuto, R., Hajnoczky, G., and Su, T.P. (2009). MAM: more than just a housekeeper. Trends Cell Biol *19*, 81-88.

He, S., and Fox, T.D. (1997). Membrane translocation of mitochondrially coded Cox2p: distinct requirements for export of N and C termini and dependence on the conserved protein Oxa1p. Mol Biol Cell *8*, 1449-1460.

Heggeness, M.H., Simon, M., and Singer, S.J. (1978). Association of mitochondria with microtubules in cultured cells. Proc Natl Acad Sci U S A *75*, 3863-3866.

Heinz, E., and Lithgow, T. (2013). Back to basics: A revealing secondary reduction of the mitochondrial protein import pathway in diverse intracellular parasites. Biochimica et Biophysica Acta (BBA) - Molecular Cell Research *1833*, 295-303.

Hell, K., Neupert, W., and Stuart, R.A. (2001). Oxa1p acts as a general membrane insertion machinery for proteins encoded by mitochondrial DNA. EMBO J *20*, 1281-1288.

Hermann, G.J., King, E.J., and Shaw, J.M. (1997). The yeast gene, MDM20, is necessary for mitochondrial inheritance and organization of the actin cytoskeleton. J Cell Biol *137*, 141-153.

Herrmann, J.M., and Kohl, R. (2007). Catch me if you can! Oxidative protein trapping in the intermembrane space of mitochondria. J Cell Biol *176*, 559-563.

Herrmann, J.M., Neupert, W., and Stuart, R.A. (1997). Insertion into the mitochondrial inner membrane of a polytopic protein, the nuclear-encoded Oxa1p. EMBO J *16*, 2217-2226.

Herrmann, J.M., and Riemer, J. (2012). Mitochondrial disulfide relay: redox-regulated protein import into the intermembrane space. J Biol Chem *287*, 4426-4433.

Hewitt, V., Alcock, F., and Lithgow, T. (2011). Minor modifications and major adaptations: the evolution of molecular machines driving mitochondrial protein import. Biochim Biophys Acta *1808*, 947-954.

Hewitt, V.L., Heinz, E., Shingu-Vazquez, M., Qu, Y., Jelicic, B., Lo, T.L., Beilharz, T.H., Dumsday, G., Gabriel, K., Traven, A., and Lithgow, T. (2012). A model system for mitochondrial biogenesis reveals evolutionary rewiring of protein import and membrane assembly pathways. Proc Natl Acad Sci U S A *109*, E3358-3366.

Hill, K., Model, K., Ryan, M.T., Dietmeier, K., Martin, F., Wagner, R., and Pfanner, N. (1998). Tom40 forms the hydrophilic channel of the mitochondrial import pore for preproteins [see comment]. Nature *395*, 516-521.

Hiller, S., Abramson, J., Mannella, C., Wagner, G., and Zeth, K. (2010). The 3D structures of VDAC represent a native conformation. Trends Biochem Sci *35*, 514-521.

Hines, V., Brandt, A., Griffiths, G., Horstmann, H., Brutsch, H., and Schatz, G. (1990). Protein import into yeast mitochondria is accelerated by the outer membrane protein MAS70. EMBO J *9*, 3191-3200.

Honlinger, A., Bomer, U., Alconada, A., Eckerskorn, C., Lottspeich, F., Dietmeier, K., and Pfanner, N. (1996). Tom7 modulates the dynamics of the mitochondrial outer membrane translocase and plays a pathway-related role in protein import. EMBO J *15*, 2125-2137.

Hoppins, S., Collins, S.R., Cassidy-Stone, A., Hummel, E., Devay, R.M., Lackner, L.L., Westermann, B., Schuldiner, M., Weissman, J.S., and Nunnari, J. (2011). A mitochondrial-focused genetic interaction map reveals a scaffold-like complex required for inner membrane organization in mitochondria. J Cell Biol *195*, 323-340.

Hoppins, S., Lackner, L., and Nunnari, J. (2007a). The machines that divide and fuse mitochondria. Annu Rev Biochem *76*, 751-780.

Hoppins, S., and Nunnari, J. (2009). The molecular mechanism of mitochondrial fusion. Biochim Biophys Acta *1793*, 20-26.

Hoppins, S.C., Go, N.E., Klein, A., Schmitt, S., Neupert, W., Rapaport, D., and Nargang, F.E. (2007b). Alternative splicing gives rise to different isoforms of the *Neurospora crassa* Tob55 protein that vary in their ability to insert beta-barrel proteins into the outer mitochondrial membrane. Genetics *177*, 137-149.

Hoppins, S.C., and Nargang, F.E. (2004). The Tim8-Tim13 complex of Neurospora crassa functions in the assembly of proteins into both mitochondrial membranes. J Biol Chem *279*, 12396-12405.

Horie, C., Suzuki, H., Sakaguchi, M., and Mihara, K. (2003). Targeting and assembly of mitochondrial tail-anchored protein Tom5 to the TOM complex depend on a signal distinct from that of tail-anchored proteins dispersed in the membrane. J Biol Chem *278*, 41462-41471.

Horiike, T., Hamada, K., Kanaya, S., and Shinozawa, T. (2001). Origin of eukaryotic cell nuclei by symbiosis of Archaea in Bacteria is revealed by homology-hit analysis. Nat Cell Biol *3*, 210-214.

Hulett, J.M., Lueder, F., Chan, N.C., Perry, A.J., Wolynec, P., Likic, V.A., Gooley, P.R., and Lithgow, T. (2008). The transmembrane segment of Tom20 is recognized by Mim1 for docking to the mitochondrial TOM complex. J Mol Biol *376*, 694-704.

Humphries, A.D., Streimann, I.C., Stojanovski, D., Johnston, A.J., Yano, M., Hoogenraad, N.J., and Ryan, M.T. (2005). Dissection of the mitochondrial import and assembly pathway for human Tom40. J Biol Chem *280*, 11535-11543.

Imai, K., Gromiha, M.M., and Horton, P. (2008). Mitochondrial beta-barrel proteins, an exclusive club? Cell *135*, 1158-1159; author reply 1159-1160.

Ishikawa, D., Yamamoto, H., Tamura, Y., Moritoh, K., and Endo, T. (2004). Two novel proteins in the mitochondrial outer membrane mediate beta-barrel protein assembly. J Cell Biol *166*, 621-627.

Jazwinski, S.M. (2013). The retrograde response: when mitochondrial quality control is not enough. Biochim Biophys Acta *1833*, 400-409.

Jiang, J.H., Davies, J.K., Lithgow, T., Strugnell, R.A., and Gabriel, K. (2011). Targeting of Neisserial PorB to the mitochondrial outer membrane: an insight on the evolution of beta-barrel protein assembly machines. Mol Microbiol *82*, 976-987.

Jiang, J.H., Tong, J., Tan, K.S., and Gabriel, K. (2012). From Evolution to Pathogenesis: The Link Between beta-Barrel Assembly Machineries in the Outer Membrane of Mitochondria and Gram-Negative Bacteria. International journal of molecular sciences *13*, 8038-8050.

Jin, S.M., and Youle, R.J. (2012). PINK1- and Parkin-mediated mitophagy at a glance. J Cell Sci *125*, 795-799.

John, G.B., Shang, Y., Li, L., Renken, C., Mannella, C.A., Selker, J.M., Rangell, L., Bennett, M.J., and Zha, J. (2005). The mitochondrial inner membrane protein mitofilin controls cristae morphology. Mol Biol Cell *16*, 1543-1554.

Johnson, A.E., and Jensen, R.E. (2004). Barreling through the membrane. Nat Struct Mol Biol *11*, 113-114.

Kadokura, H., Tian, H., Zander, T., Bardwell, J.C., and Beckwith, J. (2004). Snapshots of DsbA in action: detection of proteins in the process of oxidative folding. Science *303*, 534-537.

Kaneko, T., Nakamura, Y., Sato, S., Asamizu, E., Kato, T., Sasamoto, S., Watanabe, A., Idesawa, K., Ishikawa, A., Kawashima, K., Kimura, T., Kishida, Y., Kiyokawa, C., Kohara, M., Matsumoto, M., Matsuno, A., Mochizuki, Y., Nakayama, S., Nakazaki, N., Shimpo, S., Sugimoto, M., Takeuchi, C., Yamada, M., and Tabata, S. (2000). Complete genome structure of the nitrogen-fixing symbiotic bacterium *Mesorhizobium loti*. DNA research : an international journal for rapid publication of reports on genes and genomes *7*, 331-338.

Karlberg, O., Canback, B., Kurland, C.G., and Andersson, S.G. (2000). The dual origin of the yeast mitochondrial proteome. Yeast *17*, 170-187.

Kato, A., Kurashima, K., Chae, M., Sawada, S., Hatakeyama, S., Tanaka, S., and Inoue, H. (2010). Deletion of a novel F-box protein, MUS-10, in *Neurospora crassa* leads to

altered mitochondrial morphology, instability of mtDNA and senescence. Genetics *185*, 1257-1269.

Kato, H., and Mihara, K. (2008). Identification of Tom5 and Tom6 in the preprotein translocase complex of human mitochondrial outer membrane. Biochem Biophys Res Commun *369*, 958-963.

Keeping, A., Deabreu, D., Dibernardo, M., and Collins, R.A. (2011). Gel-based mass spectrometric and computational approaches to the mitochondrial proteome of Neurospora. Fungal Genet Biol *48*, 526-536.

Kemper, C., Habib, S.J., Engl, G., Heckmeyer, P., Dimmer, K.S., and Rapaport, D. (2008). Integration of tail-anchored proteins into the mitochondrial outer membrane does not require any known import components. J Cell Sci *121*, 1990-1998.

Kerscher, O., Holder, J., Srinivasan, M., Leung, R.S., and Jensen, R.E. (1997). The Tim54p-Tim22p complex mediates insertion of proteins into the mitochondrial inner membrane. J Cell Biol *139*, 1663-1675.

Khachane, A.N., Timmis, K.N., and Martins dos Santos, V.A. (2007). Dynamics of reductive genome evolution in mitochondria and obligate intracellular microbes. Mol Biol Evol *24*, 449-456.

Kiebler, M., Keil, P., Schneider, H., van der Klei, I.J., Pfanner, N., and Neupert, W. (1993). The mitochondrial receptor complex: a central role of MOM22 in mediating preprotein transfer from receptors to the general insertion pore. Cell *74*, 483-492.

Kiebler, M., Pfaller, R., Sollner, T., Griffiths, G., Horstmann, H., Pfanner, N., and Neupert, W. (1990). Identification of a mitochondrial receptor complex required for recognition and membrane insertion of precursor proteins. Nature *348*, 610-616.

Klein, A., Israel, L., Lackey, S.W., Nargang, F.E., Imhof, A., Baumeister, W., Neupert, W., and Thomas, D.R. (2012). Characterization of the insertase for beta-barrel proteins of the outer mitochondrial membrane. J Cell Biol *199*, 599-611.

Koehler, C.M., Jarosch, E., Tokatlidis, K., Schmid, K., Schweyen, R.J., and Schatz, G. (1998a). Import of mitochondrial carriers mediated by essential proteins of the intermembrane space. Science *279*, 369-373.

Koehler, C.M., Merchant, S., Oppliger, W., Schmid, K., Jarosch, E., Dolfini, L., Junne, T., Schatz, G., and Tokatlidis, K. (1998b). Tim9p, an essential partner subunit of Tim10p for the import of mitochondrial carrier proteins. EMBO J *17*, 6477-6486.

Koehler, C.M., Merchant, S., and Schatz, G. (1999). How membrane proteins travel across the mitochondrial intermembrane space. Trends Biochem Sci *24*, 428-432.

Komiya, T., Rospert, S., Koehler, C., Looser, R., Schatz, G., and Mihara, K. (1998). Interaction of mitochondrial targeting signals with acidic receptor domains along the protein import pathway: evidence for the 'acid chain' hypothesis. EMBO J *17*, 3886-3898.

Komiya, T., Rospert, S., Schatz, G., and Mihara, K. (1997). Binding of mitochondrial precursor proteins to the cytoplasmic domains of the import receptors Tom70 and Tom20 is determined by cytoplasmic chaperones. EMBO J *16*, 4267-4275.

Komuro, Y., Miyashita, N., Mori, T., Muneyuki, E., Saitoh, T., Kohda, D., and Sugita, Y. (2013). Energetics of the presequence-binding poses in mitochondrial protein import through Tom20. J Phys Chem B *117*, 2864-2871.

Kondo-Okamoto, N., Shaw, J.M., and Okamoto, K. (2003). Mmm1p spans both the outer and inner mitochondrial membranes and contains distinct domains for targeting and foci formation. J Biol Chem *278*, 48997-49005.

Kondo-Okamoto, N., Shaw, J.M., and Okamoto, K. (2008). Tetratricopeptide repeat proteins Tom70 and Tom71 mediate yeast mitochondrial morphogenesis. EMBO Rep *9*, 63-69.

Koopman, W.J., Willems, P.H., and Smeitink, J.A. (2012). Monogenic mitochondrial disorders. N Engl J Med *366*, 1132-1141.

Korner, C., Barrera, M., Dukanovic, J., Eydt, K., Harner, M., Rabl, R., Vogel, F., Rapaport, D., Neupert, W., and Reichert, A.S. (2012). The C-terminal domain of Fcj1 is required for formation of crista junctions and interacts with the TOB/SAM complex in mitochondria. Mol Biol Cell *23*, 2143-2155.

Kornmann, B., Currie, E., Collins, S.R., Schuldiner, M., Nunnari, J., Weissman, J.S., and Walter, P. (2009). An ER-mitochondria tethering complex revealed by a synthetic biology screen. Science *325*, 477-481.

Kozjak-Pavlovic, V., Ott, C., Gotz, M., and Rudel, T. (2011). *Neisserial* Omp85 protein is selectively recognized and assembled into functional complexes in the outer membrane of human mitochondria. J Biol Chem *286*, 27019-27026.

Kozjak-Pavlovic, V., Ross, K., Benlasfer, N., Kimmig, S., Karlas, A., and Rudel, T. (2007). Conserved roles of Sam50 and metaxins in VDAC biogenesis. EMBO Rep *8*, 576-582.

Kozjak, V., Wiedemann, N., Milenkovic, D., Lohaus, C., Meyer, H.E., Guiard, B., Meisinger, C., and Pfanner, N. (2003). An essential role of Sam50 in the protein sorting and assembly machinery of the mitochondrial outer membrane. J Biol Chem *278*, 48520-48523.

Krayl, M., Lim, J.H., Martin, F., Guiard, B., and Voos, W. (2007). A cooperative action of the ATP-dependent import motor complex and the inner membrane potential drives mitochondrial preprotein import. Mol Cell Biol *27*, 411-425.

Kulp, A., and Kuehn, M.J. (2010). Biological Functions and Biogenesis of Secreted Bacterial Outer Membrane Vesicles. Annual Review of Microbiology, Vol 64, 2010 *64*, 163-184.

Kunkele, K.P., Heins, S., Dembowski, M., Nargang, F.E., Benz, R., Thieffry, M., Walz, J., Lill, R., Nussberger, S., and Neupert, W. (1998). The preprotein translocation channel of the outer membrane of mitochondria. Cell *93*, 1009-1019.

Kurland, C.G., and Andersson, S.G. (2000). Origin and evolution of the mitochondrial proteome. Microbiol Mol Biol Rev *64*, 786-820.

Kuroda, T., Tani, M., Moriguchi, A., Tokunaga, S., Higuchi, T., Kitada, S., and Kuge, O. (2011). FMP30 is required for the maintenance of a normal cardiolipin level and mitochondrial morphology in the absence of mitochondrial phosphatidylethanolamine synthesis. Mol Microbiol *80*, 248-265.

Kutik, S., Stojanovski, D., Becker, L., Becker, T., Meinecke, M., Kruger, V., Prinz, C., Meisinger, C., Guiard, B., Wagner, R., Pfanner, N., and Wiedemann, N. (2008). Dissecting membrane insertion of mitochondrial beta-barrel proteins. Cell *132*, 1011-1024.

Kutik, S., Stroud, D.A., Wiedemann, N., and Pfanner, N. (2009). Evolution of mitochondrial protein biogenesis. Biochim Biophys Acta *1790*, 409-415.

Lackey, S.W., Wideman, J.G., Kennedy, E.K., Go, N.E., and Nargang, F.E. (2011). The *Neurospora crassa* TOB complex: analysis of the topology and function of Tob38 and Tob37. PLoS One *6*, e25650.

Lackner, L.L., and Nunnari, J.M. (2009). The molecular mechanism and cellular functions of mitochondrial division. Biochim Biophys Acta *1792*, 1138-1144.

Lake, J.A., Henderson, E., Oakes, M., and Clark, M.W. (1984). Eocytes: a new ribosome structure indicates a kingdom with a close relationship to eukaryotes. Proc Natl Acad Sci U S A *81*, 3786-3790.

Lake, J.A., and Rivera, M.C. (1994). Was the nucleus the first endosymbiont? Proc Natl Acad Sci U S A *91*, 2880-2881.

Lang, B.F., Burger, G., O'Kelly, C.J., Cedergren, R., Golding, G.B., Lemieux, C., Sankoff, D., Turmel, M., and Gray, M.W. (1997). An ancestral mitochondrial DNA resembling a eubacterial genome in miniature. Nature *387*, 493-497.

Lazarou, M., Jin, S.M., Kane, L.A., and Youle, R.J. (2012). Role of PINK1 binding to the TOM complex and alternate intracellular membranes in recruitment and activation of the E3 ligase Parkin. Dev Cell *22*, 320-333.

Lenaz, G., and Genova, M.L. (2009). Structural and functional organization of the mitochondrial respiratory chain: a dynamic super-assembly. Int J Biochem Cell Biol *41*, 1750-1772.

Likic, V.A., Perry, A., Hulett, J., Derby, M., Traven, A., Waller, R.F., Keeling, P.J., Koehler, C.M., Curran, S.P., Gooley, P.R., and Lithgow, T. (2005). Patterns that define the four domains conserved in known and novel isoforms of the protein import receptor Tom20. J Mol Biol *347*, 81-93.

Lill, R. (2009). Function and biogenesis of iron-sulphur proteins. Nature *460*, 831-838.

Lill, R., and Muhlenhoff, U. (2005). Iron-sulfur-protein biogenesis in eukaryotes. Trends Biochem Sci *30*, 133-141.

Lindmark, D.G., and Muller, M. (1973). Hydrogenosome, a cytoplasmic organelle of the anaerobic flagellate Tritrichomonas foetus, and its role in pyruvate metabolism. J Biol Chem *248*, 7724-7728.

Lithgow, T., Junne, T., Suda, K., Gratzer, S., and Schatz, G. (1994). The mitochondrial outer membrane protein Mas22p is essential for protein import and viability of yeast. Proc Natl Acad Sci U S A *91*, 11973-11977.

Lithgow, T., and Schneider, A. (2010). Evolution of macromolecular import pathways in mitochondria, hydrogenosomes and mitosomes. Philos Trans R Soc Lond B Biol Sci *365*, 799-817.

Liu, Q., D'Silva, P., Walter, W., Marszalek, J., and Craig, E.A. (2003). Regulated cycling of mitochondrial Hsp70 at the protein import channel. Science *300*, 139-141.

Liu, Z., Li, X., Zhao, P., Gui, J., Zheng, W., and Zhang, Y. (2011). Tracing the evolution of the mitochondrial protein import machinery. Computational Biology and Chemistry *35*, 336-340.

Lopez-Garcia, P., and Moreira, D. (1999). Metabolic symbiosis at the origin of eukaryotes. Trends Biochem Sci *24*, 88-93.

Macasev, D., Whelan, J., Newbigin, E., Silva-Filho, M.C., Mulhern, T.D., and Lithgow, T. (2004). Tom22', an 8-kDa trans-site receptor in plants and protozoans, is a conserved feature of the TOM complex that appeared early in the evolution of eukaryotes. Mol Biol Evol *21*, 1557-1564.

Malhotra, K., Sathappa, M., Landin, J.S., Johnson, A.E., and Alder, N.N. (2013). Structural changes in the mitochondrial Tim23 channel are coupled to the proton-motive force. Nat Struct Mol Biol *20*, 965-972.

Malinverni, J.C., Werner, J., Kim, S., Sklar, J.G., Kahne, D., Misra, R., and Silhavy, T.J. (2006). YfiO stabilizes the YaeT complex and is essential for outer membrane protein assembly in *Escherichia coli*. Mol Microbiol *61*, 151-164.

Margulis, L. (1993). Origins of species: acquired genomes and individuality. Biosystems *31*, 121-125.

Martin, W., Hoffmeister, M., Rotte, C., and Henze, K. (2001). An overview of endosymbiotic models for the origins of eukaryotes, their ATP-producing organelles (mitochondria and hydrogenosomes), and their heterotrophic lifestyle. Biol Chem *382*, 1521-1539.

Martin, W., and Koonin, E.V. (2006). Introns and the origin of nucleus-cytosol compartmentalization. Nature *440*, 41-45.

Martin, W., and Muller, M. (1998). The hydrogen hypothesis for the first eukaryote. Nature *392*, 37-41.

Martin, W.F. (2011). Early evolution without a tree of life. Biology direct *6*, 36.

Mayer, A., Nargang, F.E., Neupert, W., and Lill, R. (1995a). MOM22 is a receptor for mitochondrial targeting sequences and cooperates with MOM19. EMBO J *14*, 4204-4211.

Mayer, A., Neupert, W., and Lill, R. (1995b). Mitochondrial protein import: reversible binding of the presequence at the trans side of the outer membrane drives partial translocation and unfolding. Cell *80*, 127-137.

McBride, H., and Scorrano, L. (2013). Mitochondrial dynamics and physiology. Biochim Biophys Acta *1833*, 148-149.

McBride, H.M., Neuspiel, M., and Wasiak, S. (2006). Mitochondria: more than just a powerhouse. Curr Biol *16*, R551-560.

Meineke, B., Engl, G., Kemper, C., Vasiljev-Neumeyer, A., Paulitschke, H., and Rapaport, D. (2008). The outer membrane form of the mitochondrial protein Mcr1 follows a TOM-independent membrane insertion pathway. FEBS Lett *582*, 855-860.

Meisinger, C., Pfannschmidt, S., Rissler, M., Milenkovic, D., Becker, T., Stojanovski, D., Youngman, M.J., Jensen, R.E., Chacinska, A., Guiard, B., Pfanner, N., and Wiedemann, N. (2007). The morphology proteins Mdm12/Mmm1 function in the major beta-barrel assembly pathway of mitochondria. EMBO J *26*, 2229-2239.

Meisinger, C., Rissler, M., Chacinska, A., Szklarz, L.K., Milenkovic, D., Kozjak, V., Schonfisch, B., Lohaus, C., Meyer, H.E., Yaffe, M.P., Guiard, B., Wiedemann, N., and Pfanner, N. (2004). The mitochondrial morphology protein Mdm10 functions in assembly of the preprotein translocase of the outer membrane. Dev Cell *7*, 61-71.

Meisinger, C., Ryan, M.T., Hill, K., Model, K., Lim, J.H., Sickmann, A., Muller, H., Meyer, H.E., Wagner, R., and Pfanner, N. (2001). Protein import channel of the outer mitochondrial membrane: a highly stable Tom40-Tom22 core structure differentially interacts with preproteins, small tom proteins, and import receptors. Mol Cell Biol *21*, 2337-2348.

Meisinger, C., Wiedemann, N., Rissler, M., Strub, A., Milenkovic, D., Schonfisch, B., Muller, H., Kozjak, V., and Pfanner, N. (2006). Mitochondrial protein sorting: differentiation of beta-barrel assembly by Tom7-mediated segregation of Mdm10. J Biol Chem *281*, 22819-22826.

Merklinger, E., Gofman, Y., Kedrov, A., Driessen, A.J., Ben-Tal, N., Shai, Y., and Rapaport, D. (2012). Membrane integration of a mitochondrial signal-anchored protein does not require additional proteinaceous factors. Biochem J *442*, 381-389.

Michel, A.H., and Kornmann, B. (2012). The ERMES complex and ER-mitochondria connections. Biochem Soc Trans *40*, 445-450.

Midzak, A., Rone, M., Aghazadeh, Y., Culty, M., and Papadopoulos, V. (2011). Mitochondrial protein import and the genesis of steroidogenic mitochondria. Molecular and cellular endocrinology *336*, 70-79.

Milenkovic, D., Kozjak, V., Wiedemann, N., Lohaus, C., Meyer, H.E., Guiard, B., Pfanner, N., and Meisinger, C. (2004). Sam35 of the mitochondrial protein sorting and assembly machinery is a peripheral outer membrane protein essential for cell viability. J Biol Chem *279*, 22781-22785.

Millar, D.G., and Shore, G.C. (1993). The signal anchor sequence of mitochondrial Mas70p contains an oligomerization domain. J Biol Chem *268*, 18403-18406.

Miquel, J., Economos, A.C., Fleming, J., and Johnson, J.E., Jr. (1980). Mitochondrial role in cell aging. Exp Gerontol *15*, 575-591.

Moczko, M., Bomer, U., Kubrich, M., Zufall, N., Honlinger, A., and Pfanner, N. (1997). The intermembrane space domain of mitochondrial Tom22 functions as a trans binding site for preproteins with N-terminal targeting sequences. Mol Cell Biol *17*, 6574-6584.

Moczko, M., Ehmann, B., Gartner, F., Honlinger, A., Schafer, E., and Pfanner, N. (1994). Deletion of the receptor MOM19 strongly impairs import of cleavable preproteins into Saccharomyces cerevisiae mitochondria. J Biol Chem *269*, 9045-9051.

Moczko, M., Gartner, F., and Pfanner, N. (1993). The protein import receptor MOM19 of yeast mitochondria. FEBS Lett *326*, 251-254.

Model, K., Meisinger, C., and Kuhlbrandt, W. (2008). Cryo-electron microscopy structure of a yeast mitochondrial preprotein translocase. J Mol Biol *383*, 1049-1057.

Model, K., Meisinger, C., Prinz, T., Wiedemann, N., Truscott, K.N., Pfanner, N., and Ryan, M.T. (2001). Multistep assembly of the protein import channel of the mitochondrial outer membrane. Nat Struct Biol *8*, 361-370.

Model, K., Prinz, T., Ruiz, T., Radermacher, M., Krimmer, T., Kuhlbrandt, W., Pfanner, N., and Meisinger, C. (2002). Protein translocase of the outer mitochondrial membrane: role of import receptors in the structural organization of the TOM complex. J Mol Biol *316*, 657-666.

Mokranjac, D., and Neupert, W. (2010). The many faces of the mitochondrial TIM23 complex. Biochim Biophys Acta *1797*, 1045-1054.

Moreira, D., and Lopez-Garcia, P. (1998). Symbiosis between methanogenic archaea and delta-proteobacteria as the origin of eukaryotes: the syntrophic hypothesis. J Mol Evol *47*, 517-530.

Mossmann, D., Meisinger, C., and Vogtle, F.N. (2012). Processing of mitochondrial presequences. Biochim Biophys Acta *1819*, 1098-1106.

Muller, M. (1993). The hydrogenosome. J Gen Microbiol *139*, 2879-2889.

Muto, T., Obita, T., Abe, Y., Shodai, T., Endo, T., and Kohda, D. (2001). NMR identification of the Tom20 binding segment in mitochondrial presequences. J Mol Biol *306*, 137-143.

Nakai, M., and Endo, T. (1995). Identification of yeast MAS17 encoding the functional counterpart of the mitochondrial receptor complex protein MOM22 of *Neurospora crassa*. FEBS Lett *357*, 202-206.

Nakai, M., Kinoshita, K., and Endo, T. (1995). Mitochondrial receptor complex protein. The intermembrane space domain of yeast MAS17 is not essential for its targeting or function. J Biol Chem *270*, 30571-30575.

Nargang, F.E., Kunkele, K.P., Mayer, A., Ritzel, R.G., Neupert, W., and Lill, R. (1995). 'Sheltered disruption' of *Neurospora crassa* MOM22, an essential component of the mitochondrial protein import complex. EMBO J *14*, 1099-1108.

Nargang, F.E., Rapaport, D., Ritzel, R.G., Neupert, W., and Lill, R. (1998). Role of the negative charges in the cytosolic domain of TOM22 in the import of precursor proteins into mitochondria. Mol Cell Biol *18*, 3173-3181.

Neupert, W., and Brunner, M. (2002). The protein import motor of mitochondria. Nat Rev Mol Cell Biol *3*, 555-565.

Neupert, W., and Herrmann, J.M. (2007). Translocation of proteins into mitochondria. Annu Rev Biochem *76*, 723-749.

Neuspiel, M., Schauss, A.C., Braschi, E., Zunino, R., Rippstein, P., Rachubinski, R.A., Andrade-Navarro, M.A., and McBride, H.M. (2008). Cargo-selected transport from the mitochondria to peroxisomes is mediated by vesicular carriers. Curr Biol *18*, 102-108.

Nicastro, D., Frangakis, A.S., Typke, D., and Baumeister, W. (2000). Cryo-electron tomography of *Neurospora* mitochondria. J Struct Biol *129*, 48-56.

Noinaj, N., Kuszak, A.J., Gumbart, J.C., Lukacik, P., Chang, H., Easley, N.C., Lithgow, T., and Buchanan, S.K. (2013). Structural insight into the biogenesis of beta-barrel membrane proteins. Nature.

Nunnari, J., and Suomalainen, A. (2012). Mitochondria: in sickness and in health. Cell *148*, 1145-1159.

O'Malley, M.A. (2010). The first eukaryote cell: an unfinished history of contestation. Studies in history and philosophy of biological and biomedical sciences *41*, 212-224.

Obita, T., Muto, T., Endo, T., and Kohda, D. (2003). Peptide library approach with a disulfide tether to refine the Tom20 recognition motif in mitochondrial presequences. J Mol Biol *328*, 495-504.

Okamoto, K., Brinker, A., Paschen, S.A., Moarefi, I., Hayer-Hartl, M., Neupert, W., and Brunner, M. (2002). The protein import motor of mitochondria: a targeted molecular ratchet driving unfolding and translocation. EMBO J *21*, 3659-3671.

Okamoto, K., and Shaw, J.M. (2005). Mitochondrial morphology and dynamics in yeast and multicellular eukaryotes. Annu Rev Genet *39*, 503-536.

Osman, C., Haag, M., Potting, C., Rodenfels, J., Dip, P.V., Wieland, F.T., Brugger, B., Westermann, B., and Langer, T. (2009). The genetic interactome of prohibitins: coordinated control of cardiolipin and phosphatidylethanolamine by conserved regulators in mitochondria. J Cell Biol *184*, 583-596.

Osman, C., Voelker, D.R., and Langer, T. (2011). Making heads or tails of phospholipids in mitochondria. J Cell Biol *192*, 7-16.

Ota, K., Kito, K., Okada, S., and Ito, T. (2008). A proteomic screen reveals the mitochondrial outer membrane protein Mdm34p as an essential target of the F-box protein Mdm30p. Genes Cells *13*, 1075-1085.

Otera, H., Taira, Y., Horie, C., Suzuki, Y., Suzuki, H., Setoguchi, K., Kato, H., Oka, T., and Mihara, K. (2007). A novel insertion pathway of mitochondrial outer membrane proteins with multiple transmembrane segments. J Cell Biol *179*, 1355-1363.

Ott, C., Ross, K., Straub, S., Thiede, B., Gotz, M., Goosmann, C., Krischke, M., Mueller, M.J., Krohne, G., Rudel, T., and Kozjak-Pavlovic, V. (2012). Sam50 functions in mitochondrial intermembrane space bridging and biogenesis of respiratory complexes. Mol Cell Biol *32*, 1173-1188.

Papic, D., Krumpe, K., Dukanovic, J., Dimmer, K.S., and Rapaport, D. (2011). Multispan mitochondrial outer membrane protein Ugo1 follows a unique Mim1-dependent import pathway. J Cell Biol *194*, 397-405.

Paschen, S.A., Neupert, W., and Rapaport, D. (2005). Biogenesis of beta-barrel membrane proteins of mitochondria. Trends Biochem Sci *30*, 575-582.

Paschen, S.A., Rothbauer, U., Kaldi, K., Bauer, M.F., Neupert, W., and Brunner, M. (2000). The role of the TIM8-13 complex in the import of Tim23 into mitochondria. EMBO J *19*, 6392-6400.

Paschen, S.A., Waizenegger, T., Stan, T., Preuss, M., Cyrklaff, M., Hell, K., Rapaport, D., and Neupert, W. (2003). Evolutionary conservation of biogenesis of beta-barrel membrane proteins. Nature *426*, 862-866.

Petrakis, N., Alcock, F., and Tokatlidis, K. (2009). Mitochondrial ATP-independent chaperones. IUBMB Life *61*, 909-914.

Pfanner, N. (2000). Protein sorting: recognizing mitochondrial presequences. Curr Biol *10*, R412-415.

Pfanner, N., and Chacinska, A. (2002). The mitochondrial import machinery: preprotein-conducting channels with binding sites for presequences. Biochim Biophys Acta *1592*, 15-24.

Pfanner, N., Wiedemann, N., Meisinger, C., and Lithgow, T. (2004). Assembling the mitochondrial outer membrane. Nat Struct Mol Biol *11*, 1044-1048.

Piko, L., Hougham, A.J., and Bulpitt, K.J. (1988). Studies of sequence heterogeneity of mitochondrial DNA from rat and mouse tissues: evidence for an increased frequency of deletions/additions with aging. Mech Ageing Dev *43*, 279-293.

Plumper, E., Bradley, P.J., and Johnson, P.J. (2000). Competition and protease sensitivity assays provide evidence for the existence of a hydrogenosomal protein import machinery in *Trichomonas vaginalis*. Mol Biochem Parasitol *106*, 11-20.

Poole, A., and Penny, D. (2001). Does endo-symbiosis explain the origin of the nucleus? Nat Cell Biol *3*, E173-174.

Poole, A., and Penny, D. (2007a). Eukaryote evolution: engulfed by speculation. Nature *447*, 913.

Poole, A.M. (2006). Did group II intron proliferation in an endosymbiont-bearing archaeon create eukaryotes? Biology direct *1*, 36.

Poole, A.M., and Penny, D. (2007b). Evaluating hypotheses for the origin of eukaryotes. Bioessays *29*, 74-84.

Popov-Celeketic, J., Waizenegger, T., and Rapaport, D. (2008). Mim1 functions in an oligomeric form to facilitate the integration of Tom20 into the mitochondrial outer membrane. J Mol Biol *376*, 671-680.

Preuss, M., Ott, M., Funes, S., Luirink, J., and Herrmann, J.M. (2005). Evolution of mitochondrial oxa proteins from bacterial YidC. Inherited and acquired functions of a conserved protein insertion machinery. J Biol Chem *280*, 13004-13011.

Pusnik, M., Schmidt, O., Perry, A.J., Oeljeklaus, S., Niemann, M., Warscheid, B., Lithgow, T., Meisinger, C., and Schneider, A. (2011). Mitochondrial preprotein translocase of trypanosomatids has a bacterial origin. Curr Biol *21*, 1738-1743.

Pusnik, M., Schmidt, O., Perry, A.J., Oeljeklaus, S., Niemann, M., Warscheid, B., Meisinger, C., Lithgow, T., and Schneider, A. (2012). Response to Zarsky et al. Current Biology *22*, R481-R482.

Qiu, J., Wenz, L.S., Zerbes, R.M., Oeljeklaus, S., Bohnert, M., Stroud, D.A., Wirth, C., Ellenrieder, L., Thornton, N., Kutik, S., Wiese, S., Schulze-Specking, A., Zufall, N., Chacinska, A., Guiard, B., Hunte, C., Warscheid, B., van der Laan, M., Pfanner, N., Wiedemann, N., and Becker, T. (2013). Coupling of mitochondrial import and export translocases by receptor-mediated supercomplex formation. Cell *154*, 596-608.

Qu, Y., Jelicic, B., Pettolino, F., Perry, A., Lo, T.L., Hewitt, V.L., Bantun, F., Beilharz, T.H., Peleg, A.Y., Lithgow, T., Djordjevic, J.T., and Traven, A. (2012). Mitochondrial sorting and assembly machinery subunit Sam37 in *Candida albicans*: insight into the roles of mitochondria in fitness, cell wall integrity, and virulence. Eukaryot Cell *11*, 532-544.

Rabl, R., Soubannier, V., Scholz, R., Vogel, F., Mendl, N., Vasiljev-Neumeyer, A., Korner, C., Jagasia, R., Keil, T., Baumeister, W., Cyrklaff, M., Neupert, W., and

Reichert, A.S. (2009). Formation of cristae and crista junctions in mitochondria depends on antagonism between Fcj1 and Su e/g. J Cell Biol *185*, 1047-1063.

Rada, P., Dolezal, P., Jedelsky, P.L., Bursac, D., Perry, A.J., Sedinova, M., Smiskova, K., Novotny, M., Beltran, N.C., Hrdy, I., Lithgow, T., and Tachezy, J. (2011). The core components of organelle biogenesis and membrane transport in the hydrogenosomes of *Trichomonas vaginalis*. PLoS One *6*, e24428.

Ramage, L., Junne, T., Hahne, K., Lithgow, T., and Schatz, G. (1993). Functional cooperation of mitochondrial protein import receptors in yeast. EMBO J *12*, 4115-4123.

Rapaport, D. (2003). Finding the right organelle. Targeting signals in mitochondrial outer-membrane proteins. EMBO Rep *4*, 948-952.

Rapaport, D., Kunkele, K.P., Dembowski, M., Ahting, U., Nargang, F.E., Neupert, W., and Lill, R. (1998). Dynamics of the TOM complex of mitochondria during binding and translocation of preproteins. Mol Cell Biol *18*, 5256-5262.

Rapaport, D., and Neupert, W. (1999). Biogenesis of Tom40, core component of the TOM complex of mitochondria. J Cell Biol *146*, 321-331.

Rapaport, D., Neupert, W., and Lill, R. (1997). Mitochondrial protein import. Tom40 plays a major role in targeting and translocation of preproteins by forming a specific binding site for the presequence. J Biol Chem *272*, 18725-18731.

Rassow, J., Dekker, P.J., van Wilpe, S., Meijer, M., and Soll, J. (1999). The preprotein translocase of the mitochondrial inner membrane: function and evolution. J Mol Biol *286*, 105-120.

Rehling, P., Pfanner, N., and Meisinger, C. (2003). Insertion of hydrophobic membrane proteins into the inner mitochondrial membrane--a guided tour. J Mol Biol *326*, 639-657.

Reichert, A.S., and Neupert, W. (2002). Contact sites between the outer and inner membrane of mitochondria-role in protein transport. Biochim Biophys Acta *1592*, 41-49.

Ribeiro, S., and Golding, G.B. (1998). The mosaic nature of the eukaryotic nucleus. Mol Biol Evol *15*, 779-788.

Rivera, M.C., and Lake, J.A. (2004). The ring of life provides evidence for a genome fusion origin of eukaryotes. Nature *431*, 152-155.

Roesch, K., Curran, S.P., Tranebjaerg, L., and Koehler, C.M. (2002). Human deafness dystonia syndrome is caused by a defect in assembly of the DDP1/TIMM8a-TIMM13 complex. Hum Mol Genet *11*, 477-486.

Rojo, E.E., Stuart, R.A., and Neupert, W. (1995). Conservative sorting of F0-ATPase subunit 9: export from matrix requires delta pH across inner membrane and matrix ATP. EMBO J *14*, 3445-3451.

Ryan, M.T. (2004). Chaperones: inserting beta barrels into membranes. Curr Biol *14*, R207-209.

Ryan, M.T., Muller, H., and Pfanner, N. (1999). Functional staging of ADP/ATP carrier translocation across the outer mitochondrial membrane. J Biol Chem *274*, 20619-20627.

Sagan, L. (1967). On the origin of mitosing cells. J Theor Biol *14*, 255-274.

Saint-Georges, Y., Garcia, M., Delaveau, T., Jourdren, L., Le Crom, S., Lemoine, S., Tanty, V., Devaux, F., and Jacq, C. (2008). Yeast mitochondrial biogenesis: a role for the PUF RNA-binding protein Puf3p in mRNA localization. PLoS One *3*, e2293.

Saitoh, T., Igura, M., Obita, T., Ose, T., Kojima, R., Maenaka, K., Endo, T., and Kohda, D. (2007). Tom20 recognizes mitochondrial presequences through dynamic equilibrium among multiple bound states. EMBO J *26*, 4777-4787.

Saraste, M. (1999). Oxidative phosphorylation at the fin de siecle. Science *283*, 1488-1493.

Schlossmann, J., Lill, R., Neupert, W., and Court, D.A. (1996). Tom71, a novel homologue of the mitochondrial preprotein receptor Tom70. J Biol Chem *271*, 17890-17895.

Schlossmann, J., and Neupert, W. (1995). Assembly of the preprotein receptor MOM72/MAS70 into the protein import complex of the outer membrane of mitochondria. J Biol Chem *270*, 27116-27121.

Schmidt, O., Harbauer, A.B., Rao, S., Eyrich, B., Zahedi, R.P., Stojanovski, D., Schonfisch, B., Guiard, B., Sickmann, A., Pfanner, N., and Meisinger, C. (2011). Regulation of mitochondrial protein import by cytosolic kinases. Cell *144*, 227-239.

Schmidt, O., Pfanner, N., and Meisinger, C. (2010). Mitochondrial protein import: from proteomics to functional mechanisms. Nat Rev Mol Cell Biol *11*, 655-667.

Schmitt, S., Ahting, U., Eichacker, L., Granvogl, B., Go, N.E., Nargang, F.E., Neupert, W., and Nussberger, S. (2005). Role of Tom5 in maintaining the structural stability of the TOM complex of mitochondria. J Biol Chem *280*, 14499-14506.

Schmitt, S., Prokisch, H., Schlunck, T., Camp, D.G., 2nd, Ahting, U., Waizenegger, T., Scharfe, C., Meitinger, T., Imhof, A., Neupert, W., Oefner, P.J., and Rapaport, D. (2006). Proteome analysis of mitochondrial outer membrane from *Neurospora crassa*. Proteomics *6*, 72-80.

Schneiter, R., Brugger, B., Sandhoff, R., Zellnig, G., Leber, A., Lampl, M., Athenstaedt, K., Hrastnik, C., Eder, S., Daum, G., Paltauf, F., Wieland, F.T., and Kohlwein, S.D. (1999). Electrospray ionization tandem mass spectrometry (ESI-MS/MS) analysis of the lipid molecular species composition of yeast subcellular membranes reveals acyl chain-based sorting/remodeling of distinct molecular species en route to the plasma membrane. J Cell Biol *146*, 741-754.

Schon, E.A., and Przedborski, S. (2011). Mitochondria: the next (neurode)generation. Neuron *70*, 1033-1053.

Schulke, N., Sepuri, N.B., Gordon, D.M., Saxena, S., Dancis, A., and Pain, D. (1999). A multisubunit complex of outer and inner mitochondrial membrane protein translocases stabilized in vivo by translocation intermediates. J Biol Chem *274*, 22847-22854.

Schulke, N., Sepuri, N.B., and Pain, D. (1997). In vivo zippering of inner and outer mitochondrial membranes by a stable translocation intermediate. Proc Natl Acad Sci U S A *94*, 7314-7319.

Selkrig, J., Mosbahi, K., Webb, C.T., Belousoff, M.J., Perry, A.J., Wells, T.J., Morris, F., Leyton, D.L., Totsika, M., Phan, M.D., Celik, N., Kelly, M., Oates, C., Hartland, E.L., Robins-Browne, R.M., Ramarathinam, S.H., Purcell, A.W., Schembri, M.A., Strugnell, R.A., Henderson, I.R., Walker, D., and Lithgow, T. (2012). Discovery of an archetypal protein transport system in bacterial outer membranes. Nat Struct Mol Biol *19*, 506-510, S501.

Sesaki, H., and Jensen, R.E. (1999). Division versus fusion: Dnm1p and Fzo1p antagonistically regulate mitochondrial shape. J Cell Biol *147*, 699-706.

Sherman, E.L., Go, N.E., and Nargang, F.E. (2005). Functions of the small proteins in the TOM complex of *Neurospora crassa*. Mol Biol Cell *16*, 4172-4182.

Shiota, T., Mabuchi, H., Tanaka-Yamano, S., Yamano, K., and Endo, T. (2011). In vivo protein-interaction mapping of a mitochondrial translocator protein Tom22 at work. Proc Natl Acad Sci U S A *108*, 15179-15183.

Shiota, T., Maruyama, M., Miura, M., Tamura, Y., Yamano, K., Esaki, M., and Endo, T. (2012). The Tom40 assembly process probed using the attachment of different intramitochondrial sorting signals. Mol Biol Cell *23*, 3936-3947.

Sirrenberg, C., Endres, M., Folsch, H., Stuart, R.A., Neupert, W., and Brunner, M. (1998). Carrier protein import into mitochondria mediated by the intermembrane proteins Tim10/Mrs11 and Tim12/Mrs5. Nature *391*, 912-915.

Sloan, D.B., Alverson, A.J., Chuckalovcak, J.P., Wu, M., McCauley, D.E., Palmer, J.D., and Taylor, D.R. (2012). Rapid evolution of enormous, multichromosomal genomes in flowering plant mitochondria with exceptionally high mutation rates. PLoS Biol *10*, e1001241.

Sogo, L.F., and Yaffe, M.P. (1994). Regulation of mitochondrial morphology and inheritance by Mdm10p, a protein of the mitochondrial outer membrane. J Cell Biol *126*, 1361-1373.

Sollner, T., Griffiths, G., Pfaller, R., Pfanner, N., and Neupert, W. (1989). MOM19, an import receptor for mitochondrial precursor proteins. Cell *59*, 1061-1070.

Soubannier, V., McLelland, G.L., Zunino, R., Braschi, E., Rippstein, P., Fon, E.A., and McBride, H.M. (2012). A vesicular transport pathway shuttles cargo from mitochondria to lysosomes. Curr Biol *22*, 135-141.

Spencer, D.F., Schnare, M.N., and Gray, M.W. (1984). Pronounced structural similarities between the small subunit ribosomal RNA genes of wheat mitochondria and *Escherichia coli*. Proc Natl Acad Sci U S A *81*, 493-497.

Stan, T., Ahting, U., Dembowski, M., Kunkele, K.P., Nussberger, S., Neupert, W., and Rapaport, D. (2000). Recognition of preproteins by the isolated TOM complex of mitochondria. EMBO J *19*, 4895-4902.

Starita, L.M., Lo, R.S., Eng, J.K., von Haller, P.D., and Fields, S. (2012). Sites of ubiquitin attachment in *Saccharomyces cerevisiae*. Proteomics *12*, 236-240.

Steger, H.F., Sollner, T., Kiebler, M., Dietmeier, K.A., Pfaller, R., Trulzsch, K.S., Tropschug, M., Neupert, W., and Pfanner, N. (1990). Import of ADP/ATP carrier into mitochondria: two receptors act in parallel. J Cell Biol *111*, 2353-2363.

Stojanovski, D., Guiard, B., Kozjak-Pavlovic, V., Pfanner, N., and Meisinger, C. (2007). Alternative function for the mitochondrial SAM complex in biogenesis of alpha-helical TOM proteins. J Cell Biol *179*, 881-893.

Stojanovski, D., Muller, J.M., Milenkovic, D., Guiard, B., Pfanner, N., and Chacinska, A. (2008). The MIA system for protein import into the mitochondrial intermembrane space. Biochim Biophys Acta *1783*, 610-617.

Stroud, D.A., Becker, T., Qiu, J., Stojanovski, D., Pfannschmidt, S., Wirth, C., Hunte, C., Guiard, B., Meisinger, C., Pfanner, N., and Wiedemann, N. (2011). Biogenesis of mitochondrial beta-barrel proteins: the POTRA domain is involved in precursor release from the SAM complex. Mol Biol Cell *22*, 2823-2833.

Sutak, R., Dolezal, P., Fiumera, H.L., Hrdy, I., Dancis, A., Delgadillo-Correa, M., Johnson, P.J., Muller, M., and Tachezy, J. (2004). Mitochondrial-type assembly of FeS centers in the hydrogenosomes of the amitochondriate eukaryote *Trichomonas vaginalis*. Proc Natl Acad Sci U S A *101*, 10368-10373.

Tamm, L.K., Arora, A., and Kleinschmidt, J.H. (2001). Structure and assembly of beta-barrel membrane proteins. J Biol Chem *276*, 32399-32402.

Tamm, L.K., Hong, H., and Liang, B. (2004). Folding and assembly of beta-barrel membrane proteins. Biochim Biophys Acta *1666*, 250-263.

Tamura, Y., Endo, T., Iijima, M., and Sesaki, H. (2009). Ups1p and Ups2p antagonistically regulate cardiolipin metabolism in mitochondria. J Cell Biol *185*, 1029-1045.

Taylor, R.D., McHale, B.J., and Nargang, F.E. (2003). Characterization of *Neurospora crassa* Tom40-deficient mutants and effect of specific mutations on Tom40 assembly. J Biol Chem *278*, 765-775.

Terada, K., Kanazawa, M., Yano, M., Hanson, B., Hoogenraad, N., and Mori, M. (1997). Participation of the import receptor Tom20 in protein import into mammalian mitochondria: analyses in vitro and in cultured cells. FEBS Lett *403*, 309-312.

Terziyska, N., Grumbt, B., Bien, M., Neupert, W., Herrmann, J.M., and Hell, K. (2007). The sulfhydryl oxidase Erv1 is a substrate of the Mia40-dependent protein translocation pathway. FEBS Lett *581*, 1098-1102.

Theves, C., Keyser-Tracqui, C., Crubezy, E., Salles, J.P., Ludes, B., and Telmon, N. (2006). Detection and quantification of the age-related point mutation A189G in the human mitochondrial DNA. J Forensic Sci *51*, 865-873.

Thornton, N., Stroud, D.A., Milenkovic, D., Guiard, B., Pfanner, N., and Becker, T. (2010). Two modular forms of the mitochondrial sorting and assembly machinery are involved in biogenesis of alpha-helical outer membrane proteins. J Mol Biol *396*, 540-549.

Tommassen, J. (2007). Biochemistry. Getting into and through the outer membrane. Science *317*, 903-904.

Tong, J., Dolezal, P., Selkrig, J., Crawford, S., Simpson, A.G., Noinaj, N., Buchanan, S.K., Gabriel, K., and Lithgow, T. (2011). Ancestral and derived protein import pathways in the mitochondrion of *Reclinomonas americana*. Mol Biol Evol *28*, 1581-1591.

Toulmay, A., and Prinz, W.A. (2011). Lipid transfer and signaling at organelle contact sites: the tip of the iceberg. Curr Opin Cell Biol *23*, 458-463.

Tovar, J., Fischer, A., and Clark, C.G. (1999). The mitosome, a novel organelle related to mitochondria in the amitochondrial parasite Entamoeba histolytica. Mol Microbiol *32*, 1013-1021.

Tsaousis, A.D., Gaston, D., Stechmann, A., Walker, P.B., Lithgow, T., and Roger, A.J. (2011). A functional Tom70 in the human parasite *Blastocystis sp.*: implications for the evolution of the mitochondrial import apparatus. Mol Biol Evol *28*, 781-791.

Ujwal, R., Cascio, D., Colletier, J.P., Faham, S., Zhang, J., Toro, L., Ping, P., and Abramson, J. (2008). The crystal structure of mouse VDAC1 at 2.3 A resolution reveals mechanistic insights into metabolite gating. Proc Natl Acad Sci U S A *105*, 17742-17747.

Ulrich, T., Gross, L.E., Sommer, M.S., Schleiff, E., and Rapaport, D. (2012). Chloroplast beta-barrel proteins are assembled into the mitochondrial outer membrane in a process that depends on the TOM and TOB complexes. J Biol Chem *287*, 27467-27479.

van der Giezen, M. (2009). Hydrogenosomes and mitosomes: conservation and evolution of functions. J Eukaryot Microbiol *56*, 221-231.

van der Giezen, M., Birdsey, G.M., Horner, D.S., Lucocq, J., Dyal, P.L., Benchimol, M., Danpure, C.J., and Embley, T.M. (2003). Fungal hydrogenosomes contain mitochondrial heat-shock proteins. Mol Biol Evol *20*, 1051-1061.

van der Laan, M., Bohnert, M., Wiedemann, N., and Pfanner, N. (2012). Role of MINOS in mitochondrial membrane architecture and biogenesis. Trends Cell Biol *22*, 185-192.

van der Laan, M., Hutu, D.P., and Rehling, P. (2010). On the mechanism of preprotein import by the mitochondrial presequence translocase. Biochim Biophys Acta *1803*, 732-739.

van Wilpe, S., Ryan, M.T., Hill, K., Maarse, A.C., Meisinger, C., Brix, J., Dekker, P.J., Moczko, M., Wagner, R., Meijer, M., Guiard, B., Honlinger, A., and Pfanner, N. (1999). Tom22 is a multifunctional organizer of the mitochondrial preprotein translocase. Nature *401*, 485-489.

Vesteg, M., and Krajcovic, J. (2011). The falsifiability of the models for the origin of eukaryotes. Curr Genet *57*, 367-390.

Vestweber, D., Brunner, J., Baker, A., and Schatz, G. (1989). A 42K outer-membrane protein is a component of the yeast mitochondrial protein import site. Nature *341*, 205-209.

Vestweber, D., and Schatz, G. (1989). DNA-protein conjugates can enter mitochondria via the protein import pathway. Nature *338*, 170-172.

Vogel, F., Bornhovd, C., Neupert, W., and Reichert, A.S. (2006). Dynamic subcompartmentalization of the mitochondrial inner membrane. J Cell Biol *175*, 237-247.

von der Malsburg, K., Muller, J.M., Bohnert, M., Oeljeklaus, S., Kwiatkowska, P., Becker, T., Loniewska-Lwowska, A., Wiese, S., Rao, S., Milenkovic, D., Hutu, D.P., Zerbes, R.M., Schulze-Specking, A., Meyer, H.E., Martinou, J.C., Rospert, S., Rehling, P., Meisinger, C., Veenhuis, M., Warscheid, B., van der Klei, I.J., Pfanner, N., Chacinska, A., and van der Laan, M. (2011). Dual role of mitofilin in mitochondrial membrane organization and protein biogenesis. Dev Cell *21*, 694-707.

Voulhoux, R., and Tommassen, J. (2004). Omp85, an evolutionarily conserved bacterial protein involved in outer-membrane-protein assembly. Res Microbiol *155*, 129-135.

Wagner, K., Gebert, N., Guiard, B., Brandner, K., Truscott, K.N., Wiedemann, N., Pfanner, N., and Rehling, P. (2008). The assembly pathway of the mitochondrial carrier translocase involves four preprotein translocases. Mol Cell Biol *28*, 4251-4260.

Waizenegger, T., Habib, S.J., Lech, M., Mokranjac, D., Paschen, S.A., Hell, K., Neupert, W., and Rapaport, D. (2004). Tob38, a novel essential component in the biogenesis of beta-barrel proteins of mitochondria. EMBO Rep *5*, 704-709.

Waizenegger, T., Schmitt, S., Zivkovic, J., Neupert, W., and Rapaport, D. (2005). Mim1, a protein required for the assembly of the TOM complex of mitochondria. EMBO Rep *6*, 57-62.

Waizenegger, T., Stan, T., Neupert, W., and Rapaport, D. (2003). Signal-anchor domains of proteins of the outer membrane of mitochondria: structural and functional characteristics. J Biol Chem *278*, 42064-42071.

Walther, D.M., Bos, M.P., Rapaport, D., and Tommassen, J. (2010). The mitochondrial porin, VDAC, has retained the ability to be assembled in the bacterial outer membrane. Mol Biol Evol *27*, 887-895.

Walther, D.M., Papic, D., Bos, M.P., Tommassen, J., and Rapaport, D. (2009a). Signals in bacterial beta-barrel proteins are functional in eukaryotic cells for targeting to and assembly in mitochondria. Proc Natl Acad Sci U S A *106*, 2531-2536.

Walther, D.M., Rapaport, D., and Tommassen, J. (2009b). Biogenesis of beta-barrel membrane proteins in bacteria and eukaryotes: evolutionary conservation and divergence. Cell Mol Life Sci *66*, 2789-2804.

Wang, C., and Youle, R.J. (2009). The role of mitochondria in apoptosis*. Annu Rev Genet *43*, 95-118.

Wattenberg, B., and Lithgow, T. (2001). Targeting of C-terminal (tail)-anchored proteins: understanding how cytoplasmic activities are anchored to intracellular membranes. Traffic *2*, 66-71.

Webb, C.T., Gorman, M.A., Lazarou, M., Ryan, M.T., and Gulbis, J.M. (2006). Crystal structure of the mitochondrial chaperone TIM9.10 reveals a six-bladed alpha-propeller. Mol Cell *21*, 123-133.

Webb, C.T., Heinz, E., and Lithgow, T. (2012). Evolution of the beta-barrel assembly machinery. Trends Microbiol *20*, 612-620.

Weis, B.L., Schleiff, E., and Zerges, W. (2013). Protein targeting to subcellular organelles via MRNA localization. Biochim Biophys Acta *1833*, 260-273.

Wideman, J.G., Go, N.E., Klein, A., Redmond, E., Lackey, S.W., Tao, T., Kalbacher, H., Rapaport, D., Neupert, W., and Nargang, F.E. (2010). Roles of the Mdm10, Tom7, Mdm12, and Mmm1 proteins in the assembly of mitochondrial outer membrane proteins in *Neurospora crassa*. Mol Biol Cell *21*, 1725-1736.

Wideman, J.G., Lackey, S.W., Srayko, M.A., Norton, K.A., and Nargang, F.E. (2013). Analysis of Mutations in *Neurospora crassa* ERMES Components Reveals Specific Functions Related to beta-Barrel Protein Assembly and Maintenance of Mitochondrial Morphology. PLoS One *8*, e71837.

Wiedemann, N., Kozjak, V., Chacinska, A., Schonfisch, B., Rospert, S., Ryan, M.T., Pfanner, N., and Meisinger, C. (2003). Machinery for protein sorting and assembly in the mitochondrial outer membrane. Nature *424*, 565-571.

Wiedemann, N., Truscott, K.N., Pfannschmidt, S., Guiard, B., Meisinger, C., and Pfanner, N. (2004). Biogenesis of the protein import channel Tom40 of the mitochondrial outer membrane: intermembrane space components are involved in an early stage of the assembly pathway. J Biol Chem *279*, 18188-18194.

Woese, C.R., Kandler, O., and Wheelis, M.L. (1990). Towards a natural system of organisms: proposal for the domains Archaea, Bacteria, and Eucarya. Proc Natl Acad Sci U S A *87*, 4576-4579.

Wu, T., Malinverni, J., Ruiz, N., Kim, S., Silhavy, T.J., and Kahne, D. (2005). Identification of a multicomponent complex required for outer membrane biogenesis in *Escherichia coli*. Cell *121*, 235-245.

Xie, J., Marusich, M.F., Souda, P., Whitelegge, J., and Capaldi, R.A. (2007). The mitochondrial inner membrane protein mitofilin exists as a complex with SAM50, metaxins 1 and 2, coiled-coil-helix coiled-coil-helix domain-containing protein 3 and 6 and DnaJC11. FEBS Lett *581*, 3545-3549.

Yaffe, M.P., Harata, D., Verde, F., Eddison, M., Toda, T., and Nurse, P. (1996). Microtubules mediate mitochondrial distribution in fission yeast. Proc Natl Acad Sci U S A *93*, 11664-11668.

Yamamoto, H., Fukui, K., Takahashi, H., Kitamura, S., Shiota, T., Terao, K., Uchida, M., Esaki, M., Nishikawa, S., Yoshihisa, T., Yamano, K., and Endo, T. (2009). Roles of Tom70 in import of presequence-containing mitochondrial proteins. J Biol Chem *284*, 31635-31646.

Yamamoto, H., Itoh, N., Kawano, S., Yatsukawa, Y., Momose, T., Makio, T., Matsunaga, M., Yokota, M., Esaki, M., Shodai, T., Kohda, D., Hobbs, A.E., Jensen, R.E., and Endo, T. (2011). Dual role of the receptor Tom20 in specificity and efficiency of protein import into mitochondria. Proc Natl Acad Sci U S A *108*, 91-96.

Yamano, K., Kuroyanagi-Hasegawa, M., Esaki, M., Yokota, M., and Endo, T. (2008a). Step-size analyses of the mitochondrial Hsp70 import motor reveal the Brownian ratchet in operation. J Biol Chem *283*, 27325-27332.

Yamano, K., Tanaka-Yamano, S., and Endo, T. (2010a). Mdm10 as a dynamic constituent of the TOB/SAM complex directs coordinated assembly of Tom40. EMBO Rep *11*, 187-193.

Yamano, K., Tanaka-Yamano, S., and Endo, T. (2010b). Tom7 regulates Mdm10-mediated assembly of the mitochondrial import channel protein Tom40. J Biol Chem *285*, 41222-41231.

Yamano, K., Yatsukawa, Y., Esaki, M., Hobbs, A.E., Jensen, R.E., and Endo, T. (2008b). Tom20 and Tom22 share the common signal recognition pathway in mitochondrial protein import. J Biol Chem *283*, 3799-3807.

Yang, D., Oyaizu, Y., Oyaizu, H., Olsen, G.J., and Woese, C.R. (1985). Mitochondrial origins. Proc Natl Acad Sci U S A *82*, 4443-4447.

Yano, M., Hoogenraad, N., Terada, K., and Mori, M. (2000). Identification and functional analysis of human Tom22 for protein import into mitochondria. Mol Cell Biol *20*, 7205-7213.

Ylikallio, E., and Suomalainen, A. (2012). Mechanisms of mitochondrial diseases. Annals of medicine *44*, 41-59.

Yoshii, S.R., Kishi, C., Ishihara, N., and Mizushima, N. (2011). Parkin mediates proteasome-dependent protein degradation and rupture of the outer mitochondrial membrane. J Biol Chem *286*, 19630-19640.

Young, J.C., Hoogenraad, N.J., and Hartl, F.U. (2003). Molecular chaperones Hsp90 and Hsp70 deliver preproteins to the mitochondrial import receptor Tom70. Cell *112*, 41-50.

Youngman, M.J., Hobbs, A.E., Burgess, S.M., Srinivasan, M., and Jensen, R.E. (2004). Mmm2p, a mitochondrial outer membrane protein required for yeast mitochondrial shape and maintenance of mtDNA nucleoids. J Cell Biol *164*, 677-688.

Zarsky, V., Tachezy, J., and Dolezal, P. (2012). Tom40 is likely common to all mitochondria. Curr Biol *22*, R479-481; author reply R481-472.

Zerbes, R.M., Bohnert, M., Stroud, D.A., von der Malsburg, K., Kram, A., Oeljeklaus, S., Warscheid, B., Becker, T., Wiedemann, N., Veenhuis, M., van der Klei, I.J., Pfanner, N., and van der Laan, M. (2012). Role of MINOS in mitochondrial membrane architecture: cristae morphology and outer membrane interactions differentially depend on mitofilin domains. J Mol Biol *422*, 183-191.

Zeth, K. (2010). Structure and evolution of mitochondrial outer membrane proteins of beta-barrel topology. Biochim Biophys Acta *1797*, 1292-1299.

Zeth, K., and Thein, M. (2010). Porins in prokaryotes and eukaryotes: common themes and variations. Biochem J *431*, 13-22.

Zillig, W., Klenk, H.P., Palm, P., Puhler, G., Gropp, F., Garrett, R.A., and Leffers, H. (1989). The phylogenetic relations of DNA-dependent RNA polymerases of archaebacteria, eukaryotes, and eubacteria. Canadian journal of microbiology *35*, 73-80.

Zinser, E., Sperka-Gottlieb, C.D., Fasch, E.V., Kohlwein, S.D., Paltauf, F., and Daum, G. (1991). Phospholipid synthesis and lipid composition of subcellular membranes in the unicellular eukaryote Saccharomyces cerevisiae. J Bacteriol *173*, 2026-2034.

Chapter 2. The *Neurospora crassa* TOB complex: analysis of the topology and function of Tob37 and Tob38.

Based on:

Lackey, S.W., Wideman, J.G., Kennedy, E.K., Go, N.E., and Nargang, F.E. (2011). The *Neurospora crassa* TOB complex: analysis of the topology and function of Tob38 and Tob37. PLoS One *6*, e25650.

Note: Creation and testing of ΔTob37 and ΔTob38 sheltered heterokaryon strains as well as construction of His-tagged TOB strains was performed by Go, N.E. (Fig 2.1B, F, 2.4 A-C and 2.5 B). Wideman, J.G. contributed Fig 2.4 A-C,E. Kennedy, E.K. contributed Fig 2.1D and 2.5A.

2.1 Introduction

As mentioned in section 1.6.3 the TOB complex is required for the assembly of MOM β-barrels and several MOM proteins with single C-terminal α-helical TMDs (Kozjak *et al.*, 2003; Paschen *et al.*, 2003; Wiedemann *et al.*, 2003; Ishikawa *et al.*, 2004; Milenkovic *et al.*, 2004; Waizenegger *et al.*, 2004; Stojanovski *et al.*, 2007; Becker *et al.*, 2010; Thornton *et al.*, 2010; Becker *et al.*, 2011). Tob38 is proposed to recognize and bind incoming β-barrel precursors, while Tob37 has roles in β-barrel release from the complex and insertion of C-terminal α-helically anchored MOM proteins, yet little is understood about how these proteins function at the molecular level (Chan and Lithgow, 2008; Imai *et al.*, 2008; Kutik *et al.*, 2008; Dukanovic *et al.*, 2009; Becker *et al.*, 2010; Yamano *et al.*, 2010). Analogous functions of the TOB complex homologues from different organisms are observed despite low sequence identity and variant topologies (notably for Tob37). Theory suggests that functional domains should display a relatively high level of conservation, while non-conserved regions should be prone to increased evolutionary divergence.

Several proteins have been shown to interact with the TOB complex at specific stages during the import of certain precursors including: Mdm10 (Meisinger *et al.*, 2004; Wideman *et al.*, 2010), Mim1 (Stojanovski *et al.*, 2007; Becker *et al.*, 2008; Stroud *et al.*, 2011), Tom40, Tom22 and the small Toms (Becker *et al.*, 2010; Thornton *et al.*, 2010) . The protein-protein interactions between the TOB components and these accessory proteins are thought to be regulated by various mechanisms. However the interactions themselves should occur between specific sites which are defined by the biochemical properties and architecture of the domains. All such domains within the TOB complex required for these interactions and complex function are yet to be defined. Thus, very little is known about the biogenesis and composition of the TOB complex. In this study

we have analyzed the structure and function of the *Neurospora crassa* TOB complex using Tob37 and Tob38 knockouts and specific Tob37 mutants.

As discussed above and in the Introduction (section 1.6.3) studies of the TOB complex in *S. cerevisiae* and mammalian models have resulted in some controversies as to the nature and components of the TOB complex. Therefore, I have set out within this chapter to test a collection of working hypotheses that were developed to help understand the roles of the TOB components. My hypotheses predicted that *N. crassa* Tob37 and Tob38 would both be essential genes and that the protein products of these genes would localize to the cytosolic face of the TOB complex in the MOM. As TOB complex components, Tob37 and Tob38 would function within the complex to facilitate the assembly of TOB dependent substrates, including membrane embedded β-barrels though the actual mechanisms by which assembly is achieved remains poorly understood. Based on *in silico* analysis, I suggest that Tob37 is an integral MOM protein that possesses two C-terminal α-helical trans-membrane domains that are required for localization and association of Tob37 to the MOM/TOB complex. If Tob37 is an integral membrane protein it may aid in the static association of Tob38 to the TOB complex since Tob38 is predicted to be a peripheral membrane protein. If these hypotheses are supported then it might be further expected that disruption or removal of the C-terminal TMDs of Tob37 would adversely influence the activity and stability of the TOB complex.

The results of experiments designed to test the above hypotheses are discussed in the context of these questions and also with respect to new insights and models that arose from the experimental data.

2.2 Materials and Methods

2.2.1 Strains and growth of *N. crassa*

Strains used in this study are listed in Table 2.1. *N. crassa* was grown according to previously described procedures (Davis and De Serres, 1970). Unless otherwise stated, cells were grown at 30° C. Tests of growth rate were performed as described previously (Hoppins *et al.*, 2007) using a standard sorbose medium to induce colonial growth.

2.2.2.Construction of Tob37 and Tob38 knockout strains

A split marker approach was used to knock out the *tob37* and *tob38* genes (Figure S2.1). Approximately three kilobase regions upstream and downstream of the coding sequence for each gene were generated via PCR of cosmids containing the genes, or from genomic DNA. These regions and a PCR product containing a hygromycin resistance cassette were used in the construction of the KO plasmid via recombination in *S. cerevisiae* (strain FY2) using the pRS416 plasmid (see Appendix I). Using PCR the appropriate split markers (Colot *et al.*, 2006) for the genes as described previously for *N. crassa tob55* (Hoppins *et al.*, 2007) were amplified from the KO construct. For each gene, the two portions of the split marker were transformed into heterokaryon HP1 using electroporation (Figure S2.1B) (Nargang *et al.*, 1995; Nargang and Rapaport, 2007). Hygromycin resistant colonies were isolated, purified, and examined for replacement of the *tob37* or *tob38* gene in one of the nuclei of HP1 by Southern analysis (not shown). Strains showing the correct pattern of integration were then examined for growth characteristics. One nucleus of the heterokaryon carries an allele (*mtr*) for resistance to p-fluorophenylalanine (fpa) plus auxotrophy for histidine, while the second carries benomyl resistance (*Bml*) and pantothenate auxotrophy. Transformation of *N. crassa* typically

Table 2.1. Strains used in this study.

Strain (short name)	Genotype	Origin or reference
76-26	*his-3 mtrR a* (*mtrR* imparts fpa resistance)	R.L. Metzenberg
71-18	*pan-2 BmlR a* (*BmlR* imparts benomyl resistance)	R.L. Metzenberg
HP1	Heterokaryon of 76-26 plus 71-18.	Nargang Lab. (Nargang *et al.*, 1995)
Tob37KO- 5 (ΔTob37)	Sheltered heterokaryon. As HP1, but with replacement of *tob37* gene in 76-26 nucleus with a hygromycin resistance (*hygR*) cassette.	Transformation of HP1 with split marker fragments for *tob37* knockout.
Tob38KO-6 (ΔTob38)	Sheltered heterokaryon. As HP1, but with replacement of *tob38* gene in 76-26 nucleus with a hygromycin resistance (*hygR*) cassette.	Transformation of HP1 with split marker fragments for *tob38* knockout.
Tob37HT (9His-Tob37-2)	*his-3 mtrR a Δtob37::hygR* contains an ectopic copy of genomic *tob37* with C-terminal 9x His tag. Bleomycin resistant.	Nargang Lab (Wideman *et al.*, 2010)
Tob38HT (9His-Tob38-3)	*his-3 mtrR a Δtob38::hygR* contains an ectopic copy of genomic *tob38* with C-terminal 9x His tag. Bleomycin resistant.	Nargang Lab (Wideman *et al.*, 2010)
Tob55HT (H6C4-5)	*his-3 mtrR a Δtob55::hygR* contains an ectopic copy of genomic *tob37* with N-terminal 9x His tag. Bleomycin resistant.	Nargang Lab (Wideman *et al.*, 2010)
Tob55 Short HT	*his-3 mtrR a Δtob55::hygR* contains an ectopic copy of N-terminal 9x His tagged *tob55* cDNA specific for the short form.	Nargang Lab
Tob55 Int HT	*his-3 mtrR a Δtob55::hygR* contains an ectopic copy of N-terminal 9x His tagged *tob55* cDNA specific for the intermediate form.	Nargang Lab
Tob55 Long HT	*his-3 mtrR a Δtob55::hygR* contains an ectopic copy of N-terminal 9x His tagged *tob55* cDNA specific for the long form.	Nargang Lab
Tob37ΔTMD1-9	*his-3 mtrR a Δtob37::hygR* contains an ectopic copy of genomic *tob37ΔTMD1*. Bleomycin resistant.	Nargang Lab
Tob37ΔCHD2-3	*his-3 mtrR a Δtob37::hygR* contains an ectopic copy of genomic *tob37ΔCHD*. Bleomycin resistant.	Nargang Lab
Tob37ΔT+C12-5	*his-3 mtrR a Δtob37::hygR* contains an ectopic copy of genomic *tob37ΔT+C*. Bleomycin resistant.	Nargang Lab

occurs in only one nucleus of a multi-nucleate conidium (Grotelueschen and Metzenberg, 1995). To determine which nucleus of the heterokaryotic transformants was transformed by the split marker and carried the knockout, the strains were tested for their ability to grow on medium containing either histidine plus fpa or pantothenate plus benomyl. For isolates with the knockout in the histidine-requiring, fpa-resistant nucleus, the presence of fpa in the growth medium forces the nucleus containing the knockout to predominate numerically in the culture, resulting in a deficiency of Tob37 or Tob38 (Figure S2.1C). If the proteins are required for maximal growth rate, such knockouts should grow slowly under these conditions. One strain showing this phenotype for each gene was chosen for further analysis: for Tob37, strain Tob37KO-5; for Tob38, strain Tob38KO-6.

2.2.3 Creation of strains carrying altered versions of Tob37

Mutant alleles of *tob37* were created by site-directed PCR mutagenesis of a Bluescript plasmid containing the genomic copy of *N. crassa Tob37* and a bleomycin resistance gene (Austin *et al.*, 1990). Mutagenesis was performed to create *Hpa*I restriction sites flanking the regions containing two possible transmembrane domains (TMDs). Following mutagenesis coding regions between amino acid residues 386-405, 424-442, and 386-442 could be removed by *Hpa*I digestion and religation (Figure S2.2). Because of the coding capacity of the restriction sites, the deletions are flanked with Val (GTT) and Asn (AAC) codons. Plasmids confirmed to contain the desired mutations by sequence analysis were linearized and used to transform conidia from the sheltered heterokaryon strain Tob37KO-5.

2.2.4 Transformation of sheltered heterokaryon Tob37KO-5.

DNA was transformed into strain Tob37KO-5 by electroporation of conidia as previously described (Tanton *et al.*, 2003). The transformation mixture was plated on

medium containing histidine and fpa to select for the nucleus bearing the *tob37* knockout, as well as bleomycin to select for transformants carrying the plasmid with altered *tob37* alleles. Transformants were purified through one round of single colony isolation on medium containing fpa, histidine, and bleomycin. Colonies were picked and tested for nutritional requirements. Transformants that required histidine were homokaryons that contained the desired mutant alleles, which must be capable of restoring Tob37 function to a level sufficient for viability. The presence of the correct mutant alleles in the transformants was confirmed by sequencing PCR products of the ectopically integrated *tob37* mutant alleles from isolated genomic DNA.

2.2.5 Mitochondrial Isolation

Unless specified otherwise, mycelia were grown at 30°C, harvested by filtration, and ground in the presence of sand and SEMP isolation buffer (0.25 M sucrose, 10 mM MOPS, pH 7.2, 1 mM EDTA, 1 mM phenylmethylsulfonyl fluoride [PMSF]) using a mortar and pestle. Mitochondria were isolated by differential centrifugation as described previously (Nargang and Rapaport, 2007; Wideman *et al.*, 2010).

2.2.6 Alkaline Extraction

To determine if proteins were integral membrane proteins, alkaline extraction was performed. Mitochondria (50 µg protein) were suspended in 1 ml of 0.1 M sodium carbonate at a chosen pH (between 10.5 and 12.5) and incubated on ice for 1 hr. The mixture was then centrifuged at 50,000 rpm in a TLA55 rotor (Beckman Instruments, Palo Alto, CA) at 4°C for 60 min. The pellets were processed for electrophoresis by adding 50 µl of Laemmli cracking buffer (0.06 M Tris-Cl, pH 6.8, 2.5% SDS, 5% β-mercapto-ethanol, 5% sucrose, 0.01% bromophneol blue (Laemmli, 1970)). Proteins in the supernatant were precipitated in the presence of 7% trichloroacetic acid, centrifuged

as described above, washed with acetone, dried, and processed for electrophoresis as above (Wideman *et al.*, 2010).

2.2.7 Salt treatment of isolated mitochondria

Mitochondria (50 µg protein), were suspended in 50 µl of isolation buffer (0.25M sucrose, 1mM EDTA, 10mM MOPS, (pH 7.2) containing 1 mM PMSF) and 500 mM NaCl and left on ice for 30 min. The sample was then centrifuged at 16,250 x *g* at 4°C for 20 min in a refrigerated microcentrifuge. The mitochondrial pellets were processed for electrophoresis by dissolving in "cracking" buffer (see section 2.2.6). The supernatant was desalted using the Zeba™ Spin Desalting Column system (Pierce Biotechnology – Thermo Scientific, Rockford, IL) and then prepared for electrophoresis by adding one fifth volume of 5X cracking buffer.

2.2.8 Gel electrophoresis of proteins

Proteins were analyzed by sodium dodecyl sulphate polyacrylamide gel electrophoresis (SDS-PAGE) or blue-native gel electrophoresis (BNGE) as described previously (Laemmli, 1970; Schägger and von Jagow, 1991; Schägger *et al.*, 1994) using 30 µg or 50 µg of mitochondrial protein per lane, respectively, unless stated otherwise. For two dimensional electrophoresis, lanes from the first dimension BNGE were excised and soaked in cracking buffer for 5 min. Treated lanes were then placed between the glass gel plates, onto the stacking gel, of a pre-made gel for second dimension SDS-PAGE. Following electrophoresis, gels were transferred to either nitrocellulose or PVDF (polyvinylidene fluoride) membrane and immunodecorated with specific antibodies (Good and Crosby, 1989).

2.2.9 Electrophoretic analysis of affinity purified proteins

Affinity purification of His-tagged proteins was performed as described (Wideman *et al.*, 2010). For BNGE of purified His-tagged proteins, one tenth volume of 10X sample buffer (100 mM bis-Tris, pH 7.0; 500 mM 6-aminocaproic acid; 5% Coomassie brilliant blue G250) was added directly to the elution fractions. These were immediately subjected to BN-PAGE. After electrophoresis gels were transferred to PVDF for Western analysis.

2.2.10 Proteinase K treatment of isolated mitochondria

Isolated mitochondria (50 µg) were suspended in 150 µl of isolation buffer on ice. Following addition of proteinase K (8 µl from a stock solution of 2 mg/ml) the sample was incubated for 15 min on ice. The proteinase K was then inactivated by the addition of 1.5 µl PMSF (200 mM in ethanol) and an additional 340 µl of isolation buffer containing 1 mM PMSF. After gentle mixing the sample was centrifuged at 16,250 x *g* at 4°C for 20 min in a microcentrifuge. The mitochondrial pellets were dissolved in 50 µl of cracking buffer and subjected to SDS-PAGE.

2.2.11 Preparation of damaged mitochondria

To create mitochondria from wild-type cells that were similar to those isolated from strains containing enlarged mitochondria, we used a modified osmotic shock treatment. Isolated wild-type mitochondria in SEMP buffer (500 µg of mitochondrial protein) were pelleted by centrifugation (16,250 × *g*, 15 min, 4°C), resuspended in 1 ml of swelling buffer (1 mM KPO_4, 1 mM EDTA, pH 7.2), and incubated on ice for 30 min. Every 5 min the mitochondria were vortexed at high speed for 10 s. Mitochondria were reisolated by centrifugation (16,250 × *g*, 15 min, 4°C) and resuspended in fresh SEMP. We refer to the mitochondria obtained by this treatment as “damaged” mitochondria (Wideman *et al.*, 2010).

2.2.12 Import of mitochondrial precursor proteins

Import of precursor proteins into isolated mitochondria was performed as previously described (Harkness *et al.*, 1994). To summarize, radiolabelled precursor proteins were produced *in vitro* by transcription and translation in rabbit reticulocyte lysate (Promega TnT reticulocyte lysate system (Madison, WI)) in the presence of [^{35}S] methionine. Following incubation of radiolabelled precursor with isolated mitochondria import reactions were treated with proteinase K, washed and re-isolated to remove any unimported precursors from the mitochondria. The samples were electrophoresed using SDS-PAGE, transferred to nitrocellulose, and analyzed by autoradiography. Study of assembly and import intermediates required mitochondria to be solubilized in 1% digitonin and subjected to BNGE followed by transfer onto polyvinylidene fluoride (PVDF) membrane and visualization by autoradiography. In some cases, import of precursor proteins into mitochondria isolated from mutant strains was quantified. In these cases, bands on x-ray film were scanned and analyzed using Adobe Photoshop. Each experiment included a wild type control which was set as 100 percent. The intensity of the bands obtained using mutant mitochondria were compared to the wild type and a percentage of import was determined. The average and standard deviation were calculated from four independent experiments following 20 min of import.

2.2.13 Presentation of Figures

In some instances irrelevant lanes were removed electronically from blots or gels for the production of figures.

2.3 Results

2.3.1 Development of sheltered heterokaryons harbouring nuclei with knockouts of *tob37* or *tob38*

We generated knockouts of the *N. crassa tob37* and *tob38* genes via transformation of the HP1 heterokaryotic strain using a split marker approach as described previously for *N. crassa tob55* (Figure S2.1 B) (Hoppins *et al.*, 2007). Transformation of one of the two different nuclei in HP1 results in the creation of a sheltered heterokaryon (Figure 2.1 A). As described in the Methods, we chose one strain for each gene where the knockout was in the histidine-requiring (*his-3*), fpa resistant (*mtr*) nucleus. These sheltered heterokaryon strains will hereafter be referred to as ΔTob37 and ΔTob38. Growth of these strains in the presence of histidine and fpa results in a severely reduced growth rate (Figure 2.1B) as the knockout-containing nuclei are forced to predominate the culture to supply resistance to fpa thus reducing the levels of Tob37 or Tob38. Mitochondria isolated from liquid cultures of these strains grown in the presence of histidine and fpa were examined for the presence of various mitochondrial proteins (Figure 2.1C). Reduction of Tob37 in ΔTob37 also resulted in a reduction of the level of Tob38 but reduction of Tob38 in ΔTob38 had only a minor effect on Tob37 levels. This agrees with previous suggestions that Tob37 may be involved in the association of Tob38 with mitochondria or its stability. Both sheltered heterokaryons grown in the presence of histidine and fpa show a reduction in all β-barrel proteins examined (Mdm10, Tob55, Tom40, and porin). Tom5, Tom6, and Tom22 of the outer membrane were also reduced. Slight reductions of the intermembrane space proteins Tim8 and Tim13 were observed. Levels of the inner membrane protein Tim23 and the outer membrane protein Tom70 were unaffected. These observations are consistent with a role for the TOB complex in the import of β-barrel proteins and certain α-helical anchored proteins of the TOM complex. The reduction in the intermembrane space

Figure 2.1. Isolation and characterization of *N. crassa* strains with reduced levels of Tob37 or Tob38. (A) Sheltered heterokaryons with deletions of either *tob37* or *tob38* in one nucleus of the heterokaryon were constructed using a split marker approach (see Figure S2.1 for details). Boxes symbolize heterokaryons while circles within the boxes represent the different component nuclei of the heterokaryon. The Figure shows an example for *tob37*, but the process was identical for *tob38*. The starting heterokaryon (HP1) contained nuclei with different genetic markers: either *his-3* and *mtr* (provides resistance to fpa) or *pan-2* and *Bml* (provides resistance to benomyl). Strains chosen for further work carried the knockouts in the *his-3 mtr* nucleus (see Methods section 2.2.2). (B) Serial dilutions of conidiaspores (actual numbers spotted shown at top of panel) from the strains indicated on the left were spotted onto plates containing either minimal medium (min), which maintains both nuclei of the heterokaryon approximately equally; minimal medium containing pantothenate and benomyl (pan ben), which forces the nucleus carrying benomyl resistance (*Bml*, Figure 2.1A) to predominate the culture; or minimal medium containing histidine plus fpa (his fpa), which forces the nucleus carrying fpa resistance (*mtr*, Figure 2.1A) to predominate the culture. The control was strain HP1. (C) Cells from the indicated strains (top of panel) were grown in the presence of histidine (His) and fpa to force the predominance of the nucleus bearing the deletion of either *tob37* or *tob38*. This results in reduction of the levels of Tob37 or Tob38, respectively. Mitochondria were isolated and subjected to SDS-PAGE followed by transfer to nitrocellulose, and immunodecoration with the antibodies indicated on the left. The control strain was HP1. Multiple bands in the Tob55 lane correspond to different isoforms of the protein (Hoppins *et al.*, 2007). (D) Mitochondria isolated from the indicated strains were either untreated (Mitos) or incubated in the presence of proteinase K (Mitos + pK) for 15 min. Mitochondrial proteins were then subjected to SDS-PAGE and western blotting. The blot was examined for the presence of the outer membrane

protein Tom70 and the intermembrane space protein CCHL. (E) As in panel C, except strains were grown in minimal medium which maintains the numbers of both types of nuclei in the culture approximately equally. (F) Conidia produced from the sheltered heterokaryons (ΔTob37 and ΔTob38) were streaked onto medium containing histidine and pantothenate. Individual colonies were isolated and tested for nutritional requirements to determine if they were histidine-requiring homokaryons (His-req), pantothenate requiring homokaryons (Pan-req), or heterokaryons (Het).

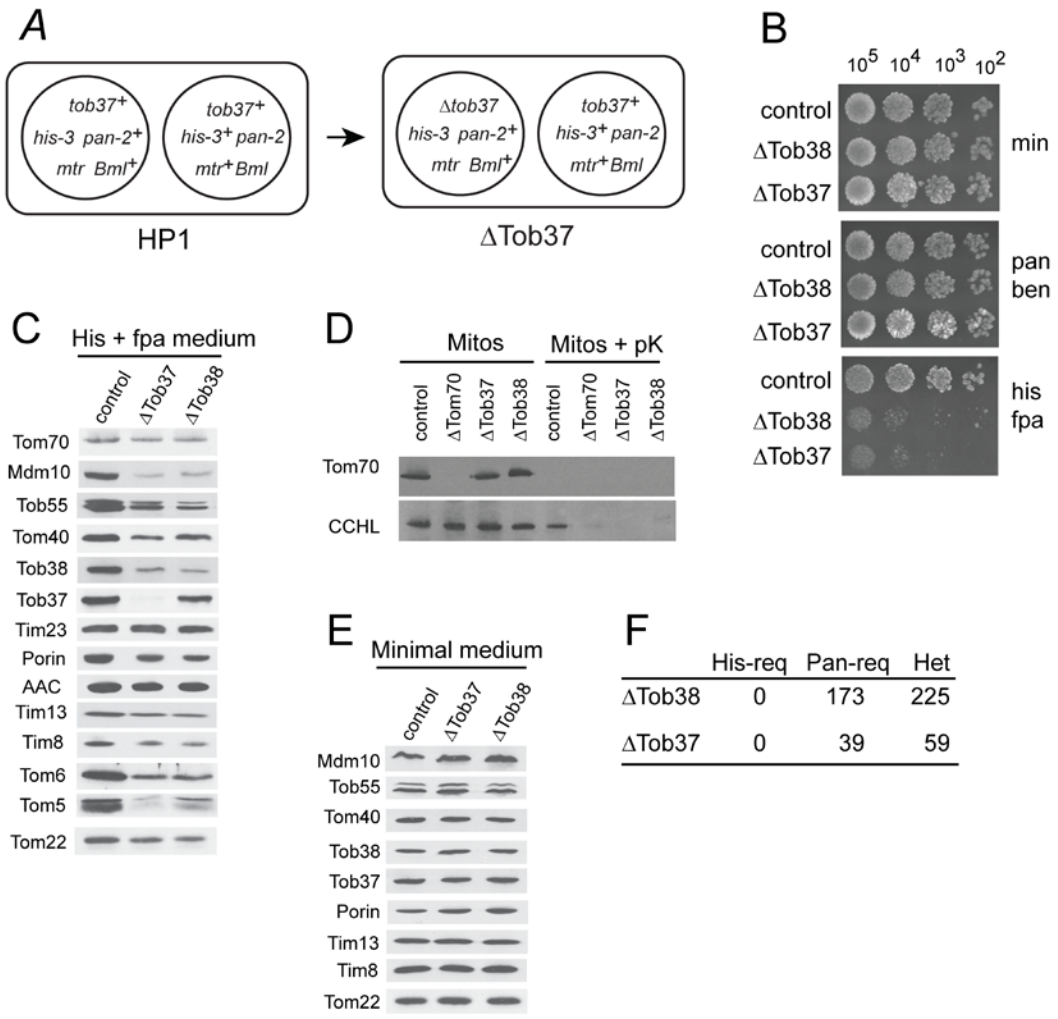

F

	His-req	Pan-req	Het
ΔTob38	0	173	225
ΔTob37	0	39	59

proteins Tim8 and Tim13 suggests possible breakage of mitochondrial outer membranes during the isolation of mitochondria as we have observed previously for other mutants affecting mitochondrial outer membrane proteins (Grad *et al.*, 1999; Wideman *et al.*, 2010). We investigated this further by examining isolated mitochondria for the presence of the intermembrane space protein cytochrome *c* heme lyase (CCHL) following exposure to proteinase K. In mitochondria from ΔTob37, ΔTob38, and ΔTom70, a mutant previously shown to have mitochondria that were damaged upon isolation (Grad *et al.*, 1999), the CCHL was degraded by the proteinase (Figure 2.1D). This demonstrates increased accessibility of the proteinase to the intermembrane space. It should also be noted that levels of CCHL in untreated mitochondria are similar in all the strains examined, as for Tim23 and Tom70 (Figures 2.1C and D). When ΔTob37 and ΔTob38 were grown in minimal medium, which forces the strains to grow as heterokaryons with relatively equal contributions from both nuclei due to the complementing auxotrophic mutations, all proteins examined in isolated mitochondria were essentially at wild type levels (Figure 2.1E). To determine if Tob37 and Tob38 were essential for viability, we examined the nutritional requirements of colonies arising from conidiaspores produced by the ΔTob37 and ΔTob38 strains (see Figure S2.1 for details of possible conidiaspores that can be produced). No histidine-requiring auxotrophs were found for either strain (Figure 2.1F). This demonstrates that both Tob37 and Tob38 are essential for viability in *N. crassa*.

2.3.2 Import/assembly of mitochondrial precursor proteins in mitochondria deficient for Tob37 or Tob38

Next, we examined import and assembly of mitochondrial precursor proteins in mitochondria isolated from ΔTob37 and ΔTob38 grown in the presence of histidine and fpa to reduce the levels of Tob37 and Tob38, respectively. Import of the matrix targeted

precursor $F_1\beta$ was found to be slightly reduced to 64% (standard deviation of 11%) of the control in ΔTob37 and to 43% (standard deviation 17%) in ΔTob38 mitochondria (Figure 2.2A). Similarly, import of AAC was slightly reduced to 64% (standard deviation 18%) of the control in ΔTob37 and 47% (standard deviation 10%) in ΔTob38 mitochondria (Figure 2.2A). Alterations in the assembly of the β-barrel protein Tom40 (Figure 2.2B) were also observed with both mutants. In wild type mitochondria the Tom40 precursor is imported across the outer membrane and can then be detected associated with the TOB complex as intermediate I of 250 kDa. The precursor is then integrated into the membrane where it forms intermediate II of 100 kDa containing an endogenous Tom40 molecule and a Tom5 subunit. The precursor then proceeds to the fully assembled 400 kDa complex (see Figure 1.2) (Rapaport and Neupert, 1999; Model *et al.*, 2001; Taylor *et al.*, 2003; Wiedemann *et al.*, 2003). Particularly striking for Tom40 assembly in mitochondria deficient in Tob37 or Tob38 was the lack of accumulation of the precursor at the 250 kDa first intermediate stage of assembly (Figure 2.2B), which represents a Tom40 precursor protein interacting with the TOB complex. A substantial amount of Tom40 does seem to reach the final assembled state in the 400 kDa complex in a time dependent fashion. This is similar to the assembly pattern we observed for mitochondria depleted of Tob55 (Hoppins *et al.*, 2007). To ensure that the Tom40 observed in the 400 kDa complex was properly assembled, the import was repeated and followed by treatment with proteinase K, which cleaves assembled *N. crassa* Tom40 into 26 kDa and 12 kDa fragments (Rapaport and Neupert, 1999). The ratio of these fragments in the mutants compared to control mitochondria was similar to the ratios observed for the undigested protein in fully assembled TOM complex (compare Figure 2.2B and Figure 2.2C). These fragments were also shown to be resistant to alkali extraction (Figure 2.2C) consistent with the idea that Tom40 had been integrated into the membrane. We conclude

Figure 2.2. Import/assembly of mitochondrial precursor proteins into mitochondria deficient in Tob37 or Tob38. (A) Radiolabeled matrix precursor $F_1\beta$ and inner membrane precursor AAC were incubated (for 5 min or 20 min, as indicated) with mitochondria isolated from heterokaryotic strains (indicated at the top of the panel) grown in the presence of histidine and fpa to reduce levels of Tob37 or Tob38 in the respective mutants. Following import, mitochondria were subjected to SDS-PAGE. Proteins were transferred to nitrocellulose membrane, and import was analyzed by autoradiography. (control, strain HP1; lys, 33% of the radiolabeled lysate added to each import reaction; bp, "bypass import" in mitochondria treated with trypsin to remove surface receptors prior to the import reaction; p, precursor protein; m, mature protein.) (B) Radiolabelled Tom40 precursor was incubated for 5 min and 20 min with mitochondria isolated from the strains indicated (top of panel) grown in the presence of histidine and fpa. Mitochondria were dissolved in 1% digitonin and subjected to BNGE. The proteins were transferred to PVDF membrane and analyzed by autoradiography. The size of the mature TOM complex (400 kDa), and assembly intermediates I (250 kDa) and II (100 kDa) are indicated on the left. * indicates an undefined band. (C) Tom40 was imported into mitochondria isolated from the strains indicated for 20 min. Following import, proteinase K was added to each import reaction for 15 min on ice. PMSF was added to inactivate the proteinase, each reaction was divided into equal halves, and mitochondria were pelleted. One half was suspended in SDS-PAGE cracking buffer (Mitos). The other half was suspended in sodium carbonate (pH 11.5) and incubated on ice for 30 min. The membrane sheets were pelleted and suspended in cracking buffer (Carb pellet). Both sets of reactions were subjected to SDS-PAGE and the proteins were transferred to nitrocellulose membrane and examined by autoradiography. The positions of Tom40 and the 26 kDa and 12 kDa fragments generated by proteinase K digestion are indicated. (D) As in panel B except that mitochondria were incubated with the

radiolabeled precursor of porin. The numbers on the left indicate the position of molecular weight markers. (E) Assembly of Tom22. As in panel D, except mitochondria were incubated with radiolabeled Tom22.

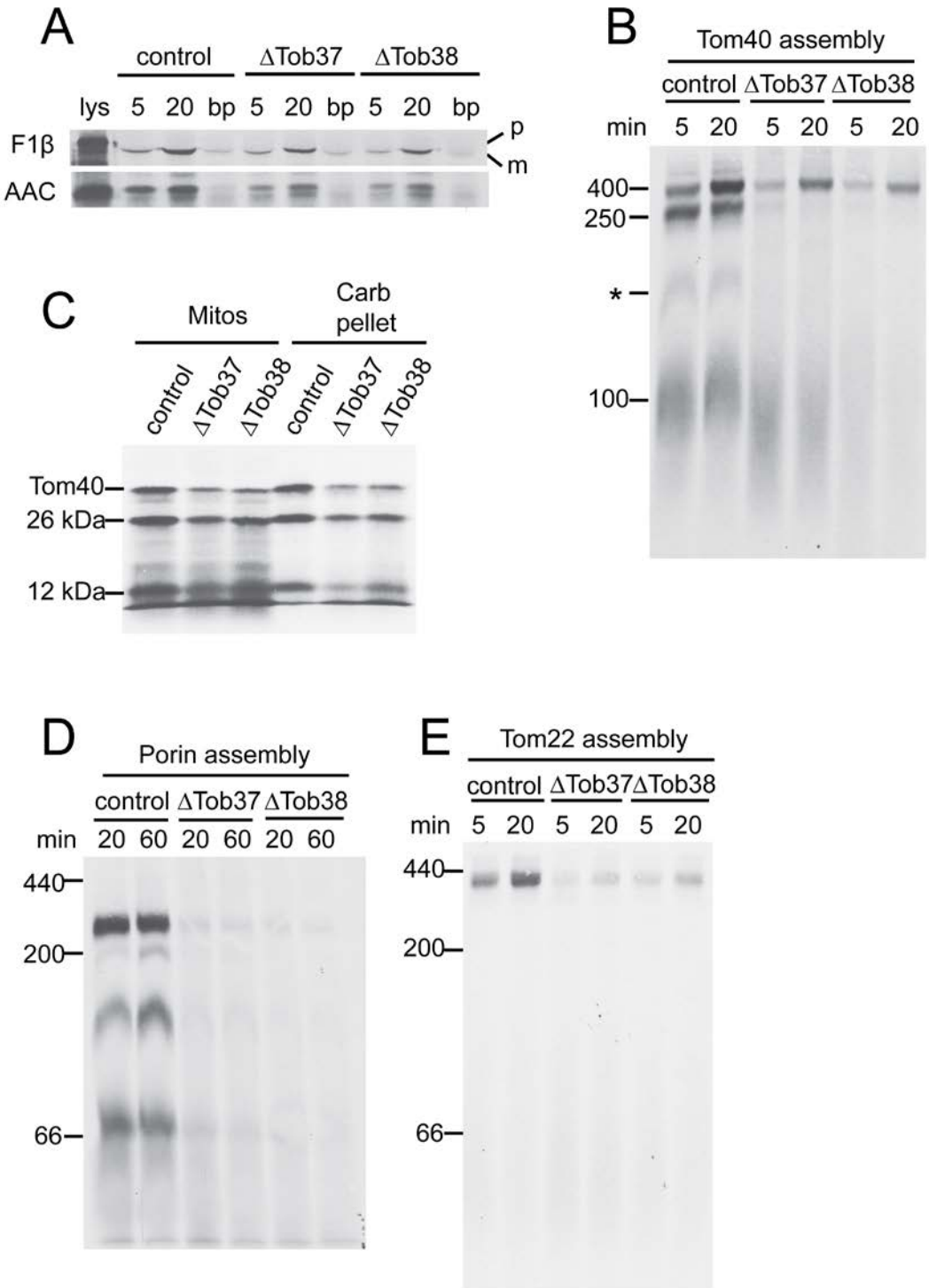
A
control
ΔTob37
ΔTob38
lys 5 20 bp 5 20 bp 5 20 bp
F1β
AAC
p
m
B
Tom40 assembly
control ΔTob37 ΔTob38
min 5 20 5 20 5 20
400
250
*
100
C
Mitos
Carb pellet
control
ΔTob37
ΔTob38
control
ΔTob37
ΔTob38
Tom40
26 kDa
12 kDa
D
Porin assembly
control ΔTob37 ΔTob38
min 20 60 20 60 20 60
440
200
66
E
Tom22 assembly
control ΔTob37 ΔTob38
min 5 20 5 20 5 20
440
200
66

that some Tom40 precursor is assembled into mitochondria containing reduced levels of Tob37 and Tob38 and is correctly integrated into the TOM complex.

One difference between the ΔTob37 and ΔTob38 mitochondria with respect to Tom40 assembly was the low level of material evident at the 100 kDa position of intermediate II for ΔTob38. The ΔTob37 mitochondria contained a substantial amount of precursor in this region, but the band was more diffuse and lower in molecular weight than in the control mitochondria. These observations demonstrate specificity of function for each protein and imply that Tob37 acts following membrane integration of Tom40 while Tob38 acts in an earlier step. The assembly pattern for porin showed a much reduced efficiency for assembly into all complexes in the mutant mitochondria (Figure 2.2D). The exact nature of the different porin complexes is not understood, though we have shown that the highest molecular weight complex contains porin precursor bound to the TOB complex (Hoppins *et al.*, 2007). Finally, we demonstrated that the assembly of Tom22 precursor into the TOM complex was also reduced in both mutants (Figure 2.2E).

The decrease of AAC import (Figure 2.2A) and the slight deficiency of Tim8 and Tim13 in mitochondria reduced for Tob37 or Tob38 (Figure 2.1C) was reminiscent of previous observations for mutants lacking the Mdm10 protein (Wideman *et al.*, 2010). In the latter case, we demonstrated that loss of the small Tim proteins was likely due to breakage of the outer mitochondrial membrane during the isolation of mitochondria from mutant cells. Since the small Tim proteins are known to be involved in the assembly of both AAC (Curran *et al.*, 2002a; Curran *et al.*, 2002b; Vasiljev *et al.*, 2004; Webb *et al.*, 2006) and β-barrel proteins (Hoppins and Nargang, 2004; Wiedemann *et al.*, 2004; Habib *et al.*, 2005), we showed that the effects on AAC import, but not the effects on the β-barrels could be explained by the loss of the small Tim proteins from the intermembrane space during the isolation of mitochondria lacking Mdm10 (Wideman *et al.*, 2010). Similar experiments in this study revealed that control mitochondria, in which the outer

membranes had been purposefully damaged to allow loss of intermembrane space components like Tim8 and Tim13, were more severely affected in their ability to import AAC than mitochondria lacking Tob37 or Tob38. However, the damaged control mitochondria were much more efficient at import and assembly of Tom40 and porin than were Tob37 or Tob38 deficient mitochondria (Figure 2.3). Thus, reductions in the level of Tob37 or Tob38 are the major factor responsible for the deficiencies in the assembly of β-barrel proteins while reduced in vitro import of AAC appears to be at least partly due to the loss of factors from the intermembrane space. However, it should be noted that Tob37 was originally characterized as having an effect on the import of AAC (Gratzer *et al.*, 1995). Since our observations suggest that steady state levels of AAC are also slightly reduced in strains depleted of either Tob37 or Tob38 (Figure 2.1C) it is conceivable that these proteins also play a minor or indirect role in AAC import/assembly.

2.3.3 TOB complexes in *N. crassa* mitochondria

The import data discussed above for strains with reduced levels of Tob37 or Tob38, together with our previous findings for Tob55 (Hoppins *et al.*, 2007), demonstrate that the three proteins have similar functions in the import of β-barrel proteins into the outer membrane. We have previously shown that the proteins co-purify as a complex (Wideman *et al.*, 2010), but the number of TOB complexes, their components, and their size has not been investigated in *N. crassa*. BNGE examination of the complexes purified from mitochondria containing His-tagged versions of the different TOB core-complex components reveals that Tob55, Tob38, and Tob37 are all found together in two complexes of about 280 kDa and 190 kDa (Figure 2.4A). In addition, Tob55 appears alone in two smaller complexes of about 75 and 140 kDa and one larger complex of 370 kDa. These latter three complexes are virtually devoid of Tob37 or Tob38, though a small amount of Tob38 is detectable in the 140 kDa form. Two-dimensional gel electrophoresis

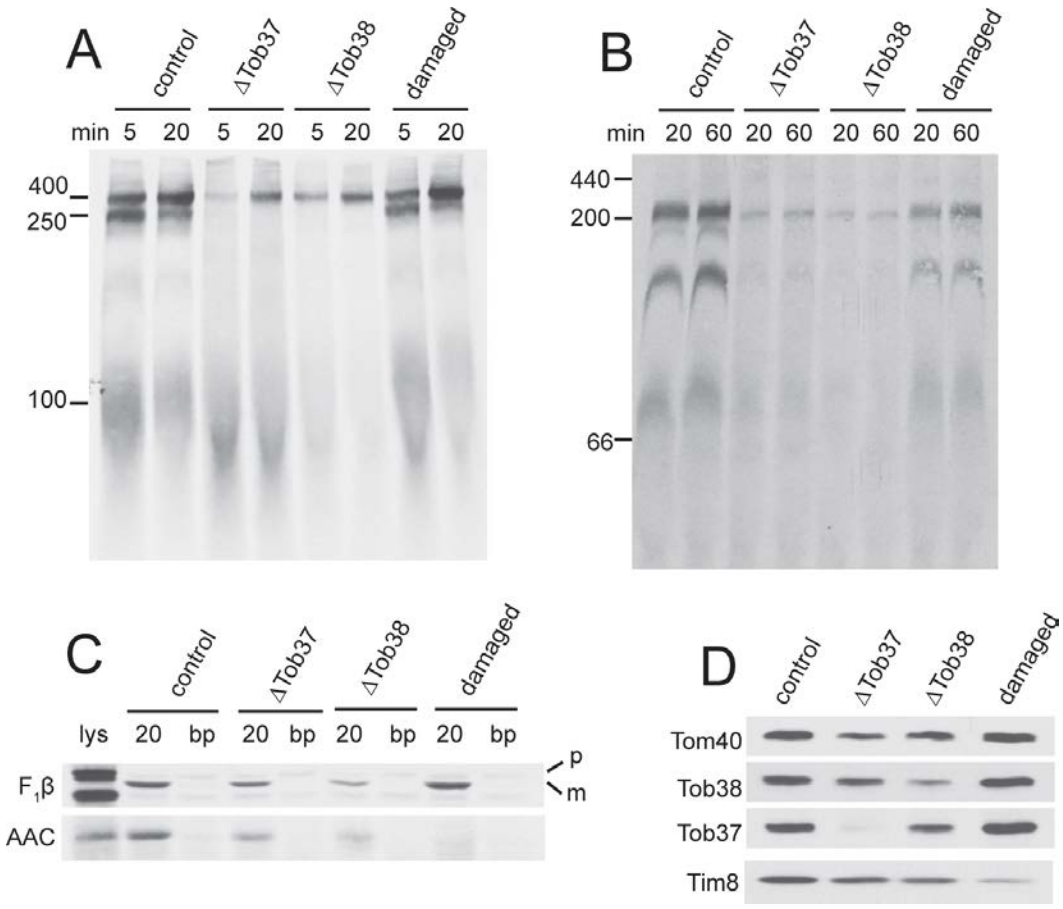

Figure 2.3. Controls for effect of damaged outer membranes in isolated mitochondria from mutant strains on mitochondrial protein import/assembly. Mitochondria from control strain HP1 grown in the presence of histidine and fpa were subjected to brief periods of vortexing in the presence of swelling buffer to produce mitochondria with damaged outer membranes as described previously (see Methods section 2.2.11). These mitochondria were then compared to undamaged control mitochondria and mitochondria from strains ΔTob37 and ΔTob38 grown in the presence of histidine and fpa to reduce levels of Tob37 and Tob38. (A) Assembly of Tom40. (B) Assembly of porin. (C) Import of $F_1\beta$ and AAC. (D) Mitochondria were isolated and subjected to SDS-PAGE followed by transfer to nitrocellulose, and immunodecoration with the antibodies indicated on the left.

Figure 2.4. The *N. crassa* TOB complex. (A) Number and protein content of *N. crassa* TOB complexes. Mitochondria were isolated from strains expressing only His-tagged versions (instead of the endogenous versions) of either Tob55 (Tob55HT), Tob38 (Tob38HT), or Tob37 (Tob37HT) as indicated for each lane at the top of the panel. TOB complexes were purified using Ni-NTA resin. Purified complexes were subjected to BNGE, transferred to PVDF membrane, and decorated with antibodies to Tob55, Mdm10, Tob37, or Tob38 as indicated at the bottom of each panel. Mock purifications using control mitochondria with no His-tagged proteins show no bands correlating with these complexes when stained with antibodies to Tob55, Tob38, Tob37, or Mdm10 (Wideman *et al.*, 2010). The position of molecular weight markers (kDa) is shown on the left and the estimated size (kDa) of complexes is shown on the right. (B) TOB complex was purified from a strain carrying His-tagged Tob55 and subjected to first dimension BNGE (1^{st} dim) in two separate lanes of the gel. One lane was transferred to PVDF, and decorated with antibody to Tob55 (top lane in panel). The second lane was removed for second dimension (2^{nd} dim) electrophoresis by SDS-PAGE as described in the Methods. Following SDS-PAGE, the gel was transferred to nitrocellulose. The membrane was cut into strips corresponding to the molecular weights of Tob55, Tob38, and Tob37 and probed with antibodies to those proteins, respectively (indicated on the left). Sizes of TOB complex following 1^{st} dimension BNGE are indicated at the top of the panel. (C) As in panel B, except the purification was performed using mitochondria containing His-tagged Tob38 and the SDS-PAGE blot was examined with antibodies to Tob38 and Mdm10. (D) As in panel B except that whole mitochondria were examined for the presence of TOB complexes. (E) As in panel A, except TOB complex was purified from mitochondria isolated from cells expressing only His-tagged versions of different Tob55 isoforms (Hoppins *et al.*, 2007): short Tob55 (Tob55 Short HT), intermediate Tob55

(Tob55 Int HT), or long Tob55 (Tob55 Long HT) as indicated at the top of the panels. Blots were immunodecorated with the antibodies indicated at the bottom of the panels.

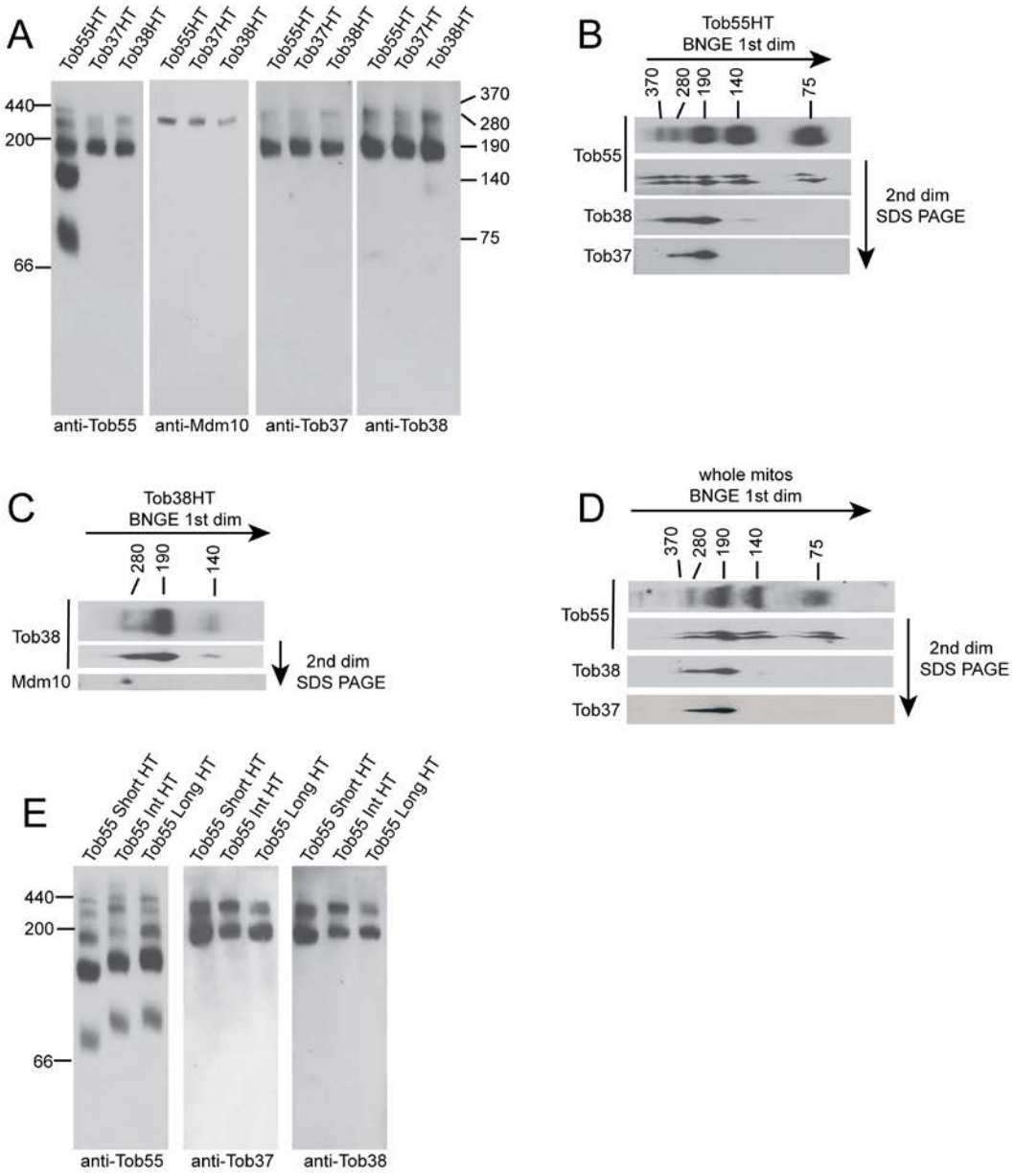
A
Tob55HT
Tob37HT
Tob38HT
440
200
66
370
280
190
140
75
anti-Tob55
anti-Mdm10
anti-Tob37
anti-Tob38
B
Tob55HT
BNGE 1st dim
370
280
190
140
75
Tob55
Tob38
Tob37
2nd dim
SDS PAGE
C
Tob38HT
BNGE 1st dim
280
190
140
Tob38
Mdm10
2nd dim
SDS PAGE
D
whole mitos
BNGE 1st dim
370
280
190
140
75
Tob55
Tob38
Tob37
2nd dim
SDS PAGE
E
Tob55 Short HT
Tob55 Int HT
Tob55 Long HT
440
200
66
anti-Tob55
anti-Tob37
anti-Tob38

(BNGE followed by SDS-PAGE) of TOB complex purified from mitochondria containing His-tagged Tob55 confirms these observations (Figure 2.4B), as does the finding that the 370 kDa, 140 kDa, and 75 kDa complexes are not observed when purification is performed using His-tagged Tob37 or Tob38 (Figure 2.4A). As noted in section 1.6.3, Mdm10 has been found in association with the TOB complex in *S. cerevisiae* (Meisinger *et al.*, 2004) and *N. crassa* (Wideman *et al.*, 2010). The protein appears to be present only in the 280 kDa complex (Figure 2.4A). This was also confirmed by two-dimensional gel analysis (Figure 2.4C) of TOB complex purified from mitochondria containing His-tagged Tob38. Thus, the 190 and 280 kDa complexes appear to correlate with the TOB core- and holo-complexes (see section 1.6.3), respectively, that have been defined in *S. cerevisiae* (Ishikawa *et al.*, 2004; Meisinger *et al.*, 2004; Milenkovic *et al.*, 2004; Waizenegger *et al.*, 2004; Meisinger *et al.*, 2007; Yamano *et al.*, 2010). It should be noted that in mock purifications using control mitochondria without His-tagged proteins that no bands correlating with these complexes are observed when blots are immunodecorated with antibodies to Tob55, Tob38, Tob37, or Mdm10 (Wideman *et al.*, 2010). When whole mitochondria were examined by western blot for Tob55 following BNGE or two-dimensional gel electrophoresis, a pattern similar to that observed for purified complexes was seen (Figure 2.4D). Thus, it appears unlikely that any of the complexes observed are artifacts of the purification procedure. However, we cannot be certain that all bands detected represent physiologically relevant complexes or if some are breakdown products resulting from BNGE. It seems likely that complexes containing the three or four components of the complex that co-purify are functionally relevant. The observation that no lower molecular weight forms of Tob37 or Tob38 were detected suggests that the complexes containing only Tob55 might not be simple breakdown products and could also have some functional relevance. *N. crassa* contains three different isoforms (short, intermediate and long) of Tob55 (Hoppins *et al.*, 2007).

To determine if any of these was specific for a given complex or set of complexes, mitochondria were isolated from strains expressing only the His-tagged versions of either the short, intermediate, or long form of Tob55. TOB complexes were purified and analyzed by BNGE and western blot. In each case, all five TOB complexes described above were present (Figure 2.4E). In addition, the distribution of Tob37 and Tob38 was similar to cells expressing all three isoforms. We conclude that the different Tob55 isoforms are not involved in the formation of specific TOB complexes.

2.3.4 Topology of Tob37 and Tob38

Both Tob37 and Tob38 are susceptible to degradation by proteinase K added to isolated mitochondria (Figure 2.5A), showing that the proteins have domains exposed on the outer surface of the outer membrane as does the control protein Tom70. The intermembrane space protein Tim8, and the matrix protein Hsp70 are protected from the externally added protease. We also examined the properties of *N. crassa* Tob37 and Tob38 by alkali extraction at varying pHs. The soluble protein Tim13, appears in the extracted, supernatant phase at all pH levels tested while the β-barrel proteins Tom40 and Tob55 partition with the pelleted membrane sheets (Figure 2.5B). For Tob38, about half the protein is removed from the membrane at pH 11.5 and the majority is removed at pH 12.0 (Figure 2.5B). Thus, the behaviour of the protein is similar to the Tom70 protein which is known to have a single membrane spanning domain (Söllner *et al.*, 1990; Shore *et al.*, 1995; Schlossmann *et al.*, 1996). However, analysis of the Tob38 amino acid sequence reveals no strong candidates for a membrane spanning helix. Tob37 is more resistant to alkali extraction than Tob38. Very little of the protein is removed from the membrane at pH 11.5, but at pH 12.0 it is roughly equally partitioned between the membrane and supernatant fractions (Figure 2.5B). Thus, it appears to be a membrane anchored protein as it is slightly more resistant to extraction than Tom70. However, the

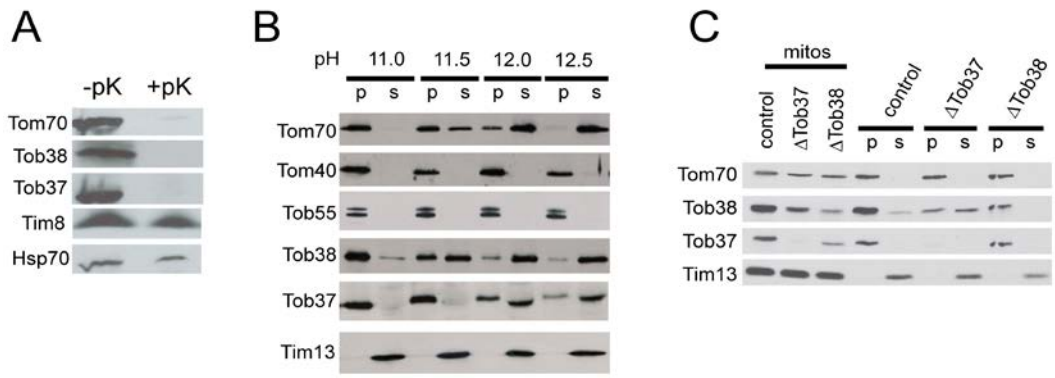

Figure 2.5. Topology of Tob37 and Tob38. (A) Mitochondria isolated from wild type cells (strain 76-26) were treated with proteinase K (+pK) as in Figure 2.2C or not (-pK). Mitochondria were washed and subjected to SDS-PAGE. The gel was blotted to nitrocellulose and examined by immunodecoration with the antibodies indicated on the left. (B) Mitochondria from the control strain (76-26) were subjected to extraction with 0.1 M sodium carbonate at the pHs indicated at the top of the panel. Following the treatment, membrane sheets were pelleted and supernatants were subjected to trichloroacetic acid precipitation. Membrane pellets (p) and supernatant precipitates (s) were subjected to SDS-PAGE. Proteins in the gel were transferred to nitrocellulose and the membrane was examined with the antibodies indicated on the left. (C) As in panel B except extractions were done at pH 11.0 from control (HP1), ΔTob37, and ΔTob38 strains grown in the presence of histidine and fpa. The three lanes on the left show the protein levels in whole mitochondria (mitos), while the six lanes on the right show the pellets and supernatants resulting from alkali extraction.

protein is more easily removed from the membrane than are the β-barrel membrane proteins Tom40 and Tob55. It has been suggested that Tob37 anchors Tob38 to the mitochondrial membrane in mammals (Armstrong *et al.*, 1999) or that Tob37 is required for stability of Tob38 in yeast (Chan and Lithgow, 2008; Dukanovic *et al.*, 2009). We examined this possibility by subjecting mitochondria depleted for Tob37 to alkali extraction at pH 11.0. In control mitochondria, Tob38 stays almost entirely associated with the pelleted membrane sheets. However, in the absence of Tob37, the reduced amount of Tob38 that remains in mitochondria is about equally portioned between the pellet and supernatant fractions (Figure 2.5C). These data support a role for Tob37 in binding Tob38 to mitochondria, but also suggest that Tob38 is bound to the membrane by other interactions. Analysis of the Tob37 amino acid sequence suggests the presence of two possible TMDs (Figure 2.6A). The first occurs in a position that ends 35 residues before the C-terminus. This placement of the TMD resembles the position of the TMD of mammalian Mtx1 and we refer to the domain as TMD1. The second comprises the last 19 residues of the protein and is referred to as the C-terminal hydrophobic domain (CHD). Taken together, the above data suggest that Tob37 is anchored to the mitochondrial membrane by one or two TMDs. On the other hand, Tob38 is likely a peripheral membrane protein that is strongly associated with Tob37 and other factors in the outer membrane.

2.3.5 Role of transmembrane domains (TMDs) in Tob37

To assess the roles of the two possible TMDs of Tob37, we removed one or both of the domains from the protein coding sequence as shown in Figure 2.6A using site-directed mutagenesis (see Methods section 2.2.3). Plasmid constructs encoding these mutant forms of Tob37 were used to transform the ΔTob37 sheltered heterokaryon. Histidine-requiring homokaryons expressing only the mutant forms of Tob37 were

Figure 2.6. Role of predicted TMDs of Tob37. (A) The WT row shows the sequence of the 63 amino acids at the C-terminus of wild type *N. crassa* Tob37. ΔTMD1 is the deletion constructed for the first possible transmembrane domain and is the name of the strain expressing this form of Tob37. Similarly for CHD, the second possible TMD found at the C-terminus of the protein, and for ΔT+C, the deletion of the last 56 amino acids of the protein which removes both possible TMDs. (B) Mitochondria and post-mitochondrial supernatants (cytosol) were isolated from strains expressing the mutant forms of Tob37 described in panel A. Samples of each were subjected to SDS-PAGE and transferred to nitrocellulose. The membrane was immunodecorated with the antibodies indicated on the left. The control was strain 76-26. Arginase represents a cytosolically localized control protein that is synthesized from two different start codons of the same locus (Marathe *et al.*, 1998) so that two bands of 41 kDa and 36 kDa are observed. (C) As in panel B for mitochondria, except that the isolated mitochondria were treated for 30 min on ice with isolation buffer containing 0.5 M NaCl. Following the incubation period, mitochondria were pelleted. The supernatant was collected and desalted. The mitochondria were washed in isolation buffer and pelleted. Pelleted mitochondria and the desalted supernatant were subjected to SDS-PAGE. Proteins were transferred to nitrocellulose and the membrane was probed with the antibodies indicated on the left. (D) Mitochondria from the strains indicated above the panel were subjected to alkali treatment using 0.1 M sodium carbonate at pH 11.0, 11.5, and 12.5 (indicated below each panel) as described in the legend to Figure 2.5B. (E) Mitochondria were isolated from each of the Tob37 deletion protein strains and treated with proteinase K as described in the Materials and Methods and Figure 2.5A. (F) Model for Tob37 topology. The large circle represents the cytosolic domain of Tob37, the filled box is TMD1, and the open box is the CHD. Two horizontal lines represent the mitochondrial outer membrane. The predicted arrangement of the domains for wild type and each of the TMD/CHD deletions

is shown. (G) Comparison of potential tail-anchoring sequences of *N. crassa* (Nc) Tob37 and *H. sapiens* (Hs) Mtx1. The potential TMD is indicated by the solid line. The position of the region within each protein is indicated by the numbers flanking each amino acid sequence. The overall length of the *N. crassa* protein is 442 residues. The *H. sapiens* protein is 304 residues. Positively charged residues in the immediate flanking regions are indicated by the plus sign.

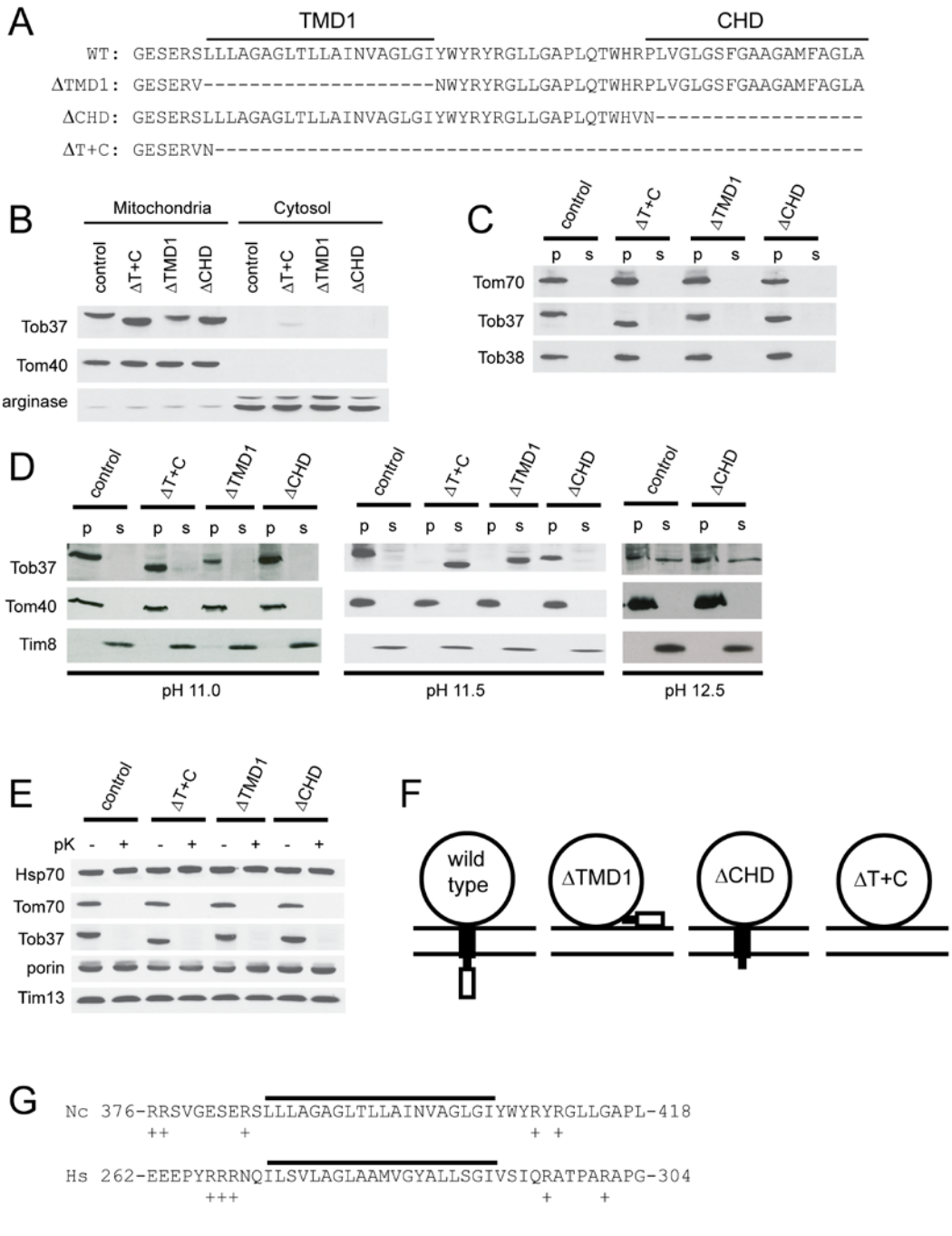
A
TMD1
CHD
WT: GESERSLLLAGAGLTLLAINVAGLGIYWYRYRGLLGAPLQTWHRPLVGLGSFGAAGAMFAGLA
ΔTMD1: GESERV----------NWYRYRGLLGAPLQTWHRPLVGLGSFGAAGAMFAGLA
ΔCHD: GESERSLLLAGAGLTLLAINVAGLGIYWYRYRGLLGAPLQTWHVN----------
ΔT+C: GESERVN----------
B
Mitochondria
Cytosol
control
ΔT+C
ΔTMD1
ΔCHD
Tob37
Tom40
arginase
C
Tom70
Tob37
Tob38
D
pH 11.0
pH 11.5
pH 12.5
Tim8
E
pK
Hsp70
Tom70
Tob37
porin
Tim13
F
wild type
ΔTMD1
ΔCHD
ΔT+C
G
Nc 376-RRSVGESERSLLLAGAGLTLLAINVAGLGIYWYRYRGLLGAPL-418
Hs 262-EEEPYRRRNQILSVLAGLAAMVGYALLSGIVSIQRATPARAPG-304

isolated, indicating that the ΔTob37 nucleus of the sheltered heterokaryon (Figure 2.1A) could be rescued by any of the three mutant versions of the protein. One strain from each transformation was chosen for further analysis: ΔTMD1-9 (lacking TMD1, Figure 2.6A), ΔCHD2-3 (lacking CHD), and ΔT+C12-5 (lacking both TMD1 and CHD). Mitochondria and post-mitochondrial pellet (referred to as cytosol) fractions were isolated from each strain. Western blot analysis showed that despite the removal of either or both of the domains, the shortened versions of Tob37 were targeted to, and remained associated with, mitochondria during standard isolation conditions while the control protein arginase (Borkovich and Weiss, 1987; Marathe *et al.*, 1998) was found predominantly in the cytosol fraction as predicted (Figure 2.6B). When mitochondria were treated with buffer containing 500 mM NaCl, all three mutant proteins still remained associated with the mitochondria (Figure 2.6C). Mitochondria isolated from each of the mutant strains were then subjected to alkali extraction with sodium carbonate at pH 11.0, 11.5, and 12.5 (Figure 2.6D). At pH 11.0, all versions of the protein remain in the membrane fraction. At pH 11.5, the wild type protein and the mutant lacking only the CHD were resistant to extraction from the membrane and remained in the pellet as did the control protein Tom40. However, the mutant proteins lacking either TMD1, or TMD1 and CHD were completely removed from the membrane by the alkali treatment. At pH 12.5, the behaviour of the protein lacking CHD is indistinguishable from the wild type protein. These data strongly suggest that TMD1 is a membrane spanning domain, but the CHD is not. This was further tested by examining the susceptibility of the mutant proteins to proteinase K treatment. If both TMD1 and CHD were membrane spanning domains, then loss of one of the domains could conceivably result in mislocalization of the large domain in the cytosol to the intermembrane space. However, all three mutant forms were shown to be digested when mitochondria were treated with proteinase K, as was the control protein Tom70. The intermembrane space control protein Tim13 was not digested. This

suggests that no change in the location of the cytosolic domain resulted from deletion of either or both TMD1 and CHD (Figure 2.6E). This is consistent with the conclusion that only TMD1 spans the outer membrane and suggests that absence of TMD1 likely results in mislocalization of the small CHD to the cytosol (Figure 2.6F). Taken together, these data suggest that TMD1 serves as a membrane spanning tail-anchoring domain for *N. crassa* Tob37 (Figure 2.6F).

The position of TMD1 within the protein is similar to the analogous region from the human Mtx1 protein (Figure 2.6G). In both proteins, the predicted TMD is flanked by regions containing positive charges, which is a characteristic of tail-anchoring mitochondrial sequences (Armstrong *et al.*, 1997; Horie *et al.*, 2002; Rapaport and Nargang, 2004). The growth rates of strains expressing the mutant alleles of Tob37 were virtually identical to the control strain (Figure 2.7A) and there were no apparent alterations in the steady state levels of mitochondrial proteins (Figure 2.7B). However, lysis of isolated mitochondria with digitonin, followed by BNGE and western blot analysis revealed that the ratio of larger to smaller TOB complexes is somewhat reduced in mitochondria containing Tob37 proteins missing TMD1, or TMD1 plus CHD (Figure 2.7C). These data suggest that TMD1 of Tob37 plays a role in TOB complex assembly and/or stability. We also investigated the import/assembly of mitochondrial proteins into mitochondria isolated from the strains containing the Tob37 mutant proteins. Import of $F_1\beta$ and AAC was indistinguishable from controls (Figure 2.8A). However, differences were observed with respect to the import of β-barrel proteins. For Tom40 (Figure 2.8B), mitochondria containing Tob37 lacking TMD1 assemble Tom40 into the final 400 kDa TOM complex at a slightly increased rate and accumulation of Tom40 precursor at the 250 kDa TOB complex intermediate stage is greatly reduced. However, mitochondria containing Tob37 lacking the CHD, or both TMD1 and the CHD, are only slightly different from the wild type control with respect to appearance of the precursor into the

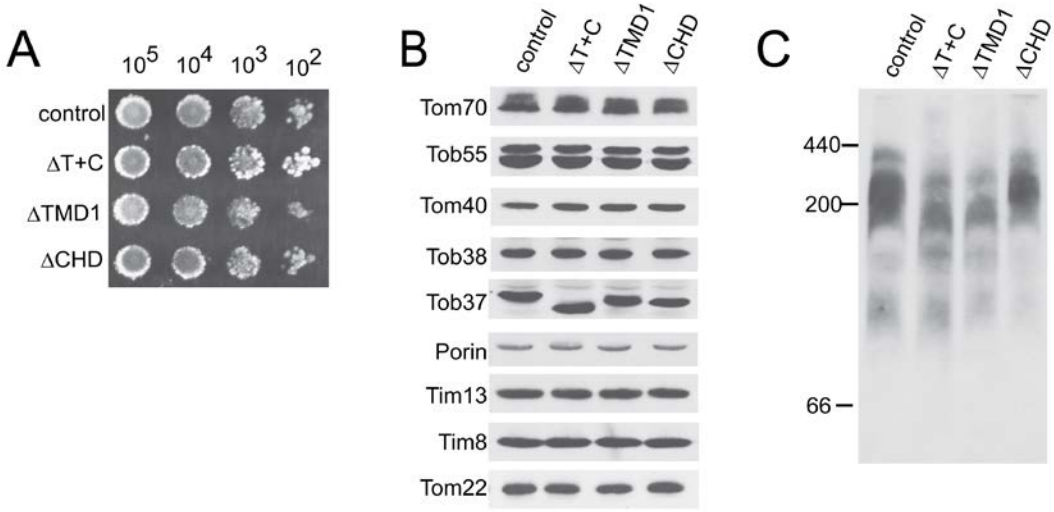

Figure 2.7. Characteristics of Tob37 C-terminal deletion strains. (A) Conidia from the strains indicated on the left were plated as described in the legend to Figure 2.1B. (B) Mitochondria were isolated form the strains indicated at the top of the panel and analyzed as described in the legend to Figure 2.1C. The control was strain 76-26. (C) Mitochondria isolated from the strains indicated at the top of the panel were dissolved in 1% digitonin, subjected to BNGE, transferred to PVDF, and decorated with antibody to Tob55. The position of molecular weight markers is indicated on the left.

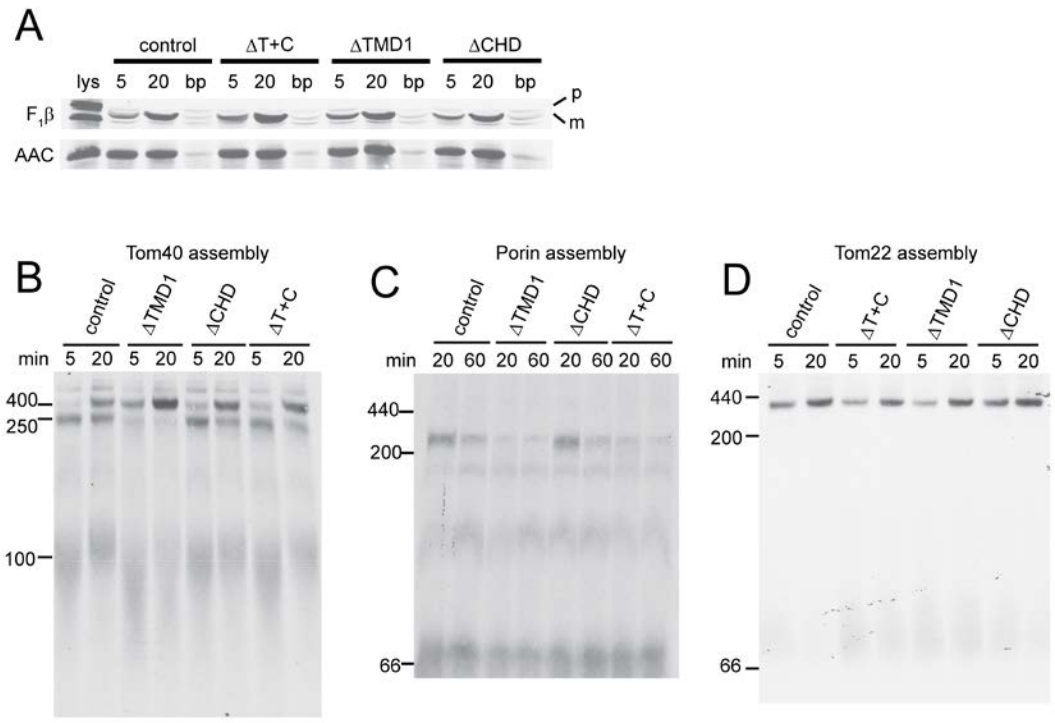

Figure 2.8. Role of Tob37 predicted TMDs on the import of mitochondrial precursor proteins into mitochondria. Import and assembly were analyzed as described in the legend to Figure 2.2 for the indicated precursors. (A) Import of $F_1\beta$ and AAC. (B) Assembly of Tom40. (C) Assembly of porin. (D) Assembly of Tom22.

250 kDa intermediate I and the final assembled complex. For porin (Figure 2.8C), mitochondria containing Tob37 lacking the CHD are indistinguishable from the wild type control. However, mitochondria with Tob37 lacking TMD1 do not efficiently form the highest molecular weight form (240 kDa). Other porin complexes are present at or near control levels. We have previously shown the 240 kDa form represents porin precursor bound to the TOB complex (Hoppins *et al.*, 2007). Assembly of the porin precursor in mitochondria lacking TMD1 plus the CHD resembles the pattern seen in those lacking only TMD1. Thus, the loss of TMD1 alone reduces the level of both Tom40 and porin precursors bound at the TOB complex. However, there is a clear difference in the assembly of the two precursors in the ΔT+C mitochondria. For Tom40 assembly is similar to the control, but for porin it is similar to the ΔTMD1 mitochondria. As shown in Figure 2.2E, the TOB complex is also required for the assembly of Tom22. Examination of Tom22 assembly into mitochondria with the TMD deletions revealed a slightly lower rate of assembly when TMD1 or TMD1 plus the CHD were deleted (Figure 2.8D), which is most clearly seen at the 5 min time point.

2.4 Discussion

Despite the limited sequence similarity among the Tob37 and Tob38 proteins from different organisms (Figure S2.3), many of their characteristics and functions are conserved. *N. crassa* Tob37 and Tob38 are found in complexes with either Tob55 or with Tob55 and Mdm10, which are analogous to the core- and holo-TOB complexes, respectively, that have been described in *S. cerevisiae* (Ishikawa *et al.*, 2004; Meisinger *et al.*, 2004; Milenkovic *et al.*, 2004; Waizenegger *et al.*, 2004; Meisinger *et al.*, 2007; Yamano *et al.*, 2010). Tob38 is essential in both *N. crassa* and *S. cerevisiae* (Ishikawa *et al.*, 2004; Milenkovic *et al.*, 2004; Waizenegger *et al.*, 2004). Its function in β-barrel import is common to these two organisms as well as mammals (Kozjak-Pavlovic *et al.*,

2007), as is its topology as an alkali extractable peripheral membrane protein. Tob37 is an essential protein in *N. crassa* and is required for embryonic development in mice (Bornstein *et al.*, 1995). Although the *S. cerevisiae* protein is not essential, knockouts have growth defects at high temperatures (Gratzer *et al.*, 1995). Loss of Tob37 in *C. albicans* leads to a much reduced growth rate (Dagley *et al.*, 2011). Tob37 is involved in β-barrel protein assembly in *S. cerevisiae* (Wiedemann *et al.*, 2003) and *N. crassa* (this study). This has not been shown directly in mammals, but Mtx1(Tob37 homologue) is known to associate with Mtx2 (Tob38 homologue) and its levels decrease in Mtx2 knockdowns suggesting a functional relationship between the two proteins (Armstrong *et al.*, 1999; Kozjak-Pavlovic *et al.*, 2007). The *N. crassa* and mammalian Tob37 proteins both contain a tail-anchoring domain. Although potential TMDs were detected in the *S. cerevisiae* protein (Gratzer *et al.*, 1995), it was concluded that it is a peripheral membrane protein based on alkaline extractability (Ryan *et al.*, 1999). In mammals deletion of the anchoring domain has a severe effect on targeting Mtx1 to mitochondria (Armstrong *et al.*, 1997). Deletion of TMD1 in the *N. crassa* protein results in loss of resistance to alkaline extraction. However, when TMD1 is absent, the *N. crassa* protein still associates with mitochondria. Thus, *N. crassa* Tob37 seems to possess a mixture of the properties found in the *S. cerevisiae* and mammalian proteins. The finding that mammalian Mtx1 and Mtx2 interact led to the suggestion that Mtx2 is bound to the mitochondrial membrane by Mtx1 (Armstrong *et al.*, 1999). Similarly, one of the suggested roles of *S. cerevisiae* Tob37 is to stabilize the Tob38 protein or the TOB complex in general (Chan and Lithgow, 2008; Dukanovic *et al.*, 2009). Our finding that Tob38 is greatly reduced in the Tob37 knockout, but Tob37 is only slightly reduced in the Tob38 knockout agrees with these suggestions. However, our results also show that when *N. crassa* Tob37 levels are reduced to virtually undetectable levels, about half of the Tob38 that associates with mitochondria is still resistant to alkali extraction, suggesting that Tob38 also binds tightly

to other components of the outer membrane, possibly by a specific interaction with Tob55 (Kutik *et al.*, 2008). Our observation of the three TOB proteins in complexes with or without Mdm10 is in agreement with findings in *S. cerevisiae*. However, we also detected additional complexes that appear to contain only Tob55. The physiological relevance and role of these complexes remains to be determined. Since the original publication of this chapter as a paper, the size, composition, and structural organization of the *N. crassa* TOB complex has been defined. The 140 kDa complex has a stoichiometry of 1:1:1 for each of the TOB_{core} components (Tob55, Tob37 and Tob38) while a very small fraction of TOB complexes associate with a single Mdm10 (Klein *et al.*, 2012). Import of radiolabeled Tom40 precursor into ΔTob37 or ΔTob38 mitochondria was reduced. Some accumulation into the fully assembled complex was observed, but no precursor was detected in an intermediate that would represent a lower molecular weight version of the TOB complex that lacked a core subunit. These results differ from those observed in previous studies of Tob37 deficient mitochondria of *S. cerevisiae* where accumulation of the Tom40 precursor was observed in a lower molecular weight TOB complex lacking Tob37 with only very small amounts of Tom40 reaching the final assembled state (Wiedemann *et al.*, 2003; Meisinger *et al.*, 2004; Dukanovic *et al.*, 2009). On the other hand, our finding that some Tom40 does reach the assembled complex is similar to a more recent study in *S. cerevisiae* where substantial assembly was observed after 60 min of import in mitochondria lacking Tob37 (Becker *et al.*, 2010). Our results for Tom40 assembly into mitochondria deficient in Tob38 are similar to one previous study in *S. cerevisiae* that used mitochondria with reduced levels of Tob38. In that report, Tom40 precursor reached the fully assembled TOM complex in a time-dependent manner, in amounts similar to controls, with no accumulation at lower molecular weight intermediates, though it was also shown that a proportion of the protein was not properly assembled (Ishikawa *et al.*, 2004). In the present study we observed somewhat reduced

levels of Tom40 reaching the assembled TOM complex. Alkali extraction and protease susceptibility studies demonstrated that most, if not all, of that protein was properly assembled into the membrane. Curiously, compared to our findings and the aforementioned yeast work, others have reported quite different results for the effects of Tob38 depletion in *S. cerevisiae*. In one study, virtually no Tom40 precursor reached the final TOM complex and the amount of the precursor accumulated at intermediate I was reduced (Waizenegger *et al.*, 2004). Similar results were seen using a temperature-sensitive allele of Tob38 (Milenkovic *et al.*, 2004). Whether these differences reflect minor alterations in the mitochondria resulting from experimental approaches, or differences between organisms or strains, remains to be determined.

The assembly of porin was also reduced in mitochondria deficient in Tob37 or Tob38. These results are similar to findings with *S. cerevisiae* cells deficient in Tob37 (Wiedemann *et al.*, 2003; Dukanovic *et al.*, 2009) or Tob38 (Ishikawa *et al.*, 2004; Milenkovic *et al.*, 2004; Waizenegger *et al.*, 2004) though the effects in *N. crassa* appear to be more dramatic. Mammalian mitochondria depleted of Mtx2 also show decreased import of both porin and Tom40 (Kozjak-Pavlovic *et al.*, 2007). Our assembly assays for Tom40 or porin in Tob37 or Tob38 deficient mitochondria show much reduced or undetectable levels of precursors bound at the TOB complex. Two explanations for similar observations have been given previously (Meisinger *et al.*, 2007; Dukanovic *et al.*, 2009). Deficiency of the proteins may influence the efficiency of binding precursors to the complex. Alternatively, delays in processing precursor bound to the complex, might make them susceptible to increased degradation. Interestingly, when ΔTob37 mitochondria are used in our Tom40 assembly assays, there is accumulation of labelled precursor in a smear at the position of the 100 kDa intermediate II. In the ΔTob38 mitochondria there is virtually no material seen in this region. This suggests that precursor may be less efficiently integrated into the membrane when Tob38 is absent.

When Tob37 is deficient, the Tom40 precursor appears to enter the membrane but may not be properly assembled with other Tom subunits to give a discrete 100 kDa form. If true, this observation lends support to an earlier suggestion that intermediate II may still be associated with the TOB complex (Chan and Lithgow, 2008).

We observed a slight reduction in the import of the matrix targeted F1β and the inner membrane protein AAC in mitochondria deficient in Tob37 and Tob38. Various results have been reported for the effects of deficiencies of Tob37, Tob38, or metaxins on the import of matrix and inner membrane precursors into mitochondria. In some studies the import of at least some of these proteins is reduced (Gratzer *et al.*, 1995; Armstrong *et al.*, 1997; Abdul *et al.*, 2000; Dukanovic *et al.*, 2009), in others it is not (Wiedemann *et al.*, 2003; Ishikawa *et al.*, 2004; Milenkovic *et al.*, 2004; Waizenegger *et al.*, 2004; Kozjak-Pavlovic *et al.*, 2007; Chan and Lithgow, 2008). One explanation might be that different strategies used to eliminate or reduce Tob37 and Tob38 levels or activity result in variations of the steady state levels of other proteins required for import of proteins to other subcompartments. In fact, one study has shown that increasing TOM complex stability by overexpressing Tom6 improved the import of matrix precursor proteins in Tob37 deficient mitochondria (Dukanovic *et al.*, 2009).

The steady state levels of various proteins in ΔTob37 and ΔTob38 mitochondria were reduced, most notably Tom5 and Mdm10. Thus, it might be argued that the defects in β- barrel assembly observed in our experiments, and at least some other previous studies, are due to reduced levels of other mitochondrial proteins that are involved in import or assembly. However, this seems unlikely. The non-core TOB complex proteins most likely to have an effect on β-barrel assembly would be TOM complex components, the small Tim proteins, and Mdm10. The patterns of assembly for Tom40 and porin in ΔTob37 and ΔTob38 mitochondria do not resemble those observed when the small Tim proteins (Hoppins and Nargang, 2004) (Figure 2.3), the small Tom proteins (Sherman *et*

al., 2005), or Mdm10 (Wideman *et al.*, 2010) are depleted. On the other hand, the assembly patterns observed in the present study are similar to those observed when Tob55 levels are depleted (Hoppins *et al.*, 2007). Furthermore, the phenotypes observed for Tom40 and porin assembly are very similar in ΔTob37 mitochondria and ΔTMD1 mitochondria, which would argue that a similar process is affected in both cases. In ΔTMD1 mitochondria import of $F_1\beta$ and AAC is not affected and no changes in the steady state levels of other mitochondrial proteins were observed, supporting the notion that alterations in the TOB proteins are responsible for the effects on β-barrel assembly.

Our studies on assembly of β-barrel proteins in mitochondria bearing Tob37 proteins with C-terminal alterations have shown that loss of the CHD has virtually no effect. However, the accumulation of the precursors for both Tom40 and porin, at the stage of interaction with the TOB complex, is severely reduced when TMD1 is removed. Interestingly, simultaneous removal of both of these domains has a different effect on the two β-barrel precursors examined. For Tom40, removal of both domains restores both the accumulation of the precursor with the TOB complex and its assembly into the TOM complex to near wild type levels. These data suggest that it is not the absence of TMD1 that affects Tom40 assembly, but the predicted mislocalization of the CHD. In a Tob37 protein lacking the tail-anchoring TMD1, the CHD would be expected to be found on the outer surface of the outer membrane, rather than in the intermembrane space (Figure 2.6F). We speculate that the mislocalized CHD alters interactions between TOB complex components such that binding of the Tom40 precursor is affected. The more rapid assembly of the precursor to the final complex suggests that when TMD1 alone is absent, the precursor is released from the TOB complex more quickly. This would be in keeping with a role for Tob37 in precursor release as suggested in two recent studies of the *S. cerevisiae* protein (Chan and Lithgow, 2008; Dukanovic *et al.*, 2009). The more rapid release in the mutant may suggest that binding at the precursor stage may represent a

quality control stage for Tom40 assembly, allowing it to achieve proper conformation and/or combining with other subunits. However, for the precursor of porin, removal of both domains gives an assembly phenotype similar to missing only TMD1. This suggests that the effects of CHD mislocalization do not have the same effect on the porin precursor. Thus, individual β-barrel precursors may associate with different features of the TOB complex to achieve maximal productive interactions. Alternatively, the nature of TOB complex/precursor interactions may specifically affect downstream assembly steps that differ between the precurors. One of many possible models to account for these observations is given in Figure 2.9. Continued investigations will be required to reach a fuller understanding of Tob37 topology and its relationship to TOB complex structure and function.

Figure 2.9. Hypothetical model for effects of Tob37 alterations on the TOB complex. Tob55 is shown as a pore-containing light grey ring embedded in the membrane. Tob37, is represented as in Fig. 2.6F with TMD1 and CHD in the outer membrane and intermembrane space, respectively. Tob38 is shown in dark grey with a domain extending into the pore of Tob55. (A) The normal TOB complex. (B) CHD absent. Loss of CHD has no effect on porin assembly and mild effects on Tom40 assembly. All members of the complex are shown in their normal configuration (C) TMD1 and CHD absent. This results in reduced accumulation of the porin precursor at the TOB complex. Effects on Tom40 are mild. A conformational change in Tob55 is shown as one possible effect caused by loss of TMD1 resulting in porin assembly defects. (D) Only TMD1 absent. This results in reduced accumulation of both porin and Tom40 precursors at the TOB complex. The conformational change in Tob55 due to lack of TMD1 is shown as in C. However, an additional change due to the suggested mislocalization of the CHD, is represented as an effect on Tob38.

Supplemental Figure S2.1. Schematic representation of knockout creation and development of sheltered heterokaryons. (A) Knock-out procedure for essential *N. crassa* genes. In this example, the histidine requiring, fpa resistant 76-26 nucleus of the HP1 heterokaryon strain undergoes knock-out of the *tob37* gene resulting in the *tob37KO* sheltered heterokaryon. It should be noted that there is an equal chance of the KO occurring in the *pan-2*, benomyl resistant (*Bml*) nucleus. However our lab prefers working with KO's in the fpa resistant nucleus and select such KO's for further work by examination of growth characteristics on media containing fpa + His and Bml + pan. (B) The knockout is created by replacing the *tob37* gene with a hygromycin resistance cassette using a split-marker approach (Colot *et al.*, 2006). Primers for amplifying 3 Kb of the 5' and 3' flanking regions of the gene of interest are used to PCR amplify these products from either genomic or cosmid DNA. These primers also contain overhangs homologous to sequences within the MCS region of the *S. cerevisiae* plasmid pRS416 and to a hygromycin resistance cassette (PCR amplified from pCSN44) as shown on the figure. All three PCR products as well as the linearized plasmid pRS416 (contains *URA3*) are transformed into *S. cerevisiae* strain FY2 (*ura3-52* mutant). Homologous recombination in FY2 creates the KO plasmid which is maintained by complementation on a uracil-free medium. The KO plasmid is isolated from FY2 and transformed into *E. coli* XL-2 for bulk plasmid isolation. The two split marker fragments are PCR amplified from the KO plasmid and transformed into *N. crassa* HP1. Knock-out is achieved when both components of the split-marker recombine at the endogenous *tob37* locus. (C) The sheltered heterokaryon KO can be grown under selective conditions (i.e. His/fpa media) that will favor the KO nucleus resulting in a numerical superiority of the KO nucleus in the culture. As the gene of interest is essential, the 71-18 nucleus containing the $tob37^{+}$ gene must be maintained at minimal required levels.

A

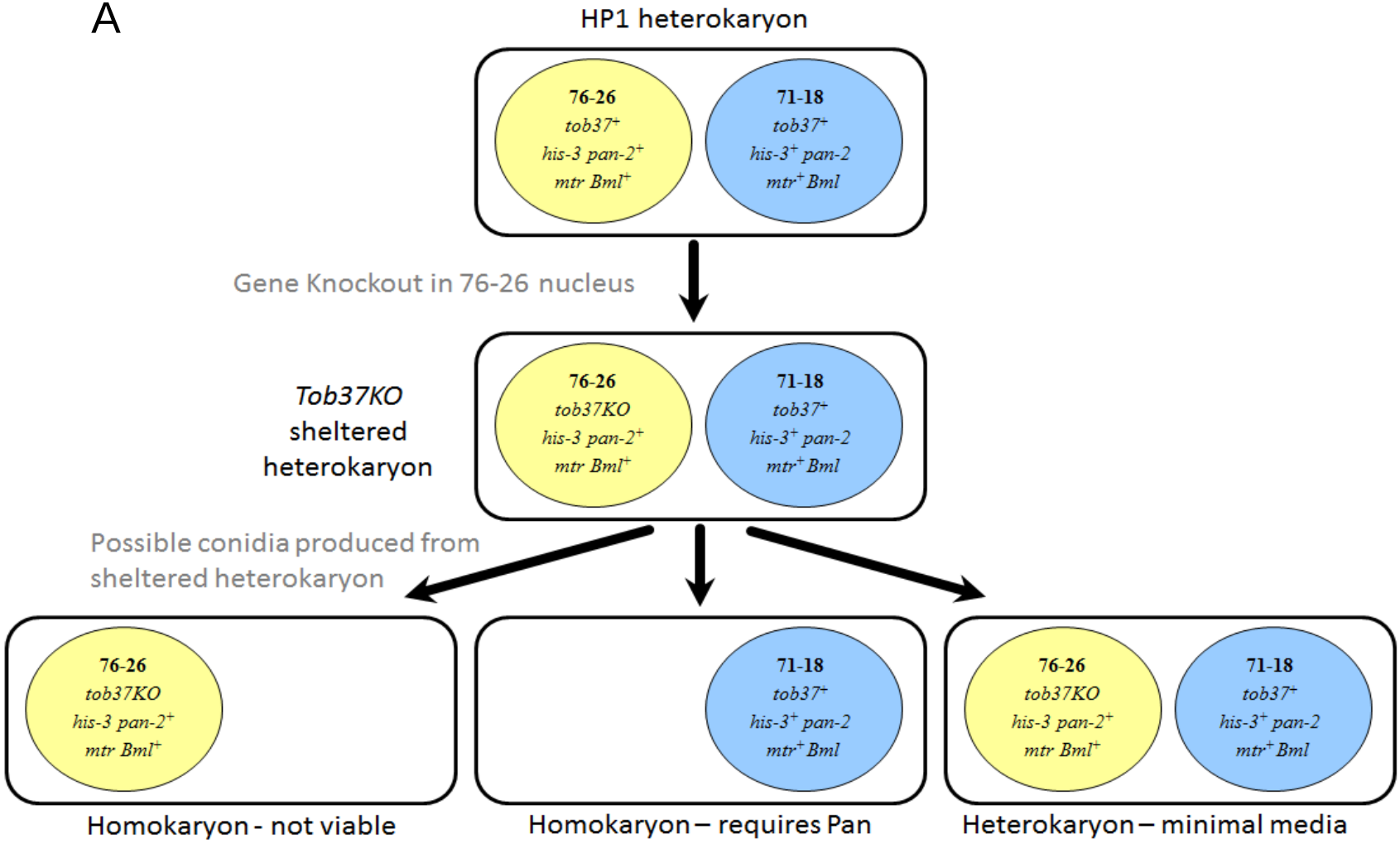
HP1 heterokaryon
76-26
tob37+
his-3 pan-2+
mtr Bml+
71-18
tob37+
his-3+ pan-2
mtr+ Bml
Gene Knockout in 76-26 nucleus
Tob37KO
sheltered
heterokaryon
76-26
tob37KO
his-3 pan-2+
mtr Bml+
71-18
tob37+
his-3+ pan-2
mtr+ Bml
Possible conidia produced from
sheltered heterokaryon
76-26
tob37KO
his-3 pan-2+
mtr Bml+
Homokaryon - not viable
71-18
tob37+
his-3+ pan-2
mtr+ Bml
Homokaryon – requires Pan
76-26
tob37KO
his-3 pan-2+
mtr Bml+
71-18
tob37+
his-3+ pan-2
mtr+ Bml
Heterokaryon – minimal media

B

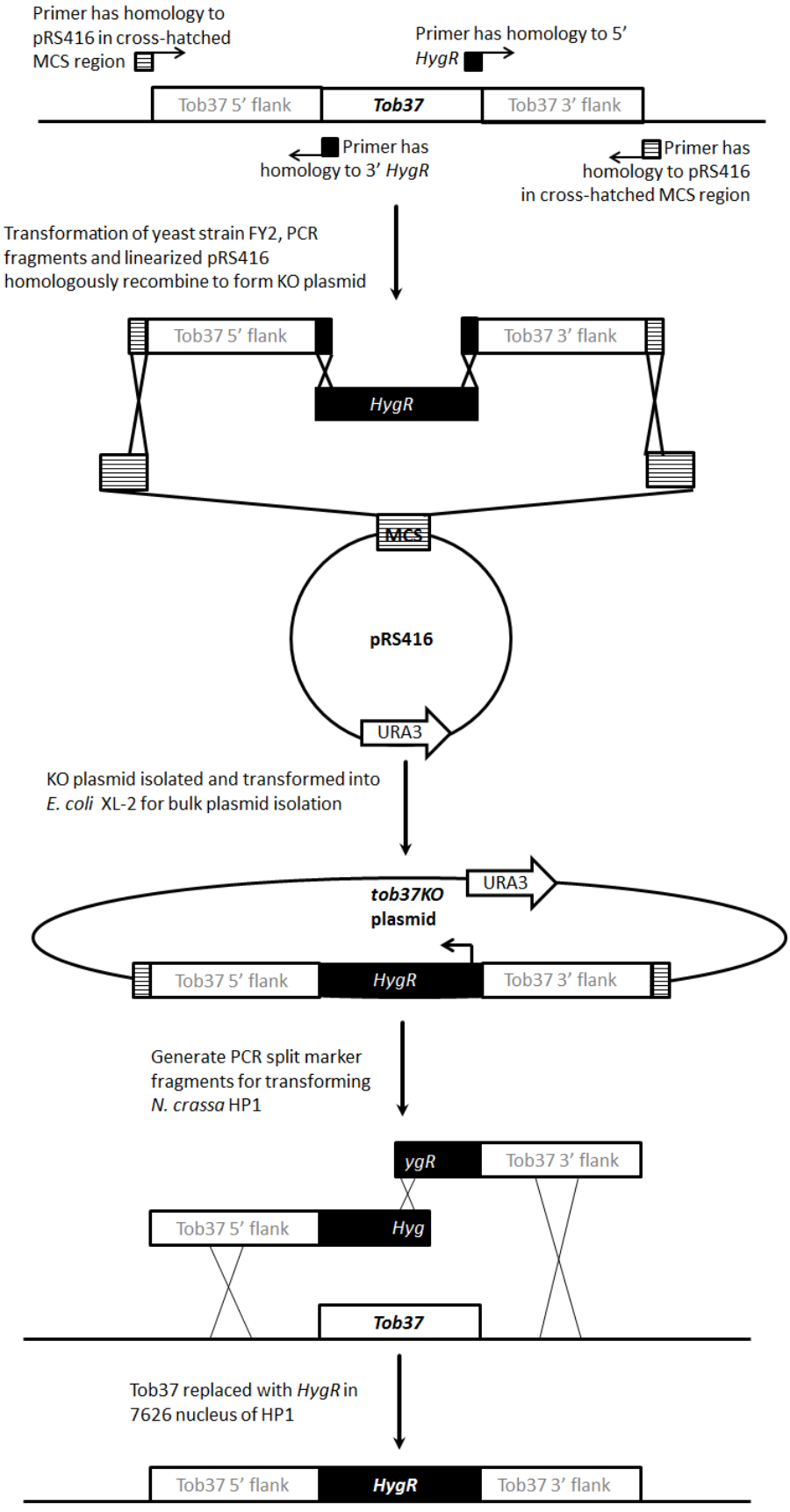
Primer has homology to pRS416 in cross-hatched MCS region
Primer has homology to 5' HygR
Tob37 5' flank
Tob37
Tob37 3' flank
Primer has homology to 3' HygR
Primer has homology to pRS416 in cross-hatched MCS region
Transformation of yeast strain FY2, PCR fragments and linearized pRS416 homologously recombine to form KO plasmid
Tob37 5' flank
Tob37 3' flank
HygR
MCS
pRS416
URA3
KO plasmid isolated and transformed into E. coli XL-2 for bulk plasmid isolation
tob37KO plasmid
URA3
Tob37 5' flank
HygR
Tob37 3' flank
Generate PCR split marker fragments for transforming N. crassa HP1
ygR
Tob37 3' flank
Tob37 5' flank
Hyg
Tob37
Tob37 replaced with HygR in 7626 nucleus of HP1
Tob37 5' flank
HygR
Tob37 3' flank

C

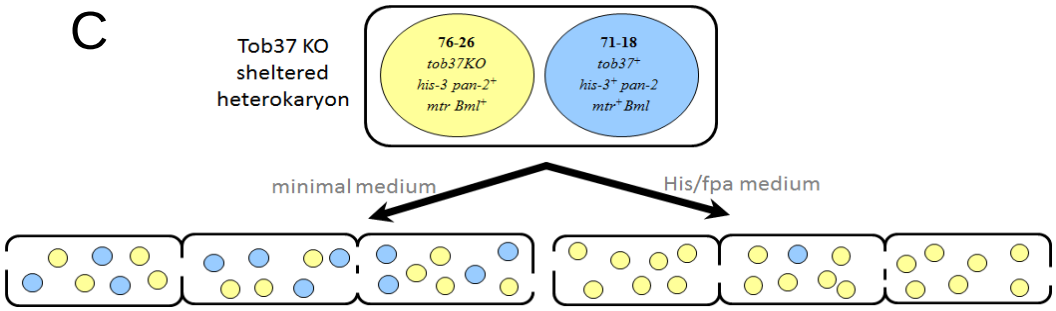
Tob37 KO
sheltered
heterokaryon
76-26
tob37KO
his-3 pan-2+
mtr Bml+
71-18
tob37+
his-3+ pan-2
mtr+ Bml
minimal medium
His/fpa medium

Supplemental Figure S2.2. Schematic representation of Tob37 mutant alleles.

The Figure shows the wildtype (Tob37) Tob37 protein and three constructs of Tob37 used to analyze the TMD topology of the protein. Using site-directed PCR mutagenesis *HpaI* sites (GTT/AAC) were inserted in place of the base-pairs coding for the amino acids that were on either side of the boundary of the predicted TMDs. Subsequent DNA restriction and ligation resulted in the mutant constructs used for transformation. Yellow represents the TMD (residues 386-405), blue the region between the two predicted TMDs (residues 406-423) and red represents the predicted C-terminal TMD. To differentiate between the two possible TMDs we refer to the C-terminal one as the C-terminal Hydrophobic Domain (CHD)(residues 424-442). Flanking amino acids that were altered are shown under each construct along with the residue substitutions that took place due to the codon change.

Tob37

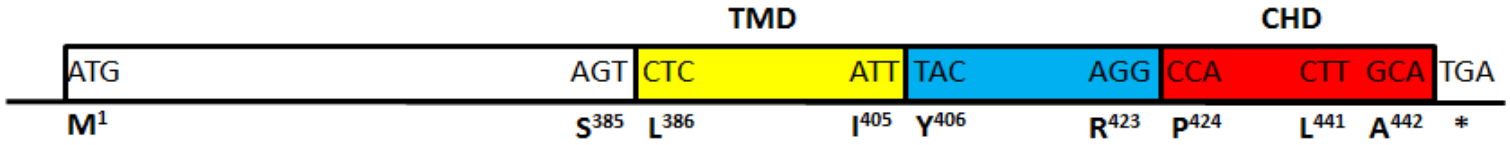

ΔTMD

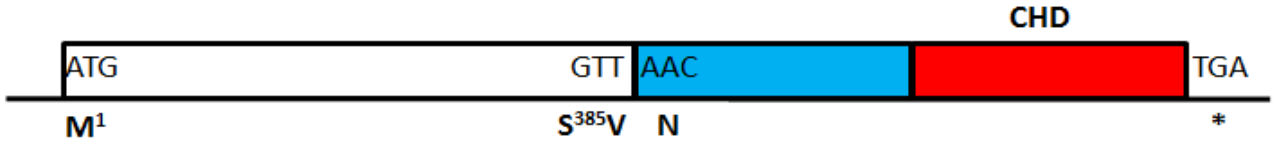

ΔCHD

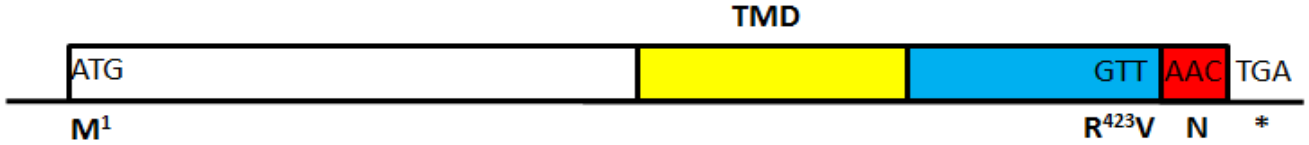

ΔT+C

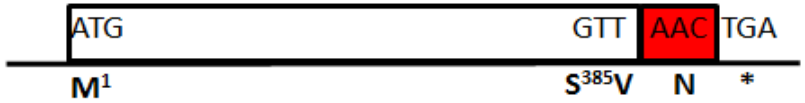

Tob37 alignment

```
N.c --MTLELHVWGPAFGLPSIDAECLATVTYFAQTLSAADYLLVQSSPSAVPS-------HH 51
H.s MAAPMELFCWSGGWGLPSVDLDSLAVLTYARFTGAPLKVHKISN-PWQSPS-------GT 52
S.c -MVKGSVHLWGKDGKASLISVDSIALVWFIKLCTSEEAKSMVAGLQIVFSNNTDLSSDGK 59
         .:. *.     . :. :.:* : :     :      : .     ..

N.c LPALYNPSTATWISGFDPIVNYLSTLQPP------SYHHPDVTTLPSRVYADSQAYKALL 105
H.s LPALR-TSHGEVISVPHKIITHLRKEK-----------YNADYDLSARQGADTLAFMSLL 100
S.c LPVLI-LDNGTKVSGYVNIVQFLHKNICTSKYEKGTDYEEDLAIVRKKDRLLEYSLLNYV 118
    **.*   . .  :*    *: .* .                   :  :      :    :

N.c TSSAAPLLALSLYVSSANYSETTRPAYSAILPFPLPWTEPLAVRAAMAARAAHLGMSSLD 165
H.s EEKLLPVLVHTFWIDTKNYVEVTRKWYAEAMPFPLNFFLP-------------------- 140
S.c DVEISRLTDYQLFLNTKNYNEYTKKLFSKLLYFPMWYNTP-------------------- 158
      .   :    :::.: ** * *:  ::  : **: :  *

N.c TDAEMERLEREEREREAAGWVQIPKALRKAVGGQNSGVKGQLSPEMKRRIKLEGLAAEVF 225
H.s -----GRMQRQYMER-----------LQLLTGEHRPEDEEELEKELYR--EARECLTLLS 182
S.c -----LQLRSQAREN-----------CEEIIGSLTLEDDEEFVESKAMESASQLAQSKTF 202
          ::. :  *.            .   *      . ::  .       .   :

N.c DVLGEVDFLEEEDGEEEEEEEEEAKEGGARIKVTLETKCLAFAYLALMLLPEVPRPWLKE 285
H.s QRLGSQKFFFG--------------------DAPASLDAFVFSYLALLLQAKLPSGKLQV 222
S.c KIAHKNKIKGK----------------------QELQQVKYNLQFDNRLQSCVSNWLAA 239
    .   . .:                           . . . :         .     *

N.c VLQKKYAGLCKFVLEYRRKTFPDSGKVLPWADRESDPAVSACDSALSIVGRFVRAVIDDI 345
H.s HLRGLHN-LCAYCTHILSLYFPWDGAEVPPQ-RQTPAGPETEEEPYRRRNQILSVLAGLA 280
S.c RKKLDDSVILSSDLLFLANLYVQLGLPDGNRIRSKLEQTFGSELLNSMSNKIDDFVHRPS 299
      :     :           :   *       *..       :      .::   :

N.c PMLGREWSRWWALRQRRVAEENSAETQLVVRRSVGESERSLLLAGAGLTLLAINVAGLGI 405
H.s AMVG------YALLSGIVSIQRATPARAPGTRTLGMAEEDEEE----------------- 317
S.c NNLE----------------QRDPQFREQGNVVMSLYNLACKYI---------------- 327
      :                 :. .  :      :.  :

N.c YWYRYRGLLGAPLQTWHRPLVGLGSFGAAGAMFAGLA 442
H.s ------------------------------------
S.c ------------------------------------
```

Tob38 alignment

```
N.c MATTSAAAPPRKWWQVPRPLQKVFDTFPLLAYDVNALPARAQSATSGDLPTLYVFSTEEE 60
H.s ------------------MSLVAEAFVSQIAAAEPWPENAT---------LYQQLKGEQ 32
S.c MVSS---------FSVPMPVKRIFDTFPLQTYAAQTDKDEAVALEIQRRSYTFTERGGGS 51
                      :. : ::*      .:.   .*          :      .

N.c ALLGAPSFNPNCLKWQAFLKLAGVKFQILP--STNHASPTGALPFILPTRSSPTDAPSPI 118
H.s ILLSD---NAASLAVQAFLQMCNLPIKVVCRANAEYMSPSGKVPFIHVGNQVVSELGPIV 89
S.c SDLTVEGTYKLGVYNVFLEANTGAALATDPWCLFVQLALCQKNGLVLPTHSQEQTPSHTC 111
      *         :    :    .  :           :      ::   ..

N.c PSSKLHDYALKYGTSNPPEVSALRLDAYQA-LLDVPIRNAWLQALYRDPEYTDLLDRFYI 177
H.s QFVKAKGHSLSDG---LEEVQKAEMKAYME-LVNNMLLTAELYLQWCDEATVGEITHARY 145
S.c N----HEMLVLSRLSNPDEALPILVEGYKKRIIRSTVAISEIMRSRILDDAEQLMYHTLL 167
         :   :        *.    :..*   ::   :  : :           : :

N.c TPASSSYWVRGALRHQLRRAAETEILKTGPGGAASTAVSLLVDEHSVYRAAVQALEALAT 237
H.s G-SPYPWPLNHILAYQKQWEVKRKMKAIGWG--KKTLDQVLEDVDQCCQALSQRLGTQP- 201
S.c DTVLYDCWITQILFCASDAQFMELYSCQKLSDSIVTPLDVENSLLQKLSAKSLKISLTKR 227
            :   *                  .    *  .:  .  .   *    :

N.c LLSESKTGWFFGAETPTIFDASVFAYTHLMLKYMSDAEGEVEGNMGFILASRKLGTMVRS 297
H.s ---------YFFNKQPTELDALVFGHLYTILTTQ--------------LTNDELSEKVKN 238
S.c NKFQFRHREIVKSMQGVYHNHHNSVNQEQVLNVLFENSKQVLLGLKDMLKSDGQPTYLHL 287
              .     .  :         :*.                * .      ::

N.c AGSGELEQHHRRLFELLWLADSNAELLDAKARGNKLLQFQLQA 340
H.s YSN--LLAFCRRIEQHYFEDRGKGRLS--------------- 263
S.c KIASYILCITNVKEPIKLKTFVENECKELVQFAQDTLKNFVQ- 329
```

Supplemental Figure S2.3. Tob37 and Tob38 Alignments. Alignments of *Neurospora crassa* (*N.c*), *Saccharomyces cerevisiae* (*S.c*), and *Homo sapiens* (*H.s*) Tob37 and Tob38 proteins. *, identical residues; :, conserved substitutions; ., semi-conserved substitutions. For the Tob37 alignment, the yellow highlight shows TMD1 in the *N. crassa* protein and the TMD of the *H. sapiens* protein, and the blue highlight shows the CHD of the *N. crassa* protein.

2.5 References

Abdul, K.M., Terada, K., Yano, M., Ryan, M.T., Streimann, I., Hoogenraad, N.J., and Mori, M. (2000). Functional analysis of human metaxin in mitochondrial protein import in cultured cells and its relationship with the TOM complex. Biochem. Biophys. Res. Commun. *276*, 1028-1034.

Armstrong, L.C., Komiya, T., Bergman, B.E., Mihara, K., and Bornstein, P. (1997). Metaxin is a component of a preprotein import complex in the outer membrane of the mammalian mitochondrion. J. Biol. Chem. *272*, 6510-6518.

Armstrong, L.C., Saenz, A.J., and Bornstein, P. (1999). Metaxin 1 interacts with metaxin 2, a novel related protein associated with the mammalian mitochondrial outer membrane. J. Cell. Biochem. *74*, 11-22.

Austin, B., Hall, R.M., and Tyler, B.M. (1990). Optimized vectors and selection for transformation of *Neurospora crassa* and *Aspergillus nidulans* to bleomycin and phleomycin resistance. Gene *93*, 157-162.

Becker, T., Guiard, B., Thornton, N., Zufall, N., Stroud, D.A., Wiedemann, N., and Pfanner, N. (2010). Assembly of the mitochondrial protein import channel: role of Tom5 in two-stage interaction of Tom40 with the SAM complex. Mol Biol Cell *21*, 3106-3113.

Becker, T., Pfannschmidt, S., Guiard, B., Stojanovski, D., Milenkovic, D., Kutik, S., Pfanner, N., Meisinger, C., and Wiedemann, N. (2008). Biogenesis of the mitochondrial TOM complex: Mim1 promotes insertion and assembly of signal-anchored receptors. J Biol Chem *283*, 120-127.

Becker, T., Wenz, L.S., Thornton, N., Stroud, D., Meisinger, C., Wiedemann, N., and Pfanner, N. (2011). Biogenesis of mitochondria: dual role of Tom7 in modulating assembly of the preprotein translocase of the outer membrane. J Mol Biol *405*, 113-124.

Borkovich, K.A., and Weiss, R.L. (1987). Relationship between two major immunoreactive forms of arginase in *Neurospora crassa*. J. Bact. *169*, 5510-5517.

Bornstein, P., McKinney, C.E., LaMarca, M.E., Winfield, S., Shingu, T., Devarayalu, S., Vos, H.L., and Ginns, E.I. (1995). Metaxin, a gene contiguous to both thrombospondin 3 and glucocerebrosidase, is required for embryonic development in the mouse: implications for Gaucher disease. Proc. Natl. Acad. Sci. USA *92*, 4547-4551.

Chan, N.C., and Lithgow, T. (2008). The peripheral membrane subunits of the SAM complex function codependently in mitochondrial outer membrane biogenesis. Mol Biol Cell *19*, 126-136.

Colot, H.V., Park, G., Turner, G.E., Ringelberg, C., Crew, C., Litvinkova, L., Weiss, R.L., Borkovich, K.A., and Dunlap, J.C. (2006). A high-throughput gene knockout procedure for *Neurospora* reveals functions for multiple transcription factors. Proc. Natl. Acad. Sci. USA *103*, 10352-10357.

Curran, S.P., Leuenberger, D., Oppliger, W., and Koehler, C.M. (2002a). The Tim9p-Tim10p complex binds to the transmembrane domains of the ADP/ATP carrier. EMBO J. *21*, 942-953.

Curran, S.P., Leuenberger, D., Schmidt, E., and Koehler, C.M. (2002b). The role of the Tim8p-Tim13p complex in a conserved import pathway for mitochondrial polytopic inner membrane proteins. J. Cell Biol. *158*, 1017-1027.

Dagley, M.J., Gentle, I.E., Beilharz, T.H., Pettolino, F.A., Djordjevic, J.T., Lo, T.L., Uwamahoro, N., Rupasinghe, T., Tull, D.L., McConville, M., Beaurepaire, C., Nantel, A., Lithgow, T., Mitchell, A.P., and Traven, A. (2011). Cell wall integrity is linked to mitochondria and phospholipid homeostasis in *Candida albicans* through the activity of the post-transcriptional regulator Ccr4-Pop2. Mol. Micro. *79*, 968-989.

Davis, R.H., and De Serres, F.J. (1970). Genetic and microbiological research techniques for *Neurospora crassa*. Methods Enzymol. *17*, 79-143.

Dukanovic, J., Dimmer, K.S., Bonnefoy, N., Krumpe, K., and Rapaport, D. (2009). Genetic and functional interactions between the mitochondrial outer membrane proteins Tom6 and Sam37. Mol Cell Biol *29*, 5975-5988.

Good, A.G., and Crosby, W.L. (1989). Anaerobic induction of alanine aminotransferase in barley root tissue. Plant Physiol *90*, 1305-1309.

Grad, L.I., Descheneau, A.T., Neupert, W., Lill, R., and Nargang, F.E. (1999). Inactivation of the Neurospora crassa mitochondrial outer membrane protein TOM70 by repeat-induced point mutation (RIP) causes defects in mitochondrial protein import and morphology. Curr Genet *36*, 137-146.

Gratzer, S., Lithgow, T., Bauer, R.E., Lamping, E., Paltauf, F., Kohlwein, S.D., Haucke, V., Junne, T., Schatz, G., and Horst, M. (1995). Mas37p, a novel receptor subunit for protein import into mitochondria. J. Cell Biol. *129*, 25-34.

Grotelueschen, J., and Metzenberg, R.L. (1995). Some property of the nucleus determines the competence of *Neurospora crassa* for transformation. Genetics *139*, 1545-1551.

Habib, S.J., Waizenegger, T., Lech, M., Neupert, W., and Rapaport, D. (2005). Assembly of the TOB complex of mitochondria. J. Biol. Chem. *280*, 6434-6440.

Harkness, T.A., Nargang, F.E., van der Klei, I., Neupert, W., and Lill, R. (1994). A crucial role of the mitochondrial protein import receptor MOM19 for the biogenesis of mitochondria. J Cell Biol *124*, 637-648.

Hoppins, S.C., Go, N.E., Klein, A., Schmitt, S., Neupert, W., Rapaport, D., and Nargang, F.E. (2007). Alternative splicing gives rise to different isoforms of the *Neurospora crassa* Tob55 protein that vary in their ability to insert beta-barrel proteins into the outer mitochondrial membrane. Genetics *177*, 137-149.

Hoppins, S.C., and Nargang, F.E. (2004). The Tim8-Tim13 complex of *Neurospora crassa* functions in the assembly of proteins into both mitochondrial membranes. J Biol Chem *279*, 12396-12405.

Horie, C., Suzuki, H., Sakaguchi, M., and Mihara, K. (2002). Characterization of signal that directs C-tail-anchored proteins to mammalian mitochondrial outer membrane. Mol. Biol. Cell *13*, 1615-1625.

Imai, K., Gromiha, M.M., and Horton, P. (2008). Mitochondrial beta-barrel proteins, an exclusive club? Cell *135*, 1158-1159; author reply 1159-1160.

Ishikawa, D., Yamamoto, H., Tamura, Y., Moritoh, K., and Endo, T. (2004). Two novel proteins in the mitochondrial outer membrane mediate beta-barrel protein assembly. J Cell Biol *166*, 621-627.

Klein, A., Israel, L., Lackey, S.W., Nargang, F.E., Imhof, A., Baumeister, W., Neupert, W., and Thomas, D.R. (2012). Characterization of the insertase for beta-barrel proteins of the outer mitochondrial membrane. J Cell Biol *199*, 599-611.

Kozjak-Pavlovic, V., Ross, K., Benlasfer, N., Kimmig, S., Karlas, A., and Rudel, T. (2007). Conserved roles of Sam50 and metaxins in VDAC biogenesis. EMBO Rep. *8*, 576-582.

Kozjak, V., Wiedemann, N., Milenkovic, D., Lohaus, C., Meyer, H.E., Guiard, B., Meisinger, C., and Pfanner, N. (2003). An essential role of Sam50 in the protein sorting and assembly machinery of the mitochondrial outer membrane. J Biol Chem *278*, 48520-48523.

Kutik, S., Stojanovski, D., Becker, L., Becker, T., Meinecke, M., Kruger, V., Prinz, C., Meisinger, C., Guiard, B., Wagner, R., Pfanner, N., and Wiedemann, N. (2008). Dissecting membrane insertion of mitochondrial beta-barrel proteins. Cell *132*, 1011-1024.

Laemmli, U.K. (1970). Cleavage of structural proteins during the assembly of the head of bacteriophage T4. Nature *227*, 680-685.

Marathe, S., Yu, Y.G., Turner, G.E., Palmier, C., and Weiss, R.L. (1998). Multiple forms of arginase are differentially expressed from a single locus in *Neurospora crassa*. J. Biol. Chem. *273*, 29776-29785.

Meisinger, C., Pfannschmidt, S., Rissler, M., Milenkovic, D., Becker, T., Stojanovski, D., Youngman, M.J., Jensen, R.E., Chacinska, A., Guiard, B., Pfanner, N., and Wiedemann, N. (2007). The morphology proteins Mdm12/Mmm1 function in the major β-barrel assembly pathway of mitochondria. EMBO J. *26*, 2229-2239.

Meisinger, C., Rissler, M., Chacinska, A., Sanjuán Szklarz, L.K., Milenkovic, D., Kozjak, V., Schönfisch, B., Lohaus, C., Meyer, H.E., Yaffe, M.P., Guiard, B., Wiedemann, N., and Pfanner, N. (2004). The mitochondrial morphology protein Mdm10 functions in assembly of the preprotein translocase of the outer membrane. Developmental Cell *7*, 61-71.

Milenkovic, D., Kozjak, V., Wiedemann, N., Lohaus, C., Meyer, H.E., Guiard, B., Pfanner, N., and Meisinger, C. (2004). Sam35 of the mitochondrial protein sorting and assembly machinery is a peripheral outer membrane protein essential for cell viability. J Biol Chem *279*, 22781-22785.

Model, K., Meisinger, C., Prinz, T., Wiedemann, N., Truscott, K.N., Pfanner, N., and Ryan, M.T. (2001). Multistep assembly of the protein import channel of the mitochondrial outer membrane. Nat. Struct. Biol. *8*, 361-370.

Nargang, F.E., Künkele, K.-P., Mayer, A., Ritzel, R.G., Neupert, W., and Lill, R. (1995). "Sheltered disruption" of *Neurospora crassa* MOM22, an essential component of the mitochondrial protein import complex. EMBO J. *14*, 1099-1108.

Nargang, F.E., and Rapaport, D. (2007). *Neurospora crassa* as a model organism for mitochondrial biogenesis. Methods Mol Biol *372*, 107-123.

Paschen, S.A., Waizenegger, T., Stan, T., Preuss, M., Cyrklaff, M., Hell, K., Rapaport, D., and Neupert, W. (2003). Evolutionary conservation of biogenesis of beta-barrel membrane proteins. Nature *426*, 862-866.

Rapaport, D., and Nargang, F.E. (2004). Mitochondrial biogenesis: Protein import into and across the outer membrane. In: Topics in Current Genetics, Vol. 8. Biogenesis of mitochondria and associated diseases., vol. 8, eds. M. Bauer and C. Koehler, Berlin Heidelberg: Springer-Verlag, 37-58.

Rapaport, D., and Neupert, W. (1999). Biogenesis of Tom40, core component of the TOM complex of mitochondria. J. Cell Biol. *146*, 321-331.

Ryan, M.T., Muller, H., and Pfanner, N. (1999). Functional staging of ADP/ATP carrier translocation across the outer mitochondrial membrane. J. Biol. Chem. *274*, 20619-20627.

Schägger, H., Cramer, W.A., and von Jagow, G. (1994). Analysis of molecular masses and oligomeric states of protein complexes by blue native electrophoresis and isolation of membrane protein complexes by two-dimensional native electrophoresis. Anal. Biochem. *217*, 220-230.

Schägger, H., and von Jagow, G. (1991). Blue native electrophoresis for isolation of membrane complexes in enzymatically active form. Anal. Biochem. *199*, 223-231.

Schlossmann, J., Lill, R., Neupert, W., and Court, D.A. (1996). Tom71, a novel homologue of the mitochondrial preprotein receptor Tom70. J. Biol. Chem. *271*, 17890-17896.

Sherman, E.L., Go, N.E., and Nargang, F.E. (2005). Functions of the small proteins in the TOM complex of *Neurospora crassa*. Mol. Biol. Cell *16*, 4172-4182.

Shore, G.C., McBride, H.M., Millar, D.G., Steenaart, N.A.M., and Nguyen, M. (1995). Import and insertion of proteins into the mitochondrial outer membrane. Eur. J. Biochem. *227*, 9-18.

Söllner, T., Pfaller, R., Griffiths, G., Pfanner, N., and Neupert, W. (1990). A mitochondrial import receptor for the ADP/ATP carrier. Cell *62*, 107-115.

Stojanovski, D., Guiard, B., Kozjak-Pavlovic, V., Pfanner, N., and Meisinger, C. (2007). Alternative function for the mitochondrial SAM complex in biogenesis of alpha-helical TOM proteins. J Cell Biol *179*, 881-893.

Stroud, D.A., Becker, T., Qiu, J., Stojanovski, D., Pfannschmidt, S., Wirth, C., Hunte, C., Guiard, B., Meisinger, C., Pfanner, N., and Wiedemann, N. (2011). Biogenesis of mitochondrial beta-barrel proteins: the POTRA domain is involved in precursor release from the SAM complex. Mol Biol Cell *22*, 2823-2833.

Tanton, L.L., Nargang, C.E., Kessler, K.E., Li, Q., and Nargang, F.E. (2003). Alternative oxidase expression in *Neurospora crassa*. Fungal Genet Biol *39*, 176-190.

Taylor, R., McHale, B., and Nargang, F.E. (2003). Characterization of *Neurospora crassa* Tom40-deficient mutants and effect of specific mutations on Tom40 assembly. J. Biol. Chem. *278*, 765-775.

Thornton, N., Stroud, D.A., Milenkovic, D., Guiard, B., Pfanner, N., and Becker, T. (2010). Two modular forms of the mitochondrial sorting and assembly machinery are involved in biogenesis of alpha-helical outer membrane proteins. J Mol Biol *396*, 540-549.

Vasiljev, A., Ahting, U., Nargang, F.E., Go, N.E., Habib, S.J., Kozany, C., Panneels, V., Sinning, I., Prokisch, H., Neupert, W., Nussberger, S., and Rapaport, D. (2004). Reconstituted TOM core complex and Tim9/Tim10 complex of mitochondria are sufficient for translocation of the ADP/ATP carrier across membranes. Mol. Biol. Cell *15*, 1445-1458.

Waizenegger, T., Habib, S.J., Lech, M., Mokranjac, D., Paschen, S.A., Hell, K., Neupert, W., and Rapaport, D. (2004). Tob38, a novel essential component in the biogenesis of beta-barrel proteins of mitochondria. EMBO Rep *5*, 704-709.

Webb, C.T., Gorman, M.A., Lazarou, M., Ryan, M.T., and Gulbis, J.M. (2006). Crystal structure of the mitochondrial chaperone TIM9-10 reveals a six-bladed α-propeller. Mol. Cell *21*, 123-133.

Wideman, J.G., Go, N.E., Klein, A., Redmond, E., Lackey, S.W., Tao, T., Kalbacher, H., Rapaport, D., Neupert, W., and Nargang, F.E. (2010). Roles of the Mdm10, Tom7, Mdm12, and Mmm1 proteins in the assembly of mitochondrial outer membrane proteins in *Neurospora crassa*. Mol Biol Cell *21*, 1725-1736.

Wiedemann, N., Kozjak, V., Chacinska, A., Schonfisch, B., Rospert, S., Ryan, M.T., Pfanner, N., and Meisinger, C. (2003). Machinery for protein sorting and assembly in the mitochondrial outer membrane. Nature *424*, 565-571.

Wiedemann, N., Truscott, K.N., Pfannschmidt, S., Guiard, B., Meisinger, C., and Pfanner, N. (2004). Biogenesis of the protein import channel Tom40 of the mitochondrial outer membrane. Intermembrane space components are involved in an early stage of the assembly pathway. J. Biol. Chem. *279*, 18188-18194.

Yamano, K., Tanaka-Yamano, S., and Endo, T. (2010). Mdm10 as a dynamic constituent of the TOB/SAM complex directs coordinated assembly of Tom40. EMBO Rep *11*, 187-193.

Chapter 3. Using Substituted Cysteine Accessibility Mapping (SCAM) to identify β-strands in the *Neurospora crassa* Tom40 protein.

Note: This project has been on-going in the Nargang lab for several years. A number of technicians and graduate students have been involved in producing the mutants and producing SCAM data (Go, N.E., Taylor, R.D., Nargang, F.E., Wong, A., Sherman, L.). I have completed the last of the planned SCAM analysis (residues 94-106 in *N. crassa* Tom40) and have put all the data in the context of existing knowledge in the literature.

3.1 Introduction

As discussed in sections 1.6.2.1 and 1.8 a structure for Tom40 has been proposed based almost entirely on computer predictions and modeling on the structure of the related β-barrel protein, porin (discussed below). Understanding the topology of Tom40 would allow us to make testable predictions on the role of individual residues on regions of the protein and lead to further understanding of the process of mitochondrial protein import, the structure of the TOM complex, and the evolution of the import machinery. The optimal situation would be to have a crystal structure of the protein. Several attempts have been made to analyze crystals of the TOM_{core} complex, but none have yet been successful (Nargang, F.E. personal communication) and no 3D structures of Tom40 have been acquired. Early computer predictions of Tom40 structure suggested 14 β-stranded models (Figure 3.1) (Court *et al.*, 1995; Mannella *et al.*, 1996; Taylor, 2003).

MOM embedded β-barrels with their complex amphipathic structures are not ideal candidates for crystallization as hydrophobicity often leads to aggregation and misfolding. However, the crystal structures of many bacterial OM β-barrels with varying functions have been solved using complex refolding techniques to acquire crystallized proteins (Galdiero *et al.*, 2007). Proteins containing 8, 10, 12, 14, 16, 18, and 22 β-strands have been identified. All these bacterial proteins have an even number of β-strands with both N- and C-termini present in the periplasmic space. The smallest of these, OmpA, has 8 β-strands and acts as a solid poreless transmembrane anchor (Pautsch and Schulz, 1998). General porins such as OmpF, OmpC, PhoE and MP3 have a 16 β-stranded pore architecture and form homotrimers to allow the passive diffusion of small molecules (Galdiero *et al.*, 2007).

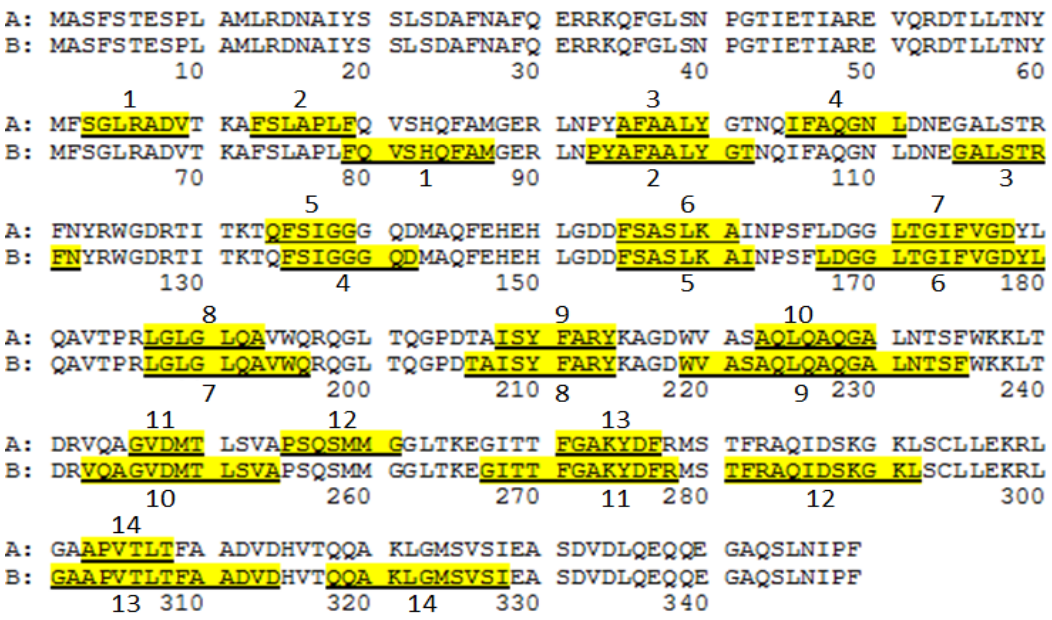

Figure 3.1 Early computer predictions led to a 14 β-stranded model for *N. crassa* Tom40 topology. Predicted β-strands are highlighted and underlined. A (top sequence) The model predicted by Court *et al.* (1995). B (bottom sequence) The model predicted by T. Schirmer via D. Rapaport (Taylor, 2003).

The only eukaryotic membrane embedded β-barrel with a known structure is porin (or VDAC). Three independent groups determined essentially the same 3D structure of human and mouse porins (VDAC) utilizing NMR and X-ray crystallography (Bayrhuber *et al.*, 2008; Hiller *et al.*, 2008; Ujwal *et al.*, 2008; Hiller and Wagner, 2009; Hiller *et al.*, 2010; Yu *et al.*, 2012). Each of these studies resulted in a model of the protein containing a 19 stranded β-barrel structure with an N-terminal α-helix plugging the pore in the closed state. The model satisfies all the structural and biophysical requirements for a functional porin to maintain a stable conformation embedded within the MOM and allow the passive diffusion of small molecules through its pore (Figure 3.2). There is general acceptance of the porin structural model (hereafter known as the "3D model") in the literature (Hiller *et al.*, 2010; Summers and Court, 2010; Bay *et al.*, 2012). However, it has been pointed out that this model conflicts with previous conclusions based on many biochemical and functional studies of porin (Blachly-Dyson *et al.*, 1990; Thomas *et al.*, 1991; Thomas *et al.*, 1993; Song and Colombini, 1996; Song *et al.*, 1998b; Colombini, 2009; McDonald *et al.*, 2009; Colombini, 2012a, b) leading to the suggestion that the 3D structure was determined on a non-native form of the protein that results from the purification protocol (see below). A model of porin structure (hereafter referred to as the "biochemical model" or BIO) based on these data suggests that the porin channel is formed by a single α-helix and 13 β-strands (Figure 3.2). Interestingly, each of the 13 β-strands predicted from the biochemical model are also present in the 19 strands in the 3D model. The existence and placement of the remaining 6 proposed β-strands of the 3D model have been said to contradict the biochemical results for various reasons (Colombini, 2009). For example, controversy arises from the fact that residue charge substitutions within these other 6 proposed β-strands resulted in no effects on channel ion selectivity, suggesting the residues are not part of the pore lumen

Figure 3.2 Two models for human porin topology. The amino acid sequence of porin from *H. sapiens* is shown in duplicate. The position of the 19 β-strands identified in the 3D NMR and X-ray structural analysis are shown on the top sequence (3D) (Bayrhuber *et al.*, 2008; Hiller *et al.*, 2008; Ujwal *et al.*, 2008). Red numbers designate the highlighted (yellow) β-strands. The 13 β-strands predicted by the biochemical model (BIO) (Blachly-Dyson *et al.*, 1990; Peng *et al.*, 1992; Song and Colombini, 1996; Song *et al.*, 1998b, a) are shown on the bottom sequence. Blue numbers designate the highlighted (blue) β-strands. The biochemical model has an N-terminal α-helical TMD that forms part of the pore wall (-----). The 3D model also predicts an N-terminal α-helix (^{11}GKSARDVFTK^{20}) but this is not thought to form part of the wall of the pore. (**…….**) represents regions predicted to be exposed in the IMS. (**_____**) represents regions predicted to be exposed to the cytosol. (* and #) show sites of FLAG epitope insertion (McDonald *et al.*, 2009). (*) Sites found to face the IMS. (#) Sites face cytosol. *1 fits both models, *2 conflicts with 3D, #3 conflicts with 3D and #4 fits both models. Figure adapted from data presented by Colombini (2009) and Hiller *et al.* (2010).

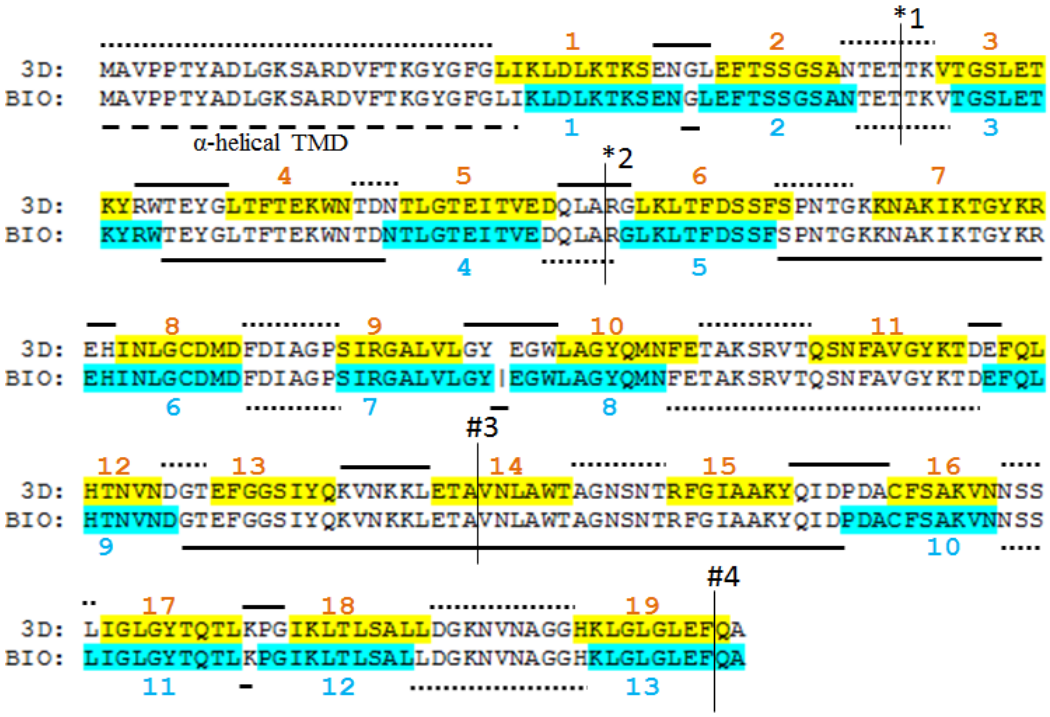
*1
3D: MAVPPTYADLGKSARDVFTKGYGFGLIKLDLKTKSENGLEFTSSGSANTETTKVTGSLET
BIO: MAVPPTYADLGKSARDVFTKGYGFGLIKLDLKTKSENGLEFTSSGSANTETTKVTGSLET
α-helical TMD
*2
3D: KYRWTEYGLTFTEKWNTDNTLGTEITVEDQLARGLKLTFDSSFSPNTGKKNAKIKTGYKR
BIO: KYRWTEYGLTFTEKWNTDNTLGTEITVEDQLARGLKLTFDSSFSPNTGKKNAKIKTGYKR
3D: EHINLGCDMDFDIAGPSIRGALVLGY EGWLAGYQMNFETAKSRVTQSNFAVGYKTDEFQL
BIO: EHINLGCDMDFDIAGPSIRGALVLGY|EGWLAGYQMNFETAKSRVTQSNFAVGYKTDEFQL
#3
3D: HTNVNDGTEFGGSIYQKVNKKLETAVNLAWTAGNSNTRFGIAAKYQIDPDACFSAKVNNSS
BIO: HTNVNDGTEFGGSIYQKVNKKLETAVNLAWTAGNSNTRFGIAAKYQIDPDACFSAKVNNSS
#4
3D: LIGLGYTQTLKPGIKLTLSALLDGKNVNAGGHKLGLGLEFQA
BIO: LIGLGYTQTLKPGIKLTLSALLDGKNVNAGGHKLGLGLEFQA

(Blachly-Dyson *et al.*, 1990; Peng *et al.*, 1992; Song and Colombini, 1996; Song *et al.*, 1998b). Furthermore, the topology of *S. cerevisiae* porin was investigated via the insertion of four FLAG epitopes at key locations within the protein (McDonald *et al.*, 2009). Two sites were found to be exposed in the IMS whereas the other two were cytosolic. The orientation of all four FLAG insertions was consistent with the biochemical model. In contrast two of the four FLAG results directly contradict the 3D structure (Figure 3.2).

The 3D NMR and crystallographic structures were determined from porin expressed in *E. coli*, isolated from inclusion bodies, and refolded (Bayrhuber *et al.*, 2008; Hiller *et al.*, 2008; Ujwal *et al.*, 2008). Refolding was achieved by first dissolving purified porin in a guanidinium hydrochloride buffer, then adding this solution slowly (dropwise or via dialysis) to refolding buffer containing lauryldimethylamine oxide (LDAO) micelles at 4˚C. A number of problems in using this approach to obtain porin crystals have been summarized by Colombini (2009, 2012a). For example, functional studies on this refolded porin have shown it lacks certain well-known signature characteristic biophysical properties of porin such as single channel conductance and voltage dependence (Peng *et al.*, 1992; Thomas *et al.*, 1993; Song *et al.*, 1998a; Colombini, 2009). These properties can be restored via treatment of the refolded protein with cholesterol and Triton X100, however the latter prevents crystallization and thus interferes with the ability to solve the structure.

Furthermore, only a minute fraction ($\sim 1/10^6$) of reconstituted porin molecules from the 3D protocols insert into membranes. The 3D structures were determined using those molecules free in solution whereas the functional studies giving rise to the BIO model are performed on the membrane embedded population. These arguments suggest the 3D models actually represent a non-native structure and Colombini (2009) has

proposed a hypothetical conformational alteration that converts the 3D model to his favored 13 β-stranded biochemical model.

My interests have not been directly focused on models of porin structure. It is currently thought that Tom40 and Porin are derived from a common ancestral β-barrel protein (Bayrhuber *et al.*, 2008; Zeth, 2010; Gessmann *et al.*, 2011; Bay *et al.*, 2012), though there is no known homologue in the OM of extant Gram –ve bacteria. Despite their common ancestry Tom40 and Porin have evolved separately to accommodate different needs in protein import and metabolite exchange, respectively. The lack of a clear bacterial homolog to Tom40 and porin can perhaps be explained by the high evolutionary demands of the newly acquired endosymbiont to have a vastly increased interaction with its new surrounding environment, the cytosol. Overall, conservation of porin primary sequences from many lineages is relatively low (Saccone *et al.*, 2003; Young *et al.*, 2007). This is likely explained by the presence of numerous paralogs in the gene family, the array of isoforms present in some species and the variety of functions porins have acquired within and between species (Saccone *et al.*, 2003; Young *et al.*, 2007; Zeth, 2010). Sequence similarity of the Tom40 protein among many species is much more evident (Gessmann *et al.*, 2011), probably due to the conserved functional specificity of the protein and the high number of protein interactions that must be maintained. Despite high sequence divergence, alignment of Tom40 and porin sequences with secondary structure predictions reveals their common ancestry (Figure 3.3).

Recent bioinformatic and phylogenetic analysis along with mass spectrometric data following limited proteolysis have resulted in computer models of the *N. crassa* (Gessmann *et al.*, 2011) and mammalian (Zeth, 2010; Mager *et al.*, 2011; Bay *et al.*, 2012) Tom40 proteins (Figure 3.3). These models have been based on the 3D structure of

Figure 3.3 Amino acid alignment of human porin, human Tom40 and *N. crassa* Tom40. The amino acid sequence of porin from *H. sapiens (H.s.)* is shown in duplicate. The position of the 13 β-strands predicted by the biochemical model (Blachly-Dyson *et al.*, 1990; Peng *et al.*, 1992; Song and Colombini, 1996; Song *et al.*, 1998b, a; Colombini, 2009) are shown (highlighted and numbered red) on the top sequence (*H.s.* p_BIO). (*) represents a sharp hairpin loop between β-strands 7 and 8 in the biochemical model. The second sequence (*H.s.* p_3D) shows the position (green) of the 19 β-strands identified by the NMR and X-ray structural studies conducted on mammalian porin (Bayrhuber *et al.*, 2008; Hiller *et al.*, 2008; Ujwal *et al.*, 2008). The third sequence (*H.s.* Tom40) shows the position (yellow) of the 19 β-stands predicted to exist using limited proteolysis followed by mass spectrometry and bioinformatics based on the homology of Tom40 and porin (Gessmann *et al.*, 2011). The bottom sequence (*N.c* Tom40) represents the *N. crassa* Tom40 with the predicted 19 β-strands shown (highlighted and numbered blue) based on homology to the predicted 3D structure of *H.s.* Tom40 and its predicted 3D structure from the solved 3D structure of *H.s.* porin (Gessmann *et al.*, 2011). The solid line between the black arrows spanning *N. crassa* residues Y94-F106 indicates the region examined in my experimental SCAM analysis. The region indicated by the dotted line shows the contiguous extension of that region by the work of others in the laboratory. This figure was adapted from Gessmann *et al.* (2011).

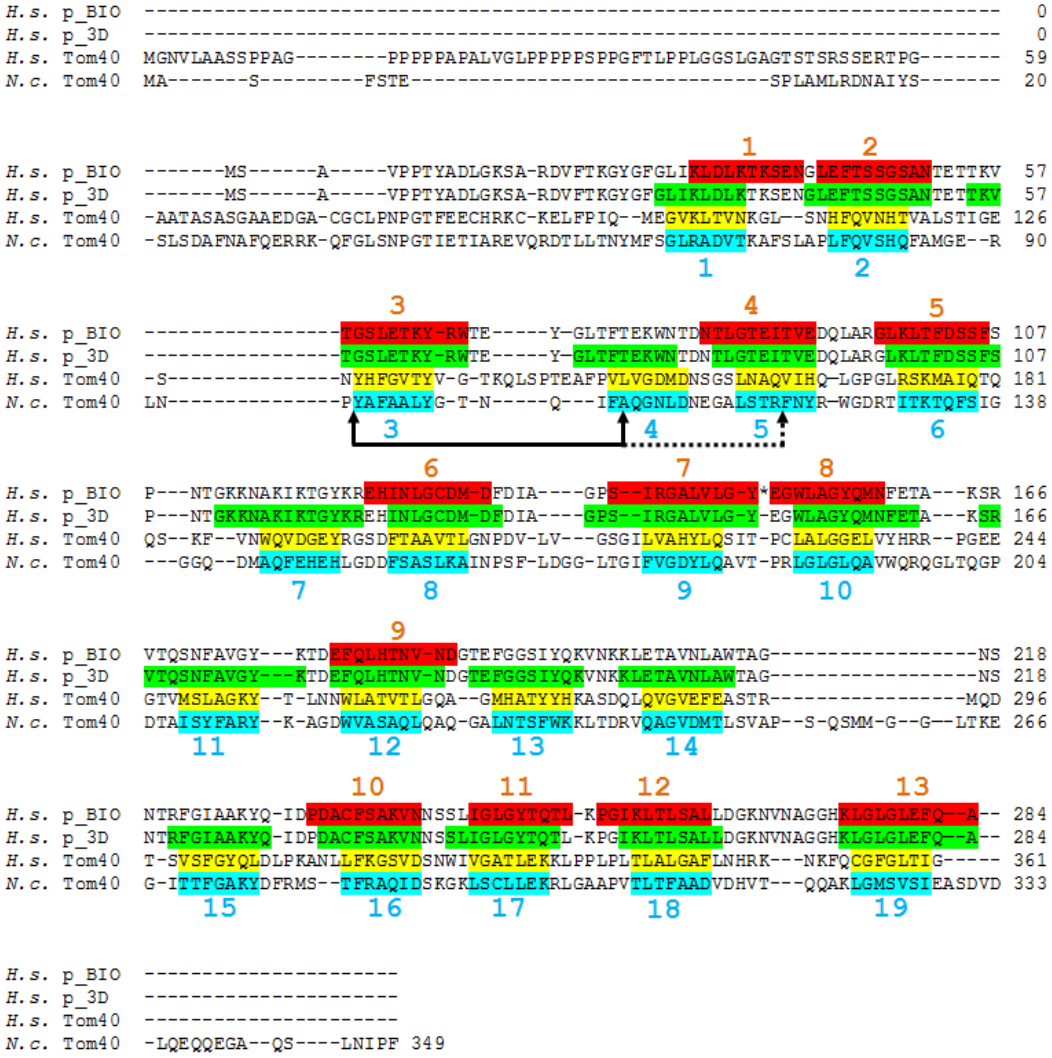
H.s. p_BIO ---------- 0
H.s. p_3D ---------- 0
H.s. Tom40 MGNVLAASSPPAG--------PPPPPAPALVGLPPPPPSPPGFTLPPLGGSLGAGTSTSRSSERTPG------- 59
N.c. Tom40 MA-------S---------FSTE----------SPLAMLRDNAIYS------- 20
1 2
H.s. p_BIO -------MS------A-----VPPTYADLGKSA-RDVFTKGYGFGLIKLDLKTKSENGLEFTSSGSANTETTKV 57
H.s. p_3D -------MS------A-----VPPTYADLGKSA-RDVFTKGYGFGLIKLDLKTKSENGLEFTSSGSANTETTKV 57
H.s. Tom40 -AATASASGAAEDGA-CGCLPNPGTFEECHRKC-KELFPIQ--MEGVKLTVNKGL--SNHFQVNHTVALSTIGE 126
N.c. Tom40 -SLSDAFNAFQERRK-QFGLSNPGTIETIAREVQRDTLLTNYMFSGLRADVTKAFSLAPLFQVSHQFAMGE--R 90
1 2
3 4 5
H.s. p_BIO ----------TGSLETKY-RWTE-----Y-GLTFTEKWNTDNTLGTEITVEDQLARGLKLTFDSSFS 107
H.s. p_3D ----------TGSLETKY-RWTE-----Y-GLTFTEKWNTDNTLGTEITVEDQLARGLKLTFDSSFS 107
H.s. Tom40 -S----------NYHFGVTYV-G-TKQLSPTEAFPVLVGDMDNSGSLNAQVIHQ-LGPGLRSKMAIQTQ 181
N.c. Tom40 LN----------PYAFAALYG-T-N-----Q---IFAQGNLDNEGALSTRFNYR-WGDRTITKTQPSIG 138
3 4 5 6
6 7 8
H.s. p_BIO P---NTGKKNAKIKTGYKREHINLGCDM-DFDIA----GPS--IRGALVLG-Y*EGWLAGYQMNFETA---KSR 166
H.s. p_3D P---NTGKKNAKIKTGYKREHINLGCDM-DFDIA----GPS--IRGALVLG-Y-EGWLAGYQMNFETA---KSR 166
H.s. Tom40 QS--KF--VNWQVDGEYRGSDFTAAVTLGNPDV-LV---GSGILVAHYLQSIT-PCLALGGELVYHRR--PGEE 244
N.c. Tom40 ---GGQ--DMAQFEHEHLGDDFSASLKAINPSF-LDGG-LTGIFVGDYLQAVT-PRLGLGLQAVWQRQGLTQGP 204
7 8 9 10
9
H.s. p_BIO VTQSNFAVGY---KTDEFQLHTNV-NDGTEFGGSIYQKVNKKLETAVNLAWTAG----------NS 218
H.s. p_3D VTQSNFAVGY---KTDEFQLHTNV-NDGTEFGGSIYQKVNKKLETAVNLAWTAG----------NS 218
H.s. Tom40 GTVMSLAGKY--T-LNNWLATVTLGQA--GMHATYYHKASDQLQVGVEFEASTR----------MQD 296
N.c. Tom40 DTAISYFARY--K-AGDWVASAQLQAQ-GALNTSFWKKLTDRVQAGVDMTLSVAP--S-QSMM-G--G--LTKE 266
11 12 13 14
10 11 12 13
H.s. p_BIO NTRFGIAAKYQ-IDPDACFSAKVNNSSLIGLGYTQTL-KPGIKLTLSALLDGKNVNAGGHKLGLGLEFQ--A-- 284
H.s. p_3D NTRFGIAAKYQ-IDPDACFSAKVNNSSLIGLGYTQTL-KPGIKLTLSALLDGKNVNAGGHKLGLGLEFQ--A-- 284
H.s. Tom40 T-SVSFGYQLDLPKANLLFKGSVDSNWIVGATLEKKLPPLPLTLALGAFLNHRK---NKFQCGFGLTIG----- 361
N.c. Tom40 G-ITTFGAKYDFRMS--TFRAQIDSKGKLSCLLEKRLGAAPVTLTFAADVDHVT---QQAKLGMSVSIEASDVD 333
15 16 17 18 19
H.s. p_BIO ----------
H.s. p_3D ----------
H.s. Tom40 ----------
N.c. Tom40 -LQEQQEGA--QS----LNIPF 349

porin (Figure 3.3). Circular dichroism spectroscopy, a method which provides details on structural composition of proteins, and Fourier-transform infrared analysis of reconstituted human Tom40 provided secondary structure results which conformed with the 19-stranded model (Mager *et al.*, 2011). These results were again obtained using refolded, recombinant Tom40 that had been reconstituted into planar membranes under specific conditions. In this instance however, the reconstituted human Tom40 displayed pore characteristics similar to *N. crassa* Tom40 purified directly from the MOM. Furthermore a novel assay using oxidative cross-linking of laterally proximate substituted Cys residues in β-strand 1 and β-strand 19 respectively has given further support to the modeled parallel orientation of these β-strands in *S. cerevisiae* porin and Tom40 (Qiu *et al.*, 2013).

Since the current prediction for Tom40 structure has been modeled after the porin 3D structure, any controversy regarding the authentic structure of porin will affect the reliability of the Tom40 model. In an attempt to test some of the predictions for the Tom40 structure we have set out to verify the topology of several predicted β-strands in endogenous *N. crassa* Tom40 in the MOM, using the substituted cysteine accessibility mapping (SCAM) technique (Song *et al.*, 1998b; Zhu and Casey, 2007). The residues within a membrane bound β-strand have a specific orientation and a general character (Figure 3.4). Side-chains (R-groups) of sequential residues alternate between generally hydrophilic residues exposed on the lumenal face of the pore and hydrophobic residues embedded in the lipid environment of the membrane. SCAM can identify the orientation of residues based on the accessibility of cysteine sulfhydryl groups to labeling by maleimide-PEG_2-biotin (van Geest and Lolkema, 2000). Accessible Cys residues would be in the lumen, non-accessible residues embedded in the membrane (Song *et al.*, 1998b). Using site-directed PCR mutagenesis, individual codons of the target are altered to

Figure 3.4 Anti-parallel β-strand schematic model. (A) A pair of anti-parallel β-strands is shown with the alternating orientation of the R-groups of neighboring residues within one strand depicted. The light orange background arrows indicate the N- to C-terminal direction of each β-strand. Dashed lines represent hydrogen bonds formed between the strands. Perceived R-group depth changes indicate their alternating orientation on either side of the β-sheet. (B) A 2-D schematic indicating the alternating orientation of R-groups in a single β-strand.

A

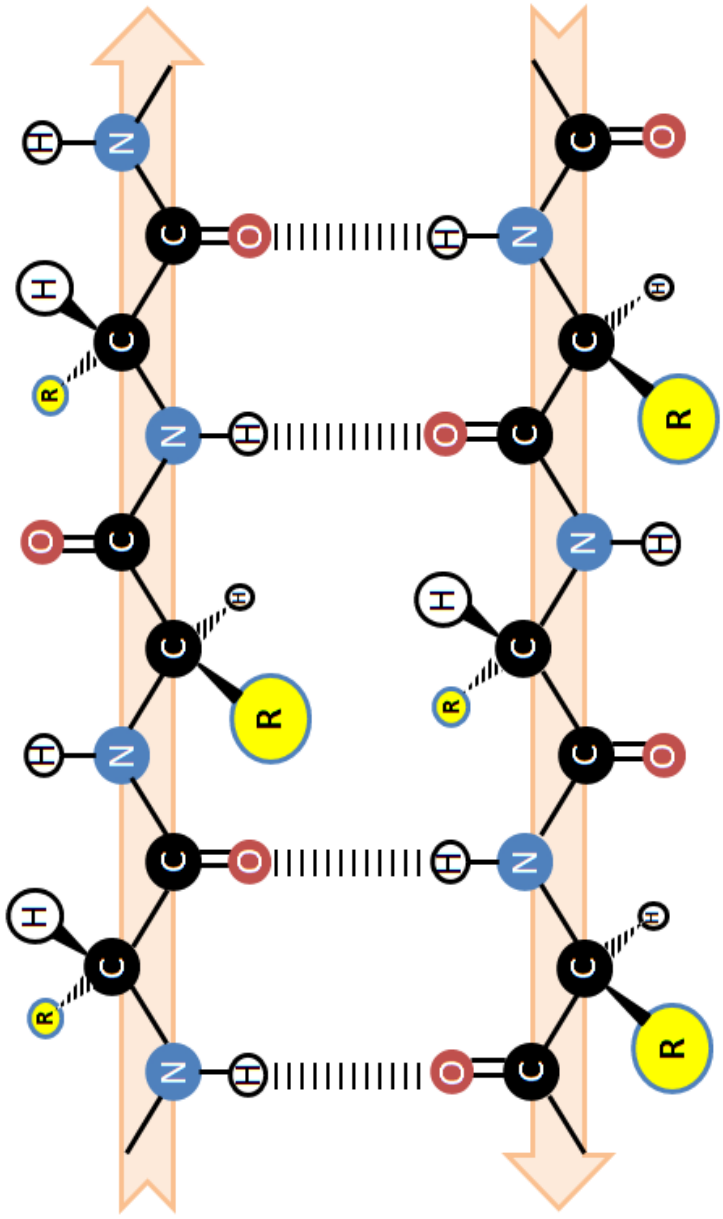

B

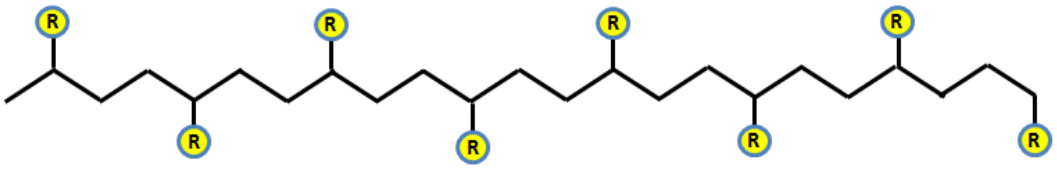

introduce Cys residues in a previously developed cysteine-less Tom40 construct. These constructs are then used to create Cys-mutant homokaryons by transformation of a nucleus carrying a *tom40KO*. Since *tom40* is an essential gene, the *tom40 KO* nucleus must be maintained in a sheltered heterokaryon and appropriate selection for the rescued nucleus must be applied to develop the appropriate *tom40-Cys* mutant homokaryons. Once the strains are produced, each one is grown in liquid culture and its mitochondria are isolated. The Cys-mutant mitochondria are exposed to a water-soluble cysteine-binding reagent carrying a biotin moiety (maleimide-PEG_2-biotin) that is capable of forming a thioether bond with exposed Cys-residues resulting in the biotinylation of such residues (Figure 3.5). The bulky biotin moiety and the hydrophilic nature of the 2-unit PEG spacer arm make the labeling reagent poorly membrane-permeant meaning it is unable to react efficiently with cysteine sulfhydryl groups embedded in the membrane or otherwise hidden (Qiu *et al.*, 1994; Pavlov and Glaser, 2002). The reagent, if bound, can then be labeled through its biotin group using streptavidin-HRP to allow for chemiluminescent detection following purification procedures, SDS-PAGE, and blotting to nitrocellulose. Cys-mutants for residues in a region of interest or the entire protein are created and analyzed using the SCAM technique. A linear sequence of alternating positive/negative binding of the labeling reagent would suggest those residues comprise a β-strand.

My experimental work on this project was centered on SCAM of a particular region of Tom40 (residues 94-106, YAFAALYGTNQIF). In the Tom40 structural model based on the 3D porin structure (Gessmann *et al.*, 2011) these residues would comprise the C-terminal end of β-strand 3, a short hairpin loop, and the beginning of β-strand 4 (Figures 3.3 and 3.6). These data were compiled along with previous work in the laboratory that completed β-strand 4 and other regions of the protein. In the biochemical

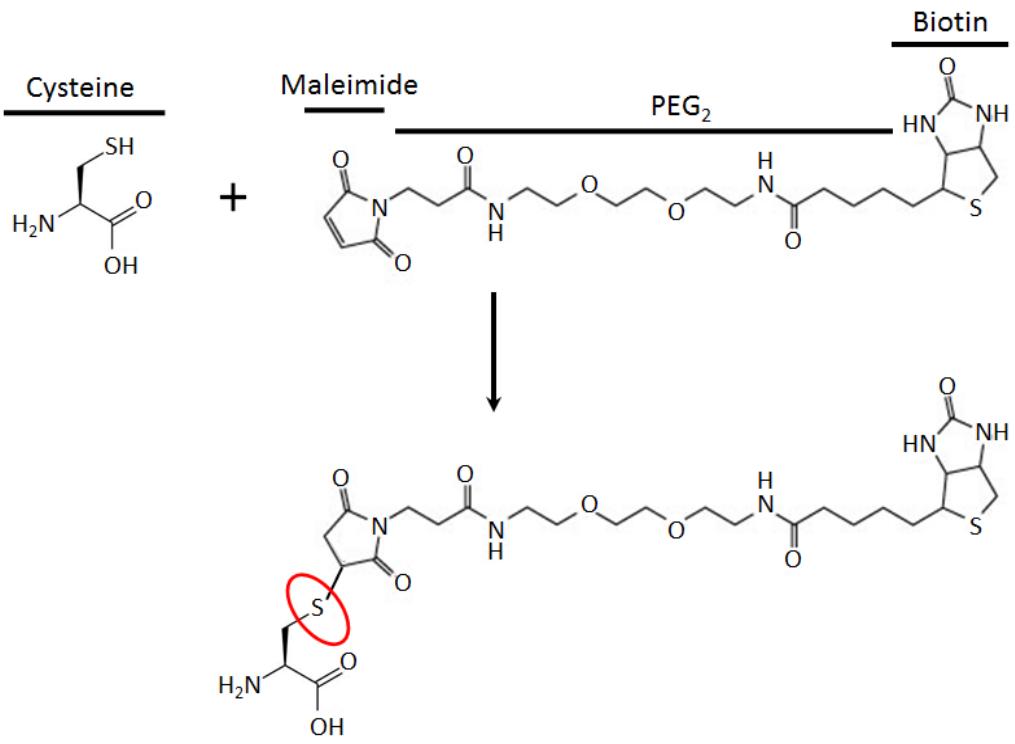

Figure 3.5 Biotin-PEG$_2$-maleimide reacts with the S atom of Cys residues. The chemical structure of biotin-PEG$_2$-maleimide and a single cysteine residue (PEG = polyethylene glycol). A thioether bond (red oval) formed between the sulfhydryl group of the cysteine residue and the unsaturated imide leads to biotin labeling of all accessible cysteine residues. The two PEG hydrophilic moieties serve to provide a spacer arm and impart increased water solubility to prevent aggregation.

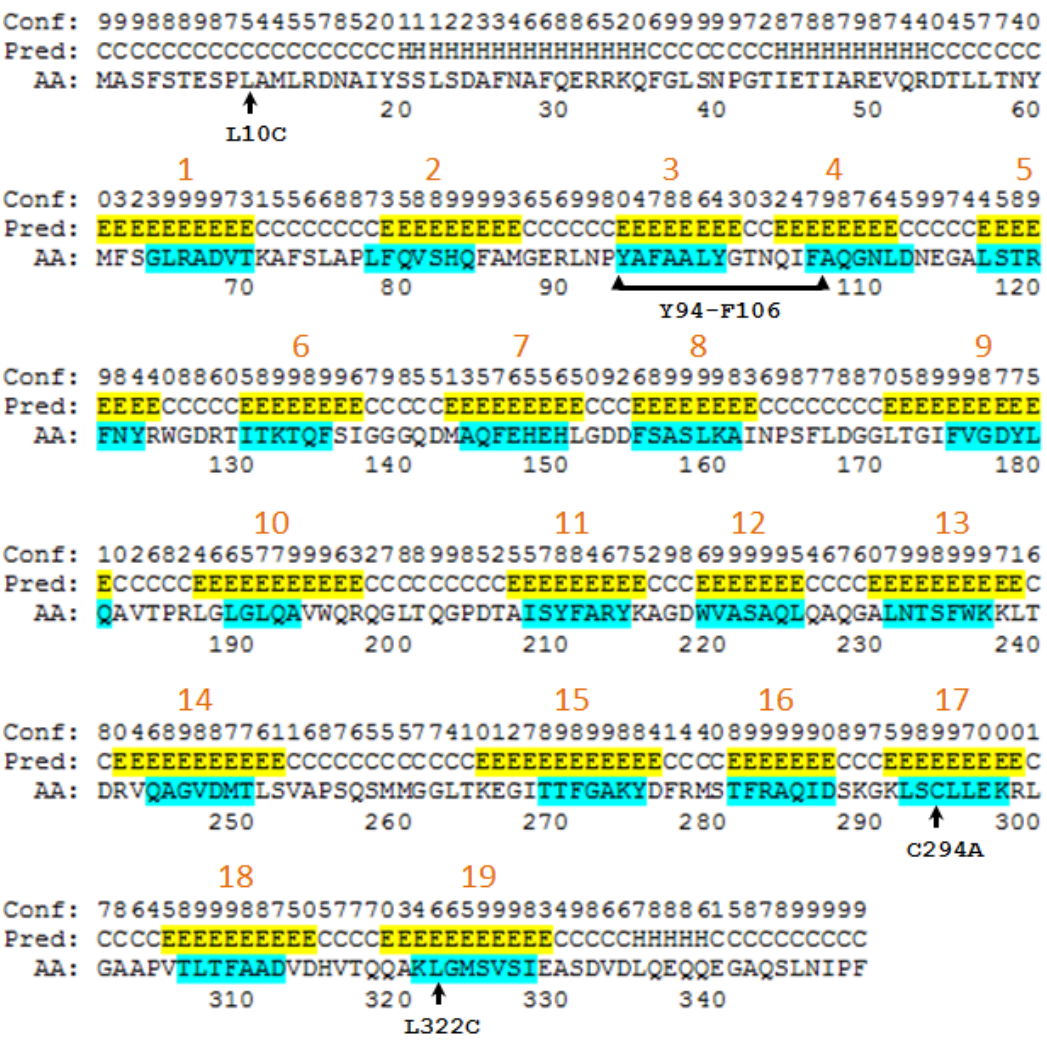

Figure 3.6 *N. crassa* Tom40 secondary structure predictions. Analysis of *N. crassa* Tom40 amino acid sequence using PSIPRED V3.3 computer program (McGuffin *et al.*, 2000). (AA) amino acid. (Pred) PSIPRED predicted topology: (C) coil, (H) α-helix, (E-yellow) β-strand. (Conf) Confidence of prediction 0 (lowest) – 9 (highest). (Blue highlight) predicted β-strands based on 3D model data (Gessmann *et al.*, 2011). Red numbers designate β-strand order. Residues examined in my work (94-106) are indicated. Additional residues done in the lab extend the analysis of β-strands 3, 4 and 5 from residues A107-R120. The locations of three controls: L10C (+) exposed cysteine, C294A (-) no cysteine and L322C (-) inaccessible cysteine are also shown.

model (Colombini, 2009) the residues of β-strand 4 from the 3D model are predicted to occur in a loop region exposed to the cytosol (Figure 3.2). As shown below, the data demonstrate the probable existence of the β-strand 3/ loop / β-strand 4 structure within the region. I have also compiled previous SCAM data gathered in our lab for *N. crassa* Tom40 and compared the findings to the most recent models of Tom40 structure (Gessmann *et al.*, 2011; Mager *et al.*, 2011) and previous results of a *N. crassa* Tom40 mutational analysis (Taylor, 2003; Taylor *et al.*, 2003; Sherman *et al.*, 2006). The SCAM results are in general agreement with the existing porin 3D-based model. Certain aspects of the mutational analysis in the context of the model suggest flexibility in Tom40 structure and function.

The working hypotheses employed at the outset of this project were that we could identify β-strands within the *N. crassa* Tom40 protein using the SCAM technique, and if true, the results obtained would support one of the models discussed above. The remainder of this chapter will address the methodology and results of our experimental examination, followed by a discussion relating the acquired results to our initial questions.

3.2 Materials and Methods

Some of the following techniques were originally described in Lackey *et al.* (2011) (Chapter 2). They have been repeated here to provide easy access and understanding to the reader. Techniques and methods adapted from other sources are referenced accordingly.

3.2.1 Strains and growth of *N. crassa*

Strains used in this study are listed in Table 3.1. *N. crassa* was grown according to previously described procedures (Davis and De Serres, 1970). Unless otherwise stated, cells were grown at 30° C. Amino acids added for nutritional supplementation of auxotrophic strains were added at a concentration of 200 µg/L of media.

3.2.2 Construction of Tom40 knockout strains

3.2.2.1 *Tom40 KO* sheltered heterokaryon

A sheltered heterokaryon carrying a knockout of the essential *tom40* gene in one nucleus was constructed in our laboratory by Nancy Go. A split marker approach was used to knock out the *tom40* gene (Figure S3.1). Approximately three kilobase regions upstream and downstream of the coding sequence for *tom40* were generated via PCR of a cosmid (pMOcosX G17:H6) containing the gene. These regions and a PCR product containing a hygromycin resistance cassette were used in the construction of the KO plasmid via recombination in *S. cerevisiae* (strain FY2) using the pRS416 plasmid (see Appendix I and Figure S2.1). Using PCR the appropriate split markers (Colot *et al.*, 2006) for the gene as described previously for *N. crassa tob55* (Hoppins *et al.*, 2007) were amplified from the KO construct. The two portions of the split marker were

transformed into heterokaryon HP1 (Figure S3.1 B) (Nargang *et al.*, 1995). Hygromycin resistant colonies were isolated, purified, and examined for replacement of the *tom40* gene in one of the nuclei of HP1 by Southern analysis (not shown). Strains showing the correct pattern of integration were then examined for growth characteristics. One nucleus of the heterokaryon carries an allele (*mtr*) for resistance to p-fluorophenylalanine (fpa) plus auxotrophy for histidine (*his-3*), while the second carries benomyl resistance (Bml) and pantothenate auxotrophy (*pan-2*) (Figure S3.1 C). Transformation of multi-nucleate *N. crassa* conidia typically results in only one nucleus being transformed (Grotelueschen and Metzenberg, 1995). Strains were grown on medium containing either histidine plus fpa or pantothenate plus benomyl to determine which nucleus of the heterokaryotic transformants was transformed by the split marker and carried the KO. For isolates with the knockout in the histidine-requiring, fpa-resistant nucleus, the presence of fpa in the growth medium forces the nucleus containing the knockout to predominate the culture, resulting in a knock-down of Tom40 (Figure S3.1 C). If the protein is required for optimal growth rate, the sheltered heterokaryon knockouts should grow slowly under these conditions. One strain Tom40 KO-5, showing this phenotype was chosen for further work. In this study the *N. crassa* Tom40 SCAM Cys mutants for residues 90-120 and 135-143 (40 in total) were created in the 7626 nucleus using the Tom40 KO-5 sheltered heterokaryon.

3.2.2.2 *Tom40*^{RIP} sheltered heterokaryon

Certain strains used in the original portion of this project were transformants of the *tom40*^{RIP}sheltered heterokaryon produced by R.D. Taylor earlier in the Nargang lab (Taylor, 2003). This includes the analysis of residues 10, 144-182, 294, 316-339 and 344. The method used by Taylor (2003) to construct the *tom40*^{RIP} sheltered heterokaryon is described in Appendix I.

3.2.3 Transformation of *N. crassa*

DNA was transformed into *N. crassa* by electroporation of conidia as previously described (Tanton *et al.*, 2003).

3.2.3.1 Creation of Tom40-Cys Mutant strains

Previously, a genomic *tom40* plasmid construct containing bleomycin resistance (pB3) was mutagenized to replace the sole endogenous *tom40* Cys codon 294 with alanine to create the pC-8 plasmid construct (Taylor, 2003). All subsequent replacement of existing codons of interest to Cys codons was performed using this "Cys-less" version of the *tom40* gene in the pC8. This plasmid was constructed in a Bluescript (pBS520) background and also carries a bleomycin (bleo) resistance cassette (*ble333*) (See appendix I Table A4). Plasmids confirmed to contain the desired mutations by DNA sequencing were linearized and used to transform conidia from one of the two previously mentioned sheltered heterokaryon strains (Tom40 KO-5 or RIP40het (isolate F40-6)). The transformation mixture was plated on medium containing His, and fpa (Tom40 KO-5) or Lys, Leu and cycloheximide (RIP40het (F40-6)) to select for the nucleus bearing the *tom40* knockout/RIP, as well as bleomycin to select for transformants carrying the plasmid. Transformants were purified as performed in Lackey *et al.* (2011) via one round of single colony isolation on selective medium (His/fpa/bleo or Lys/Leu/cyh/bleo). Colonies were picked and tested for nutritional requirements. Transformants with the correct nutritional requirements were homokaryons that contained the desired mutant alleles, which must be capable of restoring Tom40 function to a level sufficient for viability. The presence of the correct mutant alleles in the transformants was confirmed by sequencing PCR products of the ectopically integrated *tom40-Cys* mutant alleles from isolated genomic DNA.

3.2.4 Mitochondrial Isolation

Unless specified otherwise, mycelia were grown at 30°C, harvested by filtration, and ground in the presence of sand and PBSSP (phosphate buffered salts + sucrose + PMSF) isolation buffer (137 mM NaCl, 2.7 mM KCl, 10 mM Na_2HPO_4, 2 mM KH_2PO_4, pH 7.4, 0.25 M sucrose, 1 mM phenylmethylsulfonyl fluoride [PMSF]) using a mortar and pestle. Mitochondria were isolated by differential centrifugation as described previously (Nargang and Rapaport, 2007; Wideman *et al.*, 2010).

3.2.5 Gel electrophoresis of proteins

Proteins were analyzed by SDS polyacrylamide gel electrophoresis (SDS-PAGE) or blue-native gel electrophoresis (BNGE) as described previously (Laemmli, 1970; Schägger and von Jagow, 1991; Schägger *et al.*, 1994) using 50 µg of mitochondrial protein per lane, respectively, unless stated otherwise. Following electrophoresis, gels were transferred to either nitrocellulose or PVDF (polyvinylidene fluoride) membrane and immunodecorated with specific antibodies (Good and Crosby, 1989) or detected via autoradiography. In the case of biotin labeled Tom40, detection was performed with streptavidin-HRP complex as described in section 3.2.9.

3.2.6 SCAM Biotin Labeling

Mitochondria (50-200 µg protein) were suspended in 500 µL of PBSSP. 10 µL of labeling reagent (EZ-link™ maliemide-PEG2-biotin [1.2 mg/50µl in PBSSP], Thermo Fisher Scientific, Rockford IL USA) were added and the samples rocked at room temperature for 2 hrs. Mitochondria were re-isolated and washed twice with PBSSP + 1% β-mercaptoethanol to quench any excess labeling reagent.

3.2.7 Alkaline Extraction of mitochondria following SCAM biotin labelling

To minimize background signal from contaminating soluble proteins, an alkaline extraction was performed. Following the 2nd wash (section 3.2.6) the sample was suspended in 1 ml of 0.1 M sodium carbonate at pH 12.0 and incubated on ice for 1 hr. The mixture was then centrifuged at 50,000 rpm in a TLA55 rotor (Beckman Instruments, Palo Alto, CA) at 4°C for 60 min. The supernatant was discarded and the pellets were resuspended in "lysis" buffer (50 mM Tris, pH 7.4, 1% Na-deoxycholate, 0.1% Triton X-100) and rocked at 4˚C for 30 min. The sample was then clarified by centrifugation at 4˚C at 13,000 rpm (Heraeus Biofuge fresco) for 30 min. The supernatant was collected for Tom40 immunoprecipitation.

3.2.8 Immunoprecipitation of Tom40

Rabbit serum (150 µl) containing antibodies directed against *N. crassa* Tom40 was incubated with 500 µl of protein A agarose beads (Invitrogen™) to bind the IgG's to the beads. The IgG's were then cross-linked to the beads using dimethyl pimelimidate (DMP). Following cross-linking, excess DMP was quenched by washing the beads 3x in 2 ml 0.2 M ethanolamine which was subsequently removed via two washes with 2 ml PBS and then resuspending the beads in 1 ml bovine serum albumin (BSA)/PBS (1 mg BSA/ml PBS). Sample supernatant (obtained as described in 3.2.7) was added to 100µl preparation of Anti-Tom40-agarose beads and rocked overnight at 4˚C for immunoprecipitation. Beads were isolated via centrifugation at 13,000 rpm for 4 min and were then washed three times with 700 µl lysis buffer (section 3.2.7).

3.2.9 Detection of biotin labeled cysteine residues with Streptavidin-HRP

"Cracking" buffer (0.06 M Tris-HCl, pH 6.8; 2.5% SDS; 5% β-mercaptoethanol; 5% sucrose) was added to the beads with bound Tom40 (see section 3.2.8) and the mixture was shaken for 30 min followed by incubation for 20 min at 94˚C. The beads

were then removed by centrifugation at 13,000 rpm for 4 min (Heraeus Biofuge fresco). The Tom40 containing supernatant was electrophoresed through a 10% SDS-PAGE gel. Proteins were then transfered to a nitrocellulose membrane. The membrane was blocked with 3% BSA in TBS-Tween (150 mM NaCl, 12.5 mM Tris, pH 7.5, 0.005% Tween®20). The membrane was probed via incubation for 2 hr with either streptavidin-HRP conjugate or streptavidin-biotinylated HRP complex (2.5µl in 3% BSA/TBS-Tween®20). Both bind with free biotin moieties carried on the SCAM labeling reagent (both Amersham Biosciences, Buckinghamshire, England). Following three washes in TBS-Tween®20 and one in TBS the membranes were saturated with enzyme catalyzed light (ECL) reagents (KPL, Gaithersburg MD USA) and signal was detected via exposure to X-ray film (Biomax XAR, Kodak).

One problem that was apparent during the establishment of the SCAM procedure was that there was unexpected variability in the efficiency of the immunoprecipitations between samples. To alleviate the differences in protein concentrations when comparing the results for different residues, “test” runs were performed in which a set volume (25 µl) of the immunoprecipitation samples were analyzed using the protocol above. Estimations based on the “test” results were made in an attempt to equilibrate the protein amount by adjusting the load volume of each sample accordingly for subsequent runs. The SCAM results shown (Figure 3.7) are taken from different runs and each section displayed was chosen because the protein amounts loaded fell within a 2-fold threshold of each other as judged by visual inspection.

3.2.10 Import of mitochondrial precursor proteins

Import of precursor proteins into isolated mitochondria (see section 2.2.5) was performed as previously described (Harkness *et al.*, 1994). To summarize, radiolabelled precursors were produced *in vitro* by transcription and translation in rabbit reticulocyte

lysate (Promega (Madison, WI) TnT reticulocyte lysate system) in the presence of [^{35}S] methionine. Labeled proteins were incubated with isolated mitochondria for various times. Following these import reactions, samples were treated with proteinase K, washed and re-isolated to remove any unimported precursors from the mitochondria. The samples were then processed in one of two ways. For analysis of simple import (F_1B and AAC) of mitochondrial precursors, samples were subjected to SDS-PAGE, transferred to nitrocellulose, and imported proteins were detected by autoradiography. Study of assembly and import intermediates (Tom40) required mitochondria to be solubilized in 1% digitonin and subjected to BNGE followed by transfer onto polyvinylidene fluoride (PVDF) membrane and visualization by autoradiography.

Table 3.1. Strains used in this study. My experiments used only 76-26, L10C, C294A, L322C as controls and Cys-mutants for residues 94-108. Data collected by others using the other strains were compiled by me in this study. For completeness all strains are listed here.

Strain (isolate used)	**Genotype**	**Origin or reference**
7626	*his-3 mtrR a* (*mtrR* imparts fpa resistance)	R.L. Metzenberg
HP1	Heterokaryon of 76-26 and 71-18 (Figure S3.1).	Nargang Lab. (Nargang *et al.*, 1995)
Tom40 KO-5	Sheltered heterokaryon. As HP1, but with replacement of *tom40* gene in 76-26 nucleus with a hygromycin resistance (*hygR*) cassette (Figure S3.1).	Transformation of HP1 with split marker fragments for *tom40* knockout.
HostV	*cyh-2 lys-2 leu-5 mei-2 a* (Figure AI A)	Fungal Genetics Stock Center #7255
MateV	*am132 inl inv mei-2 A* (Figure AI A)	Fungal Genetics Stock Center #7265
40Dup1	*cyh-2 lys-2 leu-5 mei-2 a* contains an ectopic 1.8kb copy of *tom40*. Hygromycin resistant. (Figure AI A)	Transformation of HostV with *tom40* pRIP-4 plasmid
RIP40het (F40-6)	Sheltered heterokaryon: (*cyh-2 lys-2 leu-5 mei-2 tom40RIP + am132 inl inv mei-2)* both nuclei contain the ectopic *tom40RIP* (Figure AI B)	MateV x 40Dup1 (Taylor, 2003)
C294A (170-6)	*cyh-2 lys-2 leu-5 mei-2 tom40RIP* contains ectopic copy of *tom40* with sole Cys residue 294 changed to Ala.	Transformation of RIP40het with plasmid pC8
L10C (10-2-1)	*cyh-2 lys-2 leu-5 mei-2 tom40RIP* contains ectopic copy of *tom40* with Cys 294 changed to Ala and Leu 10 residue changed to Cys.	Transformation of RIP40het with specific SCAM plasmid construct

L322C (322-5-1)	*cyh-2 lys-2 leu-5 mei-2 tom40RIP* contains ectopic copy of *tom40* with Cys 294 changed to Ala and Leu 322 residue changed to Cys.	Transformation of RIP40het with specific SCAM plasmid construct
S344C (344-4-1)	*cyh-2 lys-2 leu-5 mei-2 tom40RIP* contains ectopic copy of *tom40* with Cys 294 changed to Ala and Ser 344 residue changed to Cys.	Transformation of RIP40het with specific SCAM plasmid construct
R90C (90-7)	*his-3 pan-2$^+$ mtr Bml$^+$ tom40KO* contains ectopic copy of *tom40* with Cys 294 changed to Ala and Arg 90 residue changed to Cys.	Transformation of Tom40 KO-5 with specific SCAM plasmid construct
L91C (91-1)	*his-3 pan-2$^+$ mtr Bml$^+$ tom40KO* contains ectopic copy of *tom40* with Cys 294 changed to Ala and Leu 91 residue changed to Cys.	Transformation of Tom40 KO-5 with specific SCAM plasmid construct
N92C (92-1)	*his-3 pan-2$^+$ mtr Bml$^+$ tom40KO* contains ectopic copy of *tom40* with Cys 294 changed to Ala and Asn 92 residue changed to Cys.	Transformation of Tom40 KO-5 with specific SCAM plasmid construct
P93C (93-1)	*his-3 pan-2$^+$ mtr Bml$^+$ tom40KO* contains ectopic copy of *tom40* with Cys 294 changed to Ala and Pro 93 residue changed to Cys.	Transformation of Tom40 KO-5 with specific SCAM plasmid construct
Y94C (94-7)	*his-3 pan-2$^+$ mtr Bml$^+$ tom40KO* contains ectopic copy of *tom40* with Cys 294 changed to Ala and Tyr 94 residue changed to Cys.	Transformation of Tom40 KO-5 with specific SCAM plasmid construct
A95C (95-2)	*his-3 pan-2$^+$ mtr Bml$^+$ tom40KO* contains ectopic copy of *tom40* with Cys 294 changed to Ala and Ala 95 residue changed to Cys.	Transformation of Tom40 KO-5 with specific SCAM plasmid construct
F96C (96-3)	*his-3 pan-2$^+$ mtr Bml$^+$ tom40KO* contains ectopic copy of *tom40* with Cys 294 changed to Ala and Phe 96 residue changed to Cys.	Transformation of Tom40 KO-5 with specific SCAM plasmid construct
A97C (97-5)	*his-3 pan-2$^+$ mtr Bml$^+$ tom40KO* contains ectopic copy of *tom40* with Cys 294 changed to Ala and Ala 97 residue changed to Cys.	Transformation of Tom40 KO-5 with specific SCAM plasmid construct

A98C (98-1)	*his-3 pan-2*$^{+}$ *mtr Bml*$^{+}$ *tom40KO* contains ectopic copy of *tom40* with Cys 294 changed to Ala and Ala 98 residue changed to Cys.	Transformation of Tom40 KO-5 with specific SCAM plasmid construct
L99C (99-11)	*his-3 pan-2*$^{+}$ *mtr Bml*$^{+}$ *tom40KO* contains ectopic copy of *tom40* with Cys 294 changed to Ala and Leu 99 residue changed to Cys.	Transformation of Tom40 KO-5 with specific SCAM plasmid construct
Y100C (100-3)	*his-3 pan-2*$^{+}$ *mtr Bml*$^{+}$ *tom40KO* contains ectopic copy of *tom40* with Cys 294 changed to Ala and Tyr 100 residue changed to Cys.	Transformation of Tom40 KO-5 with specific SCAM plasmid construct
G101C (101-23)	*his-3 pan-2*$^{+}$ *mtr Bml*$^{+}$ *tom40KO* contains ectopic copy of *tom40* with Cys 294 changed to Ala and Gly 101 residue changed to Cys.	Transformation of Tom40 KO-5 with specific SCAM plasmid construct
T102C (102-2)	*his-3 pan-2*$^{+}$ *mtr Bml*$^{+}$ *tom40KO* contains ectopic copy of *tom40* with Cys 294 changed to Ala and Thr 102 residue changed to Cys.	Transformation of Tom40 KO-5 with specific SCAM plasmid construct
N103C (103-201)	*his-3 pan-2*$^{+}$ *mtr Bml*$^{+}$ *tom40KO* contains ectopic copy of *tom40* with Cys 294 changed to Ala and Asn 103 residue changed to Cys.	Transformation of Tom40 KO-5 with specific SCAM plasmid construct
Q104C (104-1)	*his-3 pan-2*$^{+}$ *mtr Bml*$^{+}$ *tom40KO* contains ectopic copy of *tom40* with Cys 294 changed to Ala and Gln 104 residue changed to Cys.	Transformation of Tom40 KO-5 with specific SCAM plasmid construct
I105C (105-1)	*his-3 pan-2*$^{+}$ *mtr Bml*$^{+}$ *tom40KO* contains ectopic copy of *tom40* with Cys 294 changed to Ala and Ile 105 residue changed to Cys.	Transformation of Tom40 KO-5 with specific SCAM plasmid construct
F106C (106-122)	*his-3 pan-2*$^{+}$ *mtr Bml*$^{+}$ *tom40KO* contains ectopic copy of *tom40* with Cys 294 changed to Ala and Phe 106 residue changed to Cys.	Transformation of Tom40 KO-5 with specific SCAM plasmid construct
A107C (107-3)	*his-3 pan-2*$^{+}$ *mtr Bml*$^{+}$ *tom40KO* contains ectopic copy of *tom40* with Cys 294 changed to Ala and Ala 107 residue changed to Cys.	Transformation of Tom40 KO-5 with specific SCAM plasmid construct

Q108C (108-3)	*his-3 pan-2*$^{+}$ *mtr Bml*$^{+}$ *tom40KO* contains ectopic copy of *tom40* with Cys 294 changed to Ala and Gln 108 residue changed to Cys.	Transformation of Tom40 KO-5 with specific SCAM plasmid construct
G109C (109-1)	*his-3 pan-2*$^{+}$ *mtr Bml*$^{+}$ *tom40KO* contains ectopic copy of *tom40* with Cys 294 changed to Ala and Gly 109 residue changed to Cys.	Transformation of Tom40 KO-5 with specific SCAM plasmid construct
N110C (110-203)	*his-3 pan-2*$^{+}$ *mtr Bml*$^{+}$ *tom40KO* contains ectopic copy of *tom40* with Cys 294 changed to Ala and Asn 110 residue changed to Cys.	Transformation of Tom40 KO-5 with specific SCAM plasmid construct
L111C (111-1)	*his-3 pan-2*$^{+}$ *mtr Bml*$^{+}$ *tom40KO* contains ectopic copy of *tom40* with Cys 294 changed to Ala and Leu 111 residue changed to Cys.	Transformation of Tom40 KO-5 with specific SCAM plasmid construct
D112C (112-2)	*his-3 pan-2*$^{+}$ *mtr Bml*$^{+}$ *tom40KO* contains ectopic copy of *tom40* with Cys 294 changed to Ala and Asp 112 residue changed to Cys.	Transformation of Tom40 KO-5 with specific SCAM plasmid construct
N113C (113-122)	*his-3 pan-2*$^{+}$ *mtr Bml*$^{+}$ *tom40KO* contains ectopic copy of *tom40* with Cys 294 changed to Ala and Asn113 residue changed to Cys.	Transformation of Tom40 KO-5 with specific SCAM plasmid construct
E114C (114-21)	*his-3 pan-2*$^{+}$ *mtr Bml*$^{+}$ *tom40KO* contains ectopic copy of *tom40* with Cys 294 changed to Ala and Glu 114 residue changed to Cys.	Transformation of Tom40 KO-5 with specific SCAM plasmid construct
G115C (115-124)	*his-3 pan-2*$^{+}$ *mtr Bml*$^{+}$ *tom40KO* contains ectopic copy of *tom40* with Cys 294 changed to Ala and Gly 115 residue changed to Cys.	Transformation of Tom40 KO-5 with specific SCAM plasmid construct
A116C (116-122)	*his-3 pan-2*$^{+}$ *mtr Bml*$^{+}$ *tom40KO* contains ectopic copy of *tom40* with Cys 294 changed to Ala and Ala 116	Transformation of Tom40 KO-5 with specific SCAM plasmid construct
L117C (117-201)	*his-3 pan-2*$^{+}$ *mtr Bml*$^{+}$ *tom40KO* contains ectopic copy of *tom40* with Cys 294 changed to Ala and Leu 117 residue changed to Cys.	Transformation of Tom40 KO-5 with specific SCAM plasmid construct

S118C (108-23)	*his-3 pan-2*$^{+}$ *mtr Bml*$^{+}$ *tom40KO* contains ectopic copy of *tom40* with Cys 294 changed to Ala and Ser 118 residue changed to Cys.	Transformation of Tom40 KO-5 with specific SCAM plasmid construct
T119C (119-1)	*his-3 pan-2*$^{+}$ *mtr Bml*$^{+}$ *tom40KO* contains ectopic copy of *tom40* with Cys 294 changed to Ala and Thr 119 residue changed to Cys.	Transformation of Tom40 KO-5 with specific SCAM plasmid construct
R120C (120-1)	*his-3 pan-2*$^{+}$ *mtr Bml*$^{+}$ *tom40KO* contains ectopic copy of *tom40* with Cys 294 changed to Ala and Arg 120 residue changed to Cys.	Transformation of Tom40 KO-5 with specific SCAM plasmid construct
F135C (135-2)	*his-3 pan-2*$^{+}$ *mtr Bml*$^{+}$ *tom40KO* contains ectopic copy of *tom40* with Cys 294 changed to Ala and Phe 135 residue changed to Cys.	Transformation of Tom40 KO-5 with specific SCAM plasmid construct
S136C (136)	*his-3 pan-2*$^{+}$ *mtr Bml*$^{+}$ *tom40KO* contains ectopic copy of *tom40* with Cys 294 changed to Ala and Ser 136 residue changed to Cys.	Transformation of Tom40 KO-5 with specific SCAM plasmid construct
I137C (137-2)	*his-3 pan-2*$^{+}$ *mtr Bml*$^{+}$ *tom40KO* contains ectopic copy of *tom40* with Cys 294 changed to Ala and Ile 137 residue changed to Cys.	Transformation of Tom40 KO-5 with specific SCAM plasmid construct
G138C (138-3)	*his-3 pan-2*$^{+}$ *mtr Bml*$^{+}$ *tom40KO* contains ectopic copy of *tom40* with Cys 294 changed to Ala and Gly 138 residue changed to Cys.	Transformation of Tom40 KO-5 with specific SCAM plasmid construct
G139C (139)	*his-3 pan-2*$^{+}$ *mtr Bml*$^{+}$ *tom40KO* contains ectopic copy of *tom40* with Cys 294 changed to Ala and Gly 139 residue changed to Cys.	Transformation of Tom40 KO-5 with specific SCAM plasmid construct
G140C (140-1)	*his-3 pan-2*$^{+}$ *mtr Bml*$^{+}$ *tom40KO* contains ectopic copy of *tom40* with Cys 294 changed to Ala and Gly 140 residue changed to Cys.	Transformation of Tom40 KO-5 with specific SCAM plasmid construct
Q141C (141-4)	*his-3 pan-2*$^{+}$ *mtr Bml*$^{+}$ *tom40KO* contains ectopic copy of *tom40* with Cys 294 changed to Ala and Gln 141 residue changed to Cys.	Transformation of Tom40 KO-5 with specific SCAM plasmid construct

D142C (142-2)	*his-3 pan-2*$^{+}$ *mtr Bml*$^{+}$ *tom40KO* contains ectopic copy of *tom40* with Cys 294 changed to Ala and Asp 142 residue changed to Cys.	Transformation of Tom40 KO-5 with specific SCAM plasmid construct
M143C (143-1)	*his-3 pan-2*$^{+}$ *mtr Bml*$^{+}$ *tom40KO* contains ectopic copy of *tom40* with Cys 294 changed to Ala and Met 143 residue changed to Cys.	Transformation of Tom40 KO-5 with specific SCAM plasmid construct
A144C (144-3)	*cyh-2 lys-2 leu-5 mei-2 tom40RIP* contains ectopic copy of *tom40* with Cys 294 changed to Ala and Ala 144 residue changed to Cys.	Transformation of RIP40het with specific SCAM plasmid construct
Q145C (145-3)	*cyh-2 lys-2 leu-5 mei-2 tom40RIP* contains ectopic copy of *tom40* with Cys 294 changed to Ala and Gln 145 residue changed to Cys.	Transformation of RIP40het with specific SCAM plasmid construct
F146C (146-1)	*cyh-2 lys-2 leu-5 mei-2 tom40RIP* contains ectopic copy of *tom40* with Cys 294 changed to Ala and Phe 146 residue changed to Cys.	Transformation of RIP40het with specific SCAM plasmid construct
E147C (147-1)	*cyh-2 lys-2 leu-5 mei-2 tom40RIP* contains ectopic copy of *tom40* with Cys 294 changed to Ala and Glu 147 residue changed to Cys.	Transformation of RIP40het with specific SCAM plasmid construct
H148C (148-1)	*cyh-2 lys-2 leu-5 mei-2 tom40RIP* contains ectopic copy of *tom40* with Cys 294 changed to Ala and His 148 residue changed to Cys.	Transformation of RIP40het with specific SCAM plasmid construct
E149C (149-12)	*cyh-2 lys-2 leu-5 mei-2 tom40RIP* contains ectopic copy of *tom40* with Cys 294 changed to Ala and Glu 149 residue changed to Cys.	Transformation of RIP40het with specific SCAM plasmid construct
H150C (150-3)	*cyh-2 lys-2 leu-5 mei-2 tom40RIP* contains ectopic copy of *tom40* with Cys 294 changed to Ala and His 150 residue changed to Cys.	Transformation of RIP40het with specific SCAM plasmid construct
L151C (151-1)	*cyh-2 lys-2 leu-5 mei-2 tom40RIP* contains ectopic copy of *tom40* with Cys 294 changed to Ala and Leu 151 residue changed to Cys.	Transformation of RIP40het with specific SCAM plasmid construct

G152C (152-1)	*cyh-2 lys-2 leu-5 mei-2 tom40RIP* contains ectopic copy of *tom40* with Cys 294 changed to Ala and Gly 152 residue changed to Cys.	Transformation of RIP40het with specific SCAM plasmid construct
D153C (153-2)	*cyh-2 lys-2 leu-5 mei-2 tom40RIP* contains ectopic copy of *tom40* with Cys 294 changed to Ala and Asp 153 residue changed to Cys.	Transformation of RIP40het with specific SCAM plasmid construct
D154C (154-1)	*cyh-2 lys-2 leu-5 mei-2 tom40RIP* contains ectopic copy of *tom40* with Cys 294 changed to Ala and Asp 154 residue changed to Cys.	Transformation of RIP40het with specific SCAM plasmid construct
F155C (155-1)	*cyh-2 lys-2 leu-5 mei-2 tom40RIP* contains ectopic copy of *tom40* with Cys 294 changed to Ala and Phe 155 residue changed to Cys.	Transformation of RIP40het with specific SCAM plasmid construct
S156C (156-1)	*cyh-2 lys-2 leu-5 mei-2 tom40RIP* contains ectopic copy of *tom40* with Cys 294 changed to Ala and Ser 156 residue changed to Cys.	Transformation of RIP40het with specific SCAM plasmid construct
A157C (157-2)	*cyh-2 lys-2 leu-5 mei-2 tom40RIP* contains ectopic copy of *tom40* with Cys 294 changed to Ala and Ala 157 residue changed to Cys.	Transformation of RIP40het with specific SCAM plasmid construct
S158C (158-3)	*cyh-2 lys-2 leu-5 mei-2 tom40RIP* contains ectopic copy of *tom40* with Cys 294 changed to Ala and Ser 158 residue changed to Cys.	Transformation of RIP40het with specific SCAM plasmid construct
L159C (159-4)	*cyh-2 lys-2 leu-5 mei-2 tom40RIP* contains ectopic copy of *tom40* with Cys 294 changed to Ala and Leu 159 residue changed to Cys.	Transformation of RIP40het with specific SCAM plasmid construct
K160C (160-9)	*cyh-2 lys-2 leu-5 mei-2 tom40RIP* contains ectopic copy of *tom40* with Cys 294 changed to Ala and Lys 160 residue changed to Cys.	Transformation of RIP40het with specific SCAM plasmid construct
A161C (161-1)	*cyh-2 lys-2 leu-5 mei-2 tom40RIP* contains ectopic copy of *tom40* with Cys 294 changed to Ala and Ala 161 residue changed to Cys.	Transformation of RIP40het with specific SCAM plasmid construct

I162C (162-4)	*cyh-2 lys-2 leu-5 mei-2 tom40RIP* contains ectopic copy of *tom40* with Cys 294 changed to Ala and Ile 162 residue changed to Cys.	Transformation of RIP40het with specific SCAM plasmid construct
N163C (163-3)	*cyh-2 lys-2 leu-5 mei-2 tom40RIP* contains ectopic copy of *tom40* with Cys 294 changed to Ala and Asn 163 residue changed to Cys.	Transformation of RIP40het with specific SCAM plasmid construct
P164C (164-5)	*cyh-2 lys-2 leu-5 mei-2 tom40RIP* contains ectopic copy of *tom40* with Cys 294 changed to Ala and Pro 164 residue changed to Cys.	Transformation of RIP40het with specific SCAM plasmid construct
S165C (165-3)	*cyh-2 lys-2 leu-5 mei-2 tom40RIP* contains ectopic copy of *tom40* with Cys 294 changed to Ala and Ser 165 residue changed to Cys.	Transformation of RIP40het with specific SCAM plasmid construct
F166C (166-36)	*cyh-2 lys-2 leu-5 mei-2 tom40RIP* contains ectopic copy of *tom40* with Cys 294 changed to Ala and Phe 166 residue changed to Cys.	Transformation of RIP40het with specific SCAM plasmid construct
L167C (167-5)	*cyh-2 lys-2 leu-5 mei-2 tom40RIP* contains ectopic copy of *tom40* with Cys 294 changed to Ala and Leu 167 residue changed to Cys.	Transformation of RIP40het with specific SCAM plasmid construct
D168C (168-2)	*cyh-2 lys-2 leu-5 mei-2 tom40RIP* contains ectopic copy of *tom40* with Cys 294 changed to Ala and Asp 168 residue changed to Cys.	Transformation of RIP40het with specific SCAM plasmid construct
G169C (169-21)	*cyh-2 lys-2 leu-5 mei-2 tom40RIP* contains ectopic copy of *tom40* with Cys 294 changed to Ala and Gly 169 residue changed to Cys.	Transformation of RIP40het with specific SCAM plasmid construct
G170C (170)	*cyh-2 lys-2 leu-5 mei-2 tom40RIP* contains ectopic copy of *tom40* with Cys 294 changed to Ala and Gly 170 residue changed to Cys.	Transformation of RIP40het with specific SCAM plasmid construct
L171C (171-5)	*cyh-2 lys-2 leu-5 mei-2 tom40RIP* contains ectopic copy of *tom40* with Cys 294 changed to Ala and Leu 171 residue changed to Cys.	Transformation of RIP40het with specific SCAM plasmid construct

T172C (172-2)	*cyh-2 lys-2 leu-5 mei-2 tom40RIP* contains ectopic copy of *tom40* with Cys 294 changed to Ala and Thr 172 residue changed to Cys.	Transformation of RIP40het with specific SCAM plasmid construct
G173C (173-5)	*cyh-2 lys-2 leu-5 mei-2 tom40RIP* contains ectopic copy of *tom40* with Cys 294 changed to Ala and Gly 173 residue changed to Cys.	Transformation of RIP40het with specific SCAM plasmid construct
I174C (174-2)	*cyh-2 lys-2 leu-5 mei-2 tom40RIP* contains ectopic copy of *tom40* with Cys 294 changed to Ala and Ile 174 residue changed to Cys.	Transformation of RIP40het with specific SCAM plasmid construct
F175C (175-2)	*cyh-2 lys-2 leu-5 mei-2 tom40RIP* contains ectopic copy of *tom40* with Cys 294 changed to Ala and Phe 175 residue changed to Cys.	Transformation of RIP40het with specific SCAM plasmid construct
V176C (176-2)	*cyh-2 lys-2 leu-5 mei-2 tom40RIP* contains ectopic copy of *tom40* with Cys 294 changed to Ala and Val 176 residue changed to Cys.	Transformation of RIP40het with specific SCAM plasmid construct
G177C (177-3)	*cyh-2 lys-2 leu-5 mei-2 tom40RIP* contains ectopic copy of *tom40* with Cys 294 changed to Ala and Gly 177 residue changed to Cys.	Transformation of RIP40het with specific SCAM plasmid construct
D178C (178-3)	*cyh-2 lys-2 leu-5 mei-2 tom40RIP* contains ectopic copy of *tom40* with Cys 294 changed to Ala and Asp 178 residue changed to Cys.	Transformation of RIP40het with specific SCAM plasmid construct
Y179C (179-7)	*cyh-2 lys-2 leu-5 mei-2 tom40RIP* contains ectopic copy of *tom40* with Cys 294 changed to Ala and Tyr 179 residue changed to Cys.	Transformation of RIP40het with specific SCAM plasmid construct
L180C (180-4)	*cyh-2 lys-2 leu-5 mei-2 tom40RIP* contains ectopic copy of *tom40* with Cys 294 changed to Ala and Leu 180 residue changed to Cys.	Transformation of RIP40het with specific SCAM plasmid construct
Q181C (181-5)	*cyh-2 lys-2 leu-5 mei-2 tom40RIP* contains ectopic copy of *tom40* with Cys 294 changed to Ala and Gln 181 residue changed to Cys.	Transformation of RIP40het with specific SCAM plasmid construct

A182C (182-4)	*cyh-2 lys-2 leu-5 mei-2 tom40RIP* contains ectopic copy of *tom40* with Cys 294 changed to Ala and Ala 182 residue changed to Cys..	Transformation of RIP40het with specific SCAM plasmid construct
V316C (316-6-1)	*cyh-2 lys-2 leu-5 mei-2 tom40RIP* contains ectopic copy of *tom40* with Cys 294 changed to Ala and Val 316 residue changed to Cys.	Transformation of RIP40het with specific SCAM plasmid construct
T317C (317-4-1)	*cyh-2 lys-2 leu-5 mei-2 tom40RIP* contains ectopic copy of *tom40* with Cys 294 changed to Ala and Thr 317 residue changed to Cys.	Transformation of RIP40het with specific SCAM plasmid construct
Q318C (318-1-1)	*cyh-2 lys-2 leu-5 mei-2 tom40RIP* contains ectopic copy of *tom40* with Cys 294 changed to Ala and Gln 318 residue changed to Cys.	Transformation of RIP40het with specific SCAM plasmid construct
Q319C (319-7-1)	*cyh-2 lys-2 leu-5 mei-2 tom40RIP* contains ectopic copy of *tom40* with Cys 294 changed to Ala and Gln 319 residue changed to Cys.	Transformation of RIP40het with specific SCAM plasmid construct
A320C (320-1-1)	*cyh-2 lys-2 leu-5 mei-2 tom40RIP* contains ectopic copy of *tom40* with Cys 294 changed to Ala and Ala 320 residue changed to Cys.	Transformation of RIP40het with specific SCAM plasmid construct
K321C (321-2-1)	*cyh-2 lys-2 leu-5 mei-2 tom40RIP* contains ectopic copy of *tom40* with Cys 294 changed to Ala and Lys 321 residue changed to Cys.	Transformation of RIP40het with specific SCAM plasmid construct
L322C (322-5-1)	*cyh-2 lys-2 leu-5 mei-2 tom40RIP* contains ectopic copy of *tom40* with Cys 294 changed to Ala and Leu 322 residue changed to Cys.	Transformation of RIP40het with specific SCAM plasmid construct
G323C (323-5-1)	*cyh-2 lys-2 leu-5 mei-2 tom40RIP* contains ectopic copy of *tom40* with Cys 294 changed to Ala and Gly 323 residue changed to Cys.	Transformation of RIP40het with specific SCAM plasmid construct
M324C (324-1-1)	*cyh-2 lys-2 leu-5 mei-2 tom40RIP* contains ectopic copy of *tom40* with Cys 294 changed to Ala and Met 324 residue changed to Cys.	Transformation of RIP40het with specific SCAM plasmid construct

F325C (325-5-1)	*cyh-2 lys-2 leu-5 mei-2 tom40RIP* contains ectopic copy of *tom40* with Cys 294 changed to Ala and Phe 325 residue changed to Cys.	Transformation of RIP40het with specific SCAM plasmid construct
V326C (326-1-1)	*cyh-2 lys-2 leu-5 mei-2 tom40RIP* contains ectopic copy of *tom40* with Cys 294 changed to Ala and Val 326 residue changed to Cys.	Transformation of RIP40het with specific SCAM plasmid construct
S327C (327-1-1)	*cyh-2 lys-2 leu-5 mei-2 tom40RIP* contains ectopic copy of *tom40* with Cys 294 changed to Ala and Ser 327 residue changed to Cys.	Transformation of RIP40het with specific SCAM plasmid construct
I328C (328-1-1)	*cyh-2 lys-2 leu-5 mei-2 tom40RIP* contains ectopic copy of *tom40* with Cys 294 changed to Ala and Ile 328 residue changed to Cys.	Transformation of RIP40het with specific SCAM plasmid construct
G329C (329-7-1)	*cyh-2 lys-2 leu-5 mei-2 tom40RIP* contains ectopic copy of *tom40* with Cys 294 changed to Ala and Gly 329 residue changed to Cys.	Transformation of RIP40het with specific SCAM plasmid construct
A330C (330-1-1)	*cyh-2 lys-2 leu-5 mei-2 tom40RIP* contains ectopic copy of *tom40* with Cys 294 changed to Ala and Ala 330 residue changed to Cys.	Transformation of RIP40het with specific SCAM plasmid construct
S331C (331-4-1)	*cyh-2 lys-2 leu-5 mei-2 tom40RIP* contains ectopic copy of *tom40* with Cys 294 changed to Ala and Ser 321 residue changed to Cys.	Transformation of RIP40het with specific SCAM plasmid construct
D332C (322-5-1)	*cyh-2 lys-2 leu-5 mei-2 tom40RIP* contains ectopic copy of *tom40* with Cys 294 changed to Ala and Asp 332 residue changed to Cys.	Transformation of RIP40het with specific SCAM plasmid construct
V333C (333-1-1)	*cyh-2 lys-2 leu-5 mei-2 tom40RIP* contains ectopic copy of *tom40* with Cys 294 changed to Ala and Val 333 residue changed to Cys.	Transformation of RIP40het with specific SCAM plasmid construct
D334C (334-1-1)	*cyh-2 lys-2 leu-5 mei-2 tom40RIP* contains ectopic copy of *tom40* with Cys 294 changed to Ala and Asp 334 residue changed to Cys.	Transformation of RIP40het with specific SCAM plasmid construct

L335C (335-3-1)	*cyh-2 lys-2 leu-5 mei-2 tom40RIP* contains ectopic copy of *tom40* with Cys 294 changed to Ala and Leu 335 residue changed to Cys.	Transformation of RIP40het with specific SCAM plasmid construct
Q336C (336-1-1)	*cyh-2 lys-2 leu-5 mei-2 tom40RIP* contains ectopic copy of *tom40* with Cys 294 changed to Ala and Gln 336 residue changed to Cys.	Transformation of RIP40het with specific SCAM plasmid construct
G337C (337-2-1)	*cyh-2 lys-2 leu-5 mei-2 tom40RIP* contains ectopic copy of *tom40* with Cys 294 changed to Ala and Gly 337 residue changed to Cys.	Transformation of RIP40het with specific SCAM plasmid construct
Q338C (338-1-1)	*cyh-2 lys-2 leu-5 mei-2 tom40RIP* contains ectopic copy of *tom40* with Cys 294 changed to Ala and Gln 338 residue changed to Cys.	Transformation of RIP40het with specific SCAM plasmid construct
Q339C (339-1-1)	*cyh-2 lys-2 leu-5 mei-2 tom40RIP* contains ectopic copy of *tom40* with Cys 294 changed to Ala and Gln 339 residue changed to Cys.	Transformation of RIP40het with specific SCAM plasmid construct

3.3 Results and Discussion

Examination and comparison of the proposed 13 β-stranded "biochemical" (BIO) and the 19 β-stranded "3D" porin models in Figure 3.2, reveals certain regions of interest that if structurally defined would provide further support for one model over the other. For example, the residues that comprise β-strand 4 and β-strand 7 of the 3D Tom40 model (Gessmann *et al.*, 2011) are not predicted to be β-strands in the BIO model, but rather to form parts of large cytosolic loops (Colombini, 2009). In this study we have set out to biochemically define the architecture of certain regions of Tom40 using the SCAM technique to identify β-strands of functional Tom40 assembled in the MOM. Determination of the topology of residues in the regions predicted to be β-strands 4 and 7 would support one model or the other.

To perform the SCAM analysis sheltered heterokaryons containing non-functional *tom40* genes in one nucleus were developed and used in this study (Tom40 KO and RIP40het) as described in the Methods (section 3.2.2) and Appendix (Figures S3.1 and AI).

3.3.1 Substituted cysteine accessibility mapping (SCAM)

I examined the topology of amino acid residues 94-106 in this study using SCAM. Individual amino acid substitutions to Cys were introduced by site-directed mutagenesis into the "Cys-less" *tom40* gene in plasmid pC-8 (see section 3.2.3.1). Plasmids containing individual cysteine mutations for the control strains L10C, L322C and C294A (Figure 3.6) were transformed into RIP40het and were shown to rescue the $tom40^{RIP}$ lysine-leucine requiring nucleus (Taylor, 2003). Plasmids containing individual cysteine mutations for the region that I examined (residues 94-106, Figure 3.6) were transformed into Tom40 KO-5 and were shown to rescue the *tom40 KO* 76-26 His-requiring nucleus (Figure S3.1). These rescued homokaryon strains had the introduced

tom40 mutant gene PCR amplified and sequenced to verify the desired mutation in the strain. Since Tom40 is known to be essential in *N. crassa* (Taylor et al., 2003), rescue of the KO or RIP nucleus shows that the Tom40 proteins in these Tom40 Cys-mutants are functional.

The SCAM procedure is outlined in the previous sections (3.1 and 3.2). For this study EZ-link Maliemide-PEG_2-biotin (Thermo Fischer Scientific, Rockford, IL) was employed as the cysteine modifying reagent (Figure 3.5). This reagent has a 2-unit ethylene glycol spacer arm (29.1 Å in length) that increases water solubility. The 525.23 Da molecule is free to enter and pass through the TOM complex pore of ~20-22 Å diameter (Vestweber *et al.*, 1989; Hill *et al.*, 1998; Kunkele *et al.*, 1998a; Ahting *et al.*, 1999; Model *et al.*, 2002).

Others in the laboratory had examined residues 107-120 by SCAM. We were interested in having data from residues 94-120 since this region included the membrane spanning β-strand 3 (residues 94-100), a short loop (residues 101-105), β-strand 4 (residues 106-112), another short loop (residues 113-116) and the beginning of β-strand 5 (117-123) as predicted by the porin 3D model comparison (Figures 3.3 and 3.6) (Gessmann *et al.*, 2011). The biochemical model proposes that there is no β-strand that corresponds with β-strand 4 of the 3D model and that instead there is a large loop followed by a biochemical model β-strand 4 that aligns with β-strand 5 of the 3D model (Figures 3.2 and 3.3 BIO). Thus, analysis of this region should be diagnostic for the accuracy of predictions by the two models.

A PSIPRED v3.3 topology prediction proposes *N. crassa* Tom40 residues 94-101 form the entirety of β-strand 3, 102-103 form a short loop, residues 104-111 form β-strand 4, 112-116 comprise another loop, and residues 117-124 form β-strand 5 (Figure 3.6). The *N. crassa* 3D model based prediction (Gessmann *et al.*, 2011) is very similar to

the PSIPRED model except for slight discrepancies (+/- 1-2 residues) on the beginning and ending residues of the β-strands.

The combined SCAM results for residues 94-120 suggest that the predicted alternating pattern of labeling for a β-strand spanning the MOM was seen for residues 95-101, 104-112 and 114-120 (Figure 3.7). These regions correspond well with β-strands 3, 4 and 5 respectively, as predicted by PSIPRED and the 3D model. Y94 was accessible, presumably as the last residue of a loop between β2 and β3. Exactly as predicted by PSIPRED, T102-N103 showed positive labeling suggesting they do in fact form the short hairpin loop between β-strand 3 and β-strand 4. Overall, these results favor the 3D model over the BIO model. A schematic representation of the *N. crassa* Tom40 residues 94-120 topology is depicted in Figure 3.8**.**

Examination of results from all runs performed for this analysis (discussed in section 3.2.9) revealed that in some instances, certain residues (perhaps the most exemplary being residue 100) that were finally judged to be negative for labeling, would exhibit a faint positive signal (Figure S3.2). While we cannot conclusively explain these observations, we propose that the proximity of residues to the end of a given β-strand and the nature of their R-groups may influence the accessibility of the labeling reagent to that residue.

3.3.2 Functional analysis of SCAM Cys-mutants

The fact that all the Cys-mutants created are viable is perhaps the strongest argument for the mutant Tom40s being functional since the protein is known to be essential for viability (Taylor *et al.*, 2003). Nonetheless, we wished to perform a semi-quantitative analysis for several features on a few selected strains. Western blot analysis was performed on mitochondria isolated from each of the Cys-mutants (94-106) to examine the levels of various TOM complex components (Figure 3.9 A). Despite slight

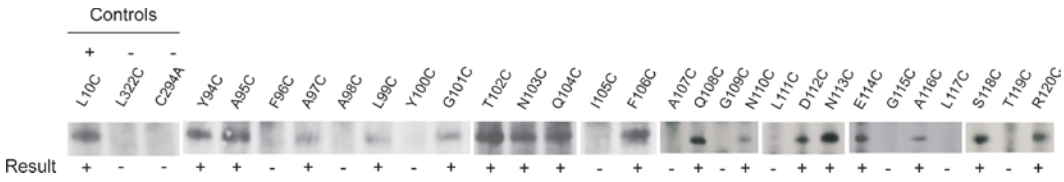

Figure 3.7 SCAM results. Mitochondria were isolated from the indicated strains (top of panel) following growth in liquid medium. Mitochondria were subjected to the SCAM biotin labeling procedure followed by transfer to nitrocellulose, and detection of biotin with streptavidin-HRP (as described in sections 3.2.6, 3.2.8 and 3.2.9). The controls strains are indicated by the black bar.

Figure 3.8 Schematic model of topology of Tom40 residues 94-120. *N. crassa* Tom40 residues 94-120 are shown (circles). Dark blue residues represent label accessible residues located in the hydrophilic environment or facing "inwards" into the pore lumen. Light blue residues are inaccessible to labeling suggesting that they are embedded in the hydrophobic lipid environment of the MOM (red texture). Neighboring β-strands undefined in this study but predicted by computer modeling based on the 3D porin structure (Gessmann *et al.*, 2011) are shown as green arrows.

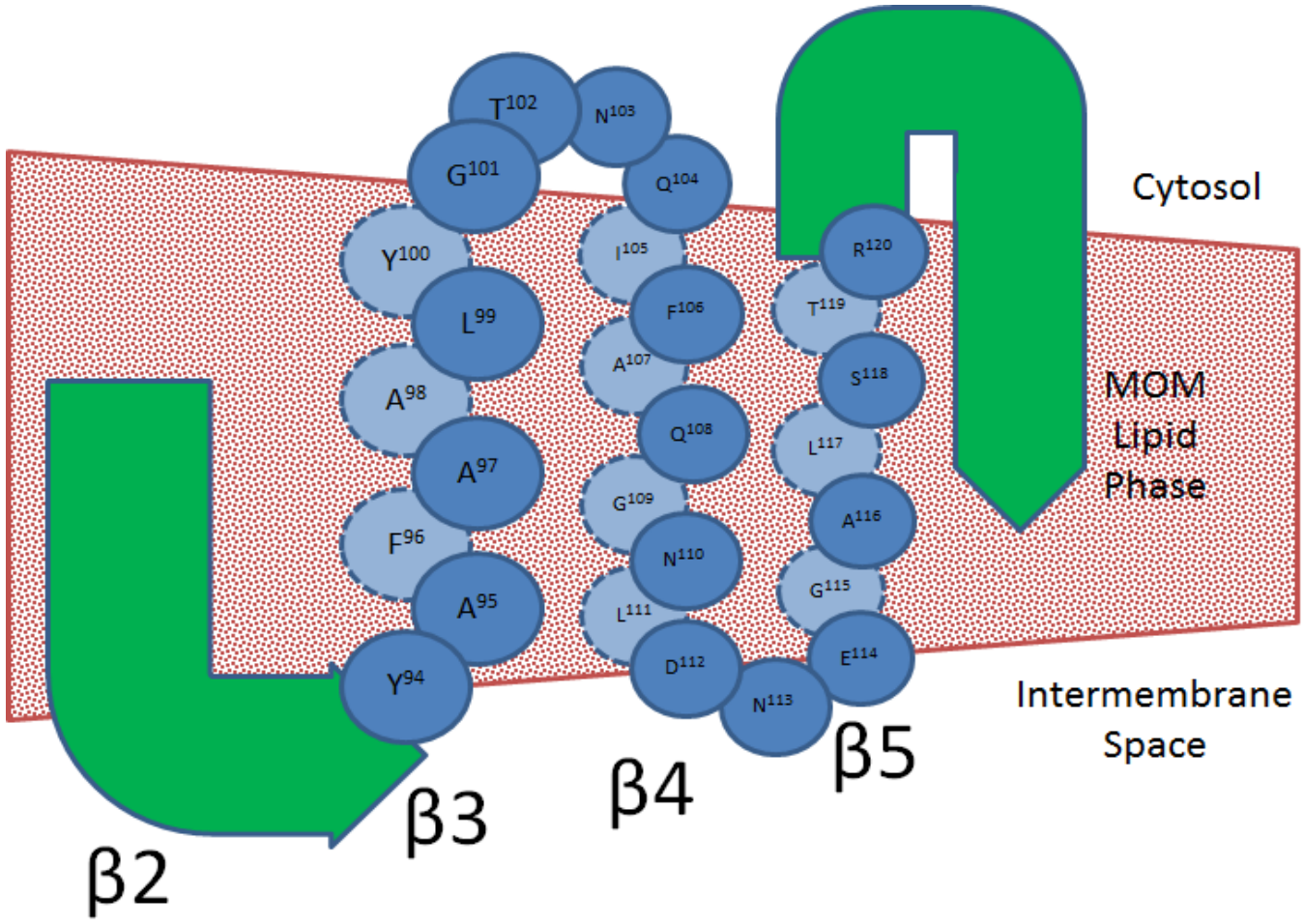
Cytosol
MOM
Lipid
Phase
Intermembrane
Space
T102
N103
G101
Q104
Y100
I105
R120
L99
F106
T119
A98
A107
S118
A97
Q108
L117
F96
G109
A116
A95
N110
G115
L111
E114
Y94
D112
N113
β2
β3
β4
β5

Figure 3.9 Analysis of mitochondrial protein content and TOM complex stability in Tom40 Cys-mutant strains. (A) Cells from the indicated strains (top of panel) were grown in liquid culture and mitochondria were isolated. Mitochondrial proteins were subjected to SDS-PAGE followed by transfer to nitrocellulose, and immunodecoration with the antibodies indicated in the middle of the two blots. The control strains were 76-26 which contains wildtype Tom40; L10C, which contains a single Cys at residue 10; L322C, which contains a single Cys at residue 322; and C294A which has no Cys residues. (B) Isolated mitochondria from the strains indicated (top of panel) were dissolved in 1% digitonin or 1% n-dodecyl-beta-D-maltoside for analysis of complex stability via BNGE. Immunodecoration with α-Tom40 antibody displayed the TOM complex or Tom40 containing products resulting from complex instability. The controls are Tom6 RIP (reduced TOM complex stability (Sherman *et al.*, 2005)) and 76-26, which contains wildtype Tom40.

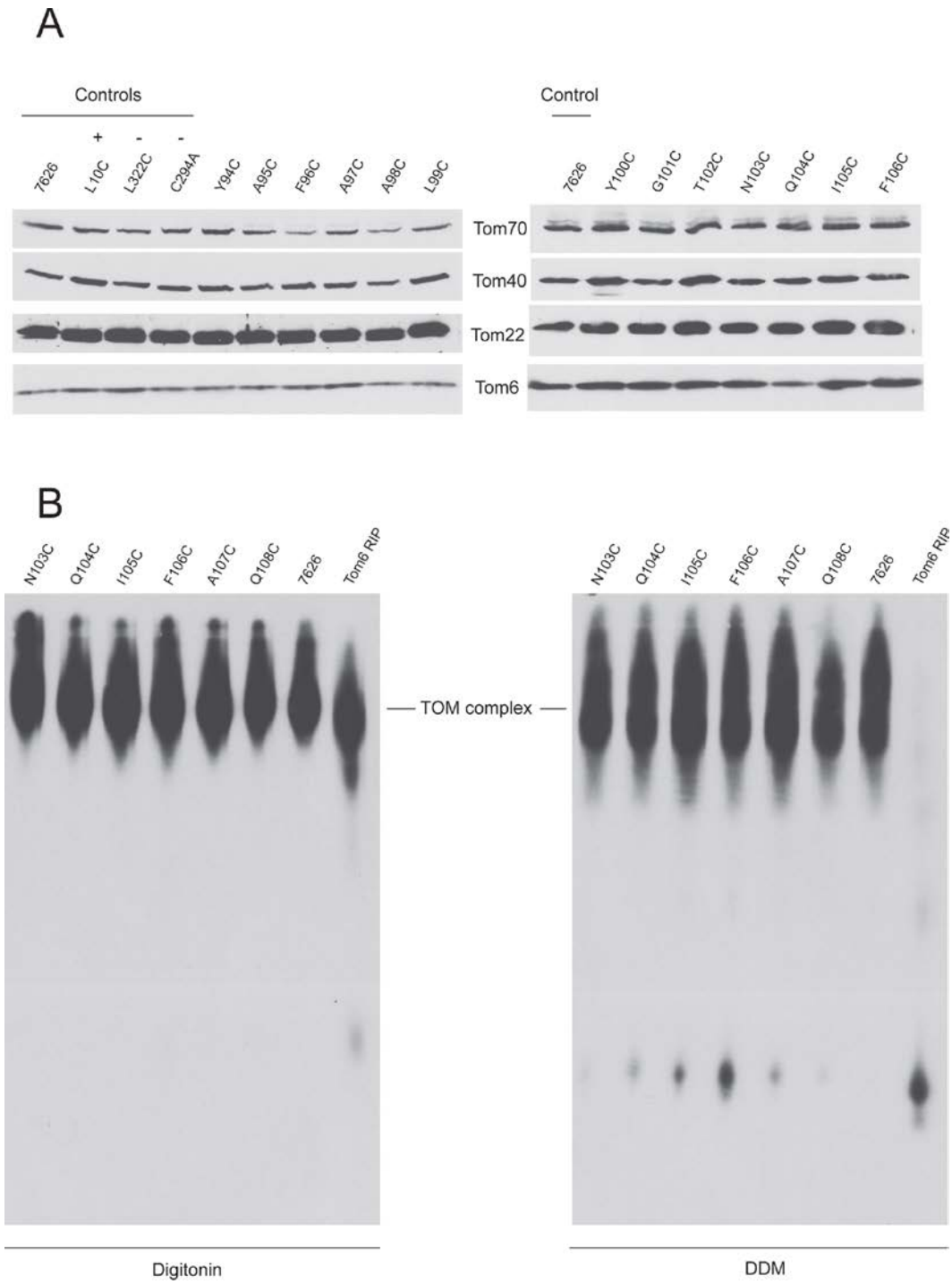
A
Controls
Control
+
-
-
7626
L10C
L322C
C294A
Y94C
A95C
F96C
A97C
A98C
L99C
7626
Y100C
G101C
T102C
N103C
Q104C
I105C
F106C
Tom70
Tom40
Tom22
Tom6
B
N103C
Q104C
I105C
F106C
A107C
Q108C
7626
Tom6 RIP
TOM complex
Digitonin
DDM

differences in protein level between strains, it appears that TOM components are not severely altered in any of the mutants. TOM complex stability of Cys-substitution strains 103-108 was analyzed via BNGE followed by immunodecoration to detect complexes containing Tom40 (Figure 3.9 B). All mutant mitochondria maintain near wildtype TOM complex stability under the lysis conditions tested (1% Digitonin or 1% n-Dodecyl-beta-D-Maltoside).

To further demonstrate that Cys–mutant TOM complexes were functional as a general import pore, *in vitro* import of radiolabelled F1β and AAC was performed on mitochondria isolated from the Cys-substitution strains 104-108. F1β (F1 β-subunit of ATP synthase) is a TIM23 complex dependent matrix targeted precursor while AAC (ADP/ATP carrier) requires TIM22 complex dependent insertion into the MIM. The observed import and assembly of these precursors into mitochondria confirm that the Tom40 Cys-mutant TOM complexes maintain their ability to act as the GIP (Figure 3.10A).

We also examined the ability of Cys-mutant TOM complexes to import and assemble wildtype Tom40 precursor into the TOM complex. The presence of the precursor in the two Tom40 assembly intermediates (see section 1.6.3.5 and Figure 1.2) and the fully assembled TOM complex suggests that the Tom40 assembly pathway is functional in the mutant strains examined (Figure 3.10B). However, some variability amongst the mutant strains was observed. For example Cys-mutant A107C has an overall reduction in Tom40 import compared to the control and other strains examined (Figure 3.10B). However, all intermediates are observed at both time points suggesting a normal, but slightly delayed assembly process. Thus, despite small quantitative differences all the mutants are viable and capable of importing and assembling the wildtype precursor proteins tested.

Figure 3.10 Import/assembly of mitochondrial proteins in Cys-mutant strains. (A) Radiolabeled matrix precursor $F_1\beta$ and inner membrane precursor AAC were incubated (for 5 min or 20 min, as indicated) with mitochondria isolated from the Tom40 Cys-substitution strains and the 7626 control (indicated at the top of the panel) grown in the presence of His. Following import, mitochondria were subjected to SDS-PAGE. Proteins were transferred to nitrocellulose membrane, and import was analyzed by autoradiography. "1/3 Lysate" represents 33% of the radiolabelled lysate added to each import reaction. (B) Radiolabelled Tom40 precursor was incubated for 5 min and 20 min with mitochondria isolated from the Tom40 Cys-substitution strains indicated (top of panel) as well as the 7626 control grown in the presence of His. Mitochondria were dissolved in 1% digitonin and subjected to BNGE. The proteins were transferred to PVDF membrane and analyzed by autoradiography. The size of the mature TOM complex (400 kDa), and assembly intermediates I (250 kDa) and II (100 kDa) are indicated on the left. * indicates an undefined band.

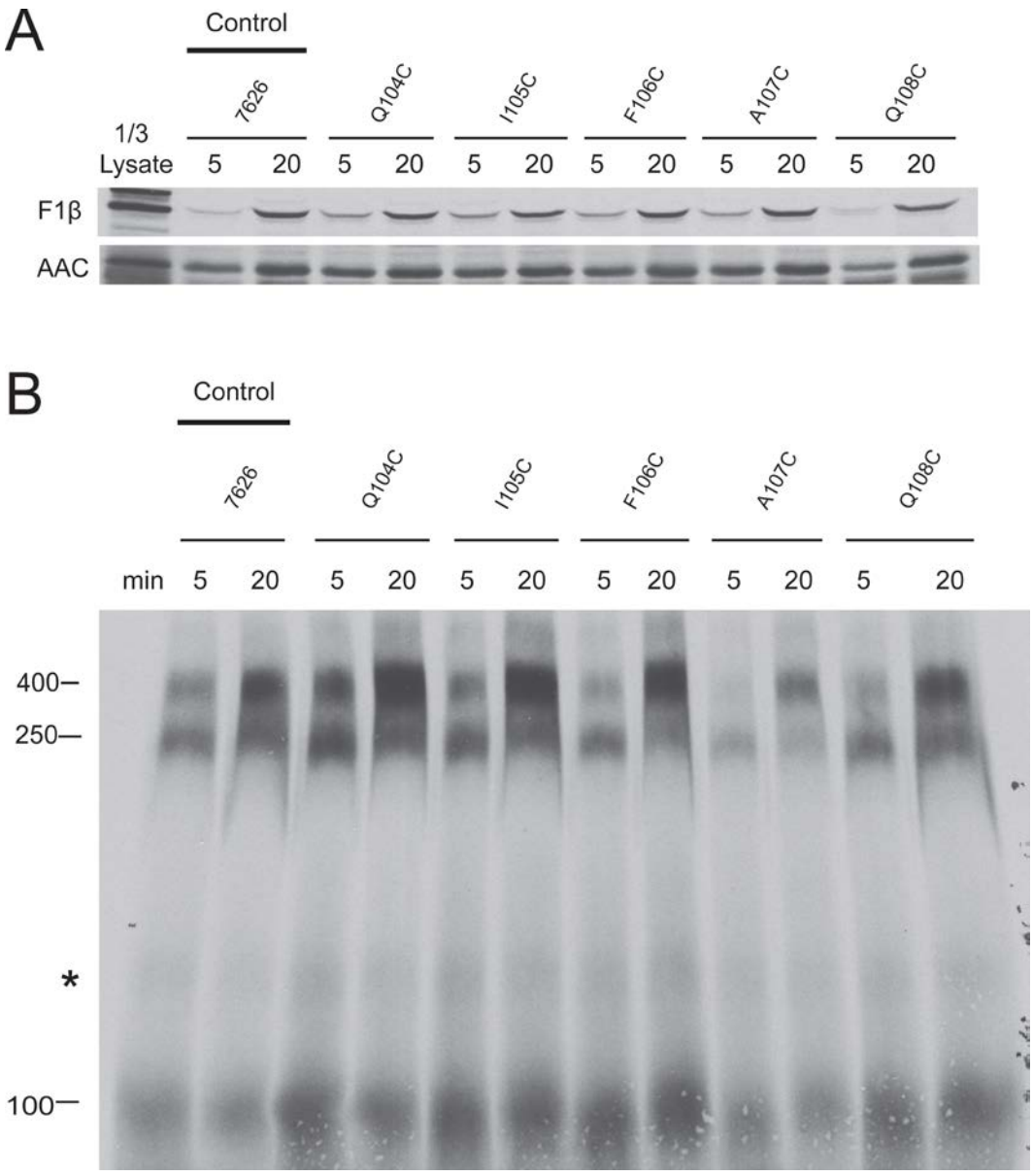
A
Control
7626
Q104C
I105C
F106C
A107C
Q108C
1/3 Lysate
5 20 5 20 5 20 5 20 5 20 5 20
F1β
AAC
B
Control
7626
Q104C
I105C
F106C
A107C
Q108C
min
5 20 5 20 5 20 5 20 5 20 5 20
400
250
*
100

3.3.3 Consideration of previous SCAM data in the context of current Tom40 models.

Our lab has previously produced SCAM data on several other regions of Tom40 which have yet to be published (F.E. Nargang, personal communication). I have assembled these data and examined them in the context of the current Tom40 model and with respect to previous mutational studies of the *N. crassa* Tom40 (Taylor, 2003; Taylor *et al.*, 2003; Sherman *et al.*, 2006).

In total, Cys-mutants for residues 90-120, 135-182 and 316-339 (as well as residues serving as controls: L10C, C294A and S344C) have been created and analyzed in the Nargang lab (Figure 3.11). According to the Tom40 3D model based on the porin structure (Figure 3.3) (Gessmann *et al.*, 2011) the first region (residues 90-120) should contain β-strand 3 (residues 94-100), β-strand 4 (residues 106-112) and the first 4 residues of β-strand 5 (117-123). The second region (residues 135-182) should contain the last 2 residues of β-strand 6 (135 and 136), β-strand 7 (residues 144-150), β-strand 8 (residues 155-161) and β-strand 9 (residues 175-181). The third region (residues 316-339) should contain the final β-strand 19 (residues 321-327). Thus we have analyzed at least parts of 7 of the 19 predicted β-strands of the model.

The characteristic SCAM alternating labeling pattern suggestive of membrane spanning β-strands was identified for regions closely corresponding to the modeled β-strands except β-strand 8 (Figures 3.11 and 3.12). For all others, comparison of our putative SCAM β-strands with those of the model reveals only slight discrepancies with regard to the exact residues involved, however the general topology is consistent.

With regard to β-strand 8, we were able to identify an alternating β-pattern only for residues 160-162 suggesting these may be the last three C-terminal residues of the strand when put in the context of the 3D model. The lack of anticipated labeling for the N-terminal region of this strand may be due to interaction of the region with the N-terminal α-helix of the protein. The porin 3D structure, which forms the template for the

Figure 3.11 Total Tom40 SCAM results from the Nargang lab. Mitochondria were isolated from the Cys-mutants strains of the indicated residues (above each lane) following growth in liquid medium. Mitochondria were subjected to the SCAM biotin labeling procedure followed by transfer to nitrocellulose, and detection of biotin with streptavidin-HRP (as described in sections 3.2.6, 3.2.8 and 3.2.9). The results (+ or -) are indicated below each lane. The black solid lines represent β-strands suggested from this study. Red dashed lines represent β-strands proposed by the Tom40 3D model based on the solved porin 3D structure (Gessmann *et al.*, 2011). Arrows indicate that the proposed β-strands extend to the line below or beyond the residues examined in this study. The control strains are shown at the top of the figure.

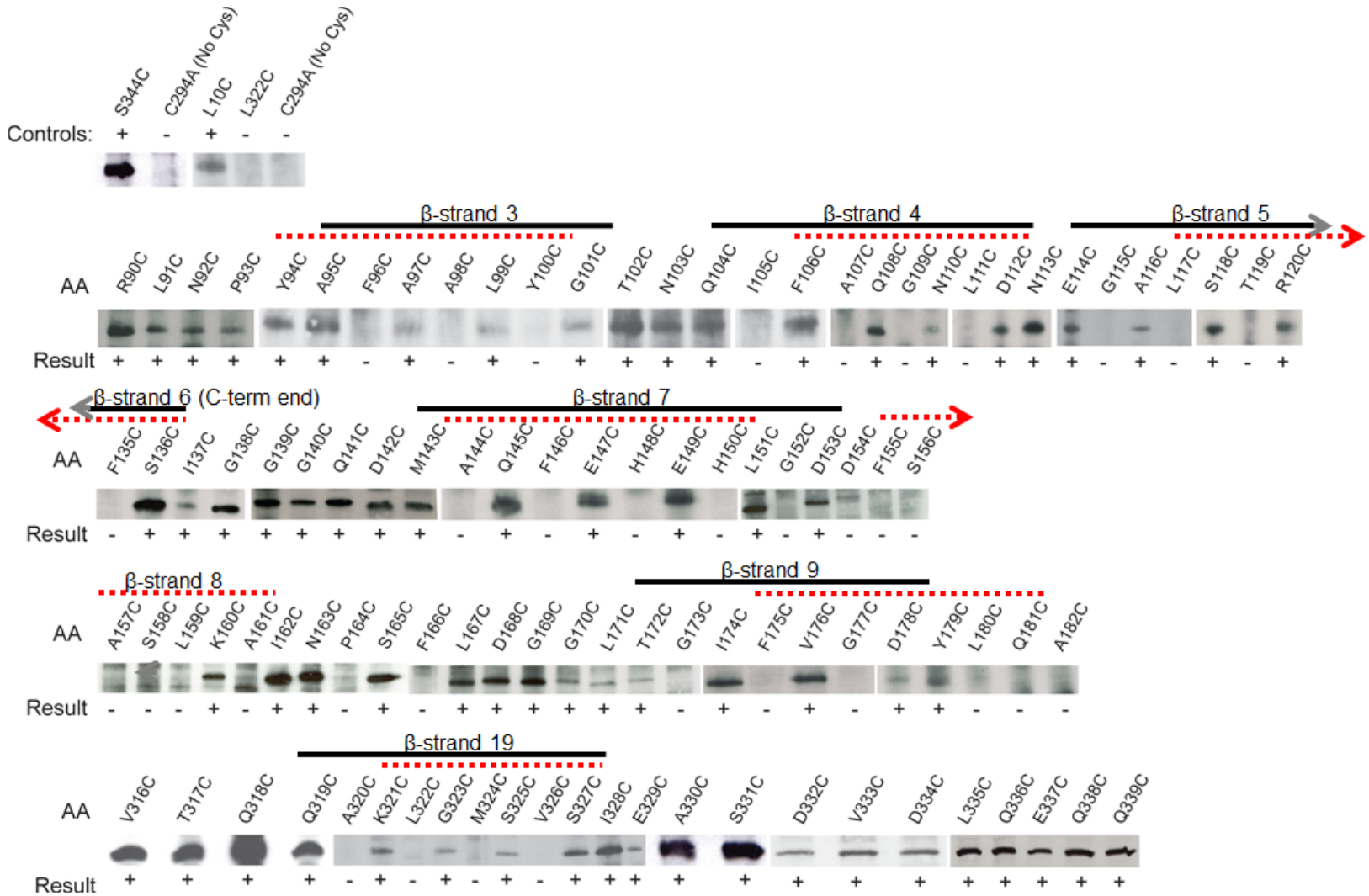
Controls:
S344C
C294A (No Cys)
L10C
L322C
C294A (No Cys)
β-strand 3
β-strand 4
β-strand 5
AA
R90C L91C N92C P93C Y94C A95C F96C A97C A98C L99C Y100C G101C T102C N103C Q104C I105C F106C A107C Q108C G109C N110C L111C D112C N113C E114C G115C A116C L117C S118C T119C R120C
Result
β-strand 6 (C-term end)
β-strand 7
AA
F135C S136C I137C G138C G139C G140C Q141C D142C M143C A144C Q145C F146C E147C H148C E149C H150C L151C G152C D153C D154C F155C S156C
Result
β-strand 8
β-strand 9
AA
A157C S158C L159C K160C A161C I162C N163C P164C S165C F166C L167C D168C G169C G170C L171C T172C G173C I174C F175C V176C G177C D178C Y179C L180C Q181C A182C
Result
β-strand 19
AA
V316C T317C Q318C Q319C A320C K321C L322C G323C M324C S325C V326C S327C I328C E329C A330C S331C D332C V333C D334C L335C Q336C E337C Q338C Q339C
Result

Figure 3.12 Alignment of human porin, humanTom40 and *N. crassa* Tom40 with the *N. crassa* Tom40 SCAM results shown. This figure is essentially a duplication of Figure 3.3 but with the SCAM results added. The amino acid sequence of porin from *H. sapiens (H.s)* is shown in duplicate. The positions of the 13 β-strands predicted by the biochemical model (Blachly-Dyson *et al.*, 1990; Peng *et al.*, 1992; Song and Colombini, 1996; Song *et al.*, 1998a, b; Colombini, 2009) are shown (highlighted and numbered red) on the top sequence (*H.s* p_BIO). (*) represents a sharp (zero residue) hairpin loop between β-strands 7 and 8 in the biochemical model. The second sequence (*H.s* p_3D) shows the positions (green) of the 19 β-strands identified by the NMR and X-ray structural studies conducted on mammalian porin (Bayrhuber *et al.*, 2008; Hiller *et al.*, 2008; Ujwal *et al.*, 2008). The third sequence (*H.s* Tom40) shows the positions (yellow) of the 19 β-stands predicted to exist using limited proteolysis followed by mass spectrometry and bioinformatics based on the homology of Tom40 and porin (Gessmann *et al.*, 2011). The bottom sequence (*N.c.* Tom40) represents the *Neurospora crassa* Tom40 aligned with the other sequences based on identity and similarity to the predicted 3D structure of *H.s* Tom40 and the solved 3D structure of *H.s* porin (Gessmann *et al.*, 2011). The predicted 19 β-strands are shown (highlighted and numbered blue). All SCAM results from this project and previous studies in the Nargang laboratory are displayed below the *N. crassa* Tom40 sequence. Positive (+) and negative (-) labeling signals are indicated. SCAM results that suggest β-strand arrangement are shown as black bars below the sequence. This figure was adapted from Gessmann *et al.* (2011).

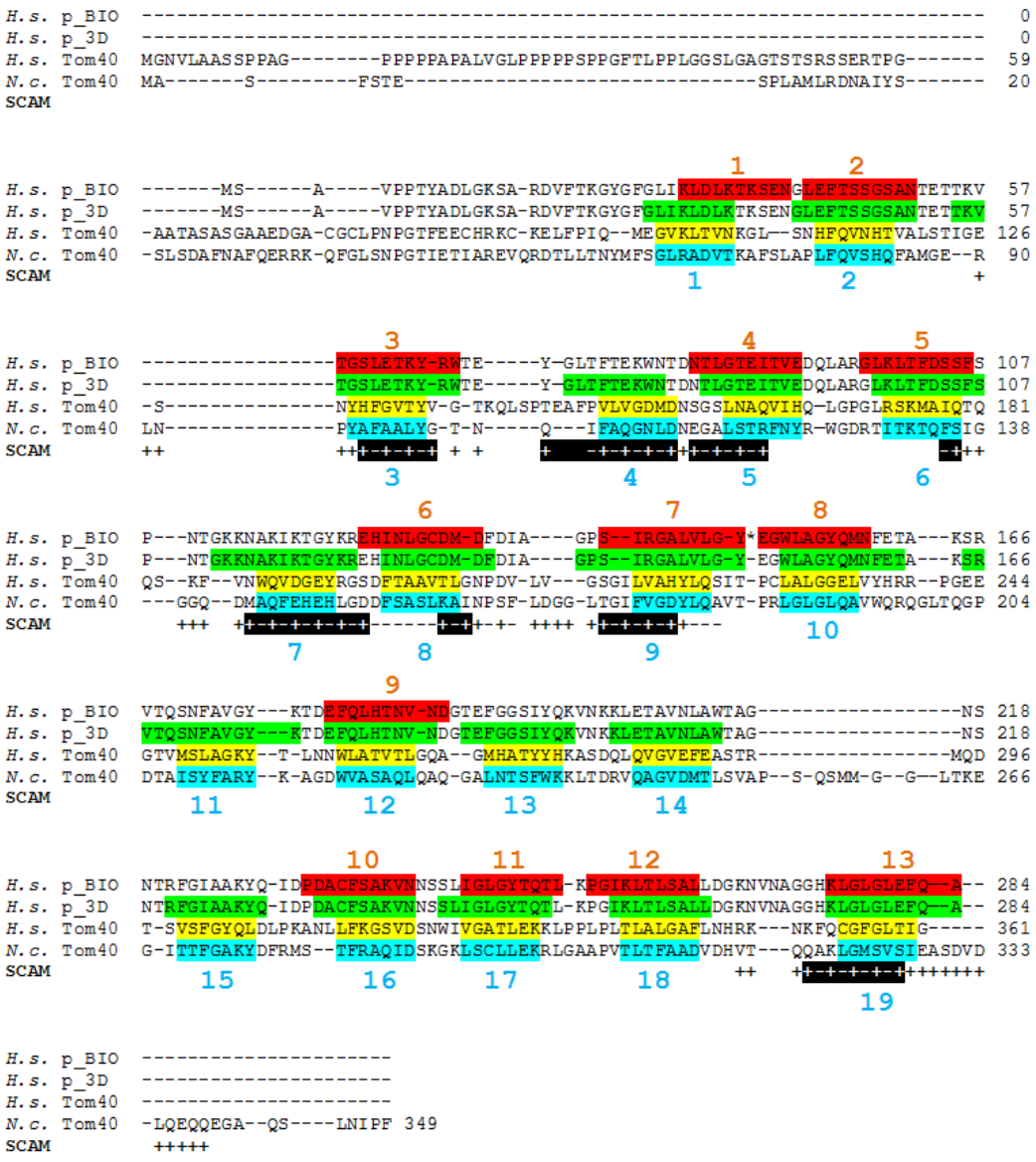
H.s. p_BIO
H.s. p_3D
H.s. Tom40
N.c. Tom40
SCAM

Tom40 models, was found to have an N-terminal α-helix that resides within the pore in certain states (Bayrhuber *et al.*, 2008; Hiller *et al.*, 2008; Ujwal *et al.*, 2008; Qiu *et al.*, 2013). This structurally defined α-helix (De Pinto *et al.*, 2007) is believed to be involved in the gating of the pore and thus undergoes conformational shifts under certain biophysical conditions (Koppel *et al.*, 1998). Studies have shown that in an "open" state this α-helical plug is ejected from the lumen of the pore to allow passage of larger molecules (Song *et al.*, 1998a). In the closed state, this α-helix aligns and interacts with certain regions of the pore lumen. Hiller *et al.* (2008) using NOESY (nuclear Overhauser effect spectroscopy) identified a small hydrophobic patch of the pore lumen involving β-strands 9 and 10 that interacts with defined residues of the α-helix. Another study came to the conclusion that the α-helix was orientated adjacently to β-strands 8-19 with specific hydrogen bonds identified between residues 2 (Ala) and 4 (Pro) of the α-helix and residues 122 (His) and 124 (Asn) at the N-terminal end of β-strand 8 (Ujwal *et al.*, 2008). These bonds act to stabilize the N-terminal α-helix with β-strand 8. Porin residues H122 and N124 that interact with the N-terminal α-helix are located in the N-terminal portion of β-strand 8 which correlates to the region lacking anticipated labeling in our SCAM data (Figure 3.12). Thus, if a similar conserved orientation of the α-helix exists for the Tom40 N-terminus in the Tom40 pore, this may explain the non-labeling results that were seen around the N-terminal end of β-strand 8. Notably, recent oxidative cross-linking studies have shown the Tom40 N-terminal α-helix to reside within the pore channel in close proximity to β-strand 9 (Qiu *et al.*, 2013).

As mentioned earlier the proposed 13 β-strands of the biochemical model align reasonably with 13 of the 19 β-strands in the porin 3D structure. The remaining six β-strands (4, 7, 11, 13, 14, 15) of the 3D porin structure (and Tom40 models) are absent in the corresponding regions of the biochemical model (Figures 3.2 and 3.12). In this study we have provided support for the 3D structures and models as applied to Tom40 since

our results suggest that β-strand 4 and β-strand 7 of the 3D structure do exist as native membrane spanning β-strands of functional and stable *N. crassa* Tom40 (Figure 3.12). We have no data on the other four strands that are predicted to differ between the two porin models.

The SCAM findings supporting the existence of β-strand 19 are especially important because the region has been suggested to play a critical role in Tom40 assembly via the TOB complex recognition of the β-signal contained within the most C-terminal β-strand (β-strand 19) of the Tom40 precursor (Kutik *et al.*, 2008a; Qiu *et al.*, 2013).

While stretches of positive labeling were observed for some exposed loop regions flanking β-strands (for example residues 328-339 following β-strand 19: Figures 3.11 and 3.12), certain regions and residues (residues154-159, 164, 166 and 180-182) provided unexpected patches with no labeling (Figure 3.11). As discussed above, residues 154-159 may be part of β-strand 8 but shielded from labeling via interactions with the N-terminal α-helical domain (Figures 3.11 and 3.12). The SCAM results also suggest residues 180-182 should be accessible to labeling as part of the exposed loop between β-strands 9 and 10. However, it has been shown (Loo and Clarke, 1995) that residues of small loops between membrane spanning α-helices can sometimes be inaccessible to Cys-labeling reagents. A similar situation may occur between β-strands. Also, the potential for shielding of certain residues via proteinaceous interactions needs to be considered when addressing these aberrant results. Shielding may inhibit the accessibility of residues that would otherwise be exposed to labeling. There are 7 proteins interacting to form the TOM complex in *N. crassa* (see section 1.6.2). Numerous protein-protein interactions are required to maintain TOM complex structure and function. Such interactions in the native complex may be responsible for shielding residues of the loops between β-strands on both the cytosolic and IMS side of the protein. Furthermore intra-protein interactions may

also be responsible for non-labeling, especially for residues predicted to be exposed in the pore lumen.

3.3.4 Interpretation of additional Tom40 mutants in the context of the 3D structural model.

In the years prior to resolution of the porin 3D structure and proposition of the Tom40 3D models, research in the Nargang lab was performed to characterize *N. crassa* Tom40 mutants (Rapaport *et al.*, 2001; Taylor *et al.*, 2003; Sherman *et al.*, 2006). Now that our SCAM data support the general validity of the 3D model we wished to re-address these mutants and perhaps provide new insight into their phenotypes with respect to the structural properties of the protein. I have chosen 32 previously described Tom40 mutants and aligned them with the 3D Tom40 model (Gessmann *et al.*, 2011) and our SCAM results (Figure 3.13).

An investigation into Tom40 mutants with truncations in the N-terminal region of the protein not involved in the β-barrel topology (Δ2-20, Δ2-40 and Δ41-60 (Rapaport *et al.*, 2001)) revealed that removal of the first 20 residues (Δ2-20) resulted in no significant defects with respect to insertion of the protein into the MOM (Rapaport *et al.*, 2001). The Δ2-40 and Δ41-60 mutants displayed normal localization to mitochondria but were inhibited in their ability to insert efficiently into the MOM. The Δ41-60 mutant precursor was unable to assemble into the final TOM complex in wildtype mitochondria *in vitro*. A Δ2-60 mutant construct could not rescue a *tom40*^{RIP} nucleus. This suggested that while some of the more N-terminal residues are not essential, the first 60 residues collectively contain crucial signals for Tom40 assembly (Rapaport and Neupert, 1999; Rapaport *et al.*, 2001). Thus, the residues of the predicted N-terminal α-helix (residues 48-57 (Gessmann *et al.*, 2011), those N-terminal to the α-helix and those linking the α-

Figure 3.13 Previously studied mutants of *N. crassa* Tom40 aligned with the 3D model and SCAM results. The first sequence is the wildtype *N. crassa* Tom40 protein with the 19 modeled β-strands shown (Highlighted and numbered blue). All SCAM results from this project and previous work in the Nargang laboratory are displayed below the *N. crassa* Tom40 sequence. Positive (+) and negative (-) labeling signals are indicated. SCAM results that suggest β-strand arrangement are shown as black bars below the wildtype Tom40 sequence. Below the SCAM results is a depiction of the region containing the amino acid deletions (-) or alanine substitutions (a) of each Tom40 mutant analyzed. All mutations have been described previously (Rapaport *et al.*, 2001; Taylor *et al.*, 2003; Sherman *et al.*, 2006). The actual affected regions of each mutant are highlighted in yellow.


N.c. Tom40 3D MASFSTESPLAMLRDNAIYSSLSDAFNAFQERRKQFGLSNPGTIETIAREVQRDTLLTNY 60
SCAM
Δ2-20 M----------SLSDAFNAFQERRKQFGLSNPGTIETIAREVQRDTLLTNY 60
Δ2-40 M----------PGTIETIAREVQRDTLLTNY 60
Δ41-60 MASFSTESPLAMLRDNAIYSSLSDAFNAFQERRKQFGLSN---------- 60
ΔNPGT MASFSTESPLAMLRDNAIYSSLSDAFNAFQERRKQFGLS----IETIAREVQRDTLLTNY 60
NPGT to AAAA MASFSTESPLAMLRDNAIYSSLSDAFNAFQERRKQFGLSaaaaIETIAREVQRDTLLTNY 60
Δ40-48 MASFSTESPLAMLRDNAIYSSLSDAFNAFQERRKQFGLS---------aEVQRDTLLTNY 60
ΔRD MASFSTESPLAMLRDNAIYSSLSDAFNAFQERRKQFGLSNPGTIETIAREVQ--TLLTNY 60
ΔRDTLL MASFSTESPLAMLRDNAIYSSLSDAFNAFQERRKQFGLSNPGTIETIAREVQ-----TNY 60
Δ51-60 MASFSTESPLAMLRDNAIYSSLSDAFNAFQERRKQFGLSNPGTIETIARa---------- 60
1 2 3 4 5
N.c. Tom40 3D MFSGLRADVTKAFSLAPLFQVSHQFAMGERLNPYAFAALYGTNQIFAQGNLDNEGALSTR 120
SCAM
ΔGLRAD MFS-----VTKAFSLAPLFQVSHQFAMGERLNPYAFAALYGTNQIFAQGNLDNEGALSTR 120
GLRAD to AAAAA MFSaaaaaVTKAFSLAPLFQVSHQFAMGERLNPYAFAALYGTNQIFAQGNLDNEGALSTR 120
ΔSHQ MFSGLRADVTKAFSLAPLFQV---FAMGERLNPYAFAALYGTNQIFAQGNLDNEGALSTR 120
SHQ to AAA MFSGLRADVTKAFSLAPLFQVaaaFAMGERLNPYAFAALYGTNQIFAQGNLDNEGALSTR 120
ΔGLND MFSGLRADVTKAFSLAPLFQVSHQFAMGERLNPYAFAALYGTNQIFAQ----NEGALSTR 120
GLND to AAAA MFSGLRADVTKAFSLAPLFQVSHQFAMGERLNPYAFAALYGTNQIFAQaaaaNEGALSTR 120
6 7 8 9
N.c. Tom40 3D FNYRWGDRTITKTQFSIGGGQDMAQFEHEHLGDDFSASLKAINPSFLDGGLTGIFVGDYL 180
SCAM
ΔTK FNYRWGDRTI--TQFSIGGGQDMAQFEHEHLGDDFSASLKAINPSFLDGGLTGIFVGDYL 180
TK to AA FNYRWGDRTIaaTQFSIGGGQDMAQFEHEHLGDDFSASLKAINPSFLDGGLTGIFVGDYL 180
ΔQFEHE FNYRWGDRTITKTQFSIGGGQDMA-----HLGDDFSASLKAINPSFLDGGLTGIFVGDYL 180
QFEHE to AAAAA FNYRWGDRTITKTQFSIGGGQDMAaaaaaHLGDDFSASLKAINPSFLDGGLTGIFVGDYL 180
ΔNP FNYRWGDRTITKTQFSIGGGQDMAQFEHEHLGDDFSASLKAI--SFLDGGLTGIFVGDYL 180
NP to AA FNYRWGDRTITKTQFSIGGGQDMAQFEHEHLGDDFSASLKAIaaSFLDGGLTGIFVGDYL 180
10 11 12 13
N.c. Tom40 3D QAVTPRLGLGLQAVWQRQGLTQGPDTAISYFARYKAGDWVASAQLQAQGALNTSFWKKLT 240
SCAM --
ΔVTP QA---RLGLGLQAVWQRQGLTQGPDTAISYFARYKAGDWVASAQLQAQGALNTSFWKKLT 240
VTP to AAA QAaaaRLGLGLQAVWQRQGLTQGPDTAISYFARYKAGDWVASAQLQAQGALNTSFWKKLT 240
ΔP QAVT-RLGLGLQAVWQRQGLTQGPDTAISYFARYKAGDWVASAQLQAQGALNTSFWKKLT 240
ΔKK QAVTPRLGLGLQAVWQRQGLTQGPDTAISYFARYKAGDWVASAQLQAQGALNTSFW--LT 240
KK to AA QAVTPRLGLGLQAVWQRQGLTQGPDTAISYFARYKAGDWVASAQLQAQGALNTSFWaaLT 240
14 15 16 17
N.c. Tom40 3D DRVQAGVDMTLSVAPSQSMMGGLTKEGITTFGAKYDFRMSTFRAQIDSKGKLSCLLEKRL 300
SCAM
ΔEKR DRVQAGVDMTLSVAPSQSMMGGLTKEGITTFGAKYDFRMSTFRAQIDSKGKLSCLL---L 300
EKR to AAA DRVQAGVDMTLSVAPSQSMMGGLTKEGITTFGAKYDFRMSTFRAQIDSKGKLSCLLaaaL 300
18 19
N.c. Tom40 3D GAAPVTLTFAADVDHVTQQAKLGMSVSIEASDVDLQEQQEGAQSLNIPF 349
SCAM
ΔKLG GAAPVTLTFAADVDHVTQQA---MSVSIEASDVDLQEQQEGAQSLNIPF 349
KLG to AAA GAAPVTLTFAADVDHVTQQAaaaMSVSIEASDVDLQEQQEGAQSLNIPF 349
ΔVDH GAAPVTLTFAAD---VTQQAKLGMSVSIEASDVDLQEQQEGAQSLNIPF 349
VDH to AAA GAAPVTLTFAADaaaVTQQAKLGMSVSIEASDVDLQEQQEGAQSLNIPF 349

helix to β-strand 1 (residues 64-70) within the pore appear to play an important role in Tom40 assembly.

To further dissect the role of the residues in this non-β-barrel N-terminal region (residues 1-64), six additional mutants (ΔNPGT, NPGT to AAAA, Δ40-48 (Rapaport *et al.*, 2001), ΔRD, ΔRDTLL and Δ51-60 (Taylor *et al.*, 2003)) were created. The position of these mutations in *N. crassa* Tom40 is shown in Figure 3.13. All were found to be capable of rescuing the *tom40*^{RIP} nucleus of the sheltered heterokaryon (strain RIP40het) (Rapaport *et al.*, 2001; Taylor *et al.*, 2003). Strains ΔNPGT, NPGT to AAAA and Δ40-48 displayed defects in both conidiation and climbing hyphal growth (Rapaport *et al.*, 2001). *In vitro* import and assembly assays revealed reduced incorporation of the six radiolabelled mutant precursors into the final TOM complex in wildtype mitochondria with an apparent stall at intermediate I (Tom40-TOB) of the Tom40 assembly pathway. Interestingly, BNGE of mutant mitochondria followed by TOM complex detection via western probing, revealed significantly reduced TOM complex stability, suggesting this region is crucial for the maintenance of the requisite protein-protein interactions of the complex or the topology/stability of Tom40 itself (Rapaport *et al.*, 2001; Taylor *et al.*, 2003).

The Taylor *et al.* (2003) study also examined the import and assembly of the ΔKLG and KLG to AAA mutant precursors into isolated wildtype mitochondria (Figure 3.13). Our SCAM data and the Gessmann *et al.* (2011) model, suggest that residues ^{321}KLG^{323} are part of the 9 residue final β-strand 19 at position 320-328 of the protein (Figure 3.13). The most C-terminal β-strand of MOM β-barrels houses the so-called β-signal (x**P**x**G**xx**H**x**H**; P – polar residue, H – hydrophobic residue) required for recognition of incoming β-precursors by Tob38 (Imai *et al.*, 2008; Kutik *et al.*, 2008a; Kutik *et al.*, 2008b). *N. crassa* β-strand 19 (A**K**L**G**MS**V**S**I**) matches the proposed β-

signal. Import of radiolabelled ΔKLG precursor into wildtype mitochondria revealed that the protein was absent from intermediate I at restrictive temperatures and stalled at intermediate I under normal import conditions with no precursor assembling into the final TOM complex (Taylor *et al.*, 2003). Therefore the ΔKLG Tom40 precursor can be recognized by and associate with the TOB complex but will not be inserted into the membrane. Removal of the KLG residues shortens the length of β-strand 19 and thus may prevent the strand from adequately spanning the MOM perhaps inhibiting Tom40 assembly into the membrane. Interestingly, the KLG to AAA precursor displayed a near wildtype assembly phenotype (Taylor *et al.*, 2003) suggesting that the polar and glycine residues of the conserved sequence are not mandatory for insertion and assembly of Tom40. These findings support the theory that an adequate span of β-strand 19 across the MOM is required for viability. The ΔKLG construct was unable to rescue the *tom40*^{RIP} nucleus whereas KLG to AAA did rescue and showed normal import phenotypes for the precursors tested. However, the KLG to AAA mutant showed reduced complex stability (Taylor *et al.*, 2003) suggesting that the integrity of the complex/Tom40 is also dependent on residues of the β-strand 19.

Another study characterized a further 21 Tom40 mutants (Figure 3.13) involving deletion or alanine substitution of residues in the main central region of the protein (residues 64-315) (Sherman *et al.*, 2006). According to the *N. crassa* Tom40 3D model, 14 of the 21 mutants have deletions or alanine substitutions of residues contained in predicted β-strands while the remaining 7 mutants affect residues in predicted loop regions.

Four of the mutant constructs (ΔSHQ, ΔVTP, ΔKK and ΔEKR; Figure 3.13) failed to rescue the *tom40*^{RIP} nucleus. The ΔVTP mutation is in the short loop between β-strands 9 and 10. Interestingly, the VTP to AAA and ΔP mutations did rescue the

tom40^{RIP} nucleus and the rescued mutants showed no aberrant phenotypes in growth, TOM complex stability and import/assembly experiments. On the other hand, import of radiolabelled ΔVTP, VTP to AAA and ΔP precursors into wildtype mitochondria resulted in a stall and accumulated smear at intermediate II, with very little precursor assembling into the final TOM complex. The three other non-rescuing mutants had missing residues at the C-terminal end of the modeled β-strand 2 (ΔSHQ), β-strand 13 (ΔKK) and β-strand 17 (ΔEKR). A similar *in vitro* assembly phenotype was seen for the three mutants with most mutant precursor stalled at intermediate I with very little reaching the TOM complex in wildtype mitochondria. Interestingly the respective alanine substitution mutants of these three regions all rescued the *tom40*^{RIP} nucleus and showed minimal Tom40 import/assembly defects yet displayed moderate to severe complex instability as determined by dissolving mitochondria in non-ionic detergents and observing Tom40 complexes following BNGE.

Surprisingly four additional deletion constructs affecting residues in predicted β-strands 1 (ΔGLRAD), 4 (ΔGLND), 6 (ΔTK) and 7 (ΔQFEHE) were able to rescue the *tom40*^{RIP} nucleus unlike the ΔKLG mutant of β-strand 19 (Taylor *et al.*, 2003; Sherman *et al.*, 2006). These mutants displayed reduced growth phenotypes and varying degrees of TOM complex instability. All mitochondria from these mutants were deficient in the *in vitro* import of at least the porin precursor. *In vitro* import of these rescuing β-strand mutant precursors into wildtype mitochondria revealed that all stalled at intermediate I with very little precursor progressing to the TOM complex (ΔQFEHE had an additional accumulation at intermediate II). The corresponding alanine substitutions appeared to have alleviated most phenotypes.

Radiolabelled precursors for four rescuing constructs (ΔNP, NP to AA, ΔVDH and VDH to AAA) affecting residues present in loop regions between β-strands showed only a slight stall at Intermediate I during *in vitro* import into wildtype mitochondria. No

growth phenotypes were observed in these rescued strains but isolated mitochondria of these mutants showed significant import phenotypes for all precursors tested. The ΔVDH and VDH to AAA mutants also displayed reduced TOM complex stability.

The results described above suggest that Tom40 β-strand/barrel topology is flexible to a certain extent and that some mutant proteins have the intrinsic ability to adapt and function as a viable general import pore, despite inefficiencies and structural instability. Particularly interesting is the fact that some mutants lacking portions of predicted β-strands can still assemble into a functional pore (strains ΔGLRAD, ΔGLND, ΔTK and ΔQFEHE). However, some residues and structural features are indispensable for the assembly and/or function of Tom40 into the TOM complex (strains Δ2-60, ΔKLG, ΔSHQ, ΔVTP, ΔKK, ΔEKR).

3.3.5 Orientation of the Tom40 β-barrel in the MOM.

MOM embedded β-barrels are generally composed of multiple single-pass β-strands that form a cylindrical β-sheet that spans the membrane. The antiparallel orientation of sequential β-strands means that β-barrels with an even number of single-pass structures (β-strands and α-helical TMDs) will generally have their termini exposed on/or facing the same side of the membrane. Conversely, proteins with an odd number of single-pass structures like porin (19 β-strands) should have their termini localized on opposing sides of the membrane. Investigations using peptide specific antibodies, protease accessibility, SCAM and modern biophysical techniques have been conducted to determine the localization (i.e. exposure to the cytosol/IMS or membrane embedded) of the N- and C-termini of porin. There is a consensus on the membrane embedded nature of the C-terminus as β-strand 19 (De Pinto *et al.*, 1991; Stanley *et al.*, 1995; Song *et al.*, 1998b; Summers and Court, 2010). The N-terminal results however are somewhat conflicting, perhaps attributable to various groups working with porin in differing gated

states reflecting the dynamic nature of the N-terminal α-helix which either resides within the pore lumen or is ejected to allow the "open" state (De Pinto *et al.*, 1991; Stanley *et al.*, 1995; Song *et al.*, 1998b; Summers and Court, 2010). Topological studies on *N. crassa* Tom40 reconstituted into planar lipid membranes using antibodies directed to epitopes at either terminus suggest that both are found on the same side of the membrane and protease accessibility studies on isolated mitochondria and mitoplasts suggested both termini were exposed to the IMS side (Kunkele *et al.*, 1998b). Conversely, protease accessibility studies on *S. cerevisiae* Tom40 suggested an IMS localization of the C-terminus whereas the N-terminus was exposed to the cytosol (Hill *et al.*, 1998). Studies on rat Tom40 (Tom40A) and a novel Tom40B isoform with a truncated N-terminal domain that is conserved across mammals, revealed that while the C-termini of both isoforms were located in the IMS the N-terminus of Tom40A was exposed to the cytosol while the Tom40B N-terminus was in the IMS (Kinoshita *et al.*, 2007). Consideration of all these data and the recent 19 β-stranded model suggests that the C-terminus of *N. crassa* Tom40 is localized in the IMS. An uneven number of β-strands (19) would then imply that the N-terminus would have a cytosolic localization. However a dynamic orientation and association of the N-terminal α-helix within the pore lumen (similar to porin) may explain accessibility data that indicates an IMS localization. Another approach used by the Nargang lab to verify the proposed orientation of the N- and C-termini as well as the inter β-strand loops was to insert protease factor Xa sites at specific locations within *N. crassa* Tom40 (personal communication, F. Nargang, data unpublished). Analysis of cleavage products from intact isolated mitochondria and disrupted mitoplasts of Xa site containing proteins added further biochemical support to our SCAM results and the proposed orientation of the 19 β-stranded 3D model of *N. crassa* Tom40.

Supplemental Figure S3.1 Schematic representation of Tom40 KO sheltered heterokaryons. (A) Knock-out procedure for essential genes. In this example, the histidine requiring, fpa resistant (*mtr*) 76-26 nucleus of the HP1 heterokaryon strain undergoes knock-out of the *tom40* gene resulting in the *tom40 KO* sheltered heterokaryon. It should be noted that there is an equal chance of the KO occurring in the *pan-2*, benomyl resistant (*Bml*) nucleus. However our lab prefers working with KO's in the fpa resistant nucleus and select such KO's for further work by examination of growth characteristics on media containing fpa + His or Bml + Pan. (B) The knockout is created by replacing the *tom40* gene with a hygromycin resistance cassette using a split-marker approach (Colot *et al.*, 2006). Knock-out is achieved when both components of the split-marker recombine at the *tom40* locus. (C) The sheltered heterokaryon KO can be grown under selective conditions (i.e. media containing His and fpa) that will result in numerical superiority of the KO nucleus in the culture. As the gene of interest is essential, the 71-18 nucleus containing the $tom40^{+}$ gene must be maintained at minimal required levels in this medium.

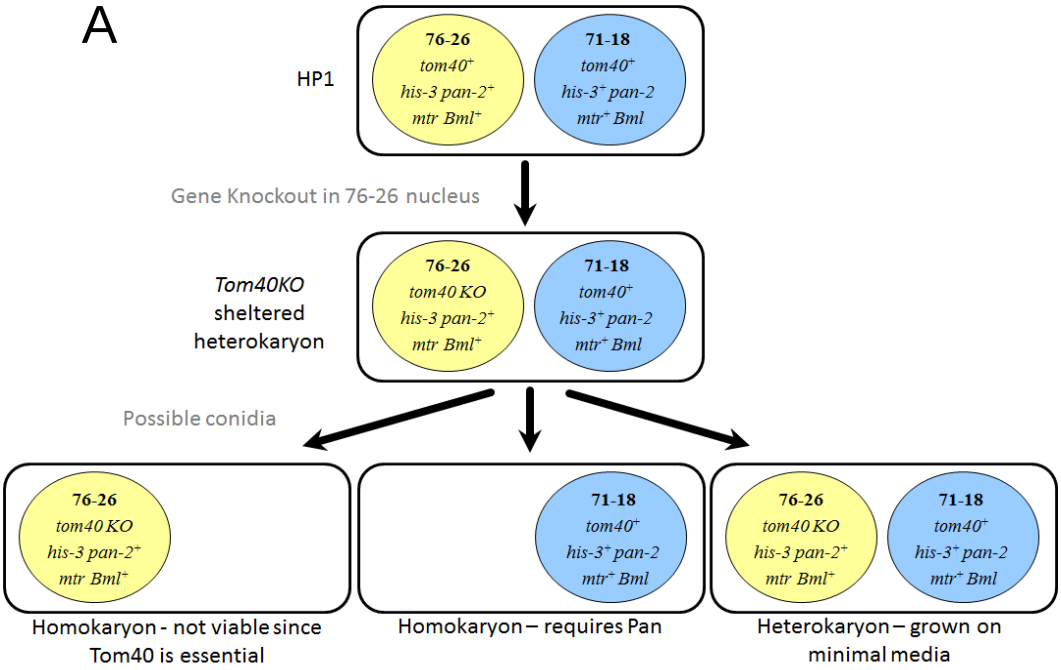
A
HP1
76-26
tom40+
his-3 pan-2+
mtr Bml+
71-18
tom40+
his-3+ pan-2
mtr+ Bml
Gene Knockout in 76-26 nucleus
Tom40KO
sheltered
heterokaryon
76-26
tom40 KO
his-3 pan-2+
mtr Bml+
71-18
tom40+
his-3+ pan-2
mtr+ Bml
Possible conidia
76-26
tom40 KO
his-3 pan-2+
mtr Bml+
Homokaryon - not viable since
Tom40 is essential
71-18
tom40+
his-3+ pan-2
mtr+ Bml
Homokaryon – requires Pan
76-26
tom40 KO
his-3 pan-2+
mtr Bml+
71-18
tom40+
his-3+ pan-2
mtr+ Bml
Heterokaryon – grown on
minimal media

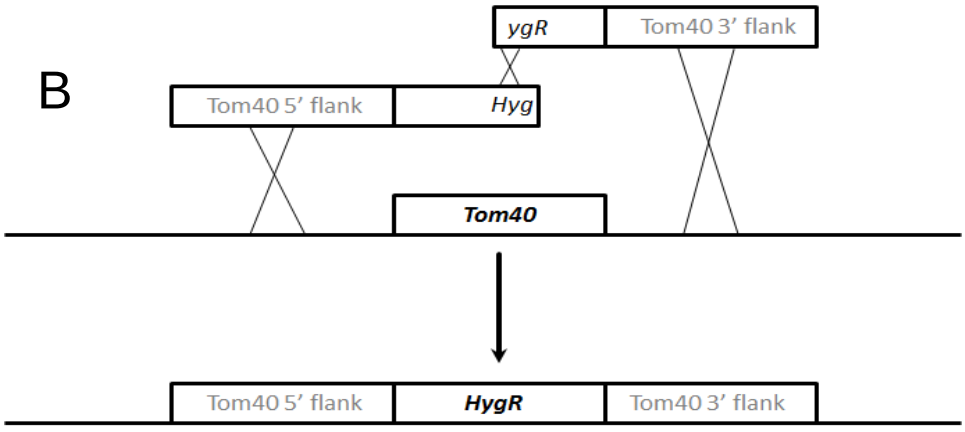
B
ygR
Tom40 3' flank
Tom40 5' flank
Hyg
Tom40
Tom40 5' flank
HygR
Tom40 3' flank

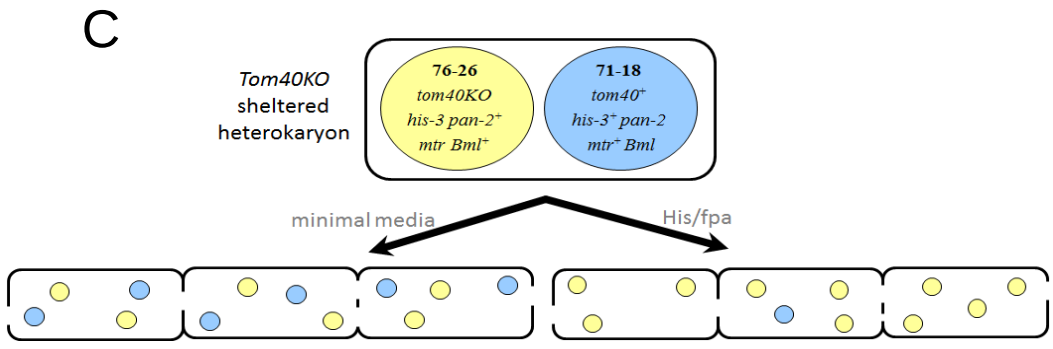
C
Tom40KO
sheltered
heterokaryon
76-26
tom40KO
his-3 pan-2+
mtr Bml+
71-18
tom40+
his-3+ pan-2
mtr+ Bml
minimal media
His/fpa

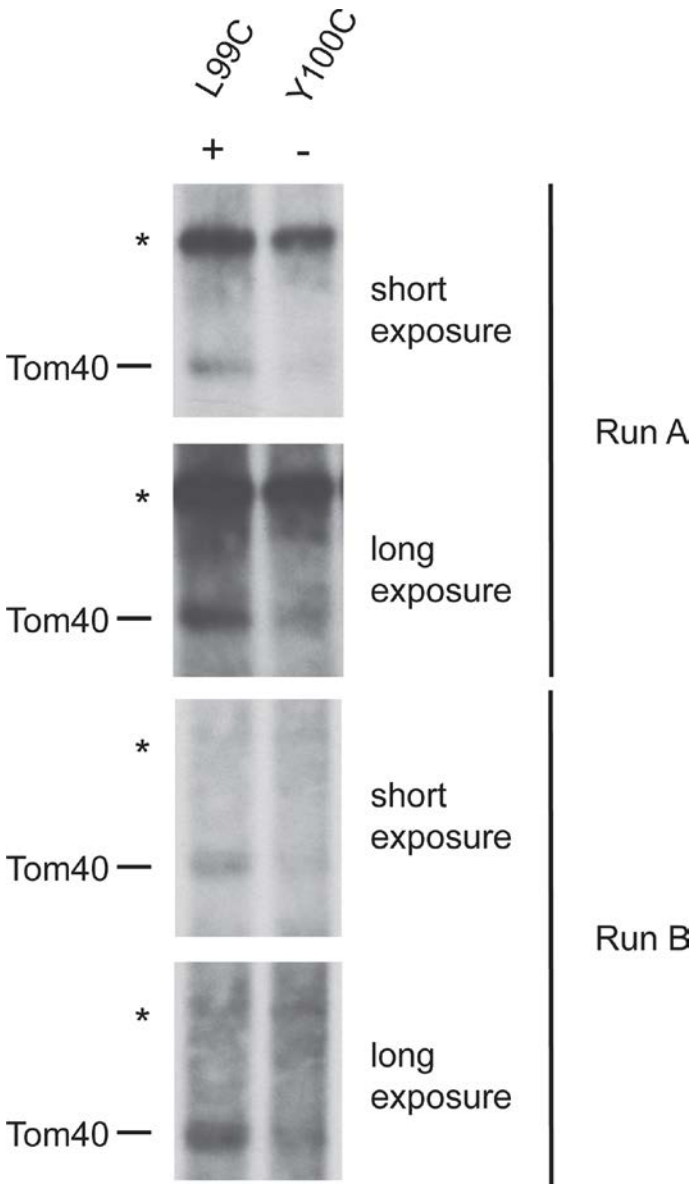

Supplemental Figure S3.2 Inconsistent SCAM labeling of residue 100. The results of two separate SCAM runs (labeled A and B) for residues 99 and 100 are shown. Residue 99 clearly displays positive (+) labeling in all four instances and was thus deemed accessible to the labeling reagent. Residue 100 was judged to be negative (-) in our analysis however in certain instances a faint band can be observed suggesting labeling to a small extent when compared to labeling for residue 99. A longer time exposure of X-ray film to the run blots makes visualization of the faint band easier. (*) represents a distinct background band observed that serves as a loading control.

3.4 References

Ahting, U., Thun, C., Hegerl, R., Typke, D., Nargang, F.E., Neupert, W., and Nussberger, S. (1999). The TOM core complex: the general protein import pore of the outer membrane of mitochondria. J Cell Biol *147*, 959-968.

Bay, D.C., Hafez, M., Young, M.J., and Court, D.A. (2012). Phylogenetic and coevolutionary analysis of the beta-barrel protein family comprised of mitochondrial porin (VDAC) and Tom40. Biochim Biophys Acta *1818*, 1502-1519.

Bayrhuber, M., Meins, T., Habeck, M., Becker, S., Giller, K., Villinger, S., Vonrhein, C., Griesinger, C., Zweckstetter, M., and Zeth, K. (2008). Structure of the human voltage-dependent anion channel. Proc Natl Acad Sci U S A *105*, 15370-15375.

Blachly-Dyson, E., Peng, S., Colombini, M., and Forte, M. (1990). Selectivity changes in site-directed mutants of the VDAC ion channel: structural implications. Science *247*, 1233-1236.

Colombini, M. (2009). The published 3D structure of the VDAC channel: native or not? Trends Biochem Sci *34*, 382-389.

Colombini, M. (2012a). Mitochondrial Outer Membrane Channels. Chem Rev.

Colombini, M. (2012b). VDAC structure, selectivity, and dynamics. Biochim Biophys Acta *1818*, 1457-1465.

Colot, H.V., Park, G., Turner, G.E., Ringelberg, C., Crew, C.M., Litvinkova, L., Weiss, R.L., Borkovich, K.A., and Dunlap, J.C. (2006). A high-throughput gene knockout procedure for *Neurospora* reveals functions for multiple transcription factors. Proc Natl Acad Sci U S A *103*, 10352-10357.

Court, D., Lill, R., and Neupert, W. (1995). The protein import apparatus of the mitochondrial outer membrane. Can. J. Bot. *73*, S193-S197

Davis, R.H., and De Serres, F.J. (1970). Genetic and microbiological research techniques for *Neurospora crassa*. Methods Enzymol. *17*, 79-143.

De Pinto, V., Prezioso, G., Thinnes, F., Link, T.A., and Palmieri, F. (1991). Peptide-specific antibodies and proteases as probes of the transmembrane topology of the bovine heart mitochondrial porin. Biochemistry *30*, 10191-10200.

De Pinto, V., Tomasello, F., Messina, A., Guarino, F., Benz, R., La Mendola, D., Magri, A., Milardi, D., and Pappalardo, G. (2007). Determination of the conformation of the human VDAC1 N-terminal peptide, a protein moiety essential for the functional properties of the pore. Chembiochem *8*, 744-756.

Galdiero, S., Galdiero, M., and Pedone, C. (2007). beta-Barrel membrane bacterial proteins: structure, function, assembly and interaction with lipids. Curr Protein Pept Sci *8*, 63-82.

Gessmann, D., Flinner, N., Pfannstiel, J., Schlosinger, A., Schleiff, E., Nussberger, S., and Mirus, O. (2011). Structural elements of the mitochondrial preprotein-conducting

channel Tom40 dissolved by bioinformatics and mass spectrometry. Biochim Biophys Acta *1807*, 1647-1657.

Good, A.G., and Crosby, W.L. (1989). Anaerobic induction of alanine aminotransferase in barley root tissue. Plant Physiol *90*, 1305-1309.

Grotelueschen, J., and Metzenberg, R.L. (1995). Some property of the nucleus determines the competence of *Neurospora crassa* for transformation. Genetics *139*, 1545-1551.

Harkness, T.A., Nargang, F.E., van der Klei, I., Neupert, W., and Lill, R. (1994). A crucial role of the mitochondrial protein import receptor MOM19 for the biogenesis of mitochondria. J Cell Biol *124*, 637-648.

Hill, K., Model, K., Ryan, M.T., Dietmeier, K., Martin, F., Wagner, R., and Pfanner, N. (1998). Tom40 forms the hydrophilic channel of the mitochondrial import pore for preproteins [see comment]. Nature *395*, 516-521.

Hiller, S., Abramson, J., Mannella, C., Wagner, G., and Zeth, K. (2010). The 3D structures of VDAC represent a native conformation. Trends Biochem Sci *35*, 514-521.

Hiller, S., Garces, R.G., Malia, T.J., Orekhov, V.Y., Colombini, M., and Wagner, G. (2008). Solution structure of the integral human membrane protein VDAC-1 in detergent micelles. Science *321*, 1206-1210.

Hiller, S., and Wagner, G. (2009). The role of solution NMR in the structure determinations of VDAC-1 and other membrane proteins. Curr Opin Struct Biol *19*, 396-401.

Hoppins, S.C., Go, N.E., Klein, A., Schmitt, S., Neupert, W., Rapaport, D., and Nargang, F.E. (2007). Alternative splicing gives rise to different isoforms of the *Neurospora crassa* Tob55 protein that vary in their ability to insert beta-barrel proteins into the outer mitochondrial membrane. Genetics *177*, 137-149.

Imai, K., Gromiha, M.M., and Horton, P. (2008). Mitochondrial beta-barrel proteins, an exclusive club? Cell *135*, 1158-1159; author reply 1159-1160.

Kinoshita, J.Y., Mihara, K., and Oka, T. (2007). Identification and characterization of a new tom40 isoform, a central component of mitochondrial outer membrane translocase. J Biochem *141*, 897-906.

Koppel, D.A., Kinnally, K.W., Masters, P., Forte, M., Blachly-Dyson, E., and Mannella, C.A. (1998). Bacterial expression and characterization of the mitochondrial outer membrane channel. Effects of n-terminal modifications. J Biol Chem *273*, 13794-13800.

Kunkele, K.P., Heins, S., Dembowski, M., Nargang, F.E., Benz, R., Thieffry, M., Walz, J., Lill, R., Nussberger, S., and Neupert, W. (1998a). The preprotein translocation channel of the outer membrane of mitochondria. Cell *93*, 1009-1019.

Kunkele, K.P., Juin, P., Pompa, C., Nargang, F.E., Henry, J.P., Neupert, W., Lill, R., and Thieffry, M. (1998b). The isolated complex of the translocase of the outer membrane of

mitochondria. Characterization of the cation-selective and voltage-gated preprotein-conducting pore. J Biol Chem *273*, 31032-31039.

Kutik, S., Stojanovski, D., Becker, L., Becker, T., Meinecke, M., Kruger, V., Prinz, C., Meisinger, C., Guiard, B., Wagner, R., Pfanner, N., and Wiedemann, N. (2008a). Dissecting membrane insertion of mitochondrial beta-barrel proteins. Cell *132*, 1011-1024.

Kutik, S., Stojanovski, D., Becker, T., Stroud, D.A., Becker, L., Meinecke, M., Krüger, V., Prinz, C., Guiard, B., Wagner, R., Meisinger, C., Pfanner, N., and Wiedemann, N. (2008b). Response: The Mitochondrial β-Signal and Protein Sorting. Cell *135*, 1159-1160.

Lackey, S.W., Wideman, J.G., Kennedy, E.K., Go, N.E., and Nargang, F.E. (2011). The *Neurospora crassa* TOB complex: analysis of the topology and function of Tob38 and Tob37. PLoS One *6*, e25650.

Laemmli, U.K. (1970). Cleavage of structural proteins during the assembly of the head of bacteriophage T4. Nature *227*, 680-685.

Loo, T.W., and Clarke, D.M. (1995). Membrane topology of a cysteine-less mutant of human P-glycoprotein. J Biol Chem *270*, 843-848.

Mager, F., Gessmann, D., Nussberger, S., and Zeth, K. (2011). Functional refolding and characterization of two Tom40 isoforms from human mitochondria. J Membr Biol *242*, 11-21.

Mannella, C.A., Neuwald, A.F., and Lawrence, C.E. (1996). Detection of likely transmembrane beta strand regions in sequences of mitochondrial pore proteins using the Gibbs sampler. J Bioenerg Biomembr *28*, 163-169.

McDonald, B.M., Wydro, M.M., Lightowlers, R.N., and Lakey, J.H. (2009). Probing the orientation of yeast VDAC1 in vivo. FEBS Lett *583*, 739-742.

McGuffin, L.J., Bryson, K., and Jones, D.T. (2000). The PSIPRED protein structure prediction server. Bioinformatics *16*, 404-405.

Model, K., Prinz, T., Ruiz, T., Radermacher, M., Krimmer, T., Kuhlbrandt, W., Pfanner, N., and Meisinger, C. (2002). Protein translocase of the outer mitochondrial membrane: role of import receptors in the structural organization of the TOM complex. J Mol Biol *316*, 657-666.

Nargang, F.E., Künkele, K.-P., Mayer, A., Ritzel, R.G., Neupert, W., and Lill, R. (1995). "Sheltered disruption" of *Neurospora crassa* MOM22, an essential component of the mitochondrial protein import complex. EMBO J. *14*, 1099-1108.

Nargang, F.E., and Rapaport, D. (2007). *Neurospora crassa* as a model organism for mitochondrial biogenesis. Methods Mol Biol *372*, 107-123.

Pautsch, A., and Schulz, G.E. (1998). Structure of the outer membrane protein A transmembrane domain. Nat Struct Biol *5*, 1013-1017.

Pavlov, P.F., and Glaser, E. (2002). Probing the membrane topology of a subunit of the mitochondrial protein translocase, Tim44, with biotin maleimide. Biochem Biophys Res Commun *293*, 321-326.

Peng, S., Blachly-Dyson, E., Forte, M., and Colombini, M. (1992). Large scale rearrangement of protein domains is associated with voltage gating of the VDAC channel. Biophys J *62*, 123-131; discussion 131-125.

Qiu, J., Wenz, L.S., Zerbes, R.M., Oeljeklaus, S., Bohnert, M., Stroud, D.A., Wirth, C., Ellenrieder, L., Thornton, N., Kutik, S., Wiese, S., Schulze-Specking, A., Zufall, N., Chacinska, A., Guiard, B., Hunte, C., Warscheid, B., van der Laan, M., Pfanner, N., Wiedemann, N., and Becker, T. (2013). Coupling of mitochondrial import and export translocases by receptor-mediated supercomplex formation. Cell *154*, 596-608.

Qiu, X.Q., Jakes, K.S., Finkelstein, A., and Slatin, S.L. (1994). Site-specific biotinylation of colicin Ia. A probe for protein conformation in the membrane. J Biol Chem *269*, 7483-7488.

Rapaport, D., and Neupert, W. (1999). Biogenesis of Tom40, core component of the TOM complex of mitochondria. J Cell Biol *146*, 321-331.

Rapaport, D., Taylor, R.D., Kaser, M., Langer, T., Neupert, W., and Nargang, F.E. (2001). Structural requirements of Tom40 for assembly into preexisting TOM complexes of mitochondria. Mol Biol Cell *12*, 1189-1198.

Saccone, C., Caggese, C., D'Erchia, A.M., Lanave, C., Oliva, M., and Pesole, G. (2003). Molecular clock and gene function. J Mol Evol *57 Suppl 1*, S277-285.

Schägger, H., Cramer, W.A., and von Jagow, G. (1994). Analysis of molecular masses and oligomeric states of protein complexes by blue native electrophoresis and isolation of membrane protein complexes by two-dimensional native electrophoresis. Anal. Biochem. *217*, 220-230.

Schägger, H., and von Jagow, G. (1991). Blue native electrophoresis for isolation of membrane complexes in enzymatically active form. Anal. Biochem. *199*, 223-231.

Sherman, E.L., Go, N.E., and Nargang, F.E. (2005). Functions of the small proteins in the TOM complex of *Neurospora crassa*. Mol Biol Cell *16*, 4172-4182.

Sherman, E.L., Taylor, R.D., Go, N.E., and Nargang, F.E. (2006). Effect of mutations in Tom40 on stability of the translocase of the outer mitochondrial membrane (TOM) complex, assembly of Tom40, and import of mitochondrial preproteins. J Biol Chem *281*, 22554-22565.

Song, J., and Colombini, M. (1996). Indications of a common folding pattern for VDAC channels from all sources. J Bioenerg Biomembr *28*, 153-161.

Song, J., Midson, C., Blachly-Dyson, E., Forte, M., and Colombini, M. (1998a). The sensor regions of VDAC are translocated from within the membrane to the surface during the gating processes. Biophys J *74*, 2926-2944.

Song, J., Midson, C., Blachly-Dyson, E., Forte, M., and Colombini, M. (1998b). The topology of VDAC as probed by biotin modification. J Biol Chem *273*, 24406-24413.

Stanley, S., Dias, J.A., D'Arcangelis, D., and Mannella, C.A. (1995). Peptide-specific antibodies as probes of the topography of the voltage-gated channel in the mitochondrial outer membrane of Neurospora crassa. J Biol Chem *270*, 16694-16700.

Summers, W.A., and Court, D.A. (2010). Origami in outer membrane mimetics: correlating the first detailed images of refolded VDAC with over 20 years of biochemical data. Biochemistry and cell biology = Biochimie et biologie cellulaire *88*, 425-438.

Tanton, L.L., Nargang, C.E., Kessler, K.E., Li, Q., and Nargang, F.E. (2003). Alternative oxidase expression in *Neurospora crassa*. Fungal Genet Biol *39*, 176-190.

Taylor, R.D. (2003). Assembly, function and structure of Tom40, the pore-forming component of the the TOM complex in *Neurospora crassa*, University of Alberta.

Taylor, R.D., McHale, B.J., and Nargang, F.E. (2003). Characterization of *Neurospora crassa* Tom40-deficient mutants and effect of specific mutations on Tom40 assembly. J Biol Chem *278*, 765-775.

Thomas, L., Blachly-Dyson, E., Colombini, M., and Forte, M. (1993). Mapping of residues forming the voltage sensor of the voltage-dependent anion-selective channel. Proc Natl Acad Sci U S A *90*, 5446-5449.

Thomas, L., Kocsis, E., Colombini, M., Erbe, E., Trus, B.L., and Steven, A.C. (1991). Surface topography and molecular stoichiometry of the mitochondrial channel, VDAC, in crystalline arrays. J Struct Biol *106*, 161-171.

Ujwal, R., Cascio, D., Colletier, J.P., Faham, S., Zhang, J., Toro, L., Ping, P., and Abramson, J. (2008). The crystal structure of mouse VDAC1 at 2.3 A resolution reveals mechanistic insights into metabolite gating. Proc Natl Acad Sci U S A *105*, 17742-17747.

van Geest, M., and Lolkema, J.S. (2000). Membrane topology and insertion of membrane proteins: search for topogenic signals. Microbiol Mol Biol Rev *64*, 13-33.

Vestweber, D., Brunner, J., Baker, A., and Schatz, G. (1989). A 42K outer-membrane protein is a component of the yeast mitochondrial protein import site. Nature *341*, 205-209.

Wideman, J.G., Go, N.E., Klein, A., Redmond, E.K., Lackey, S.W.K., Tao, T., Kalbacher, H., Rapaport, D., Neupert, W., and Nargang, F.E. (2010). Roles of the Mdm10, Tom7, Mdm12, and Mmm1 proteins in the assembly of mitochondrial outer membrane proteins in *Neurospora crassa*. Mol. Biol. Cell *21*, 1725-1736.

Young, M.J., Bay, D.C., Hausner, G., and Court, D.A. (2007). The evolutionary history of mitochondrial porins. BMC Evol Biol *7*, 31.

Yu, T.Y., Raschle, T., Hiller, S., and Wagner, G. (2012). Solution NMR spectroscopic characterization of human VDAC-2 in detergent micelles and lipid bilayer nanodiscs. Biochim Biophys Acta *1818*, 1562-1569.

Zeth, K. (2010). Structure and evolution of mitochondrial outer membrane proteins of beta-barrel topology. Biochim Biophys Acta *1797*, 1292-1299.

Zhu, Q., and Casey, J.R. (2007). Topology of transmembrane proteins by scanning cysteine accessibility mutagenesis methodology. Methods *41*, 439-450.

Appendix I. Primers, plasmids and the construction of the *Tom40*^{RIP} sheltered heterokaryon

Table A.1. Primers used in Chapter 2.

Primer	**Sequence 5'→3'**	**Use**
hphF	ACATACGATTTAGGTGACACTATAGAACGCCCGTCGACAGAAGATGATATTGAAGGAGC	Amplification of hygromycin resistance cassette for KO protocol.
hphR	AGCTGACATCGACACCAACG	
Tom37KO 5F	GTAACGCCAGGGTTTTCCCAGTCACGACGTTGCCAAGGCGACATGTTCG	Amplification of 5' UTR of Tob37 for KO protocol.
Tom37KO 5R	ACCGGGATCCACTTAACGTTACTGAAATCCGGAGGGTCAGGTAGGGATT	
Tom37KO 3F	CGTTCTATAGTGTCACCTAAATCGTATGTGACGTTGAGGGTAGAGAACC	Amplification of 3' UTR of Tob37 for KO protocol.
Tom37KO 3R	GCGGATAACAATTTCACACAGGAAACAGCGGCATCCGAAACATCACCTC	
Met2KO 5F	GTAACGCCAGGGTTTTCCCAGTCACGACGTTTAGAACTAAGAACCGGCA	Amplification of 5' UTR of Tob38 for KO protocol.
Met2KO 5R	ACCGGGATCCACTTAACGTTACTGAAATCGGTTGCGAATCGACCTGGTA	
Met2KO 3F	CGTTCTATAGTGTCACCTTAAATCGTATGTCTCATGACGAAGGCTACGAC	Amplification of 3' UTR of Tob38 for KO protocol.
Met2KO 3R	GCGGATAACAATTTCACACAGGAAACAGCTGGAGGTGAAAGAGTGACGG	

hSM-f	AAAAAGCCTGAACTCACCGCGACG	Amplification of split marker fragment containing Tom40 5'UTR and hph (-promoter).
hSM-r	TCGCCTCGCTCCAGTCAATGACC	Amplification of split marker fragment containing Tom40 3'UTR and hph (-terminator).
EKR 3	GAAGCGTCATCGCTTCAGTTGTC	Tob38 sequencing primers
EKR 4	AATAGGCCTTCCTCAAGCTTGCC	
EKR 5	TAGGTTGCCCTCTGTTTATCCGG	
Tob38-mid	TGCTGGACAGGTTCTACATC	
EKR 8	CCAACGACAACAACCCATCCATC	Tob37 sequencing primers
EKR 10	CATCCGTTCTCGTATCATTCC	
Tob37-mid	CCTTGGTTGAAGGAAGTGTT	
SWL 1	CGTGCCACAAGGTCCAACGA	PCR amplification of ectopic Tob37 copies. 5' forward
SWL 2	CGCTTTCCCATTGGGTATCC	PCR amplification of ectopic Tob37 copies. 3' reverse complementarity
SWL 3	ATGACGCTAGAGCTCCATGT	Tob37 sequencing primer
SWL 4	CAGGAGCCATGTTCGCTGGTGTTAACTGAAGACGTTGAGGGTAGAG	Mutagenic primer creating *Hpa*I restriction site directly 3' of CHD
SWL 5	CGTTGGTGAGAGTGAACGCGTTAACTTGCTGGCTGGTGCCGGGTT	Mutagenic primer creating *Hpa*I restriction site directly 5' of TMD1
SWL 7	/5Phos/GCTGGCTATCAACGTTGCCGGCCTCAGTGTTAACTGGTACCGATACCGAGGGTTGCTGG	Mutagenic primer creating *Hpa*I restriction site directly 3' of TMD1

SWL 8	/5Phos/CGCCGTTACAGACG TGGCATGTTAACCTGGTAG GCTTGGGCAGC	Mutagenic primer creating *Hpa*I restriction site directly 5' of CHD
SWL 11	CCCAATCCCTACCTGACCC TCCG	Tob37 sequencing primer

Table A.2. Plasmids used in Chapter 2.

Name	Source	Description
pCSN44	FGSC	Contains hygromycin resistance cassette.
pRS416	FGSC	*URA-3* containing plasmid used for recombination of KO protocol fragments in FY2 (*ura3-52*) yeast.
pBS520	Nancy Go	pBSK with bleomycin cassette inserted into NotI of MCS
pBS520-T37	Nancy Go	Genomic copy of *tob37* with 500bp upstream and downstream cloned into pBS520.
pBS520-T37-his	Nargang lab (Wideman *et al.*, 2010)	As for pBS520-T37 with 9x His residues added to the C-terminus
pBS520-T38	Nargang lab (Redmond, 2008)	Genomic copy of tob38 with 1213bp upstream and 2088bp downstream cloned into pBS520
pBS520-T38-his	Nargang lab (Wideman *et al.*, 2010)	As for pBS520-T38 with 9x His residues added to the C-terminus
SWL 45	This study	pBS520-T37 mutagenized to have *Hpa*I restriction sites flanking 5' of TMD1 and 3' of CHD.
SWL 57	This study	pBS520-T37 mutagenized to have *Hpa*I restriction sites flanking TMD1.
SWL 48	This study	pBS520-T37 mutagenized to have *Hpa*I restriction sites flanking CHD.
ΔTMD 12	This study	SWL 45 post *Hpa*I restriction and ligation lacking Tob37 C-terminal 171 bp.
ΔTMD 1	This study	SWL 57 post *Hpa*I restriction and ligation lacking 60 bp encoding TMD1 resdiues.
ΔTMD 2	This study	SWL 48 post *Hpa*I restriction and ligation lacking 57 bp encoding CHD residues.

Chapter 3.

Note: Primers and plasmids used to create the Tom40^{RIP} strain (RIP40het) used in this study as well as the SCAM control strains L10C, L322C and C294S can be found in the thesis of Rebecca D. Taylor (Taylor, 2003).

Construction of the *Tom40^{RIP}* sheltered heterokaryon

The construction of the *tom40^{RIP}* sheltered heterokaryon involved the natural phenomenon of RIP (repeat induced point mutation) that occurs during crossing of *N. crassa* strains (Selker, 1990). *N. crassa* RIP occurs when one nucleus of a sexual cross carries a sequence (gene) duplication. RIP results in GC to AT transitions in both copies of the gene and is used to create null alleles of a target gene (Selker, 1990). RIP occurs post-gamete cell fusion, but before karyogamy, so that the RIP is contained to the duplications in the nucleus of interest. As *tom40* is an essential gene a sheltered RIP approach was required (Harkness *et al.*, 1994; Grotelueschen and Metzenberg, 1995). The process of sheltered RIP requires various nutritional and antibiotic resistance markers located on the same chromosome as the gene of interest. In the case of *tom40*, this is chromosome V. Furthermore, both strains of the cross must carry the *mei-2* mutation that eliminates meiotic recombination and results in the formation of aneuploid ascospores. This aneuploidy results in the majority of ascospores being inviable due to chromosomal loss. However the desired ascospore will possess a full complement of chromosomes with an extra copy of the *tom40* containing chromosome, that is, disomic for chromosome V. One of the disomic chromosomes will contain the endogenous wildtype *tom40* while the other possesses the endogenous RIPed allele, the ectopic RIPed allele may also be present depending on its insertion locus and chromosome segregation. Vegetative growth of this ascospore results in the breakdown of the disomic state to a

heterokaryon containing two different nuclei each with a normal complement of chromosomes but with different chromosome V's in each nucleus (Figure AI. A). The heterokaryotic strain can be selected on minimal medium due to complementation of the nutritional markers from each of the original disomic chromosomes. The nuclear ratios in the heterokaryon can be manipulated using the appropriate drug resistance markers and nutritional requirements (Figure AI. B).

Creation of the RIP40het strain was described previously (Taylor, 2003). Briefly, spheroplasts of the HostV strain (*tom40*$^{+}$ *lys-2 leu-2 inl*$^{+}$ *cyh-2*) were transformed with a plasmid (pRIP-4) containing a hygromycin resistance cassette and 1.8 kb of PCR generated genomic *tom40* sequence. An isolated hygromycin resistant transformant 40Dup1 carrying a duplication was identified via Southern blotting and crossed with the MateV strain (*tom40*$^{+}$ *lys-2*$^{+}$ *leu-2*$^{+}$ *inl cyh-2*$^{+}$ *am132*) (Figure AI. A). The ascospore progeny capable of growth on minimal medium were isolated and tested for growth phenotypes on lysine/leucine/cycloheximide (cyh) medium (Figure AI. B). One isolate with severe growth retardation under these selective conditions was selected and confirmed as the desired RIP40het (isolate F40-6) by Southern analysis and sequencing. In this study the *N. crassa* Tom40 SCAM Cys mutants for residues 10, 144-182, 294, 316-319, 330-339 and 344 (57 in total) were created in the HostV nucleus using the RIP40het sheltered heterokaryon.

Figure AI. Schematic representation of sheltered RIP40het. (A) Construction of RIP40het as described by (Taylor, 2003). Homokaryotic HostV strain carries the endogenous *tom40*$^{+}$allele, cycloheximide resitance (*cyh-2*) and auxotrophy for lysine (*lys-2*) and leucine (*leu-5*) all on *N. crassa* chromosome V. HostV was transformed with a plasmid carrying a 1.8kb region of *tom40* as well as a hygromycin resistance cassette to form 40Dup1. 40Dup1 was crossed with MateV which is cycloheximide sensitive and carries auxotrophy for inositol (*inl*) and leucine (*am132*) on chromosome V. During the cross prior to karyogamy the 40Dup1 nucleus undergoes the phenomenon of RIPing (see above) in the duplicate Tom40 coding sequences resulting in null Tom40 alleles contained to the 40Dup1 nucleus. Both nuclei carry a *mei-2* mutant allele that eliminates meiotic rcombinationin and results in chromosome nondisjunction. A fraction of the meiotic products will posses a full complement of chromosomes plus an additional chromosome V. One of the disomic chromosome V's will contain the *tom40*^{RIP} while the other has a wildtype copy. Vegetative growth breaks down this disomic state to heterokaryotic strain with two types of nuclei housing the respective *tom40* or *tom40*^{RIP} alleles. Spores capable of growth on minimal media were isolated as those carry both versions of chromosome V. Further analysis (see above) identified the RIP40het strain. (B) The two nuclei in RIP40het are identical except for housing different copies of linkage group V (chromosome 5) which carries *tom40* and the nutritional and drug marker alleles. Possible conidia formed from the RIP40het are shown. The *tom40*^{RIP} sheltered heterokaryon can be grown under selective conditions (i.e. medium containing Lys, Leu and cycloheximide) that will favor the *tom40*^{RIP} nucleus resulting in its numerical superiority in the growing heterokaryotic culture. As *tom40* is essential, the *tom40*$^{+}$ nucleus will be maintained at minimal required levels.

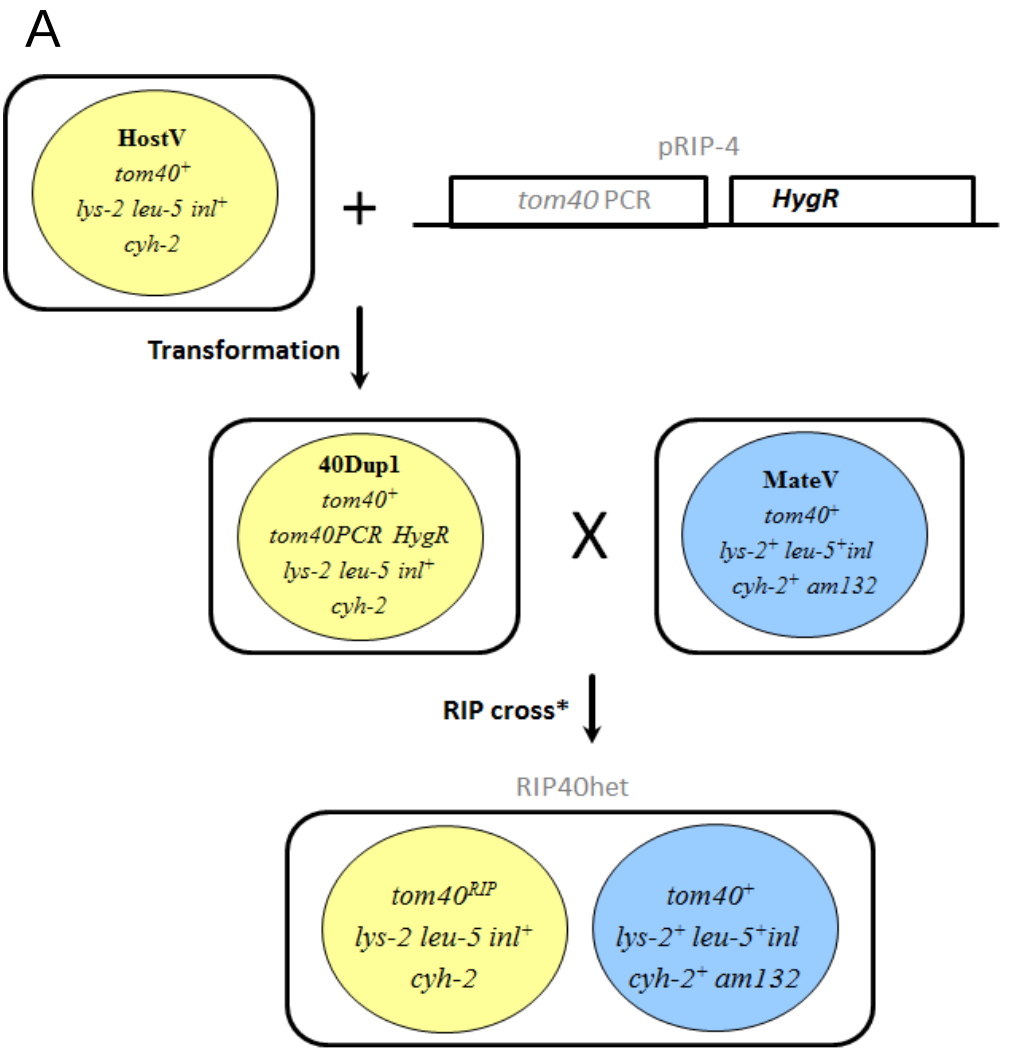

*** (Note that the *tom40PCR* will also be RIPed during the cross and may or may not be present in the heterokaryon depending on its integration site and the random segregation of chromosomes. In the case of RIP40het, *tom40PCR* was found to be present and RIPed (Taylor, 2003))**

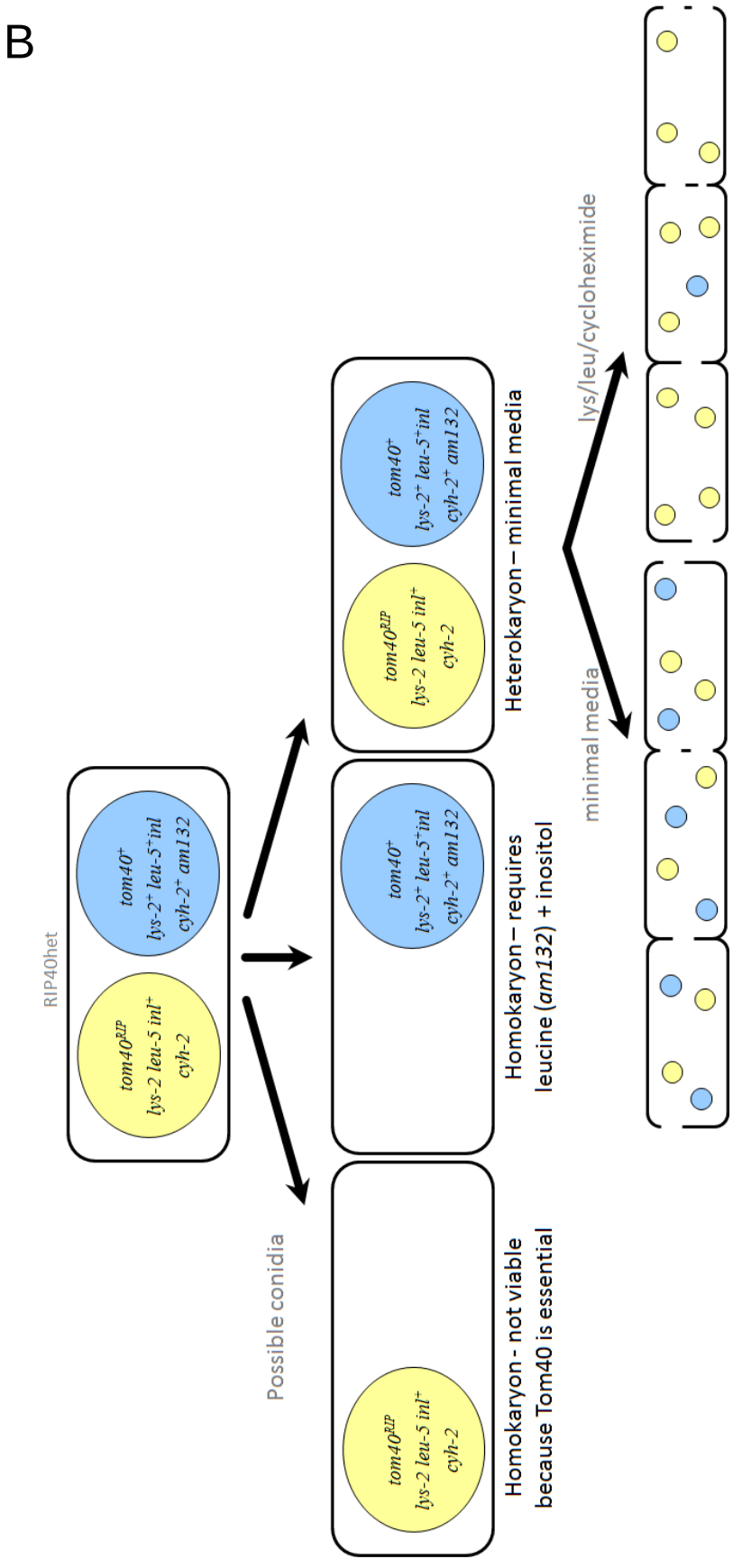
B
RIP4Ohet
tom40RIP lys-2 leu-5 inl+ cyh-2
tom40+ lys-2+ leu-5+inl cyh-2+ am132
Possible conidia
Homokaryon - not viable because Tom40 is essential
tom40+ lys-2+ leu-5+inl cyh-2+ am132
Homokaryon – requires leucine (am132) + inositol
tom40RIP lys-2 leu-5 inl+ cyh-2
tom40+ lys-2+ leu-5+inl cyh-2+ am132
Heterokaryon – minimal media
minimal media
lys/leu/cycloheximide

Table A.3. Additional primers used in Chapter 3.

Primer	Sequence 5'→3'	Use
hphF	ACATACGATTTAGGTGACACTATAGAACGCCCGTCGACAGAAGATGATATTGAAGGAGC	Amplification of hygromycin resistance cassette for KO protocol
hphR	AGCTGACATCGACACCAACG	
TOM40KO-5F	GTAACGCCAGGGTTTTCCCAGTCACGACGTGTTCCTTCAGAGGATCGGC	Amplification of 5' UTR of Tom40 for KO protocol.
TOM40KO-5R	ACCGGGATCCACTTAACGTTACTGAAATCGTCGCAGTAGACAGGGACGA	
TOM40KO-3F	CGTTCTATAGTGTCACCTAAATCGTATGTGGTGCCCAGTCCCTCAACAT	Amplification of 3' UTR of Tom40 for KO protocol.
TOM40KO-3R	GCGGATAACAATTTCACACAGGAAACAGCGCATTTGCTCGTGTGGCACC	
hSM-f	AAAAAGCCTGAACTCACCGCGACG	Amplification of split marker fragment containing Tom40 5'UTR and hph (-promoter).
hSM-r	TCGCCTCGCTCCAGTCAATGACC	Amplification of split marker fragment containing Tom40 3'UTR and hph (-terminator).
FNA 253	GGCCTCCGCGCCGACGTCACC	Tom40 sequencing primer, PCR of genomic Tom40
T40 _FOR1	GGCCGGTGACTGGGTTGCTAGC	Tom40 sequencing primers
T40_REV1	GCCCGCCACCAATCGAGAACTG	
T40_REV2	CCGAGGCCGAGTCTGGGAGTGA	PCR of genomic Tom40

Y94C	/5PHOS/ATGGGCGAGAGG TTGAACCCTTGCGCCTTT GCTGCTCTCTACGGA	Mutagenic primer creating Y94C substitution.
A95C	/5PHOS/GGCGAGAGGTTG AACCCTTATTGCTTTGCT GCTCTCTACGGAACC	Mutagenic primer creating A95C substitution.
F96C	/5PHOS/GAGAGGTTGAAC CCTTATGCCTGCGCTGCT CTCTACGGAACCAAC	Mutagenic primer creating F96C substitution.
A97C	/5PHOS/AGGTTGAACCCTT ATGCCTTTTGCGCTCTCTA CGGAACCAACCAG	Mutagenic primer creating A97C substitution.
A98C	/5PHOS/TTGAACCCTTATG CCTTTGCTTGCCTCTACG GAACCAACCAGGTA	Mutagenic primer creating A98C substitution.
L99C	/5PHOS/AACCCTTATGCCT TTGCTGCTTGCTACGGAA CCAACCAGGTATGC	Mutagenic primer creating L99C substitution.
Y100C	/5PHOS/CCTTATGCCTTTG CTGCTCTCTGCGGAACCA ACCAGGTATGCGCT	Mutagenic primer creating Y100C substitution.
G101C	/5PHOS/TATGCCTTTGCTG CTCTCTACTGCACCAACC AGGTATGCGCTTGG	Mutagenic primer creating G101C substitution.
T102C	/5PHOS/GCCTTTGCTGCTC TCTACGGATGCAACCAGG TATGCGCTTGGAGT	Mutagenic primer creating T102C substitution.
N103C	/5PHOS/TTTGCTGCTCTCT ACGGAACCTGCCAGGTAT GCGCTTGGAGTATA	Mutagenic primer creating N103C substitution.
Q104C	/5PHOS/GCTGCTCTCTACG GAACCAACTGCGTATGCG CTTGGAGTATATCC	Mutagenic primer creating Q104C substitution.
I105C	/5PHOS/CCTTTTAATCCGA GTCAACAGTGCTTCGCTC AGGGTAACCTGGAC	Mutagenic primer creating I105C substitution.

F106C	/5PHOS/TTTAATCCGAGTCAACAGATCTGCGCTCAGGGTAACCTGGACAAC	Mutagenic primer creating F106C substitution.

Table A.4. Additional plasmids used for construction of Tom40 KO (Tom40KO-5) by Nancy Go in Chapter 3.

Name	**Source**	**Description**
pMOcosX G17:H6	Orbach/Sachs cosmid library	Cosmid containing Tom40 and surrounding sequence used for KO PCR protocol.
pCSN44	FGSC	Contains hygromycin resistance cassette for KO PCR protocol .
pRS416	FGSC	*URA-3* containing plasmid used for recombination of KO protocol fragments in FY2 (*ura3-52*) yeast.
pBS520	Nancy Go	pBSK with bleomycin cassette inserted into NotI of MCS.
pBS520-T40	Nancy Go	Genomic copy of *tom40* with 500bp upstream and downstream cloned into pBS520.
pC8	R. Taylor	Genomic copy of *tom40*, no endogenous cysteine, with 500bp upstream and downstream cloned into pBS520.

Table A.5. Plasmids used to develop Cys-substituted strains for SCAM analysis in Chapter 3.

Name	Source	Description
R90C	This study (A.Wong)	pC8 with R90C substitution.
L90C	This study (A.Wong)	pC8 with L91C substitution.
N90C	This study (A.Wong)	pC8 with N92C substitution.
P90C	This study (A.Wong)	pC8 with P93C substitution.
Y94C	This study (A.Wong)	pC8 with Y94C substitution.
A95C	This study (A.Wong)	pC8 with A95C substitution.
F96C	This study (A.Wong)	pC8 with F96C substitution.
A97C	This study (A.Wong)	pC8 with A97C substitution.
A98C	This study (A.Wong)	pC8 with A98C substitution.
L99C	This study (A.Wong)	pC8 with L99C substitution.
Y100C	This study (A.Wong)	pC8 with Y100C substitution.
G101C	This study (A.Wong)	pC8 with G101C substitution.
T102C	This study (A.Wong)	pC8 with T102C substitution.
N103C	This study (A.Wong)	pC8 with N103C substitution.

Q104C	This study (A.Wong)	pC8 with Q104C substitution.
I105C	This study (A.Wong)	pC8 with I105C substitution.
F106C	This study (A.Wong)	pC8 with F106C substitution.
A107C	This study (A.Wong)	pC8 with A107C substitution.
Q108C	This study (A.Wong)	pC8 with Q108C substitution.
G109C	This study (A.Wong)	pC8 with G109C substitution.
N110C	This study (A.Wong)	pC8 with N110C substitution.
L111C	This study (A.Wong)	pC8 with L111C substitution.
D112C	This study (A.Wong)	pC8 with D112C substitution.
N113C	This study (A.Wong)	pC8 with N113C substitution.
E114C	This study (A.Wong)	pC8 with E114C substitution.
G115C	This study (A.Wong)	pC8 with G115C substitution.
A116C	This study (A.Wong)	pC8 with A116C substitution.
L117C	This study (A.Wong)	pC8 with L117C substitution.
S118C	This study (A.Wong)	pC8 with S118C substitution.
T119C	This study (A.Wong)	pC8 with T119C substitution.
R120C	This study (A.Wong)	pC8 with R120C substitution.

F135C	This study (N. Go)	pC8 with F135C substitution.
S136C	This study (N. Go)	pC8 with S136C substitution.
I137C	This study (N. Go)	pC8 with I137C substitution.
G138C	This study (N. Go)	pC8 with G138C substitution.
G139C	This study (N. Go)	pC8 with G139C substitution.
G140C	This study (N. Go)	pC8 with G140C substitution.
Q141C	This study (N. Go)	pC8 with Q141C substitution.
D142C	This study (N. Go)	pC8 with D142C substitution.
M143C	This study (N. Go)	pC8 with M143C substitution.
A144C	This study (N. Go)	pC8 with A144C substitution.
Q145C	This study (N. Go)	pC8 with Q145C substitution.
F146C	This study (N. Go)	pC8 with F146C substitution.
E147C	This study (N. Go)	pC8 with E147C substitution.
H148C	This study (N. Go)	pC8 with H148C substitution.
E149C	This study (N. Go)	pC8 with E149C substitution.
H150C	This study (N. Go)	pC8 with H150C substitution.
L151C	This study (N. Go)	pC8 with L151C substitution.

G152C	This study (N. Go)	pC8 with G152C substitution.
D153C	This study (N. Go)	pC8 with D153C substitution.
D154C	This study (N. Go)	pC8 with D154C substitution.
F155C	This study (N. Go)	pC8 with F155C substitution.
S156C	This study (N. Go)	pC8 with S156C substitution.
A157C	This study (N. Go)	pC8 with A157C substitution.
S158C	This study (N. Go)	pC8 with S158C substitution.
L159C	This study (N. Go)	pC8 with L159C substitution.
K160C	This study (N. Go)	pC8 with K160C substitution.
A161C	This study (N. Go)	pC8 with A161C substitution.
I162C	This study (N. Go)	pC8 with I162C substitution.
N163C	This study (N. Go)	pC8 with N163C substitution.
P164C	This study (N. Go)	pC8 with P164C substitution.
S165C	This study (N. Go)	pC8 with S165C substitution.
F166C	This study (N. Go)	pC8 with F166C substitution.
L167C	This study (N. Go)	pC8 with L167C substitution.
D168C	This study (N. Go)	pC8 with D168C substitution.

G169C	This study (N. Go)	pC8 with G169C substitution.
G170C	This study (N. Go)	pC8 with G170C substitution.
L171C	This study (N. Go)	pC8 with L171C substitution.
T172C	This study (N. Go)	pC8 with T172C substitution.
G173C	This study (N. Go)	pC8 with G173C substitution.
I174C	This study (N. Go)	pC8 with I174C substitution.
F175C	This study (N. Go)	pC8 with F175C substitution.
V176C	This study (N. Go)	pC8 with V176C substitution.
G177C	This study (N. Go)	pC8 with G177C substitution.
D178C	This study (N. Go)	pC8 with D178C substitution.
Y179C	This study (N. Go)	pC8 with Y179C substitution.
L180C	This study (N. Go)	pC8 with L180C substitution.
Q181C	This study (N. Go)	pC8 with Q181C substitution.
A182C	This study (N. Go)	pC8 with A182C substitution.
V316C	(Taylor, 2003)	pC8 with V316C substitution.
T317C	(Taylor, 2003)	pC8 with T317C substitution.
Q318C	(Taylor, 2003)	pC8 with Q318C substitution.

Q319C	(Taylor, 2003)	pC8 with Q319C substitution.
A320C	(Taylor, 2003)	pC8 with A320C substitution.
K321C	(Taylor, 2003)	pC8 with K321C substitution.
L322C	(Taylor, 2003)	pC8 with L322C substitution.
G323C	(Taylor, 2003)	pC8 with G323C substitution.
M324C	(Taylor, 2003)	pC8 with M324C substitution.
S325C	(Taylor, 2003)	pC8 with S325C substitution.
V326C	(Taylor, 2003)	pC8 with V326C substitution.
S327C	(Taylor, 2003)	pC8 with S327C substitution.
I328C	(Taylor, 2003)	pC8 with I328C substitution.
E329C	(Taylor, 2003)	pC8 with E329C substitution.
A330C	(Taylor, 2003)	pC8 with A330C substitution.
S331C	(Taylor, 2003)	pC8 with S331C substitution.
D332C	(Taylor, 2003)	pC8 with D332C substitution.
V333C	(Taylor, 2003)	pC8 with V333C substitution.
D334C	(Taylor, 2003)	pC8 with D334C substitution.
L335C	(Taylor, 2003)	pC8 with L335C substitution.
Q336C	(Taylor, 2003)	pC8 with Q336C substitution.
E337C	(Taylor, 2003)	pC8 with E337C substitution.
Q338C	(Taylor, 2003)	pC8 with Q338C substitution.
Q339C	(Taylor, 2003)	pC8 with Q339C substitution.

References

Grotelueschen, J., and Metzenberg, R.L. (1995). Some property of the nucleus determines the competence of *Neurospora crassa* for transformation. Genetics *139*, 1545-1551.

Harkness, T.A., Metzenberg, R.L., Schneider, H., Lill, R., Neupert, W., and Nargang, F.E. (1994). Inactivation of the *Neurospora crassa* gene encoding the mitochondrial protein import receptor MOM19 by the technique of "sheltered RIP". Genetics *136*, 107-118.

Redmond, E.K. (2008). The Role of Tob37 and Tob38 in Mitochondrial Beta-Barrel Protein Assembly, University of Alberta.

Selker, E.U. (1990). Premeiotic instability of repeated sequences in *Neurospora crassa*. Annu Rev Genet *24*, 579-613.

Taylor, R.D. (2003). Assembly, function and structure of Tom40, the pore-forming component of the the TOM complex in *Neurospora crassa*, University of Alberta.

Wideman, J.G., Go, N.E., Klein, A., Redmond, E., Lackey, S.W., Tao, T., Kalbacher, H., Rapaport, D., Neupert, W., and Nargang, F.E. (2010). Roles of the Mdm10, Tom7, Mdm12, and Mmm1 proteins in the assembly of mitochondrial outer membrane proteins in *Neurospora crassa*. Mol Biol Cell *21*, 1725-1736.

Appendix II. Analysis of a putative glutathione-S transferase (GST) domain in Tob38.

This appendix describes an attempt to demonstrate that a GST domain in Tob37 and Tob38 might be involved in maintaining an interaction between the two proteins. Since the results of the study were negative they are briefly described here rather than in a *bona fide* thesis chapter.

Analysis of sequence alignments (Figure AII.1) and BLAST analysis (Figure AII.2) revealed three regions of highly conserved amino acid residues within the Tob38 protein among several fungal species. Theoretically, the conservation of these regions suggests their importance for the correct structure and function of the protein. Additional comparison between Tob37 and Tob38, which had previously been shown to be homologues with low sequence identity (Adolph, 2005; Kozjak-Pavlovic *et al.*, 2007), revealed the conservation of a glutathione-S-transferase (GST) domain (Figure AII.3) (Armstrong *et al.*, 1997). GST domains are found in a superfamily of proteins with extremely diverse protein sequences (Koonin *et al.*, 1994). GST proteins play a key role in the regulation of the REDOX state of the cell by catalyzing the conjugation of reduced glutathione (GSH) molecules (Wilce and Parker, 1994; Sheehan *et al.*, 2001). GSH is a tripeptide that acts as an antioxidant by serving as an electron donor to reduce cellular components that have been oxidized by reactive oxygen species (ROS) (Douglas, 1987; Pompella *et al.*, 2003). GSTs in the non-active state homodimerize, however during instances of an undesirable highly reductive environment when reduced GSH needs to be sequestered GSTs separate and bind to GSH rendering it inactive as a reducing agent (Dirr *et al.*, 1994). Various GSTs exists throughout the cell with variant organellar and cytosolic localizations (Atkinson and Babbitt, 2009).

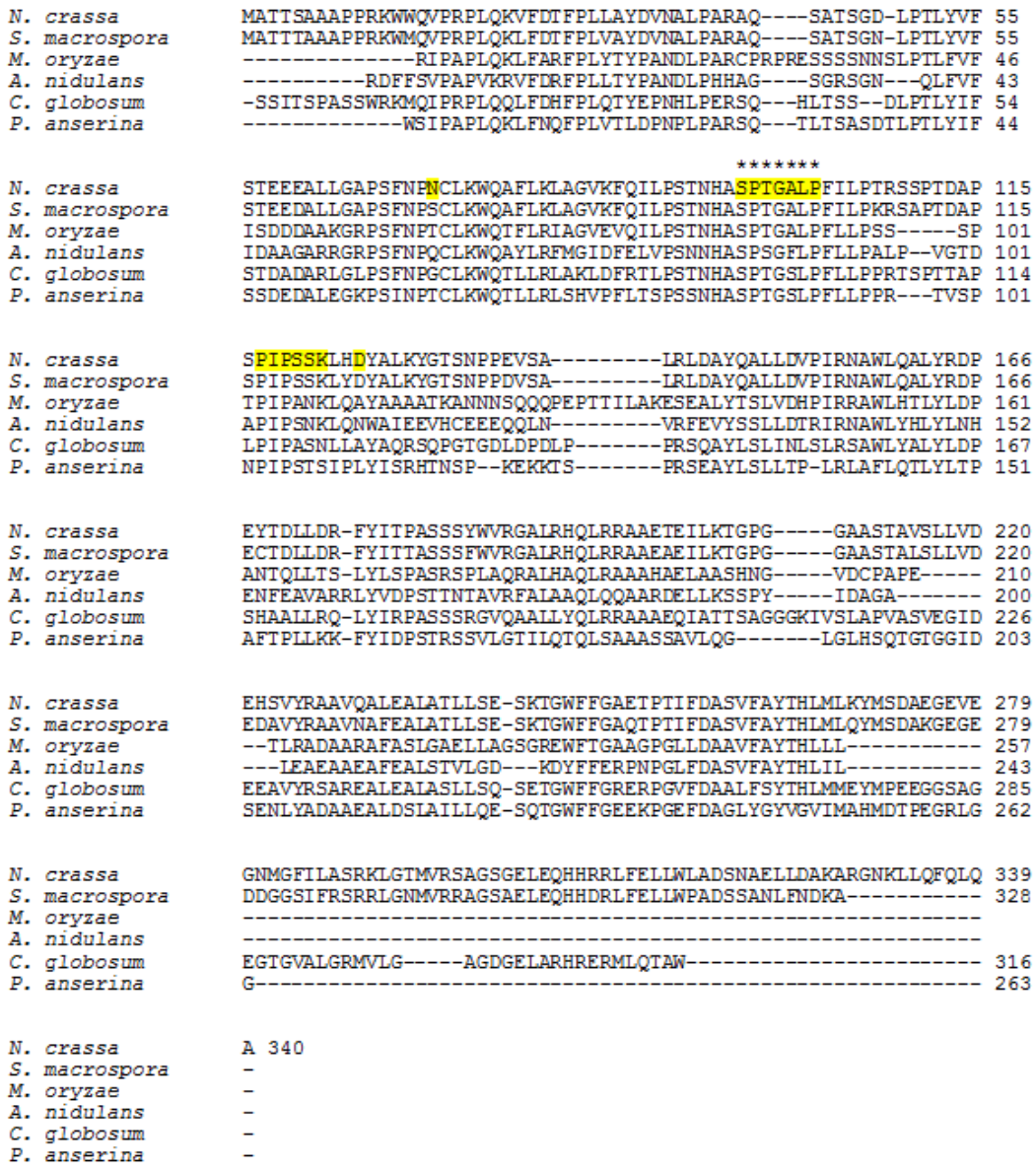

Figure AII.1 Alignment of fungal Tob38 homologues. Alignment of Tob38 amino acid sequence from varying fungal species using the Clustal W2.1 sequence alignment program (sequences from *Neurospora crassa, Sordaria macrospora, Magnaporthe oryzae, Aspergillis nidulans, Chaetomium globosum* and *Podospora anserina*). Residues ^{96}SPTGALP^{102} (*) were chosen for mutagenesis based upon near complete conservation between species. Highlighted (yellow) residues indicate the putative GST binding/homodimerization domain of *N. crassa*.

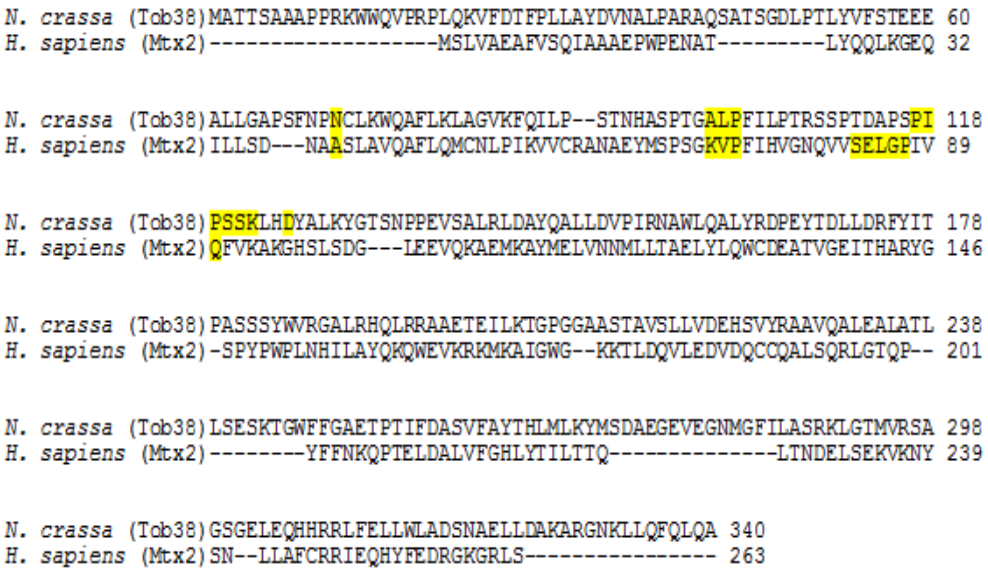

Figure AII.2 BLAST Alignment of *Neurospora crassa* Tob38 and Human Metaxin 2.

Using the Clustal W2.1 programme *Neurospora crassa* Tob8 and *Homo sapiens* Metaxin2 were aligned. Residues involved in the putative GST binding/homodimerization domain (determined by domain identification using BLAST) are shown (highlighted yellow).

```
N. crassa (Tob38) ---------------MATTSAAAPPRKWWQVPRPLQKVFDTFPLLAYDVNALPARAQSAT 45
N. crassa (Tob37) MTLELHVWGPAFGLPSIDAECLATVTYFAQTLSAADYLLVQSSPSAVPSHHLPALYNPST 60

N. crassa (Tob38) SGDLPTLYVFSTEEEALLGAPSFNPNCLKWQAFLKLAGVKFQILPSTNHASPTGALPFIL 105
N. crassa (Tob37) ATWISGFDPIVNYLSTLQPPSYHHPDVTTLPSRVYADSQAYKALLTS-SAAPLLALSLYV 119

N. crassa (Tob38) PTRSSPTDAPSPIPSSKLHDYALKYGTSNPPEVSALRLDAYQALLDVPIRNAWLQALYRD 165
N. crassa (Tob37) SSANYSETTRPAYSAILPFPLPWTEPLAVRAAMAARAAHLGMSSLDTDAEMERLEREERE 179

N. crassa (Tob38) ---PEYTDLLDRFYITPASSSYWVRGALRHQLRR--------------AAETEILKTGPG 208
N. crassa (Tob37) REAAGWVQIPKALRKAVGGQNSGVKGQLSPEMKRRIKLEGLAAEVFDVLGEVDFLEEEDG 239

N. crassa (Tob38) ------------GAASTAVSLLVDEHSVYRAAVQALEALATLLSESKTGWFFG--AETPT 254
N. crassa (Tob37) EEEEEEEEEAKEGGARIKVTLETKCLAFAYLALMLLPEVPRPWLKEVLQKKYAGLCKFVL 299

N. crassa (Tob38) IFDASVFAYTHLMLKYMS----------DAEGEVEGNMG-----------------FILA 287
N. crassa (Tob37) EYRRKTFPDSGKVLPWADRESDPAVSACDSALSIVGRFVRAVIDDIPMLGREWSRWWALR 359

N. crassa (Tob38) SRKLGTMVRSAGSGELEQHHRRLFELLWLADSNAELLDAKARGNKLLQFQLQA------- 340
N. crassa (Tob37) QRRVAEENSAETQLVVRRSVGESERSLLLAGAGLTLLAINVAGLGIYWYRYRGLLGAPLQ 419

N. crassa (Tob38) ----------------------
N. crassa (Tob37) TWHRPLVGLGSFGAAGAMFAGLA 442
```

Figure AII.3 BLAST Alignment of *Neurospora crassa* Tob38 and Tob37. Using the Clustal W2.1 programme *Neurospora crassa* Tob38 and Tob37 were aligned. Residues involved in the putative GST binding/homodimerization domain (determined by domain identification using BLAST) are shown (highlighted yellow).

The homodimerization of GSTs occurs via a dual function GSH binding/GST homodimerization domain (Wilce and Parker, 1994; Oakley, 2011). Interestingly GSTs have also been implicated in binding toxins and xenobiotics. In some instances GST family proteins have been shown have functions as transport/chaperone proteins capable of binding substrates and escorting them to the required destination (Oakley, 2011). GSTs possess a well understood protein-protein interaction mechanism facilitated by the structural arrangement and character of specific residues of the GSH binding/homodimerization domain (Dirr *et al.*, 1994; Wilce and Parker, 1994; Sheehan *et al.*, 2001; Atkinson and Babbitt, 2009). As key REDOX regulators GSTs are necessarily abundant in the ROS producing mitochondria and their immediate environment. Given the mitochondrial localization of Tob37 and Tob38 and the suggestion that they interact with one another (see section 1.6.3 and the results of Chapter 2) it seems feasible that they may have evolved from a GST-like ancestor. If this scenario were true it would also imply that the conserved GST domain, while perhaps not acting in its original capacity, may play a role in TOB complex assembly and stability. Therefore the proposed GST domain residues in Tob38 were chosen as targets for mutagenesis.

As a beginning to this study, a Biology 499 project student (Beau Desaulniers) transformed the Tob38 sheltered heterokaryon (section 2.2.2) with a Tob38 variant in which residues ^{96}SPTGALP^{102} were deleted (Figure AII.1). Transformants rescuing the *tob38 KO* nucleus were selected and purified (as in section 2.2.3). One isolate called 7bd was chosen for further analysis. I repeated this protocol using the same construct to get two further isolates called 7-1 and 7-2. Western blot analysis of mitochondrial proteins in these isolates revealed no change in the levels of the TOM and TOB proteins examined (Figure AII.4 A). However, impaired import/assembly of radiolabelled β-barrel precursors (Tom40 and porin) was observed in isolated mitochondria (Figure AII.4 B and

Figure AII.4 Import/assembly of mitochondrial precursor proteins into Tob38-7 mutant mitochondria. (A) Cells from the indicated strains (top of panel: 7-1 and 7-2 isolates produced by S. W. Lackey, 7bd produced by A. B. Desaulniers) were grown in liquid medium. Mitochondria were isolated and subjected to SDS-PAGE followed by transfer of proteins to nitrocellulose, and immunodecoration with the antibodies indicated on the left. The control strain was 76-26 (see Table 3.1). Multiple bands in the Tob55 lane correspond to different isoforms of the protein (Hoppins *et al.*, 2007). (B) Radiolabelled Tom40 precursor was incubated for 5 min and 20 min with mitochondria isolated from the strains indicated (top of panel). Mitochondria were dissolved in 1% digitonin and subjected to BNGE. The proteins were transferred to PVDF membrane and analyzed by autoradiography. The size of the mature TOM complex (400 kDa), and assembly intermediates I (250 kDa) and II (100 kDa) are indicated on the left. (C) Assembly of porin. As in panel C, except mitochondria were incubated with radiolabeled porin. (D) As in panel B except that mitochondria were incubated with the radiolabeled precursor of Tom22. The size of the mature TOM complex (400 kDa), and the mutant phenotype assembly intermediate (250 kDa) are indicated on the left.

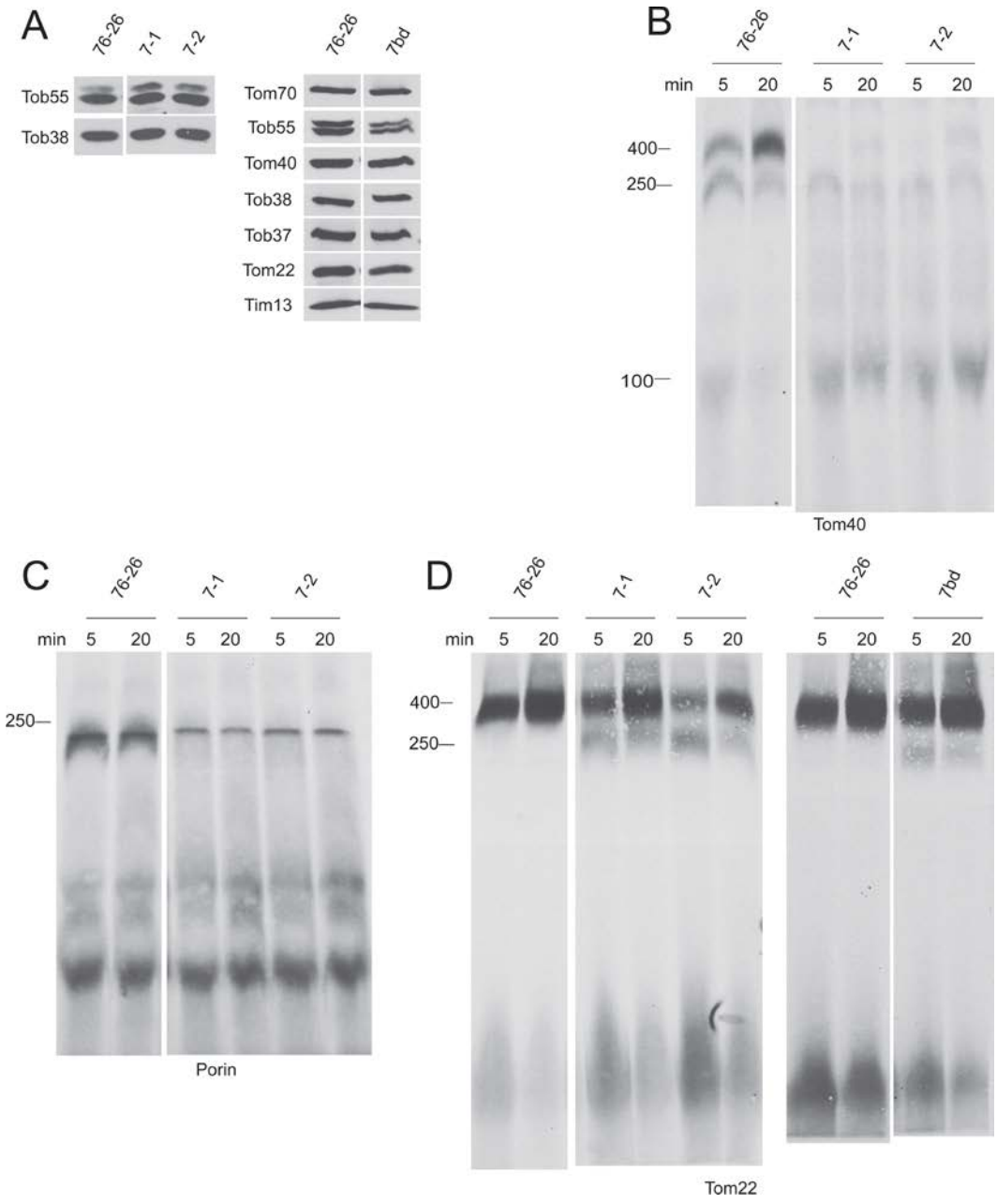
A
76-26
7-1
7-2
Tob55
Tob38
76-26
7bd
Tom70
Tob55
Tom40
Tob38
Tob37
Tom22
Tim13
B
76-26
7-1
7-2
min 5 20 5 20 5 20
400—
250—
100—
Tom40
C
76-26
7-1
7-2
min 5 20 5 20 5 20
250—
Porin
D
76-26
7-1
7-2
76-26
7bd
min 5 20 5 20 5 20 5 20 5 20
400—
250—
Tom22

C). As described in section 1.6.3.5, Tom40 assembly can be monitored through two intermediates and the final assembled TOM complex. Tom40 precursor appears to be slightly reduced at the 250kDa intermediate I (Tom40 precursor-TOB association) for both time points in the Tob38 mutants (7-1 and 7-2) (Figure AII.4 B). There also appears to be accumulation of Tom40 at the 100kDa intermediate II (Tom40 precursor-Tom40/Tom5/6). *In vitro* assembly past this intermediate to the final TOM complex is extremely inefficient as very little precursor matures into the fully assembled TOM complex (400kDa).

While little is known about the assembly of porin and the complexes observed on blue native gels during assembly assays, we do know that the highest molecular weight complex (~240 kDa) represents a porin precursor-TOB intermediate (Hoppins *et al.*, 2007). This intermediate is significantly reduced in the mutant strains while the remaining complexes appear unaffected when compared to the control strain (Figure AII.4 C).

Import of the non-β-barrel protein Tom22 into isolated mitochondria of the Tob38-7 mutants showed novel association of the Tom22 precursor with an undefined complex ~220 kDa (Figure AII.4 D). A similar phenotype has been observed in our lab before with other mutant strains (data not shown) including some mutants of the ERMES complex (described in section 1.4). Since Tom22 is inserted into the MOM via an interaction with the TOB complex (Stojanovski *et al.*, 2007; Becker *et al.*, 2008; Thornton *et al.*, 2010), we hypothesize that the ~220 kDa band represents a Tom22-TOB intermediate that persists long enough for detection when the TOB complex containing the Tob38 mutant is involved. The accumulation of this novel intermediate and the slight decrease in Tom22 precursor reaching the final TOM complex suggests a slowed and/or

inefficient dissociation of the precursor from the TOB complex. Further analysis will be required to determine the nature of this novel intermediate.

These preliminary results suggest the Δ^{96}SPTGALP^{102} mutant Tob38 alters the TOB complex in a fashion that inhibits import. Interestingly the Tom40 assembly phenotype observed appears to mostly occur at intermediate stages downstream from intermediate I where the precursor associates directly with the TOB complex. Since the residues ^{101}LP^{102} comprise the N-terminal region of the proposed GST binding domain. I created a Tob38 ΔLP mutant in an attempt to determine if these proposed GST domain residues were functionally important. When mitochondria were isolated from this strain and used for import/assembly assays as in Figure AII.4, no discernible import or assembly phenotypes were observed (data not shown). Thus, it appears the phenotype observed in the Δ^{96}SPTGALP^{102} mutants are not attributable to the LP residues thought to be conserved for functional GST protein-protein interactions. Conversely, deletion of the corresponding putative ^{52}LP^{53} GST residues in Tob37 resulted in distinct phenotypes such as reduced steady state Tob37 and porin levels, severely reduced β-barrel import and assembly and TOB complex destabilization (Redmond, 2008). These results indicate the residues in this conserved region within Tob37 are functionally important. However, we have also observed that mutation in other related GST residues (Tob37 Δ^{117}PIPSSK^{122}) does not impart any observable phenotypes (data not shown). These results suggest that the conserved putative GST domains within Tob38 and Tob37 are not essential, however disruptions to certain residues does have an effect on function. Whether these domains/residues are functioning in a GST domain-like manner or have evolved novel roles distinct from GST domains remains to be determined.

References

Adolph, K.W. (2005). Characterization of the cDNA and amino acid sequences of *Xenopus* Metaxin 3, and relationship to *Xenopus* Metaxins 1 and 2. DNA Seq *16*, 252-259.

Armstrong, L.C., Komiya, T., Bergman, B.E., Mihara, K., and Bornstein, P. (1997). Metaxin is a component of a preprotein import complex in the outer membrane of the mammalian mitochondrion. J Biol Chem *272*, 6510-6518.

Atkinson, H.J., and Babbitt, P.C. (2009). Glutathione transferases are structural and functional outliers in the thioredoxin fold. Biochemistry *48*, 11108-11116.

Becker, T., Pfannschmidt, S., Guiard, B., Stojanovski, D., Milenkovic, D., Kutik, S., Pfanner, N., Meisinger, C., and Wiedemann, N. (2008). Biogenesis of the mitochondrial TOM complex: Mim1 promotes insertion and assembly of signal-anchored receptors. J Biol Chem *283*, 120-127.

Dirr, H., Reinemer, P., and Huber, R. (1994). X-ray crystal structures of cytosolic glutathione S-transferases. Implications for protein architecture, substrate recognition and catalytic function. Eur J Biochem *220*, 645-661.

Douglas, K.T. (1987). Mechanism of action of glutathione-dependent enzymes. Advances in enzymology and related areas of molecular biology *59*, 103-167.

Hoppins, S.C., Go, N.E., Klein, A., Schmitt, S., Neupert, W., Rapaport, D., and Nargang, F.E. (2007). Alternative splicing gives rise to different isoforms of the *Neurospora crassa* Tob55 protein that vary in their ability to insert beta-barrel proteins into the outer mitochondrial membrane. Genetics *177*, 137-149.

Koonin, E.V., Mushegian, A.R., Tatusov, R.L., Altschul, S.F., Bryant, S.H., Bork, P., and Valencia, A. (1994). Eukaryotic translation elongation factor 1 gamma contains a glutathione transferase domain--study of a diverse, ancient protein superfamily using motif search and structural modeling. Protein Sci *3*, 2045-2054.

Kozjak-Pavlovic, V., Ross, K., Benlasfer, N., Kimmig, S., Karlas, A., and Rudel, T. (2007). Conserved roles of Sam50 and metaxins in VDAC biogenesis. EMBO Rep *8*, 576-582.

Oakley, A. (2011). Glutathione transferases: a structural perspective. Drug metabolism reviews *43*, 138-151.

Pompella, A., Visvikis, A., Paolicchi, A., De Tata, V., and Casini, A.F. (2003). The changing faces of glutathione, a cellular protagonist. Biochem Pharmacol *66*, 1499-1503.

Redmond, E.K. (2008). The Role of Tob37 and Tob38 in Mitochondrial Beta-Barrel Protein Assembly, University of Alberta.

Sheehan, D., Meade, G., Foley, V.M., and Dowd, C.A. (2001). Structure, function and evolution of glutathione transferases: implications for classification of non-mammalian members of an ancient enzyme superfamily. Biochem J *360*, 1-16.

Stojanovski, D., Guiard, B., Kozjak-Pavlovic, V., Pfanner, N., and Meisinger, C. (2007). Alternative function for the mitochondrial SAM complex in biogenesis of alpha-helical TOM proteins. J Cell Biol *179*, 881-893.

Thornton, N., Stroud, D.A., Milenkovic, D., Guiard, B., Pfanner, N., and Becker, T. (2010). Two modular forms of the mitochondrial sorting and assembly machinery are involved in biogenesis of alpha-helical outer membrane proteins. J Mol Biol *396*, 540-549.

Wilce, M.C., and Parker, M.W. (1994). Structure and function of glutathione S-transferases. Biochim Biophys Acta *1205*, 1-18.

Appendix III. *N. crassa* Mim2 antibody production.

The discovery of *S. cerevisiae* Mim2 (Dimmer *et al.*, 2012) by collaborators at the University of Munich led them to identify the *N. crassa* Mim2 by BLAST analysis and propose a project that would attempt to purify and crystallize the *N. crassa* MIM1/2 complex. The alignment of *S. cerevisiae* Mim2 (YLR099W-A) identified the hypothetical protein NCU16952.7 as a possible *N. crassa* Mim2 candidate (Figure AIII.1). I used a commercially produced peptide (Bio Basic Canada Inc., Markham, ON) containing residues 2-23 of NCU16952.7 as an antigen for antibody production in rats. Four rats produced serum containing antibodies that cleanly detected Mim2 via Western blotting of isolated mitochondria (Figure AIII.2). One serum was selected for further work (Mim2 4-3). To confirm the ~15kDa band represented Mim2 we used a strain expressing only an endogenous N-terminally 6x histidinyl tagged Mim1 (MIM1KO-HT-12) (Figure AIII.3) in an attempt to pulldown the MIM1/2 complex. The results show that the Mim2 protein detected with our antibody is successfully pulled down in complex with 6x His tagged Mim1 (Figure AIII.4). The protein is absent in a control strain (76-26) containing no His tag. These data suggest that the MIM1/2 complex exists in *N. crassa* and that it can be purified from our Mim1-His tag strain.

```
S. cerevisiae       MADSEDTSVILQGIDTIN--SVEGLE--EDGYLSDEDTSLSNELADAQRQWEESLQQLNK 56
N. crassa           MSTPSDSYVLHDHSPSTDNDDVDSLPSISSSILGSDDSEYDDE-SDAQKEWEQSLEQLQL 59
                    *    *  *           *  *       *   *     *  ***  ** ** **

S. cerevisiae       LLNWVLLPLLGKYIGRRMAKTLWSRFIEHFV------------------------- 87
N. crassa           LLNLVLIPFAGKFLGRKFAYWSWGRYMEWAHGVKVQWYNKTLFNIAGWIGAATPVSV 116
                    *** ** *  **  **  *   * *  *
```

Figure AIII.1 Alignment of Mim2 homologues. Mim2 amino acid sequence alignment using the Clustal W2.1 sequence alignment program. Sequences aligned are *S. cerevisiae* (YLR099W-A) and *N. crassa* (NCU16952.7) Mim2. An N-terminal *N. crassa* peptide (highlighted yellow) was used as the antigen for raising the antibody. (*) denotes conserved residues.

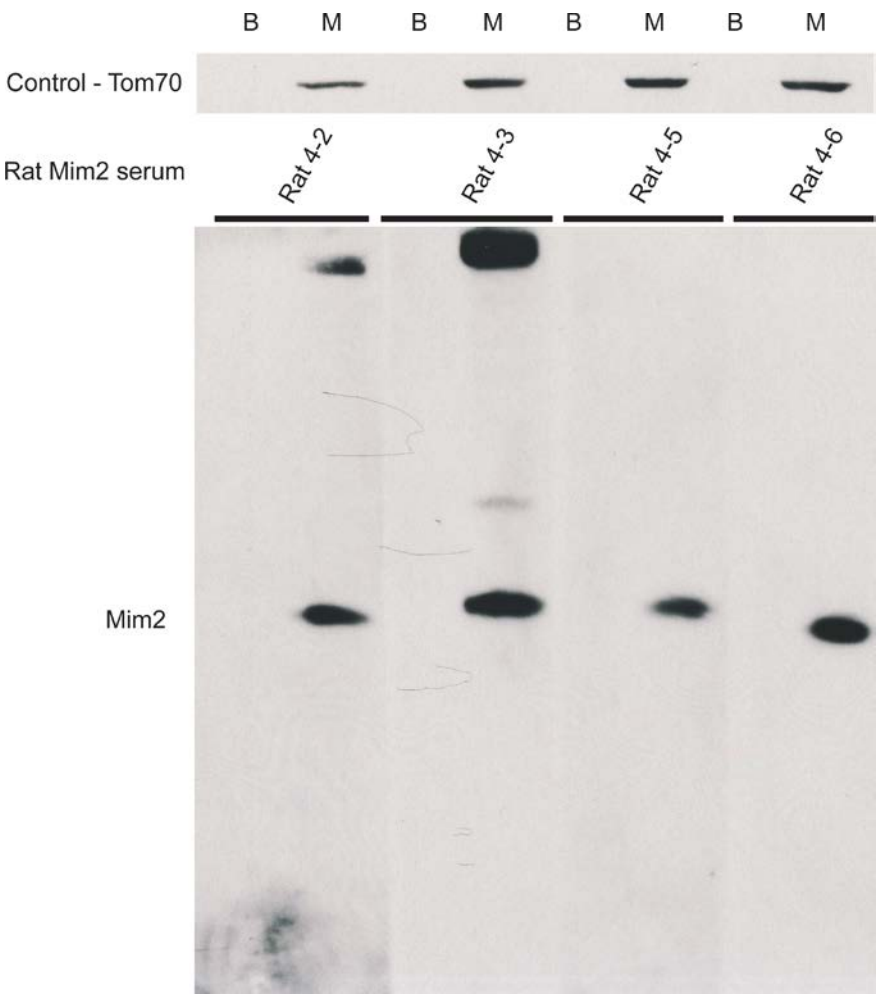

Figure AIII.2 Serum screening. Four rats designated 4-2, 4-3, 4-5 and 4-6 were selected for the antibody production protocol based on prior screening of their serum for non-reactivity with *N. crassa* mitochondrial proteins. When satisfactory signal was achieved the protocol was halted and the blood sera were isolated and used for immunodecoration and Western blotting of Mim2 from control (76-26) mitochondria. Lanes were loaded with 50µg of mitochondrial protein (M) or left blank (B). Tom70 serves as the loading control.

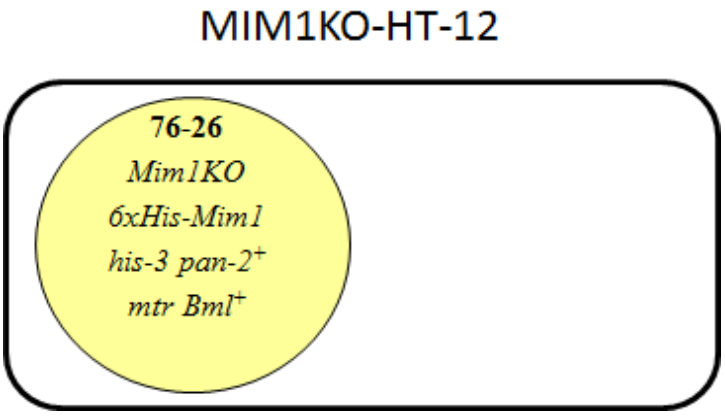

Figure AIII.3 MIM1KO-HT-12 representation. This strain (created by N.E. Go) houses an endogenous copy of a N-terminally 6 x Histidinyl tagged Mim1 integrated randomly in the genome of the 76-26 (His requiring, fpa resistant) Mim1 KO nucleus.

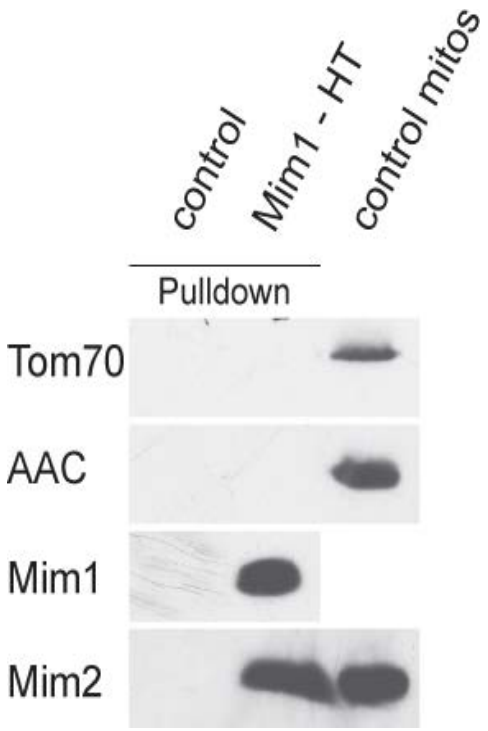

Figure AIII.4 Pulldown of MIM 1/2 complex. Cells from the control strain (76-26) or the Mim1-His tag (HT) strain (MIM1KO-HT-12) were grown in the presence of histidine (His). In the 2 "Pulldown" lanes, isolated mitochondria (1.5 mg of total mitochondrial protein) from each strain were dissolved in digitonin and subjected to a clarifying spin (28400 x g, 60 mins, 4˚C). The supernatant was removed and 1mL of NiNTA-Agarose beads (Qiagen, Cat #30230) were added. The mixture was rocked for 2 hrs at 4˚C and the beads were collected in gravity-flow column. Following two washes in imidazole buffers the bound substrate was eluted for further analysis. The "control mitos" lane contains mitochondria isolated from strain 76-26. Final samples were subjected to SDS-PAGE followed by transfer to nitrocellulose, and immunodecoration with the antibodies indicated on the left.

References

Dimmer, K.S., Papic, D., Schumann, B., Sperl, D., Krumpe, K., Walther, D.M., and Rapaport, D. (2012). A crucial role for Mim2 in the biogenesis of mitochondrial outer membrane proteins. J Cell Sci *125*, 3464-3473.